Technischen Universität München
Lehrstuhl für Bauchemie

Ersatz von Lithiumcarbonat als Beschleuniger für Calciumaluminatzemente: Untersuchungen zur Wirkung und Aufklärung des Mechanismus von beschleunigenden Biopolymeren

Alexander Adrian Engbert

Vollständiger Abdruck der von der Fakultät für Chemie der Technischen Universität München zur Erlangung des akademischen Grades eines

Doktors der Naturwissenschaften (Dr. rer. nat.)

genehmigten Dissertation.

Vorsitzender: Prof. Dr. Klaus Köhler

Prüfer der Dissertation:
1. Prof. Dr. Johann Plank
2. Prof. Dr. Thomas Brück
3. Prof. Dr. Josef Felixberger (schriftliche Beurteilung)

apl. Prof. Dr. Anton Lerf (mündliche Prüfung)

Die Dissertation wurde am 30.11.2020 bei der Technischen Universität München eingereicht und durch die Fakultät für Chemie am 01.03.2021 angenommen.

Die vorliegende Arbeit entstand in der Zeit von Dezember 2016
bis September 2020 unter der Anleitung von

Herrn Prof. Dr. Johann Plank

am Lehrstuhl für Bauchemie der Technischen Universität München.

"The greatest danger facing us is ourselves - our irrational fear of the unknown. But there's no such thing as the unknown. Only things temporarily hidden, temporarily not understood."

E. W. Roddenberry, Drehbuch für "The Corbomite Maneuver"

And at last I resolved to scale that tower,

fall though I might;

since it were better to glimpse the sky and perish,

than to live without ever beholding day.

— H. P. Lovecraft, "The Outsider"

Mein besonderer Dank gilt

Herrn Prof. Dr. Johann Plank

für die Aufnahme in seinen Arbeitskreis, sein persönliches Interesse und dafür, dass er das Gelingen dieser Arbeit ermöglicht hat. Ebenso für sein Engagement, mir einen Forschungsaufenthalt bei der Firma SE Tylose in Wiesbaden, unter Betreuung von Herrn Heiner Klehr, im Rahmen meines Masterstudiums zu ermöglichen.

Mein weiterer Dank gilt:

- der *Deutschen Forschungsgemeinschaft* (DFG) für die Förderung dieses Forschungsprojekts unter der Sachbeihilfe PL-472/13-1.
- der Firma *Imerys* (früher *Kerneos*) für die großzügige Bereitstellung von Zementen sowie Herrn Andreas Eisenreich (Fa. *Imerys*) für den fachlichen Austausch.
- den Firmen *KIMICA*, *Roeper*, *Eurogum*, *Nabertec* und *Quarzwerke* für die materielle Unterstützung mit Produktproben von Alginaten, Biopolymeren und Füllstoffen.

Persönlich möchte ich mich bedanken bei:

- meinen Teamkollegen der Faschingsvorlesung für die stets tolle Zusammenarbeit und all den Spaß an den Versuchen. Vielen Dank, Dr. Johannes Stecher, Dr. Stefanie Gruber, My Linh Vo und Christopher Schiefer sowie Matthias Werani und Matthias Theobald.
- meinen Laborgefährten Marlene Schmid, Florian Hartmann, Christopher Schiefer und My Linh Vo für das langjährige gute Miteinander.
- im Besonderen Herrn Christopher Schiefer für die freundschaftliche Zusammenarbeit und intensive Diskussion und Unterstützung im Labor.
- sowie auch Herrn Florian Hartmann für die vielen Gespräche nach Feierabend und beim Sport.
- allen verbleibenden Kollegen und Ehemaligen für die jahrlange gute Zusammenarbeit, Dr. Lei Lei, Dr. Thomas Hurnaus, Dr. Claudia Chomyn, Manuel Ilg, Timon Echt, Johann Mekulantesch, Dominik Staude und im Besonderen unserer Laborantin Dagmar Lettrich für ihre kräftige Mithilfe.

- den Studenten Christopher Schiefer, Luis Schnürer und Richard Foja für ihr Engagement und ihre Mithilfe bei der Laborarbeit im Rahmen ihrer Praktika und Abschlussarbeiten.
- Frau Dr. Oksana Storcheva für die Durchführung vieler Messungen am Festkörper NMR-Spektrometer der Fakultät für Chemie und Herrn Thomas Burger (Lehrstuhl für Technische Chemie I, Prof. Hinrichsen) für die Messungen am ICP-OES des Arbeitskreises von Prof. Nilges (Synthese und Charakterisierung innovativer Materialien).

Herzlich bedanken möchte ich mich auch bei all meinen Freunden, die mich seit der Schule über das Studium hinweg begleitet haben, auch wenn ich während meiner Promotion nur wenig Zeit mit Ihnen verbringen konnte. Im Besonderen möchte ich Herrn M. Ed. Benjamin Stöger danken für seine Unterstützung und die vielen schönen Abende und Wochenenden, die den Ausgleich zur Promotion geliefert haben. Auf viele weitere gemeinsame Jahre.

Zuletzt, aber an wichtigster Stelle, möchte ich insbesondere **meinen Eltern Miranda und Werner Engbert** meinen ewigen Dank aussprechen dafür, dass Sie mich intensiv während meiner Ausbildung unterstützt und das Studium der Chemie sowie die anschließende Promotion ermöglicht haben. Ebenso meiner Tante Lidija Olujić und meinem Onkel Mark Petri für die Unterstützung und nicht zuletzt auch für das Lesen dieser Arbeit. Auch meinen Großeltern, insbesondere meiner Großmutter Jugoslava Olujić († 2020), die die Fertigstellung dieser Arbeit nicht erleben durften, möchte ich gedenken.

Publikationen

Diese Arbeit basiert auf folgenden wissenschaftlichen Veröffentlichungen, wobei nur die Publikationen mit den Nummern 1 - 4 näher diskutiert werden:

Veröffentlichungen in internationalen Zeitschriften mit peer-review Verfahren:

1 Engbert A., Gruber S., Plank J. (2020) The effect of alginates on the hydration of calcium aluminate cement. Carbohydrate Polymers, **236**, 116038.

2 Engbert A., Plank J. (2020) Identification of Specific Structural Motifs in Biopolymers That Allow to Effectively Accelerate Calcium Alumina Cement. Industrial & Engineering Chemistry Research, **59**(26), S. 11930–11939.

3 Engbert A., Plank J. (2020) Templating effect of alginate and related biopolymers as hydration accelerator for calcium alumina cement - A mechanistic study. Materials & Design, **195**, 109054.

4 Engbert A., Plank J. (2020) Impact of Sand and Filler Materials on the Hydration Behavior of Calcium Aluminate Cement. Journal of the American Ceramic Society, **104**(2), S. 1067–1075.

Veröffentlichungen in Tagungsbänden mit peer-review Verfahren:

5 Engbert A., Plank J. “The Unusual Behaviour of Specific Biopolymers as Accelerator in Alumina Cement”, 15th International Congress on the Chemistry of Cement (ICCC), Prague (Czech Republic), 2019, Conference proceedings, Contribution ID: 101.

6 Engbert A., Plank J. “Specific biopolymers as accelerator for alumina cement”, Calcium Aluminates - Proceedings of the International Conference 2020 (Cambridge, UK), Whittles Publishing, Scotland.

7 Hartmann F., Engbert A., Plank J. “Towards understanding the ageing behaviour of SLU formulations: Impact of prehydration on individual components and role of admixtures”, Calcium Aluminates - Proceedings of the International Conference 2020 (Cambridge, UK), Whittles Publishing, Scotland.

Die Publikationen 5 - 7 sind dem Anhang unter Abschnitt 7.6 beigefügt.

Veröffentlichungen in Tagungsbänden ohne peer-review Verfahren:

8 Engbert A., Dinkel M., Plank J. "Alginate als neue Beschleuniger für Aluminatzemente", Tagung der GDCh-Fachgruppe Bauchemie, Weimar (Germany), GDCh Monographie 52, 2017, S. 53 – 58.

9 Engbert A., Dinkel M., Plank J. "Biopolymers as Novel Accelerators for Alumina Cement", 20. ibausil, Bauhaus-Universität Weimar (Germany), Tagungsband 1, 2018, S. 819 – 826.

10 Engbert A., Plank J. "Biopolymers As Novel Accelerators For Alumina Cement", European Coatings Show – Conference, Nürnberg (Germany), 2019, Contribution 20.1.

Die Publikationen 8 - 9 sind dem Anhang unter Abschnitt 7.6 beigefügt.

Alle Publikationen wurden mit Einverständnis der Rechteinhaber abgedruckt.

Inhaltsverzeichnis

Abkürzungsverzeichnis

BET	Brunauer, Emmett und Teller, Methode zur Bestimmung der spezifischen Oberfläche eines Feststoffs
Blaine	Methode zur Bestimmung der (Mahl-)Feinheit eines Pulvers über die Permeabilität gegenüber durchströmender Luft
°C	Grad Celsius
CAC	engl. calcium aluminate cement, dt. Calciumaluminatzement, auch als Aluminatzement oder Tonerdeschmelzzement bezeichnet
CCD	engl. charge-coupled device
cm^{-1}	Reziproke Zentimeter, Wellenzahl, Einheit bei FT-IR Spektroskopie
CPS	engl. cement pore solution, dt. Zementporenlösung
$d_{10/50/90}$	Einheit der Korngrößenverteilung (massengemittelter Partikeldurchmesser)
Da	Dalton, g/mol, Einheit der atomaren Masse bzw. Molekülmasse
DE	engl. degree of esterification, dt. Veresterungsgrad
DIN EN	Europäische Norm, die als Deutsche Industrienorm (DIN) übernommen wurde
FT-IR	Fourier-Transformations-Infrarotspektroskopie
g	Gramm
GPC	Gelpermeationschromatographie
ICP-OES	engl. inductively coupled plasma optical emission spectrometry, dt. optische Emissionsspektrometrie mittels induktiv gekoppelten Plasmas
J	Joule
kDa	Kilodalton, 1 kDa = 10^3 Da
kg	Kilogramm, 1 kg = 10^3 g
L	Liter, 1 L = 1 dm^3 = 1000 cm^3 = 1000 mL
LDH	engl. layered double hydroxide, dt. Mischmetallhydroxid
M	Molare Masse, Einheit: g/mol
mbar	Millibar, 1 mbar = 10^{-3} bar
mg	Milligramm, 1 mg = 10^{-3} g
min	Minute
mL	Milliliter, 1 mL = 1 cm^3 = 10^{-3} dm^3 = 10^{-3} L

mV	Millivolt, 1 mV = 10^{-3} V
mW	Milliwatt, 1 mW = 10^{-3} W
µm	Mikrometer, 1 µm = 10^{-6} m
µS	Mikrosiemens, 1 µS = 10^{-6} S
MAS	engl. magic angle spinning, Methode der Festkörper-NMR-Spektroskopie
M_n	Zahlenmittlere Molmasse eines Polymers
MPEG	*ω*-Methoxypoly(ethylenoxid)
M_w	Gewichtsmittlere Molmasse eines Polymers
M/G	Verhältnis von Mannuron- zu Guluronsäure
nm	Nanometer, 1 nm = 10^{-9} m
N/mm^2	Newton pro Quadratmillimeter, Maß für die Druck- und Biegezugfestigkeit
NMR	engl.: nuclear magnetic resonance, dt. Kernspinresonanz
OPC	engl. ordinary Portland cement, dt. Portlandzement
PCE	Polycarboxylatester/-ether
PDI	Polydispersitätsindex (M_w/M_n)
PEG	Polyethylenglykol
PGA	Propylenglykolalginat bzw. Hydroxypropylalginat
pH	pondus hydrogenii, Maß für die Säurestärke (einer Lösung), pH-Wert
REM	Rasterelektronenmikroskopie
SEM	engl. scanning electron microscopy, dt. Rasterelektronenmikroskopie
SSA	engl. specific surface area, dt. spezifische Oberfläche
Upm	Umdrehungen pro Minute
wt.%	engl. percent by weight, dt. Gewichtsprozent
w/b	Masserelation von Wasser zu Bindemittel („Wasser/Bindemittel-Wert“)
w/c	engl. water-to-cement ratio, dt. Masserelation von Wasser zu Zement
w/f	Masserelation von Wasser zu Feststoff („Wasser/Feststoff-Wert“)
w/s	engl. water-to-solid ratio, dt. Masserelation von Wasser zu Feststoff
w/z	Masserelation von Wasser zu Zement („Wasser/Zement-Wert“)
XRD	engl. X-ray diffraction, dt. Röntgenbeugung bzw. -diffraktometrie
XRF	engl. X-ray fluorescence spectroscopy, dt. Röntgenfluoreszenzanalyse

Zementchemische Notation

Historisch bedingt hat sich in der Zementchemie eine eigene Kurzschreibweise etabliert, wobei anstatt der chemischen Elementsymbole folgende Abkürzungen für die Oxide verwendet werden.

Abkürzung	Oxid
A	Aluminiumoxid (Al_2O_3)
C	Calciumoxid (CaO)
F	Eisenoxid (Fe_2O_3)
H	Wasser (H_2O)
M	Magnesiumoxid (MgO)
S	Siliciumdioxid (SiO_2)
T	Titandioxid (TiO_2)

Hieraus ergeben sich folgende Kurzschreibweisen für Klinker- bzw. Hydratphasen:

Abkürzung	Klinker-/Hydratphase
C_3A	Tricalciumaluminat, $Ca_3Al_2O_6$
$C_{12}A_7$	Mayenit, Dodecacalciumheptaaluminat, $Ca_{12}Al_{14}O_{33}$
CA	Monocalciumaluminat, $CaAl_2O_4$
CA_2	Grossit, Calciumdialuminat, $CaAl_4O_7$
C_2AS	Gehlenit, $Ca_2AlSi_2O_7$
C_4AF	Brownmillerit, Tetracalciumaluminatferrit, $Ca_2(Al_xFe_{1-x})_2O_5$
$C_{20}A_{13}M_3S_3$	Pleochroit, Q Phase, $Ca_{20}Al_{26}Mg_3Si_3O_{68}$
C_3S	Alit, Tricalciumoxysilikat, $Ca_3(SiO_4)O$
C_2S	Belit, Larnit, Dicalciumsilikat $Ca_2(SiO_4)$
CT	Perowskit, $CaTiO_3$
C_3FT	Tricalciumferrotitanat, Sharyginit, $Ca_3Fe_2TiO_8$
AH_3	Aluminiumhydroxid, $Al(OH)_3$
C-A-H	Calcium-Aluminat-Hydrat
CAH_{10}	$Ca[Al(OH)_4]_2 \cdot xH_2O$, $CaAl_2(OH)_8(H_2O)_2 \cdot xH_2O$
C_2AH_8	$Ca_2[Al(OH)_5]_2 \cdot xH_2O$, $[Ca_2Al(OH)_6]^+[Al(OH)_4 \cdot xH_2O]^-$
C_3AH_6	Katoit, $Ca_3[Al(OH)_6]_2$
C_4AH_x	$Ca_2[Al(OH)_7] \cdot xH_2O$, $2([Ca_2Al(OH)_6]^+OH^- \cdot xH_2O)$
C_2ASH_8	Strätlingit, $Ca_2Al_2SiO_7 \cdot 8H_2O$, $Ca_2Al[(OH)_6AlSiO_2(OH)_4] \cdot xH_2O$
C-S-H	Calcium-Silikat-Hydrat

1. Einleitung und Aufgabenstellung

1.1 Einleitung

Zement, aus dem Lateinischen „caementum“ für „Baustein“, ist ein Werkstoff auf anorganischer Basis, der durch Zugabe von Wasser zur Reaktion gebracht wird und zum Festkörper aushärtet. Der namensgebende „opus caementitium“, welcher bereits für die Errichtung von Bauwerken wie dem Pantheon im römischen Reich verwendet wurde, war ein Kalkmörtel mit vulkanischer Asche [1–3]. Dieser erhielt seine Festigkeit durch eine Calcium-Alumosilikat-Hydrat-Phase und Strätlingit [4]. Das Wissen um die Herstellung dieses Bindemittels verblasste mit dem Untergang des Römischen Reiches [3].

Erst gegen Ende des 18. Jahrhunderts begann durch die Beteiligung von *John Smeaton* und *James Parker* das Zeitalter des „modernen“ Zements [1–3]. Der von *James Parker* patentierte Romanzement (bei welchem es sich allerdings nicht um einen Zement im heutigen Sinne handelt) war ein Baukalk mit puzzolanischen Bestandteilen. Dieser wurde durch die Erfindung des Portlandzementes Anfang des 19. Jahrhunderts rasch aus dem Markt verdrängt. Dessen Entwicklung und weitere Verfeinerung geht auf *Joseph Aspdin* und seinen Sohn *William Aspdin* zurück [1]. Heute ist Portlandzement (kurz: OPC) mit einer Produktionsmenge von 4,1 Mrd. Tonnen im Jahr 2019 ein unverzichtbarer Baustoff [5]. Zusätzlich zum Hoch- und Tiefbau haben sich eine Vielzahl von Anwendungsgebieten im Bereich der Trockenmörtel (u.a. im Innenausbau) für OPC entwickelt.

Neben dem Portlandzement gibt es eine Vielzahl weiterer spezialisierter Zemente und Bindemittel. Hierzu zählen neuere Entwicklungen wie Calciumsulfoaluminat-Zement, Geopolymere oder Belit-Ye’elimit-Ferrit-Zement, aber auch bereits etablierte Bindemittel wie Magnesiabinder, Bariumzement, Phosphatbinder und Aluminatzement. Bezogen auf die Produktionskapazität sticht dabei der Calciumaluminatzement (kurz: CAC) wegen seiner vielfältigen Spezialanwendungen hervor [1,6–10].

Calciumaluminatzemente zeichnen sich besonders durch ihre schnelle Festigkeitsentwicklung (< 24 Std.), ihre chemische Widerstandsfähigkeit sowie ihre Temperaturbeständigkeit aus. Diese werden, verglichen mit OPC, aufgrund ihres deutlich höheren Preises nur in relativ geringer Menge hergestellt. Daher werden sie bevorzugt in Schnellreparaturmörteln, unter aggressiven Bedingungen (z.B. Schwarzwasser oder Salzwasser) und in Feuerfestanwendungen (bis 1800 °C) verwendet. Ein wichtiger Einsatzbereich für Calciumaluminatzemente ist allen voran der Trockenmörtel (binäre

und ternäre Bindemittel), in denen sie gemischt mit Calciumsulfat (Anhydrit oder Halbhydrat) und gegebenenfalls Portlandzement verwendet werden [1,2,11,12].

Chemisch unterscheiden sich CACs sowohl bezüglich ihrer Eigenschaften, ihrer Zusammensetzung als auch ihrer Reaktivität mit Wasser jedoch grundlegend von Portlandzementen. Hierbei gilt es allerdings zu beachten, dass CACs nicht für tragende Anwendungen empfohlen bzw. zugelassen sind, da diese aufgrund einer später einsetzenden chemischen Umwandlungsreaktion an Endfestigkeit verlieren. Dieses als ‚Konversion' bezeichnete Phänomen kann allerdings durch Einsatz eines niedrigen w/z-Wertes (≤ 0,4) kompensiert werden [1,2].

Für ihren Einsatzzweck können Calciumaluminatzemente durch unterschiedlichste Zusatzmittel, u.a. Verzögerer, Beschleuniger, Fließmittel, Latex-Polymere und Stellmittel, auf ihre Anwendung optimiert werden. Im Besonderen soll in dieser Arbeit die Rolle des Abbindebeschleunigers betrachtet werden. In der Anwendungspraxis werden hierfür Lithium-Salze eingesetzt, wie beispielsweise das häufig verwendete Lithiumcarbonat (Li_2CO_3).

Da Lithium allerdings für die Produktion von Li-Ionen-Akkumulatoren unabdingbar ist, war hier in den letzten Jahren ein stetig steigender Bedarf zu beobachten, der sich auch in der Preisentwicklung von Lithium wiederspiegelte [13]. Der in **Abbildung 1** gezeigte Preis einer Tonne Li_2CO_3 zeigt eine kontinuierliche Steigerung über die letzte Dekade. Parallel zum Preisanstieg ist ebenfalls kontinuierlich die Produktionskapazität für Lithium deutlich ausgebaut worden, um den Bedarf zu decken, sodass 2019 erstmals der Wert einer Tonne Lithiumcarbonat rückläufig war [14].

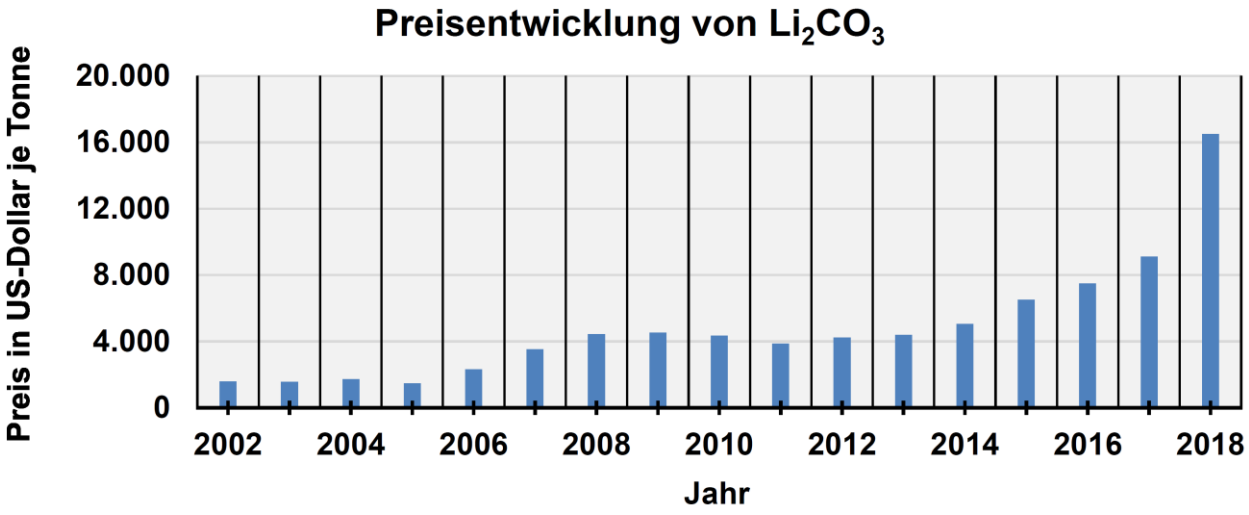

Abbildung 1: Preisentwicklung von Lithiumcarbonat zwischen 2002 und 2018, basierend auf den Daten aus [13].

Im Jahr 2019 betrug die Fördermenge an Lithium ungefähr 77.000 Tonnen und wurde zu circa 65 % für die Batterie-Produktion eingesetzt [5]. Weitere wichtige Einsatzgebiete für Lithium sind beispielsweise die Glas- und Keramikherstellung sowie Schmierstoffe.

Nach aktuellem Stand der Technik sind in der Batterie eines Elektroautos abhängig von seiner Bauart und Reichweite zwischen 3 und 13 kg Lithium verbaut, was einer Kapazität von ungefähr 20 – 100 kWh entspricht [15]. Würden nun die gesamten 50.000 Tonnen Lithium ausschließlich für die Herstellung von E-Autos eingesetzt werden, so könnte man weltweit 6 Millionen Pkws mit diesen Batterien (zu je 8 kg Lithium) produzieren. Um dies in Relation zu setzen, sei Folgendes erwähnt: Alleine in Deutschland liefen im Jahr 2019 nicht weniger als 4,6 Mio. neue Pkws vom Band. Weltweit waren es über 67 Mio. Pkws (2019), wobei noch zusätzlich 25 Mio. Nutzfahrzeuge (Busse, Lkws, etc.) dazukommen [16,17].

Diese Zahlen verdeutlichen, dass die Verfügbarkeit von Lithium eine kritische Voraussetzung für die weitere Umsetzung der Elektromobilität darstellt. Zudem ist die Verfügbarkeit weiterer Elemente wie Cobalt und Nickel, die essentiell für das Kathodenmaterial (z.B. $LiCoO_2$) in Li-Batterien sind, ebenso wie die des Lithiums begrenzt. Aktuell sind Li-freie Batterien wie z.B. die Natrium-Ionen-, Magnesium-Ionen- bzw. Aluminium-Ionen-Batterien noch in der Grundlagenforschung und kommerziell nicht konkurrenzfähig, da diese in ihrer Zyklenstabilität, Ladungsdichte und Schnellladefähigkeit weit unterlegen und unausgereift sind [18–21]. Daher ist auf absehbare Zeit kein alternatives Element in der Lage, das Lithium in Akkumulatoren zu ersetzen.

1.2 Aufgabenstellung

Aufgrund des exponentiell angestiegenen Bedarfs an Lithium war die Verfügbarkeit dieser Commodity für die Bauindustrie zeitweilig sehr schwierig. Insbesondere die verstärkte Entwicklung von Li-Ionen-Akkumulatoren im Bereich der Elektromobiltät hat die Nachfrage beeinflusst. Während ein Recycling von Lithium aus Akkumulatoren durch verschiedene Prozesse bereits industriell praktiziert wird [22–24], ist ein nachträgliches Recycling des Lithiums durch Extraktion aus Bauschutt nicht möglich. Daher gilt es anzuerkennen, dass der Einsatz der wertvollen Lithiumsalze in der Bauindustrie eine schlechte Nachhaltigkeit zur Folge hat. Entsprechend drängt sich die Frage nach einer geeigneten Alternative für Li_2CO_3 auf.

Im Rahmen einer früheren Untersuchung zur Interkalation von Biopolymeren in LDH-Strukturen am Lehrstuhl für Bauchemie wurde unerwartet ein hydratations-beschleunigender Effekt für Alginate festgestellt [25,26]. Da Polysaccharide in der Regel eine verzögernde Wirkung auf die Hydratation zeigen, indem es z.B. zu einer Blockierung („Vergiftung“) des Kristallwachstums kommt [27–32], erweckte dies Interesse an der Ursache hinter dem ungewöhnlichen Effekt von Alginat. Zudem handelt es sich bei Alginaten um einen global verfügbaren, nachwachsenden Rohstoff, der noch dazu toxikologisch unbedenklich ist. Er wird bereits häufig in der Lebensmittelindustrie sowie in der Medizin eingesetzt, wobei die gelierende Wirkung von Alginat, die in Gegenwart divalenter Kationen auftritt, genutzt wird [33–35].

Das wesentliche Ziel der vorliegenden Arbeit ist deshalb die Untersuchung und Aufklärung des Wirkmechanismus, der dem beschleunigenden Effekt von Alginat zugrunde liegt. Dies erfolgte unter Betrachtung verschiedener Aspekte. In einem ersten Schritt wurde die generelle Wirksamkeit von Alginat auf verschiedene Zemente untersucht und bestimmte chemische Eigenschaften des Alginats ausgemacht, welche dessen Wirksamkeit beeinflussen könnten. Im Folgenden wurde die chemische Struktur verschiedener Biopolymere unterschiedlicher Herkunft unter dem Aspekt einer möglichen Struktur-Wirkbeziehung studiert, um die besonderen Strukturmerkmale des Alginats zu identifizieren. Abschließend wurde unter Einsatz mehrerer analytischer Methoden (NMR, XRD, ICP-OES, Zeta-Potential und REM) das Wirkprinzip untersucht und auf Basis der gewonnenen Erkenntnisse ein Modell zum Mechanismus entwickelt.

Aufbauend auf diesen Erfahrungen wurde darüber hinaus noch der beschleunigende Effekt von feinen Füllstoffen näher betrachtet und ein Wirkmechanismus für diesen vorgeschlagen.

2. Theoretischer Hintergrund

2.1 Calciumaluminatzement

2.1.1 Herstellung und Zusammensetzung

Bereits im 19. Jahrhundert wurde die Herstellung von Aluminat-reichen Zementen erforscht, woraufhin Anfang des 20. Jahrhunderts *Jules Bied* den Calciumaluminatzement, wie er heute bekannt ist, bei *LaFarge* kommerziell zugänglich gemacht hat [1,36]. In seiner oxidischen Zusammensetzung unterscheidet er sich, wie in **Abbildung 2** zu erkennen, grundlegend vom OPC.

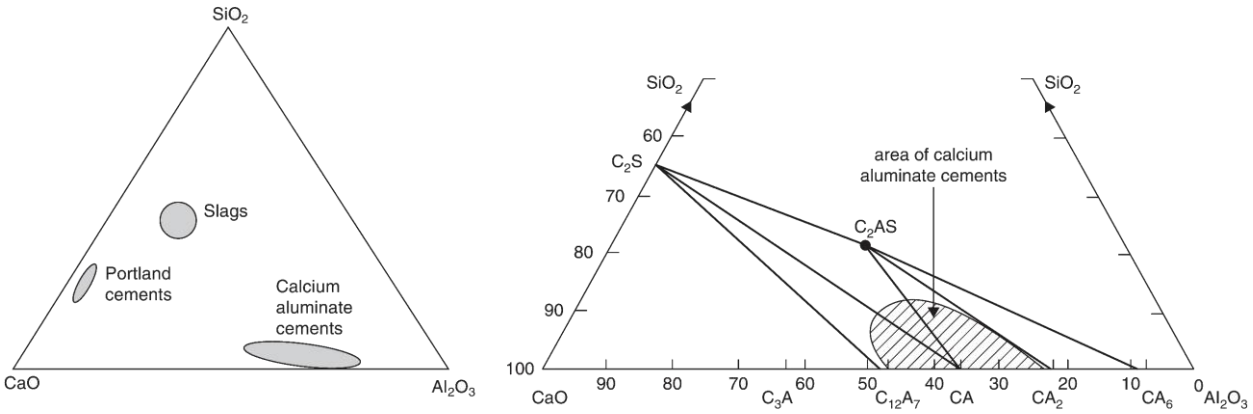

Abbildung 2: Oxidische Zusammensetzung von OPC und CAC, abgedruckt in bearbeiteter Form mit Genehmigung aus [3,11].

Aufgrund des hohen Al_2O_3-Anteils (circa 36 – 82 Gew.%) dieser Zemente wird zur erfolgreichen Synthese der gewünschten Klinkerphasen, hauptsächlich z.B. CA und CA_2 für einen weißen CAC, eine deutlich höhere Brenntemperatur als beim OPC benötigt. Dies ist aus dem Phasendiagramm in **Abbildung 3**, das die Schmelzpunkte der jeweiligen Phasen angibt, ersichtlich. Bei grauen bzw. braunen Zementen, welche zusätzlich noch Silikate und Ferrate enthalten, wird das Phasendiagramm im quaternären System entsprechend komplexer. Für diesen Prozess werden Kalkstein und Bauxit in einem Ofen gemeinsam bei bis zu 1600 °C gebrannt, wobei verschiedene Ofentypen wie beispielsweise Drehrohröfen, aber auch Lichtbogenöfen eingesetzt werden können [1,2,11,12,36,37]. Der erhaltene Klinker wird anschließend langsam abgekühlt, wodurch in dem so hergestellten Zement die Klinkerphasen hauptsächlich kristallin vorliegen und nur ein geringer Anteil in amorpher Form. Alternativ kann ein hochreaktiver Zement, in dem der Zementklinker gezielt in amorpher Form vorliegt, durch rasches Abschrecken sowie durch höhere Brenntemperaturen (1600 bis > 2000 °C) erhalten werden [38,39].

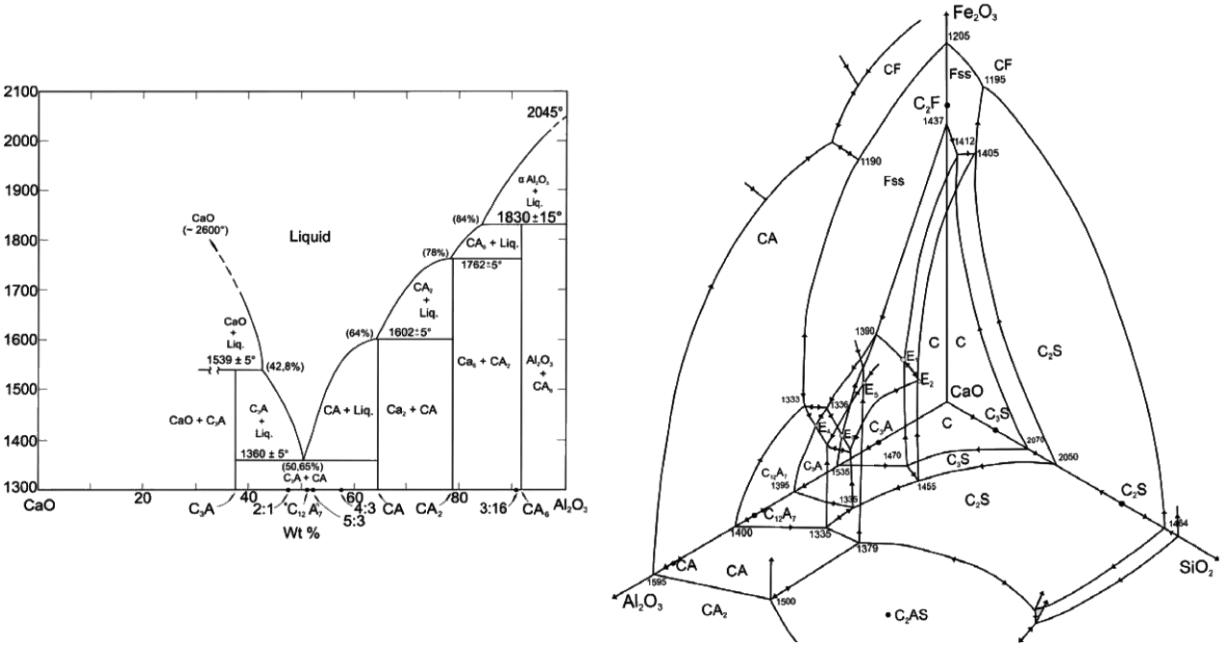

Abbildung 3: Binäres und quaternäres Phasendiagramm für die Systeme CaO/Al_2O_3 und $CaO/Al_2O_3/Fe_2O_3/SiO_2$, abgedruckt in veränderter Form mit Genehmigung aus [36].

Im Falle der Bildung kristalliner Klinkerphasen entstehen abhängig von der oxidischen Zusammensetzung des Rohmehls im Wesentlichen die folgenden hydraulischen Klinkerphasen: CA, CA_2, C_2AS und C_4AF. Weitere Bestandteile sind C_2S und $C_{12}A_7$, wobei Letzteres bestimmend für die Reaktivität des CAC ist [2,6,11,12]. Bei den Klinkerphasen nimmt die Reaktivität mit Wasser mit steigendem Verhältnis von CaO/Al_2O_3 zu [40]:

$$C_3A > C_{12}A_7 > CA > CA_2$$

Die im Rahmen dieser Arbeit verwendeten Calciumaluminatzemente, produziert von der Firma *Imerys* (bis 2019 als *Kerneos* firmiert), waren mit einem Al_2O_3-Gehalt zwischen 35 und 80 Gew.% von unterschiedlicher Phasenzusammensetzung. Mittels *Rietveld*-Analyse wurden diese unter Zuhilfenahme von Literaturwerten quantitativ analysiert (siehe **Tabelle 1**). Dabei zeigte sich, dass mit einer Ausnahme alle Zemente einen CA-Gehalt von 40 – 60 Gew.% aufweisen, was für CACs charakteristisch ist. Nur Ternal EP, welches ein $C_{12}A_7$-reiches Bindemittel ist und für die Formulierung in binären, Ettringit-bildenden Systemen konzipiert ist, bleibt hiervon ausgenommen und stellt keinen in Reinform verwendbaren Zement dar.

Tabelle 1: Mineralogische Zusammensetzung (in M.%) der in dieser Arbeit verwendeten CACs.

Klinker-phase	Phasengehalte (Gew.%) der Calciumaluminatzement-Proben					
	Ternal EP (35 % Al_2O_3)	Ciment Fondu Ternal SE (40 % Al_2O_3)	Secar 41 (45 % Al_2O_3)	Secar 51 Ternal LC (50 % Al_2O_3)	Secar 71 Secar 712 (70 % Al_2O_3)	Secar 80 (80 % Al_2O_3)
CA	1 - 5 %	47 - 57 %	54 - 66 %	64 - 74 %	54 - 64 %	35 - 45 %
CA_2	*n.d.*	*n.d.*	*n.d.*	*n.d.*	36 - 44 %	22 - 30 %
C_2AS	*n.d.*	1 - 10 %	10 - 22 %	18 - 22 %	< 1 %	*n.d.*
C_4AF	10 - 20 %	10 - 20 %	*n.d.*	*n.d.*	*n.d.*	*n.d.*
C_2S	10 - 20 %	1 - 10 %	1 - 10 %	1 - 5 %	*n.d.*	*n.d.*
$C_{12}A_7$	55 - 65 %	1 - 5 %	1 - 5 %	< 1 %	< 1 %	< 1 %
weitere Phasen	C_3A, CT	C_3FT, $C_{20}A_{13}M_3S_3$	CT, C_3FT, $C_{20}A_{13}M_3S_3$	CT, C_3FT	α-Al_2O_3 (< 2 %)	α-Al_2O_3 (35 - 45 %)

2.1.2 Hydratation von CAC

Der Mechanismus der beim Anmischen von CAC mit Wasser einsetzenden Hydratationsreaktion folgt einem weitgehend kongruenten Auflöseprozess der Klinkerphasen und anschließender Präzipitation der Hydrate aus der übersättigten Lösung [2,3,6,11,12,36,37,41–46]. Hierbei werden nach anfänglichem Kontakt mit Wasser Ca^{2+}-Ionen aufgrund ihrer besseren Löslichkeit aus dem Klinker gelöst, während Aluminium-Ionen sich an der Klinkeroberfläche anreichern und in hydroxylierter Form als Aluminium-Hydroxo-Hydrat vorliegen (siehe **Abbildung 4**) [6,42,45,47–50]. In diesem initialen Schritt, der die Induktionsperiode der Zementreaktion umfasst, wird allerdings nur ein geringer Anteil (< 1 Gew.%) des Zementes gelöst [49]. Die nachfolgende dormante Periode, welche an der fehlenden Wärmefreisetzung in der Kalorimetrie zu erkennen ist, ist durch hohe Konzentrationen an Calcium- und Aluminium-Ionen in der Zementporenlösung gekennzeichnet [3,37,40,41,44,49,51]. In Abhängigkeit von Additiven (Beschleuniger und Verzögerer) beginnt die Akzelerationsperiode, sobald durch anfängliche Nukleation Hydratphasen aus der Porenlösung sowohl homogen als auch heterogen auskristallisieren [37,46,52,53]. Die daraufhin einsetzende Sammelkristallisation führt sukzessiv unter Wärmefreisetzung zur Ausbildung eines Gefüges durch interpartikuläre Überbrückung, wodurch der Zementleim erstarrt und anschließend erhärtet [37,45]. Aufgrund der massiven Kristallisation von C-A-H-Phasen in einem kurzen Zeitraum baut CAC schnell Festigkeit auf, was ihn vom OPC, bei

welchem die C-S-H-Bildung über Wochen, Monate oder sogar Jahre erfolgen kann, grundlegend unterscheidet [11].

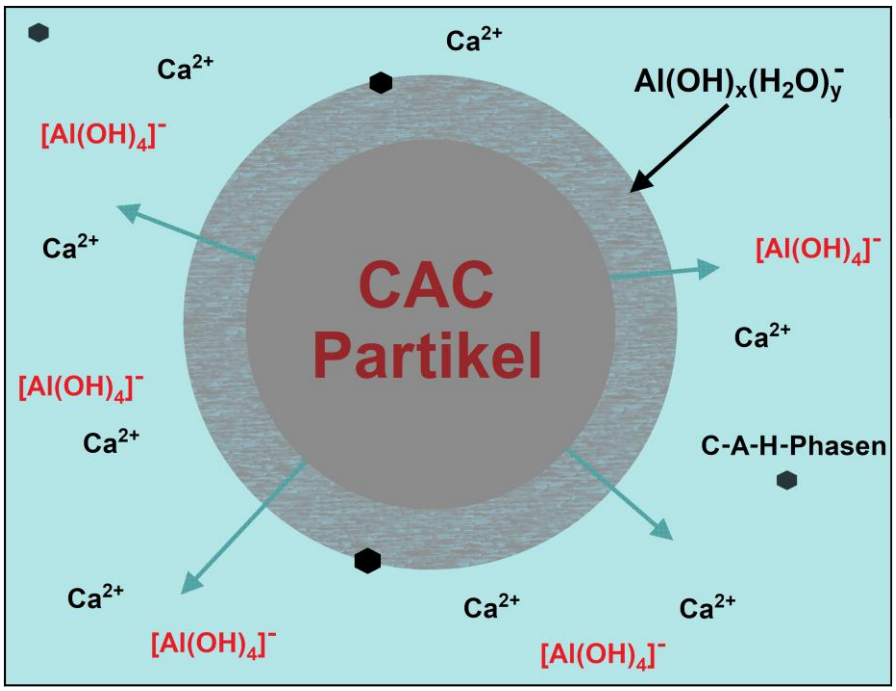

Abbildung 4: Darstellung eines angelösten Klinkerkorns mit hydroxylierter Schicht nach initialem Kontakt mit Wasser, angelehnt an [47].

Im Gegensatz zu OPC ist für Calciumaluminatzemente ein charakteristisches temperaturabhängiges Hydratationsverhalten zu beobachten [2,6,45]. Hierbei reagieren $C_{12}A_7$, CA und CA_2 entweder zu CAH_{10}, C_2AH_8 oder C_3AH_6, wobei bei Raumtemperatur ausschließlich C_3AH_6 eine thermodynamisch stabile Phase darstellt (siehe **Abbildung 5**), während CAH_{10} und C_2AH_8 unter diesen Bedingungen metastabil sind [40,43].

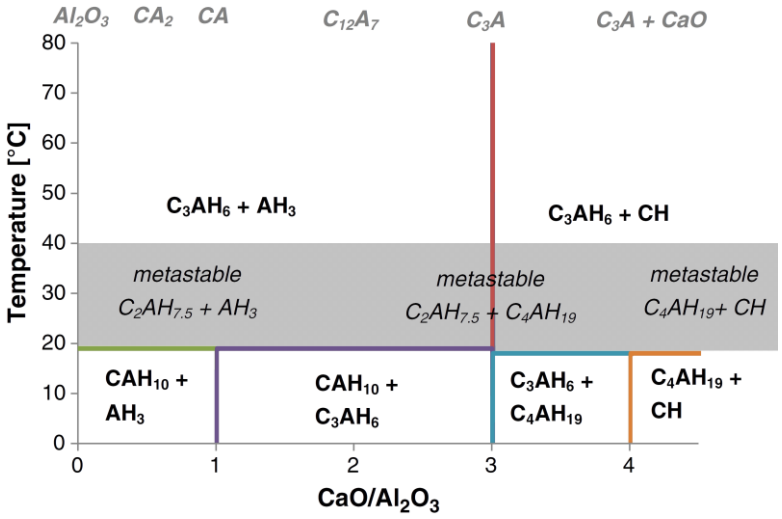

Abbildung 5: Stabile Hydratphasen im System $CaO/Al_2O_3/H_2O$ in Abhängigkeit der Temperatur, abgedruckt in bearbeiteter Form mit Genehmigung aus [43].

Die Bildung dieser Phasen erfolgt bevorzugt in den angegebenen Temperaturbereichen, entsprechend den nachfolgenden Reaktionsgleichungen, wie sie in **Tabelle 2** aufgeführt sind [6,12,36,40].

Tabelle 2: Reaktionsgleichungen der Phasen $C_{12}A_7$, CA und CA_2 mit Wasser und Umwandlung der metastabilen Hydrate in Abhängigkeit von der Temperatur in stabile Endprodukte.

< 15 °C	$C_{12}Al_{14}O_{33} + 69\ H_2O \rightarrow 6\ CaAl_2O_4{\cdot}10H_2O + 2\ Al(OH)_3 + 6\ Ca(OH)_2$
	$CaAl_2O_4 + 10\ H_2O \rightarrow CaAl_2O_4{\cdot}10H_2O\ (= CAH_{10})$
	$CaAl_4O_7 + 13\ H_2O \rightarrow CaAl_2O_4{\cdot}10H_2O + 2\ Al(OH)_3$
15 - 25 °C	$C_{12}Al_{14}O_{33} + 51\ H_2O \rightarrow 6\ Ca_2Al_2O_5{\cdot}8H_2O\ (= C_2AH_8) + 2\ Al(OH)_3$
	$2\ CaAl_2O_4 + 11\ H_2O \rightarrow Ca_2Al_2O_5{\cdot}8H_2O + 2\ Al(OH)_3$
	$2\ CaAl_4O_7 + 17\ H_2O \rightarrow Ca_2Al_2O_5{\cdot}8H_2O + 6\ Al(OH)_3$
	$2\ CaAl_2O_4{\cdot}10H_2O \rightarrow Ca_2Al_2O_5{\cdot}8H_2O + 2\ Al(OH)_3 + 9\ H_2O$
> 25 °C	$C_{12}Al_{14}O_{33} + 33\ H_2O \rightarrow 4\ Ca_3Al_2O_6{\cdot}6H_2O\ (= C_3AH_6) + 6\ Al(OH)_3$
	$3\ CaAl_2O_4 + 12\ H_2O \rightarrow Ca_3Al_2O_6{\cdot}6H_2O + 4\ Al(OH)_3$
	$3\ CaAl_4O_7 + 21\ H_2O \rightarrow Ca_3Al_2O_6{\cdot}6H_2O + 10\ Al(OH)_3$
	$3\ CaAl_2O_4{\cdot}10H_2O \rightarrow Ca_3Al_2O_6{\cdot}6H_2O + 4\ Al(OH)_3 + 18\ H_2O$
	$3\ Ca_2Al_2O_5{\cdot}8H_2O \rightarrow 2\ Ca_3Al_2O_6{\cdot}6H_2O + 2\ Al(OH)_3 + 9\ H_2O$

Die Bildung der unterschiedlichen C-A-H-Phasen CAH_{10}, C_2AH_8 und C_3AH_6 ist aufgrund ihrer unterschiedlichen Löslichkeit und der thermodynamischen Stabilität temperaturabhängig, wodurch die Zeit für das Abbinden und Erhärten des Zements ein charakteristisches temperaturabhängiges Profil zeigt. Dieses ist in **Abbildung 6** dargestellt und weist zwischen 25 – 30 °C ein Maximum auf, bei welchem aufgrund einer ungünstigen Thermodynamik die Kristallisation der Hydratphase C_2AH_8 behindert ist und hierdurch das Abbinden deutlich verzögert stattfindet [2,6,12,40,43,45,54–58].

Ebenso ist die nachfolgende Konversion der metastabilen Phasen CAH_{10} und C_2AH_8 zum Katoit abhängig von der Temperatur und kann aufgrund der Kinetik bei der jeweiligen Umgebungstemperatur über einen Zeitraum von Jahren stattfinden [2,6,11,59,60]. Parallel kommt es zu einem Verlust an Endfestigkeit durch die Umwandlung der hexagonalen, plättchenförmigen Hydrate CAH_{10} und C_2AH_8 in das dichtere kubische C_3AH_6 unter Freisetzung von AH_3 und H_2O im Zementsteingefüge, was die Porosität erhöht und die Festigkeit reduziert [3,6,11,12]. Die Morphologie der Hydratphasen ist zur Verdeutlichung in **Abbildung 7** rasterelektronenmikroskopisch dargestellt.

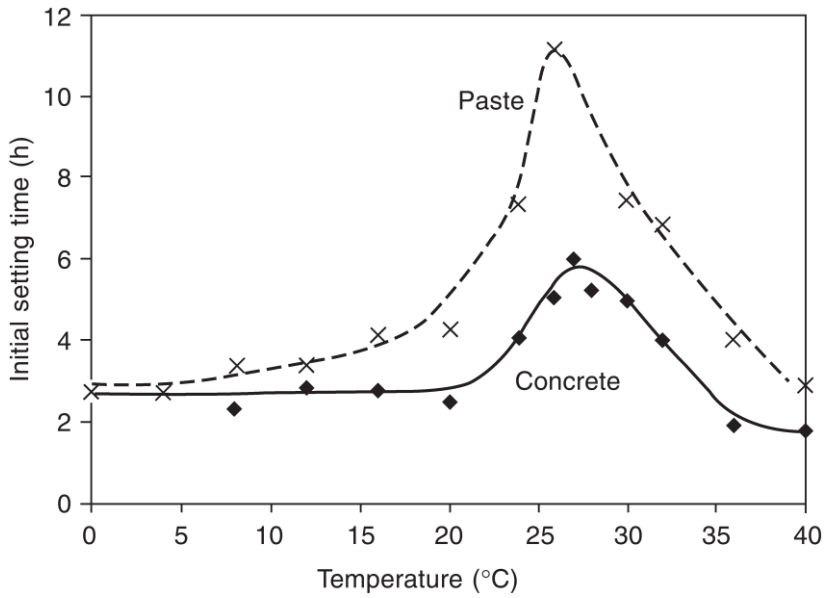

Abbildung 6: Temperaturabhängiges Abbindeverhalten eines Zementleims bzw. eines Betons mit Calciumaluminatzement als Bindemittel, abgedruckt mit Genehmigung aus [11].

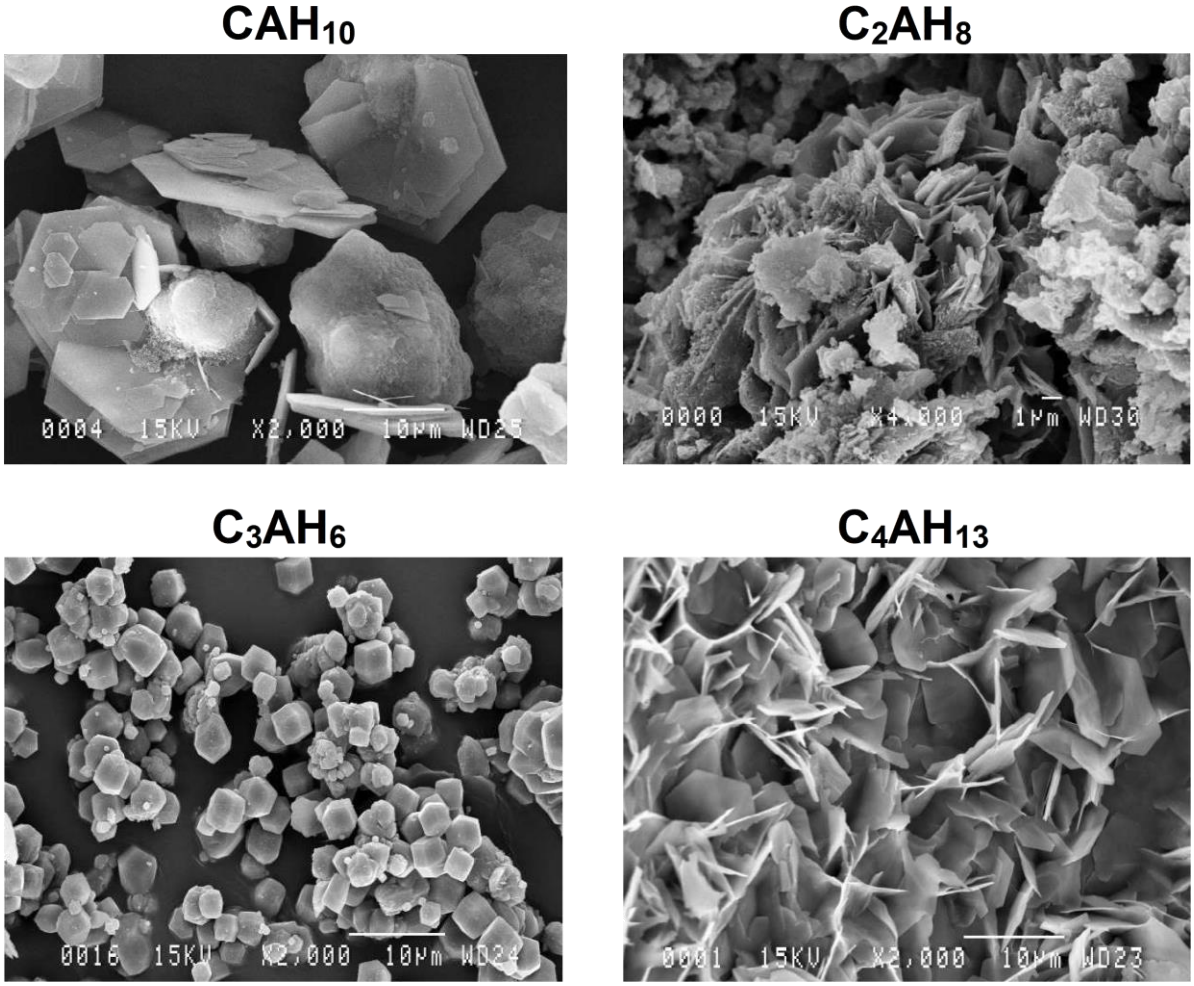

Abbildung 7: Rasterelektronenmikroskopische Aufnahmen der C-A-H-Phasen, abgedruckt in veränderter Form mit Genehmigung aus [37].

Bei den C-A-H-Phasen unterscheidet sich, wie aus **Abbildung 8** ersichtlich, der strukturelle Aufbau grundsätzlich. Während es sich bei CAH_{10} und C_3AH_6 um ein dreidimensional verknüpftes Gerüst aus Oktaedern / Polyedern (CAH_{10}) sowie Oktaedern / Dodekaedern (C_3AH_6) handelt, liegt bei C_2AH_8 eine Schichtverbindung vor [61–65]. Diese besitzt eine Hauptschicht aus AlO_6-Oktaedern und eine Zwischenschicht aus Wasser und $[Al(OH)_4]^-$-Tetraedern, wobei ein Entzug von Wasser unter Verringerung der Zwischenschichtdicke möglich ist [61,66]. Basierend auf dieser Schichtstruktur, welche auch als „layered double hydroxide“ (bzw. kurz LDH) bekannt ist, sind weitere Hydratphasen möglich. Hierzu zählt C_4AH_x, in dessen Zwischenschicht Hydroxid-Anionen sitzen, und Mono- bzw. Hemicarbonat, welches Carbonat-Anionen eingelagert hat. Diese sind unter bestimmten Umständen auch bei der Hydratation von CAC zu beobachten [12,67–69]. Ebenfalls kann es zu einer unvorteilhaften Einlagerung von Polymeren in diese Zwischenschicht kommen. Dieses Phänomen ist beispielsweise für PCE-Fließmittel bekannt und reduziert deren verflüssigende Wirkung [69–72].

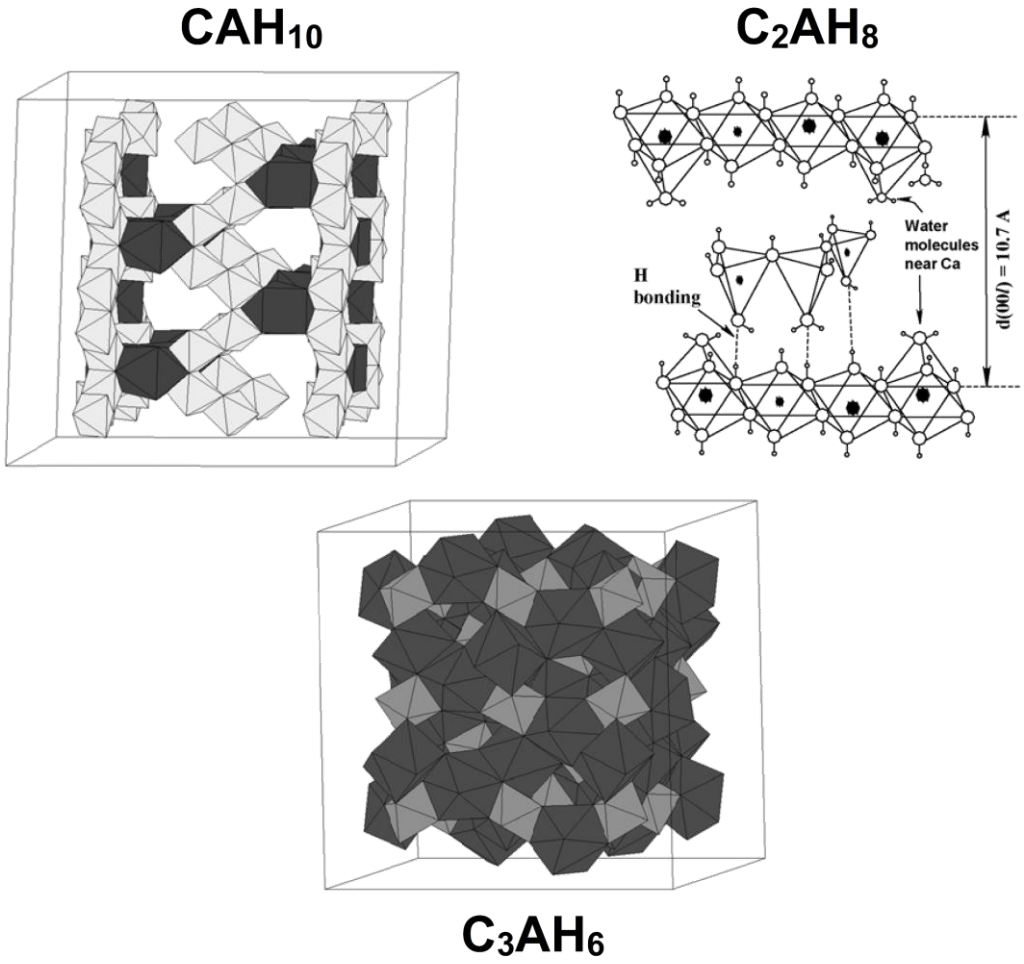

Abbildung 8: Struktur der Hydratphasen CAH_{10}, C_2AH_8 und C_3AH_6, abgedruckt in bearbeiteter Form mit Genehmigung aus [36,61].

2.1.3 Beschleunigung durch Lithium-Kationen

Um die Erstarrungszeit von Calciumaluminatzement zu kontrollieren, werden Verzögerer und Beschleuniger eingesetzt, welche die Dauer der dormanten Phasen bzw. den Beginn der Akzelerationsperiode beeinflussen. Dies ist exemplarisch in **Abbildung 9** für verschiedene anorganische (NaF, Li_2CO_3, NaOH und $Ca(OH)_2$) und organische (Apfelsäure und Cyclodextrin) Verbindungen dargestellt. Bereits literaturbekannt ist der verzögernde Effekt von organischen Verbindungen mit Hydroxyl- und/oder Carboxylat-Gruppen, welche u.a. Calcium-Ionen in der Porenlösung komplexieren bzw. präzipitieren [6,12,30,31,36,73–75]. Einen beschleunigenden Effekt zeigen neben Calcium- und Alkalihydroxiden insbesondere Lithiumsalze. Diese wirken bereits bei sehr geringen Dosierungen und werden in kommerziellen Produkten häufig eingesetzt [36,46,52,75–77]. Einen mit Lithium vergleichbaren spezifischen Kationen-Effekt zeigt kein anderes Alkali- bzw. Erdalkalisalz. Lediglich von Chrom-(III)-Salzen ist noch ein stark beschleunigender Effekt bekannt [78], der aber aufgrund der Toxizität von Chrom nicht weiter verfolgt wurde.

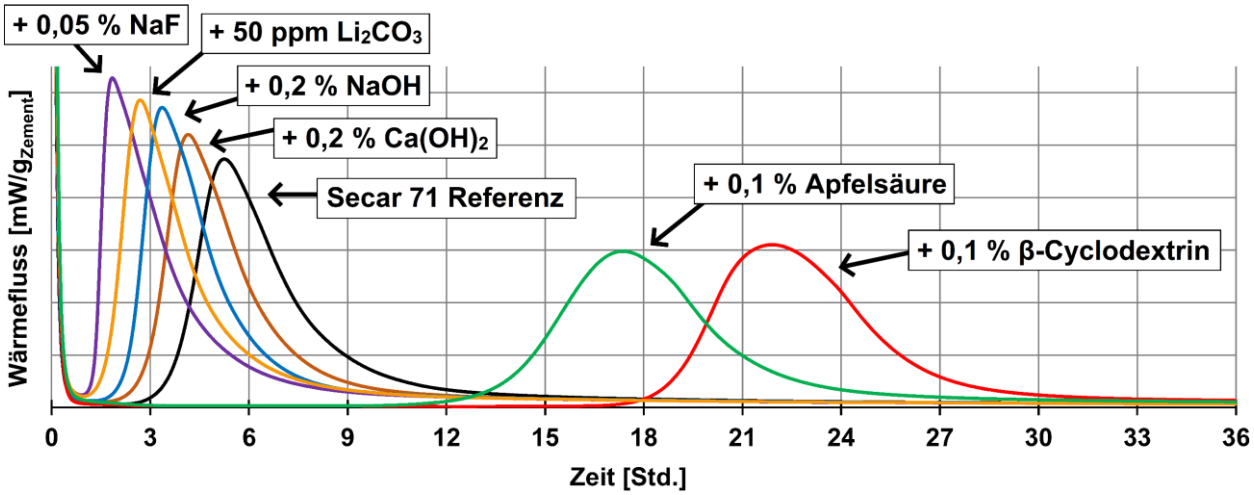

Abbildung 9: Einfluss verschiedener Zusatzmittel auf das Abbindeverhalten von CAC-Mörtel (*Secar 71*, w/z = 0,55), bestimmt mittels Wärmeflusskalorimetrie. Alle Dosierungen in Gew.% bezogen auf die Zementmasse.

Die Wirkung von Lithium-Salzen wurde bereits 1984 von *Rodger* und *Double* [79], *Matusinović* [76,80,81] und auch *Damidot* [51,82] betrachtet. Später hat *Götz-Neunhoeffer* [47,48,67,83] diese auf eine komplexe Wechselwirkung mit den CAC-Klinkerphasen und der Kristallisation zurückgeführt. Der Effekt des Lithiums basiert demnach auf dem Zusammenspiel multipler Wirkmechanismen [47,48]: (1) Durch eine erhöhte Permeabilität der Aluminium-Hydroxo-Hydrat-Schicht, welche das Zementkorn

im Zementleim passiviert, wird die Löslichkeit von Calciumaluminat (CA) verbessert. (2) Durch anschließende Nukleation des $[LiAl_2(OH)_6]^{+}{}_2\,[(OH)_2 \cdot x\,H_2O]^{2-}$ LDHs in Form einer metastabilen Zwischenphase als „Seeding“ Material. Die Struktur der Li-Al-LDH-Verbindung ist nicht isotypisch mit der des Hydratationsprodukts C_2AH_8, beide enthalten aber $[Al(OH)_6]^{3-}$ Einheiten, welche die Nukleation von C_2AH_8 ($[Ca_2Al(OH)_6]^{+}$ $[Al(OH)_4 \cdot x\,H_2O]^{-}$) begünstigen. (3) Die hierdurch verringerte Aluminium-Konzentration in der Porenlösung verschiebt das Calcium-zu-Aluminium-Verhältnis, wodurch die Bildung der Calcium-reichen C_2AH_8-Phase bevorzugt wird. (4) Durch die Abgabe von Aluminat wird das Li-Al-LDH zersetzt, wodurch die Lithium-Ionen kontinuierlich rezykliert werden, d.h. sie wirken nur katalytisch auf die Hydratation und werden dabei nicht verbraucht, sondern können zahlreiche Zyklen (Bildung von LiAl-LDH und anschließende Zersetzung) durchlaufen. (5) Hierdurch wird die Aluminium-Konzentration in der Lösung niedrig gehalten und folglich das weitere Auflösen des Aluminats gefördert. Dieser in **Abbildung 10** visualisierte Wirkmechanismus erklärt, warum ein Li-Salz bereits in geringer Konzentration sehr effektiv beschleunigt.

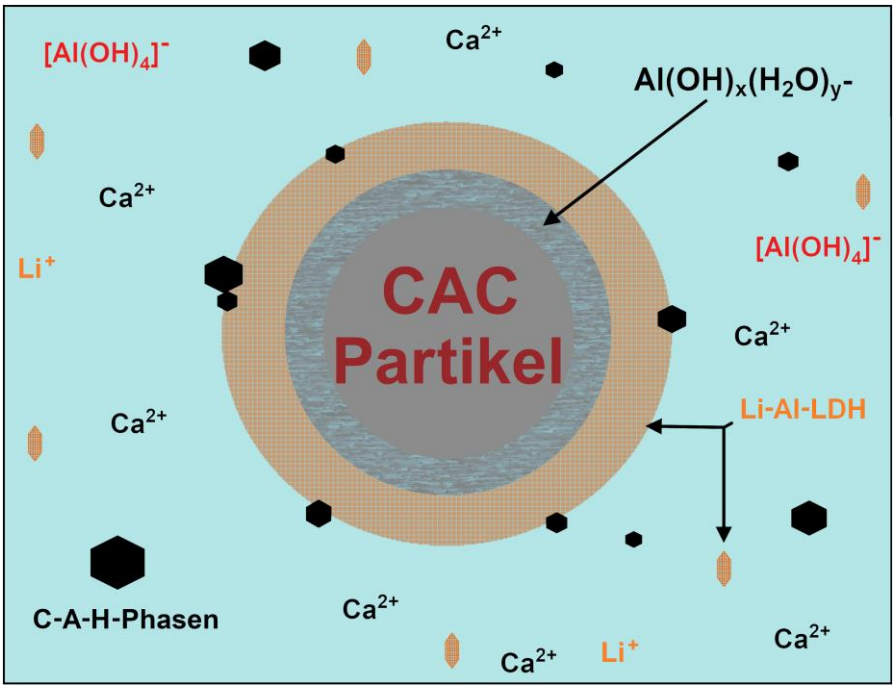

Abbildung 10: Darstellung eines hydratisierenden Klinkerkorns in Gegenwart von Lithium-Kationen, angelehnt an [47].

Eine alternative Theorie zum Wirkmechanismus, wurde von *Damidot* entwickelt. Sie besagt, dass die Nukleation von AH_3 durch Lithium beschleunigt wird [51,82,84]. Untersuchungen hierzu zeigen, dass das Li^+-Kation die Polymerisation der Aluminat-Anionen, die aufgrund elektrostatischer Abstoßung an sich erschwert ist, begünstigt.

Hierdurch werden Hydroxid-Ionen freigesetzt, wodurch die weitere Auflösung der Klinkerphasen und die Bildung der Hydratphasen begünstigt wird [85–87].

Es gilt jedoch anzumerken, dass weder das Modell nach *Götz-Neunhöffer* noch das Modell nach *Damidot* eindeutig belegt sind.

2.2 Biopolymere

Im Rahmen dieser Untersuchung wurde eine Vielzahl von verdickend wirkenden Polymeren bezüglich ihrer Wirkung auf die Hydratation von CAC geprüft. So ist beispielsweise für Celluloseether bekannt, dass diese sowohl OPC als auch CAC verzögern, wobei die Derivatisierung des Celluloseethers von entscheidender Bedeutung für dessen verzögernde Eigenschaft ist [2,88–93].

Drei natürliche Biopolymere stachen hier durch einen stark beschleunigenden Effekt auf CAC heraus und sollen nun im Folgenden näher beschrieben werden. Dabei handelt es sich um die Polysaccharide Alginat, Carrageen und Pektin, deren Strukturen in **Abbildung 11** dargestellt sind. Ein ausführlicherer Vergleich verschiedener Biopolymere (natürlichen, halbsynthetischen und mikrobiellen Ursprungs) findet sich in der angehängten **Publikation 2**.

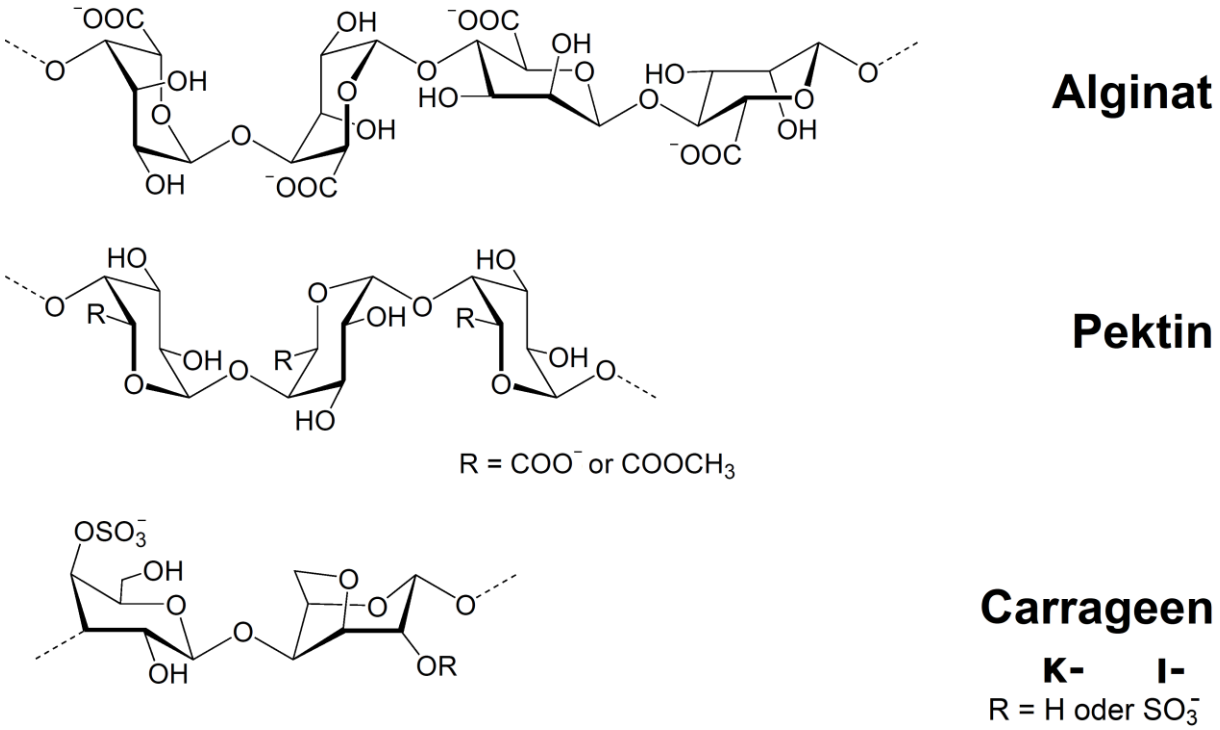

Abbildung 11: Molekulare Strukturen von Alginat, Pektin und Carrageen.

2.2.1 Alginat

Als Alginate werden lineare Copolymere zweier spezifischer Uronsäuren bezeichnet, welche in den Zellwänden von Braunalgen (*Phaeophyceae*) strukturgebend vorliegen. Diese werden durch Extraktion gewonnen und bestehen aus α-1→4 und β-1→4 glykosidisch verknüpfter α-L-Mannuronsäure (M) und β-D-Guluronsäure (G). Je nach Art der Verknüpfung der beiden Monomere (G-G-G oder M-M-M oder M-G-M) kommt es, wie in **Abbildung 12** illustriert, zu unterschiedlichen sterischen Anordnungen sowie zur Bildung von homopolymeren Blöcken. Diese sind für den Mechanismus der ionotropen Gelierung von essentieller Bedeutung und beeinflussen die Viskosität, Wechselwirkung mit Kationen sowie die Eigenschaften des Gels [33–35,90,94–100].

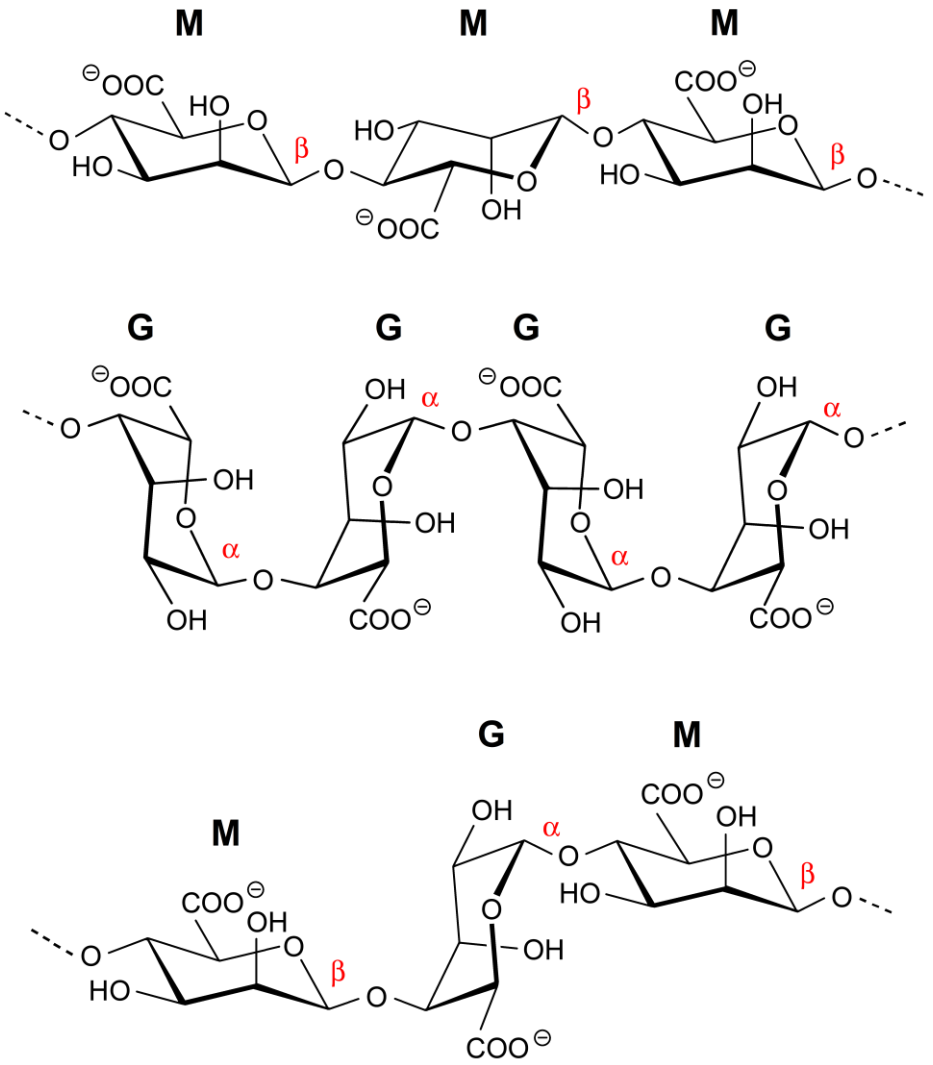

Abbildung 12: Unterschiedliche sterische Anordnung von α- bzw. β-verknüpften Einheiten von Mannuron- und Guluronsäure, adaptiert aus [100].

Bedingt durch die Biosynthese in unterschiedlichen Algengattungen und -spezies sowie deren Wachstumsbedingungen handelt es sich bei Alginaten in der chemischen

Zusammensetzung (M/G-Verhältnis, Blockstruktur und Molmasse) um ein heterogenes Naturprodukt. Kommerzielle Alginat-Produkte werden zumeist aus u.a. *Laminaria hyberborea, Laminaria digitata, Macrocystis pyrifera* oder *Lessonia nigrescens* gewonnen, wobei anzumerken ist, dass weltweit circa 2000 Braunalgen-Spezies existieren. Das erhaltene Alginat weist nach Extraktion und gegebenenfalls Depolymerisation eine durchschnittliche molare Masse von 10.000 – 600.000 Dalton auf, was einem Polymerisationsgrad von circa 50 – 3000 entspricht [33–35,90,94–101].
Die protonierte Alginsäure ist in Wasser nahezu unlöslich und wird erst durch Überführung in das deprotonierte Pendant löslich, wobei die Carboxylatgruppen dieses Polymers mit Kationen wie beispielsweise Na^+, K^+ oder NH_4^+ als Gegenion ein Salz ausbilden. Natriumalginat ist wasserlöslich und bildet ein viskoses Hydrokolloid, das durch Zugabe divalenter Kationen wie Ca^{2+}, Ba^{2+} und Kationen diverser Übergangsmetalle ein Gel ausbildet (siehe **Abbildung 13**) [94,95,98,102–108].

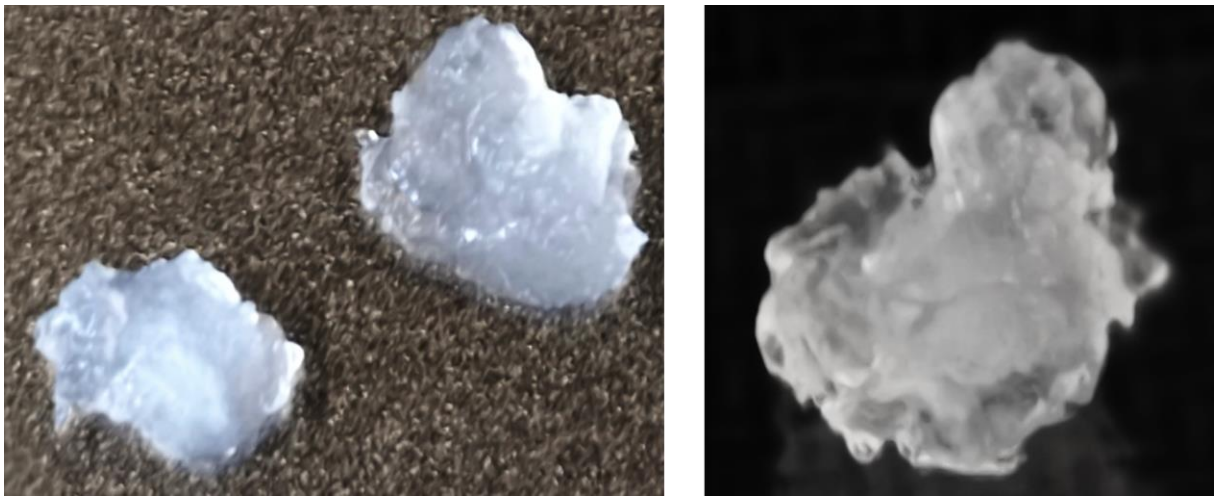

Abbildung 13: Aussehen eines selbst hergestellten Calcium-Alginat-Hydrogels.

Bei diesem Hydrogel handelt es sich um ein dreidimensional verknüpftes Polymernetzwerk mit Wassereinschluss, welches im vorliegenden Fall durch ionische Bindung verknüpft („cross-linked“) ist. Dies erfolgt für Alginat nach einem Mechanismus, der durch das sogenannte „Egg-Box“ Modell (dt. Eierschachtel-Modell), ursprünglich postuliert von *Grant et al.* [109], beschrieben wird. Bei diesem wird, wie in **Abbildung 14** illustriert, durch die Wechselwirkung der Carboxylatgruppe mit den Ca^{2+}-Ionen erst ein Monokomplex gebildet, der sich im nächsten Schritt zu Dimeren und Multimeren zusammenlagert. Dieser Komplex aus Ca^{2+}-Kationen inmitten zweier Alginat-Stränge, welche die Form einer Zick-Zack-Kette einnehmen, erinnert an die charakteristische Form eines Eierkartons, in welchem das Calcium-Kation analog zu einem Ei eingelagert

ist. Dabei kann das Ca^{2+}-Ion sowohl durch die Komplexierung mit den Carboxylat-Gruppen als auch mit den Hydroxyl-Gruppen oder dem endocyclischen Sauerstoff-Atom stabilisiert werden. Dies ist in **Abbildung 15** schematisch dargestellt. Durch quantenchemische Berechnungen ist jedoch lediglich die Bindung zwischen Carboxylatgruppen und Ca^{2+} eindeutig validiert worden, wohingegen die Beteiligung der weiteren funktionellen Gruppen an der Komplexierung des Calciums nicht abschließend geklärt ist [95,98,99,109–119].

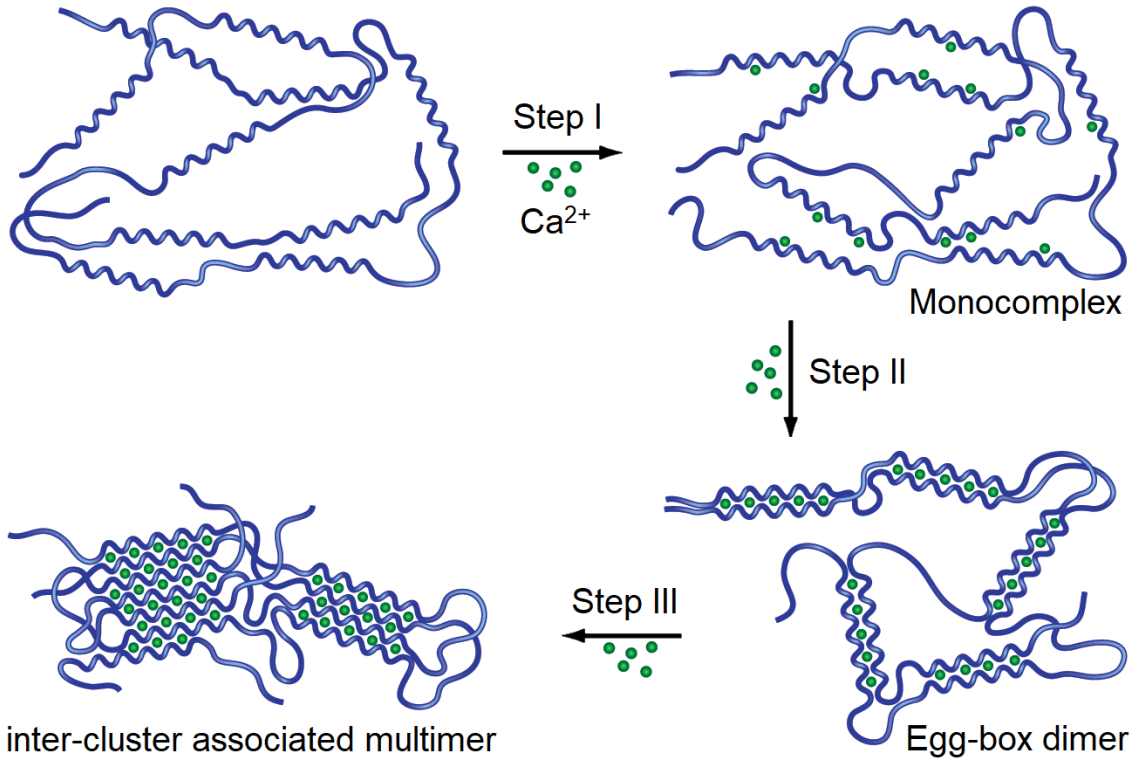

Abbildung 14: Ausbildung eines Calcium-Alginat-Hydrogels nach dem „Egg-Box“ Modell, abgedruckt in veränderter Form mit Genehmigung aus [95].

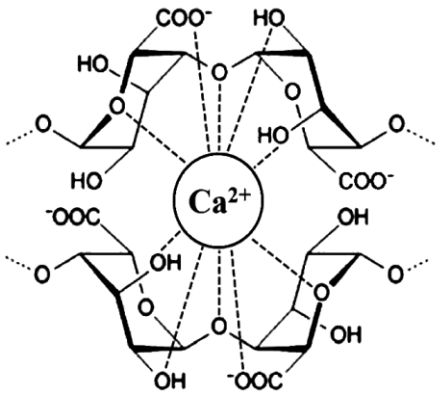

Abbildung 15: Mögliche Komplexierung von Calcium-Ionen durch die funktionellen Gruppen des Alginat-Moleküls, angelehnt an [34,120].

2.2.2 Pektin

Pektine liegen in den Zellwänden verschiedener Pflanzenarten (u.a. die Gattungen *Citrus* und *Malus*) vor, in denen sie eine festigkeitsgebende und wasserbindende Funktion erfüllen. Dieses lineare Homopolymer der D-Galakturonsäure weist eine durchschnittliche molare Masse von 50.000 – 900.000 Dalton auf und seine Carboxylatgruppen sind zu einem gewissen Anteil methoxyliert. Bei der Galacturonsäure handelt es sich wie bei der Mannuron- bzw. Guluronsäure des Alginats ebenfalls um eine Uronsäure. Dieses 1→4 verknüpfte Polymer wird durch den Einbau von Rhamnose, die mit oligomeren Seitenketten neutraler Zucker verknüpft ist, unterbrochen. Industriell wird nach der Extraktion das Polymers mit Säure behandelt, um den Veresterungsgrad zu reduzieren, wobei ebenfalls säurelabile Seitenketten austreten. Das erhaltene Produkt wird abhängig vom Veresterungsgrad als hoch- bzw. niederverestertes Pektin bezeichnet, wobei niedrigmethylierte Derivate einen Veresterungsgrad von 20 – 45 % und hochmethylierte von 55 – 75 % aufweisen [33–35,90,95,121].

Hierbei zeigen nur niederveresterte Pektine, aufgrund der freien Carboxylatgruppen, eine Wechselwirkung mit Kationen wie Ca^{2+}, durch die eine Vergelung induziert wird. Diese Gelbildung verläuft nach einem vergleichbaren Mechanismus, wie er bereits für das Alginat mittels des „Egg-Box“ Modells beschrieben wurde. Diese Parallelität ist auf die Molekülstruktur des Pektins zurückzuführen, welche spiegelsymmetrisch zu der des Alginates ist. Da die Struktur des Pektins jedoch nur eine geringere Interaktion mit den Kationen erlaubt, ist diese Vergelung schwächer ausgeprägt als beim Alginat [95,111,118,119,121–127].

2.2.3 Carrageen

Von den Alginaten und Pektinen, die strukturell eng verwandt sind, unterscheidet sich Carrageen deutlich in seiner Molekülstruktur. Dieses Copolymer aus α-1→4 und β-1→3 glykosidisch verknüpfter Galaktose und 2,6-Anhydrogalaktose ist partiell sulfatiert. Man unterscheidet zwischen κ-, ι- und λ-Carrageen, welche sich in ihrem Grad der Sulfatierung und im Falle der λ-Form auch in der Molekülstruktur unterscheiden. In kommerziellen Produkten liegt die durchschnittliche molare Masse bei 200.000 – 800.000 Dalton [33–35,90,94].

Lediglich κ- und ι-Carrageen bilden in Gegenwart von Kationen (mono- oder divalent) ein Gel aus. Der Mechanismus dieser Vergelung verläuft, wie in **Abbildung 16** gezeigt, deutlich unterschiedlich verglichen zu Alginat und Pektin. Diese benötigen zur

Agglomeration der Molekülketten divalente Kationen. Carrageen hingegen bildet bereits in Abwesenheit gelbildender Kationen ein helikales Dimer aus und wird durch die Zugabe von Kationen zur weiteren Aggregierung / Zusammenlagerung der bereits bestehenden Doppelhelices bewegt. Dabei wird durch Kationen (wie Ca^{2+}) eine Verbrückung zwischen den Sulfat-Gruppen zweier Helices aufgebaut, wodurch eine Annäherung dieser zueinander ermöglicht wird [90,94,95,128–136].

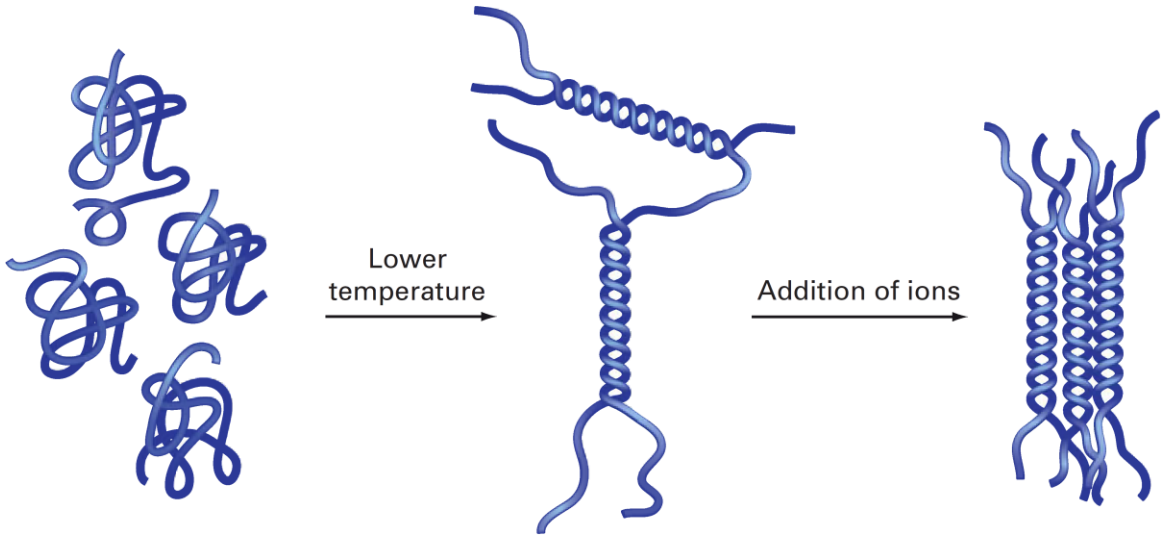

Abbildung 16: Ausbildung eines Carrageen Hydrogels durch Zugabe von Kationen, abgedruckt in bearbeiteter Form mit Genehmigung aus [95].

2.2.4 Verdickende Wirkung von Polymeren in Zement

Natürliche sowie synthetische Makromoleküle werden Mörteln und Beton zugesetzt, um deren Rheologie zu modifizieren und Wasserrückhaltevermögen zu erzielen. Dies reduziert autogenes Schwinden und stabilisiert die Suspension, indem Sedimentation bzw. Entmischen unterbunden wird. Zu diesem Zweck werden beispielsweise Celluloseether, Stärke(ether), Diutan Gum, Guar Gum, Welan Gum, Xanthan Gum oder Polyacrylamide zugegeben, deren prinzipieller Wirkmechanismus in **Abbildung 17** schematisch illustriert ist [90,92,137–141].

Hierbei bilden Wassermoleküle mit dem Polymer durch Adsorption und Bindung über Wasserstoffbrücken ein Hydrokolloid aus, das in einem ersten Schritt die Viskosität der wässrigen Lösung erhöht. Im Folgenden tritt durch Wechselwirkungen der Polymerketten untereinander eine schwache Gel-Bildung auf, welche allerdings bei ionischen Polymeren wie beispielsweise Alginat durch das ‚Cross-Linking' mit Calcium-Kationen zu einer ausgeprägten Gelierung führt. In einem weiteren Schritt kann es durch Adsorption

des Polymers auf der Partikeloberfläche zu einer Verbrückung zwischen den Partikeln kommen, womit eine weitere Steigerung der Viskosität einhergeht [139,141–145].

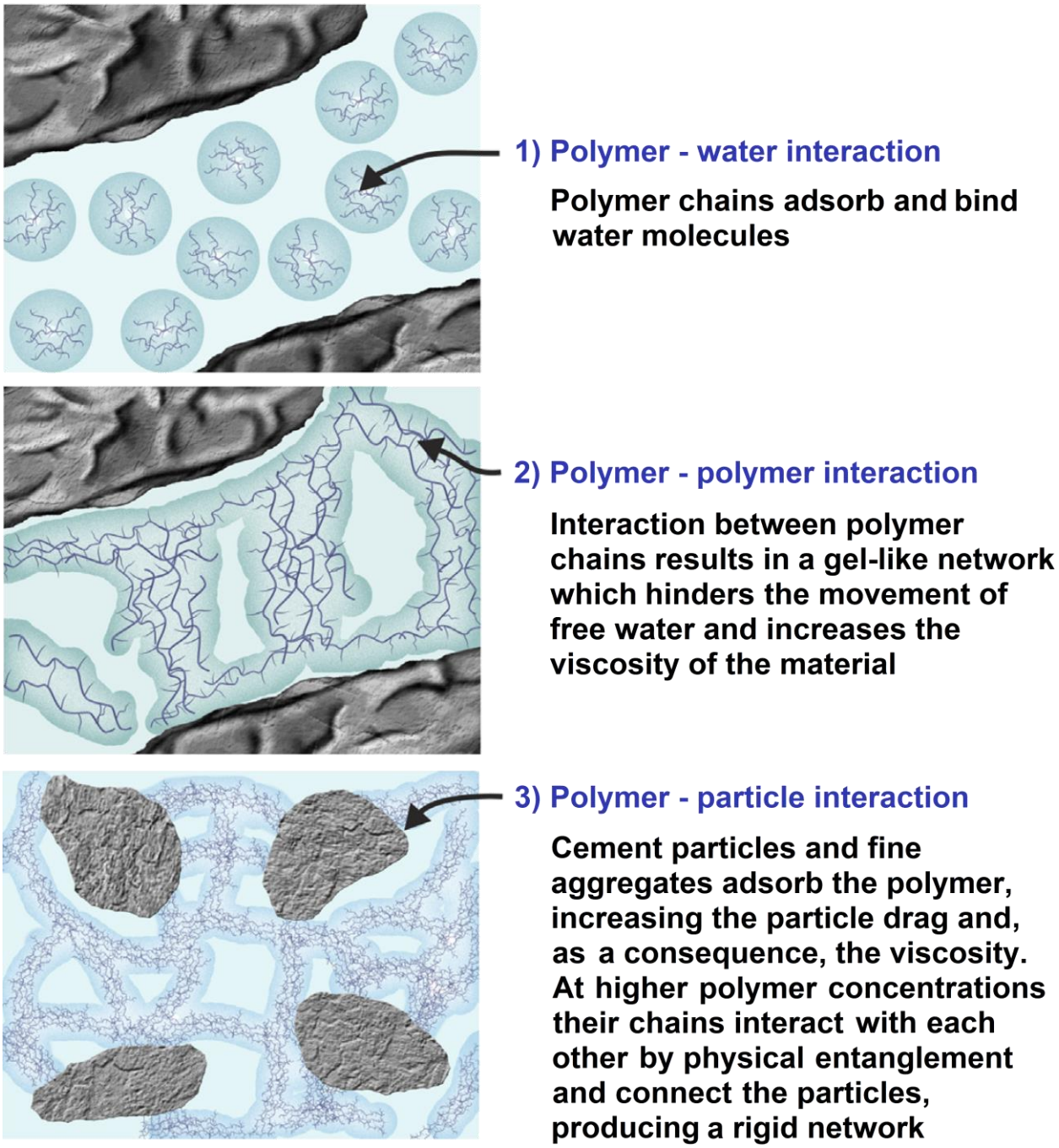

Abbildung 17: Wirkprinzip von verdickenden Polymeren auf einen Zementleim, abgedruckt in veränderter Form mit Genehmigung aus [142].

Die adsorptive Wechselwirkung verdickender Polymere mit der Zementpartikeloberfläche ist jedoch noch nicht abschließend geklärt. Für nicht-ionische Celluloseether konnte jedoch gezeigt werden, dass es zu keiner nennenswerten Adsorption an den Zementpartikeln kommt [146].

2.3 Charakterisierung bauchemischer Materialien

Der Einfluss von Zusatzmitteln auf das Reaktionsverhalten von Zement wurde mittels Wärmeflusskalorimetrie und Bestimmung der mechanischen Mörtelfestigkeiten betrachtet. Die resultierenden Reaktionsprodukte wurden mittels Röntgendiffraktometrie charakterisiert.

2.3.1 Isotherme Wärmeflusskalorimetrie

Durch isotherme (= konstant gehaltene Temperatur) Kalorimetrie bei einer definierten Temperatur wird über eine Zeitspanne der durch eine Reaktion freigesetzte oder aufgenommene Wärmefluss einer Probe aufgezeichnet. Hierbei kann eine Reaktion auf ihre thermodynamischen und kinetischen Eigenschaften reproduzierbar untersucht werden [147].

Für Zemente wie OPC und CAC, aber auch Sulfatbinder und Bindemittelmischungen, werden mittels Kalorimetrie der Wärmefluss der exothermen Abbindereaktion ermittelt, um sowohl den qualitativen Verlauf, also das Linienprofil, als auch die quantitative Wärmefreisetzung zu bestimmen [46,148–150]. Dies erlaubt einen schnellen und i.d.R. aussagekräftigen Rückschluss bezüglich der Wirkung eines Zusatzmittels auf die Hydratation des Bindemittels. So kann durch eine verspätete oder gestreckte Wärmefreisetzung eine verzögernde Wirkung oder durch eine vorzeitige bzw. schnellere Wärmeentwicklung ein beschleunigender Effekt festgestellt werden. Dies ist exemplarisch in der vorher gezeigten **Abbildung 9** für Verzögerer und Beschleuniger dargestellt.

Das verwendete Instrument der Firma *TA Instruments* (früher *Thermometric*) erlaubt die parallele Messung anhand von acht Probenkanälen, welche über je einen separaten Referenzkanal verfügen. Hierfür wird eine Temperaturkonstanz der Wärmesenke mit einer Genauigkeit von ± 0,02 °C gehalten. Die von der exothermen Hydratationsreaktion abgeführte Wärme wird dabei durch einen Wärmeflusssensor mittels des Seebeck-Effekts ermittelt. Durch den Temperaturgradienten zwischen der Referenz und der Probe wird eine Spannung durch Kontakt zweier verschiedener Metalle oder Legierungen, welche eine unterschiedliche Lage in der thermoelektrischen Spannungsreihe aufweisen, aufgebaut. Die Wärme wird anschließend durch ein Peltier-Element aus dem Gerät abgeführt. Der Aufbau dieses Wärmeflusskalorimeters, in dessen Kanälen die zu untersuchenden Proben platziert werden, ist in **Abbildung 18** schematisch illustriert [148,150].

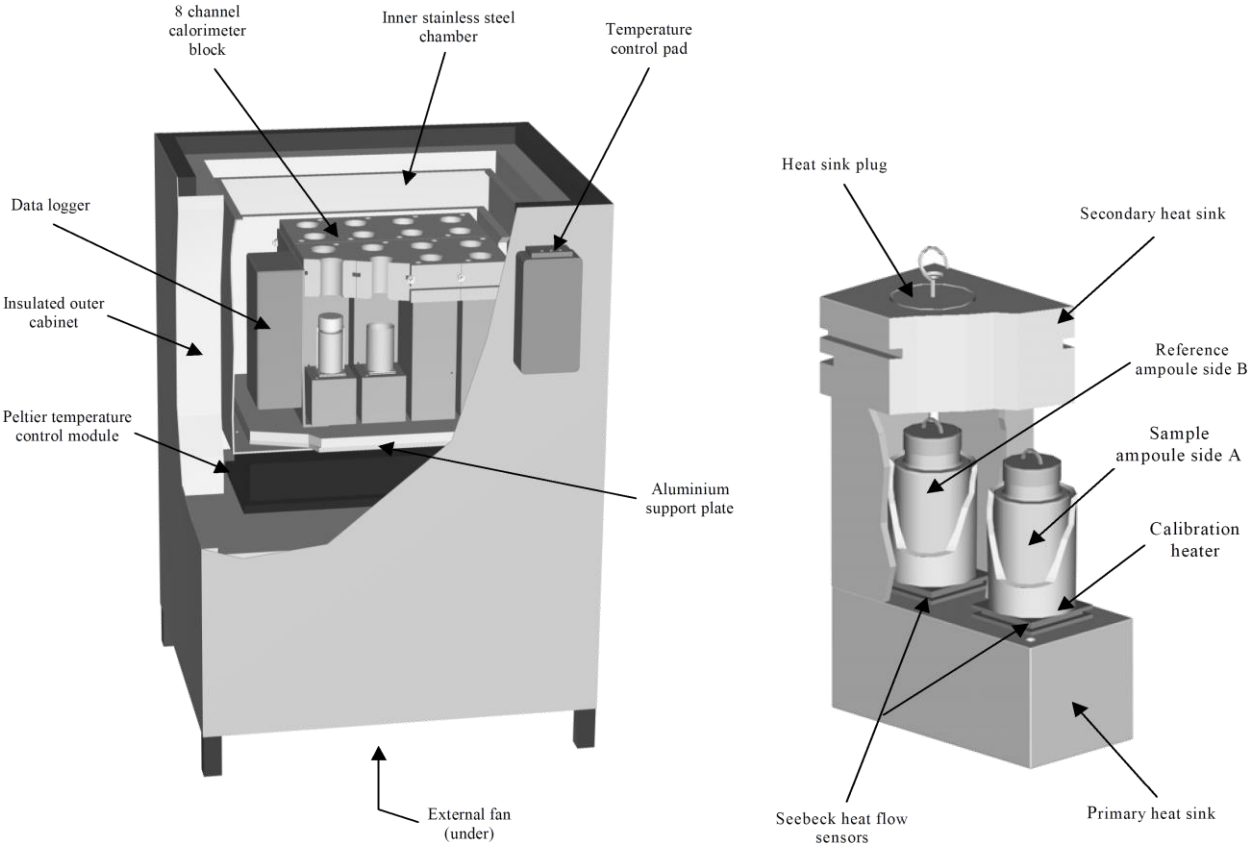

Abbildung 18: Schematischer Aufbau eines isothermen Wärmeflusskalorimeters, abgedruckt in bearbeiteter Form mit Genehmigung aus [151].

Das Anmischen der Proben erfolgt *ex-situ* mittels eines Vortex-Mischers und muss stets reproduzierbar über einen spezifischen Zeitraum durchgeführt werden. Hierbei muss sowohl auf die Mischzeit als auch auf die Durchführung zwecks Reproduzierbarkeit geachtet werden, da insbesondere Aluminatzemente eine ausgeprägte Sensibilität bzgl. des Eintrags an Mischenergie aufweisen [6]. Dieses Phänomen führt bei CAC je nach Zement bei unterschiedlichen Anmischzeiten von 30, 60, 90 oder 120 Sekunden bereits zu einer Differenz in der Abbindezeit von bis zu mehreren Stunden.

Als Probengefäße dienen Glasampullen mit 10 mL bzw. 20 mL Volumen, die mittels eines Bördel-Deckels nach Wasserzugabe verschlossen werden. Zementpasten wurden in den Ampullen mit 10 mL Volumen angemischt, während Mörtelmischungen in 20 mL Ampullen hergestellt wurden.

2.3.2 Bestimmung von Druck- und Biegezugfestigkeit

Die Wärmeflusskalorimetrie ermöglicht eine zeitlich aufgelöste Betrachtung des Hydratationsfortschritts und ist durch DIN EN 196-11 für Zementpasten genormt [150]. Komplementär hierzu muss aber die Festigkeit eines Mörtels ermittelt werden, um die

tatsächlichen Materialeigenschaften makroskopisch zu bestimmen. Insbesondere für Portlandzement ist bekannt, dass die Kalorimetrie irreführende Rückschlüsse zulässt, da beispielsweise der sogenannte „sulphate depletion peak“ trotz Wärmefreisetzung keinen wesentlichen Einfluss auf die Festigkeit ausübt. Bei dieser Reaktion im OPC kommt es lediglich zu einer Umwandlung von Ettringit zu Monosulfat, wobei keine dieser Hydratphasen festigkeitsgebend ist [152–154]. Ebenso ist von CAC und auch von OPC bekannt, dass sich die Abbindezeit einer Zementpaste von der eines Mörtels bzw. Betons unterscheidet [2,6].

Zur Bestimmung der Druck- und Biegezugfestigkeiten wurden Mörtelprismen gemäß der Norm 196-1 [155] hergestellt, indem eine gewichtete Mischung aus ¾ Normsand und ¼ Zement sowie ggfs. Zusatzmitteln, wie beispielsweise Fließmittel und Alginat, mit Wasser maschinell angemischt wurde. Die aus der Edelstahl-Form ausgeschalten erhärteten Prismen, deren Ausmaße in **Abbildung 19 (oben)** dargestellt sind, wurden in einer hydraulischen Presse, wie in **Abbildung 19 (unten)** gezeigt, abgedrückt. Hierzu wurde an den Mörtelprismen durch zentrisches Belasten im 3-Punktverfahren die Biegezugfestigkeit bestimmt und aus den jeweils resultierenden beiden Fragmenten die Druckfestigkeit ermittelt.

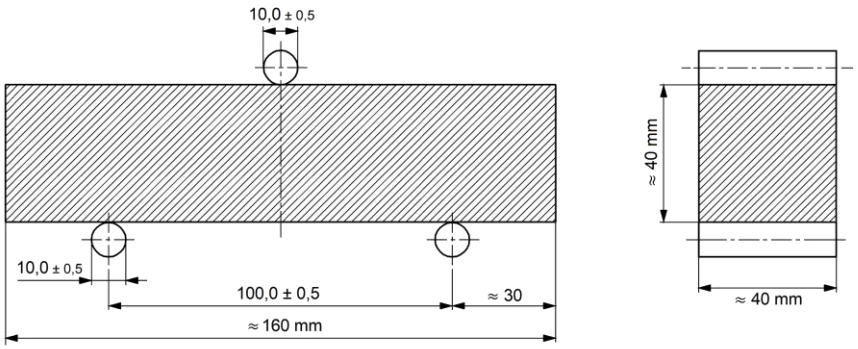

Abbildung 19: Schematischer [155] und instrumenteller Aufbau für die Bestimmung von Druck- und Biegezugfestigkeit eines Mörtels.

2.3.3 Röntgendiffraktometrie

Durch die Beugung von Röntgenstrahlung an der Elektronenhülle der jeweiligen Atome in einem Festkörper, der eine periodische Strukturanordnung aufweist, entsteht ein charakteristisches Beugungsmuster bzw. Diffraktogramm. Dieses für jede Verbindung aufgrund ihrer Kristallstruktur, Atomanordnung und Zusammensetzung charakteristische Beugungsmuster wird durch die konstruktive Interferenz der im Gitter gebeugten Wellen erhalten. Die dafür nötigen Bedingungen können anhand der *Bragg*-Gleichung, welche die konstruktive Interferenz beschreibt, hergeleitet und zur weiteren Strukturbestimmung eingesetzt werden [156,157].

$$n \cdot \lambda = 2d \cdot sin(\theta)$$

Mithilfe des in **Abbildung 20** gezeigten Diffraktometers der Firma *Bruker AXS* wird eine Probe in *Bragg-Brentano*-Geometrie vermessen. Hierzu wird der Probenhalter, welcher entweder ein Pulver oder eine mit röntgentransparenter Folie abgedeckte (Zement)Paste enthält, bestrahlt und die Intensität der gebeugten Röntgenstrahlung durch den Detektor winkelabhängig (Theta-Theta Geometrie) bestimmt [157].

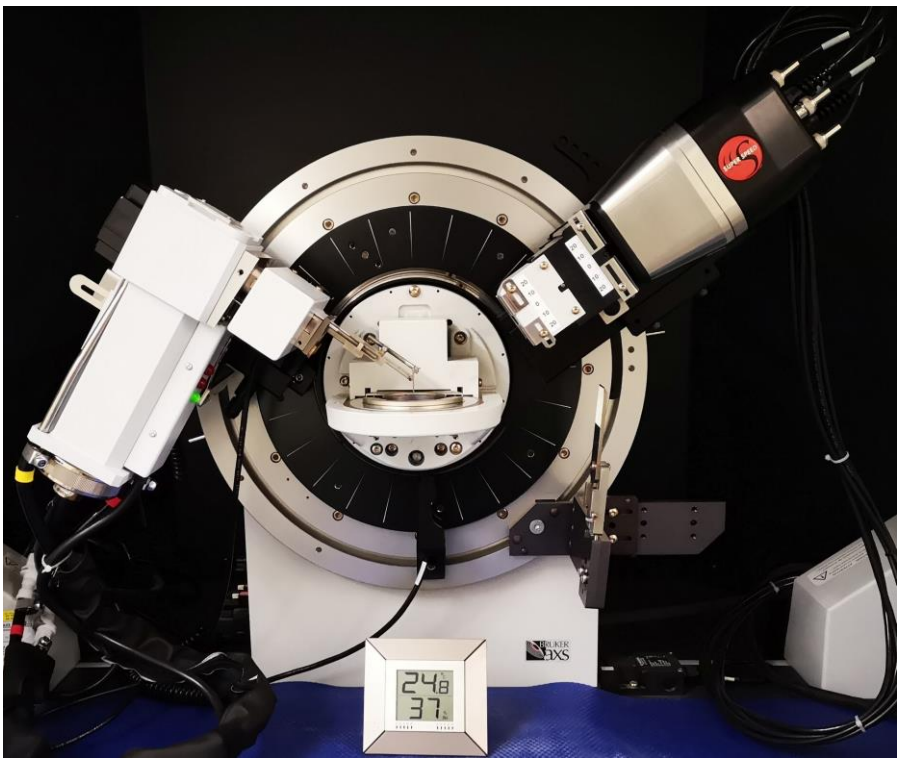

Abbildung 20: Goniometer mit Röntgenröhrenhalterung (links) und Detektor (rechts) des Röntgendiffraktometers *D8 Advance*.

Mit Hilfe der Röntgendiffraktometrie wurden die Hydratationsprodukte verschiedener CAC-Proben identifiziert und die Phasenzusammensetzung der verwendeten

Calciumaluminatzemente quantitativ bestimmt. Letzteres erfolgte unter Einsatz der *Rietveld*-Methode, die durch Abgleich und mathematische Optimierung eines theoretischen Beugungsmusters einer Verbindung mit dem gemessenen Diffraktogramm eine quantitative Analyse ermöglicht [158,159].

2.4 Analytische Methoden

2.4.1 Quantifizierung der Zementhydratation mittels MAS-NMR-Spektroskopie

Eine Quantifizierung des Hydratationsfortschritts bzw. Hydratationsgrads ist bei Aluminat-Zementen mittels Festkörper-NMR-Spektroskopie (engl. Magic-Angle-Spinning, MAS-Technik) am ^{27}Al-Kern möglich. Da es sich bei Aluminium um ein anisotopes Element (100 % ^{27}Al) handelt und der Kern eine vergleichsweise gute relative Empfindlichkeit E_r (^{1}H) aufweist, können MAS-NMR-Spektren mit kurzer Messdauer (beispielsweise 15 Minuten) aufgezeichnet werden [12,160–162].

Hierfür wurde der entsprechende CAC, teils vermengt mit Alginat, in einem Zentrifugenröhrchen oder einem Rollrandglas mit Wasser vermischt und über eine definierte Zeit bei 20 °C hydratisiert. Daraufhin wurde je nach Reaktionsfortschritt der flüssige Zementleim mit Aceton versetzt bzw. der erhärtete Zementstein in einem Achatmörser aufgemahlen. Das erhaltene Pulver wurde unmittelbar in einen Zirkonia-Rotor gefüllt und im NMR-Spektrometer (siehe **Abbildung 21**) bei 15 kHz rotiert. Die Rotation der Probe um eine Achse, die um den magischen Winkel von $(\cos \theta_m)^2 = {}^1/_3$ bzgl. der Magnetfeldrichtung verschoben ist, ermöglicht es, anisotrope Effekte des Festkörpers, die in einer Linienverbreiterung der Spektren resultieren, zu kompensieren. In der NMR-Spektroskopie von Flüssigkeiten wird durch die *Brown*‘sche Molekularbewegung die anisotrope Wechselwirkung (u.a. dipolare Kopplung und anisotrope chemische Verschiebung) gemittelt, während dies in Festkörpern aufgrund der fehlenden Mobilität der Kerne nicht möglich ist. Durch das angelegte externe Magnetfeld werden, wie es durch den *Zeeman*-Effekt beschrieben wird, die energetischen Zustände, die für die jeweilige Magnetquantenzahl quantenmechanisch entartet vorliegen, aufgespalten. Die Anregung und Relaxation dieser Übergänge in der *Larmor*-Frequenz erfolgt energetisch durch Radio- bzw. Mikrowellen (0,1 – 10 µeV) und erzeugt eine Resonanz, welche über den freien Induktionszerfall messtechnisch erfasst werden kann [12,160–166].

Durch Dekonvolution der Spektren (wie exemplarisch in den ‚Supporting Informations' von **Publikation 3** gezeigt) wurde der Anteil der vorliegenden Aluminium-Spezies (Al-VI und Al-IV) im Verlauf der Hydratationszeit bestimmt. Die Hydratphasen enthalten 6-fach koordiniertes (oktaedrisches) Aluminium, während in den Klinkerphasen 4-fach koordiniertes (tetraedrisches) Aluminium vorliegt [167–172]. Dies erlaubt den direkten Rückschluss auf den Hydratationsgrad des Zements.

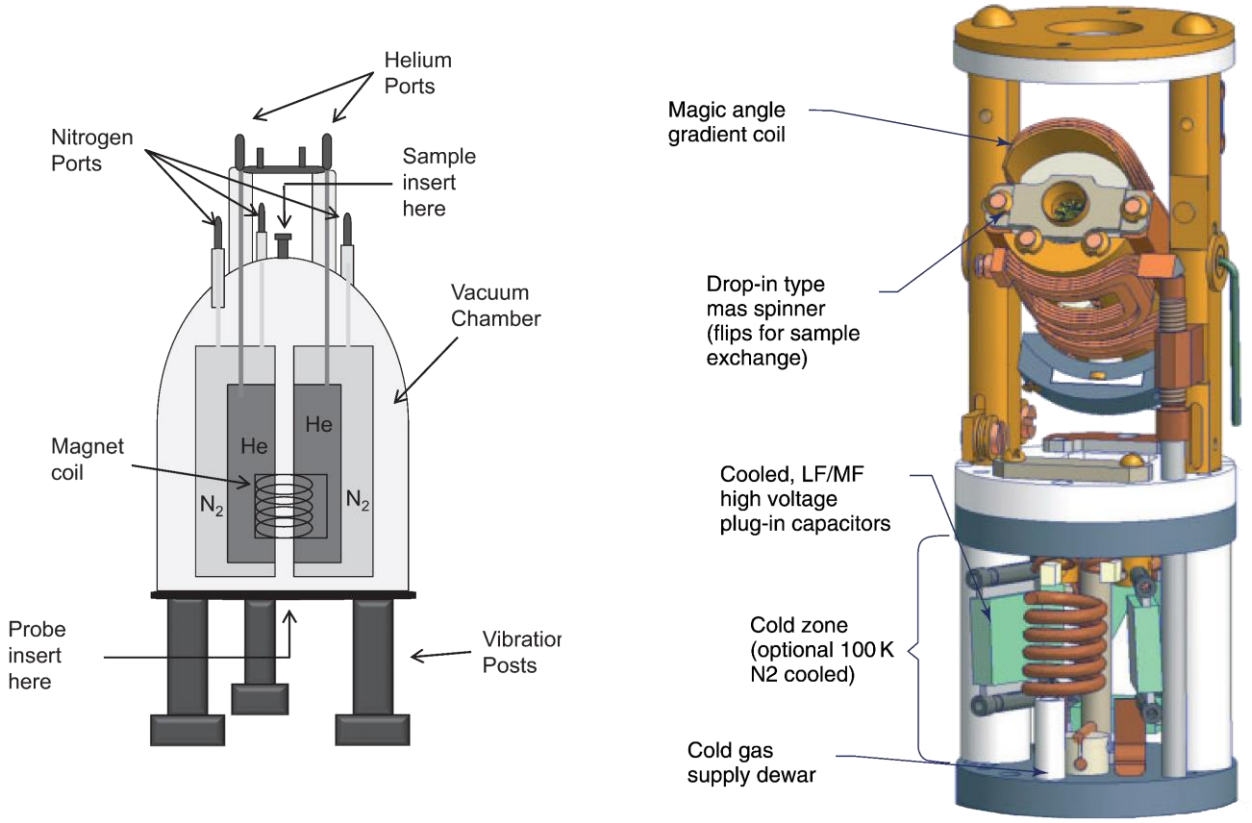

Abbildung 21: Schematischer Aufbau eines NMR Spektrometers (links) und eines MAS-Proben-/Messkopfs (rechts) für die Festkörper-NMR-Spektroskopie, abgedruckt in veränderter Form mit Genehmigung aus [165,173].

2.4.2 Ionenkonzentrationen in der Zementporenlösung (ICP-OES)

Die Hydratation von hydraulischen und latent-hydraulischen Bindemitteln wie Portland- und Calciumaluminat-Zement verläuft über einen Auflösungs- und Kristallisationsprozess, wobei Letzterer sowohl heterogen als auch homogen zur Bildung von Hydratphasen führt. Klassische Verzögerer und Beschleuniger wirken daher häufig durch Erniedrigung oder Erhöhung der freien Ionenkonzentration in der Zementporenlösung [12,53,75,87].

Um die Konzentrationen der relevanten Ionen, im vorliegenden Fall des Calciums und des Aluminiums, zu bestimmen, wurde die Atomemissionsspektrometrie gewählt. Hierzu

wurde durch Zentrifugation und anschließende Filtration von Zementleim eine Probe der Zementporenlösung gewonnen, die anschließend mit einer HCl-sauren Lösung (hierdurch wird u.a. die Carbonatisierung unterbunden) verdünnt wurde. Diese Lösung wird im Spektrometer, wie es schematisch in **Abbildung 22** dargestellt ist, von einer peristaltischen Pumpe angesaugt und nach Vermengung mit konzentrierter Salpetersäure durch einen Zerstäuber als Aerosol in die Plasmafackel eingebracht. In dieser Plasmafackel aus Argon, welches durch ein Hochfrequenzfeld induktiv erhitzt wird, wird das Probenaerosol durch die Wechselwirkung mit dem ionisierten Argon-Plasma bei 6.000 – 10.000 K atomisiert. Durch die im Plasma stattfindende Ionisierung und Rekombination der Atome kommt es zur Emittierung von elementspezifischer Strahlung, die an einem optischen Gitter gebeugt und auf einen CCD-Sensor gelenkt wird. Anhand einer Kalibrierung mit Lösungen definierter Zusammensetzung können die Konzentrationen der einzelnen Ionen in CPS berechnet werden, wodurch die Ionenbindefähigkeit von beispielsweise Alginat betrachtet werden kann [174–178].

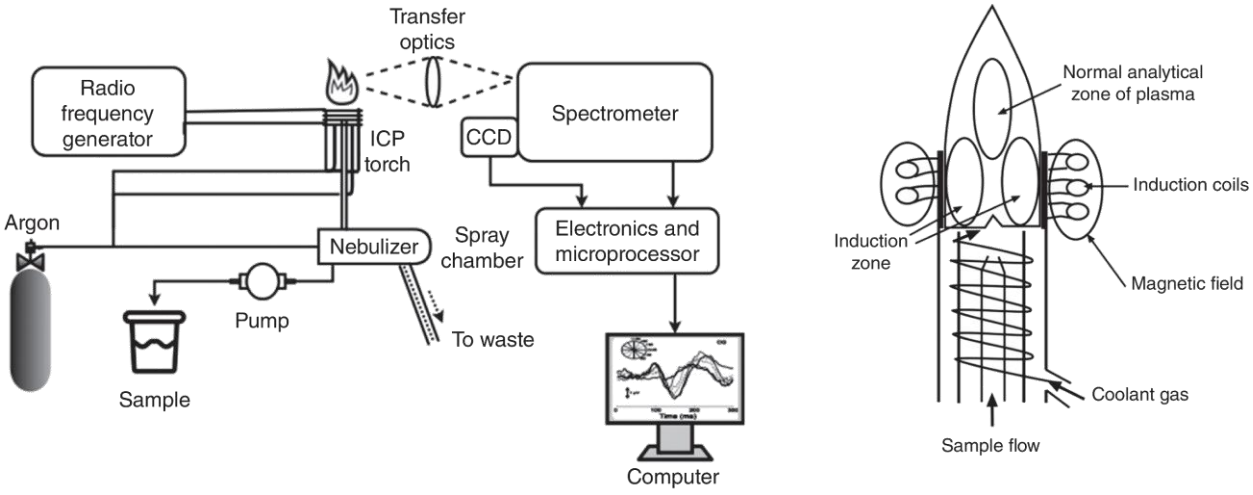

Abbildung 22: Schematischer Aufbau eines Atomemissionsspektrometers mit induktiv gekoppeltem Plasma, abgedruckt in bearbeiteter Form mit Genehmigung aus [176].

2.4.3 Bestimmung des Zeta-Potentials von Alginat

Um im Weiteren die Bindung der Ionen in der Zementporenlösung durch das Alginat zu untersuchen, wurde die Ladung bzw. das Zeta-Potential des Biopolymers in Lösung bestimmt. Dies ermöglicht es, die Wechselwirkung der verschiedenen Ionen, allen voran von Ca^{2+} und $[Al(OH)_4]^-$, mit der anionischen Polymerkette, die Carboxylat- und Hydroxyl-gruppen aufweist, zu untersuchen.

Hierzu wurden Lösungen von Natriumalginat bei einem alkalischen pH-Wert hergestellt, bei welchem das Biopolymer deprotoniert solvatisiert vorliegt. Da das Natrium-Kation nur eine schwache Wechselwirkung mit dem Alginat eingeht, zeigt das Polymer ein stark negatives Zeta-Potential. Im Folgenden wurden dieser Lösung verschiedene Konzentrationen an Ca^{2+} und $[Al(OH)_4]$ zu dosiert und nach kurzer Homogenisierung das resultierende Zeta-Potential gemessen. Dies erfolgt durch Einbringen der Lösung / Suspension in eine gefaltete Kapillarzelle, an der im Messgerät durch Elektroden ein elektrisches Feld angelegt wird. Die hieraus resultierende Elektrophorese (Wanderung geladener Teilchen) der Ionen bzw. des geladenen Polymers in der Lösung wird in Form der elektrophoretischen Mobilität bestimmt. Dies erfolgt durch Ermittelung der Phasenverschiebung der Lichtstreuung eines Laserstrahls durch die Probe und ist in **Abbildung 23** illustriert. Mithilfe der bekannten angelegten Spannung und der bestimmten Bewegungsgeschwindigkeit des Polymers kann anschließend durch die *Henry*-Gleichung, unter Verwendung der *Smoluchowski*-Näherung, das Zeta-Potential berechnet werden [179–181].

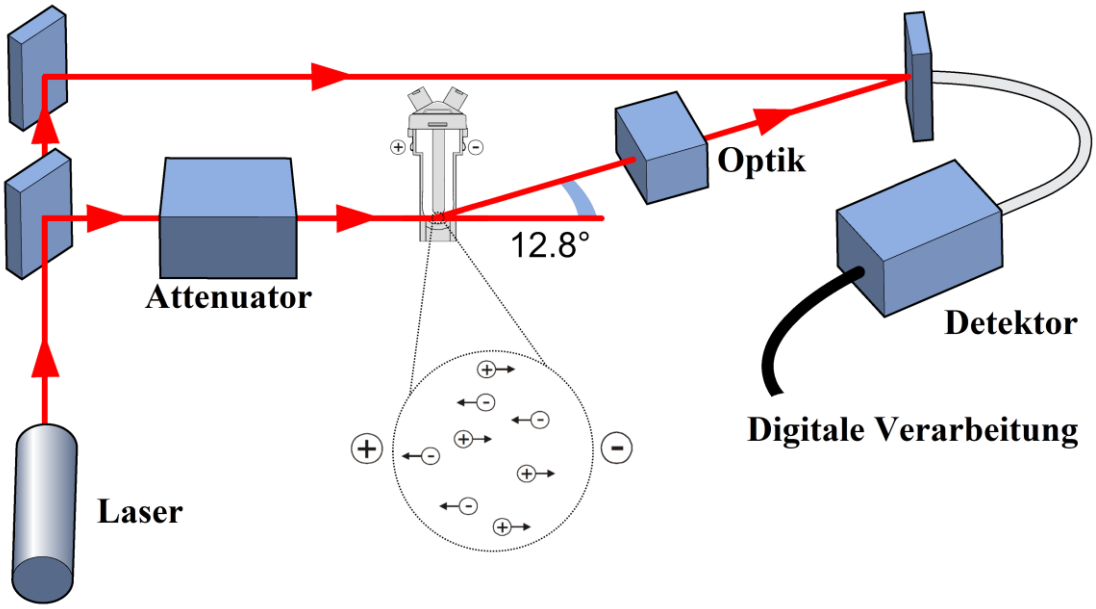

Abbildung 23: Schematischer Aufbau der elektrophoretischen Lichtstreuung, adaptiert mit Genehmigung aus [181].

2.4.4 Untersuchungen zur Kristallisation von Hydratphasen

Für die Charakterisierung der auf der Oberfläche der beschleunigenden Biopolymere durch die heterogene Nukleation gebildeten C-A-H-Phasen aus der Porenlösung wurden diese u.a. durch Rasterelektronenmikroskopie bildgebend untersucht. Hierzu wurden

Proben nach unterschiedlichen Kontaktzeiten mit Zementporenlösung hergestellt und betrachtet.

Unterschiedliche Methoden der Probenpräparation sind hierzu im Rahmen dieser Arbeit eingesetzt worden, wobei im Folgenden jene erläutert werden soll, die sich durch den besten Bezug zum realen System auszeichnete. Auf eine selbstklebende Graphit-Folie, die z.B. an einem REM-Probenhalter fixiert ist, wurde Alginat-Pulver aufgetragen. Dieser Probenhalter wurde nach Entfernen überschüssigen Pulvers in eine frisch extrahierte Zementporenlösung kopfüber eingetaucht und gelagert. Nach definierten Kontaktzeiten zwischen der Porenlösung und dem Alginat, welches unmittelbar nach Kontakt ein Hydrogel ausbildet, wird der Probenhalter entnommen und mit destilliertem Wasser gewaschen. Hieraufhin wird die Probe indirekt über eine Metallwanne mit flüssigem Stickstoff in Kontakt gebracht und eingefroren, woraufhin die Probe im Vakuum lyophilisiert wird. Dieser Prozess ist in **Abbildung 24** dargestellt und zeigt von links nach rechts die Probenpräparation durch Kontakt Alginat-CPS, das Einfrieren mit flüssigem N_2 und die fertige Probe nach der Gefriertrocknung.

Abbildung 24: Probenpräparation eines C-A-H-Alginat-Hydrogels und anschließende Trocknung für REM- und XRD-Untersuchungen.

Die trockene Probe wird nun für die Untersuchung mittels Rasterelektronenmikroskopie durch Besputterung mit Gold zur Verbesserung der elektrischen Leitfähigkeit vorbereitet. Der Probenhalter wird anschließend in das in **Abbildung 25** sowohl schematisch als auch photographisch illustrierte Mikroskop eingeschleust und dort im Hochvakuum (10^{-6} mbar) mit einem fein gebündelten Elektronenstrahl, welcher aus einer Feldemissionskathode extrahiert wird, beschossen. Dieser Strahl wird durch elektromagnetische Linsen und Blenden (engl. condenser lens & aperture) gebündelt und durch Magnetspulen (engl. scan coils) auf je einen Punkt der Probenoberfläche, die zur Bildgebung abgerastert wird, fokussiert. Durch den auftreffenden (primären) Elektronenstrahl, dessen Eindringtiefe

abhängig von der Beschleunigungsspannung ist, werden u.a. aus bzw. an der Probe Elektronen zurückgestreut (engl. backscattered electrons, BSE) oder Sekundärelektronen (SE) ausgeschlagen. Diese Elektronen werden beispielsweise durch Szintillatoren oder Halbleiterdetektoren erfasst und zur bildgebenden Ermittlung der Topographie (mittels SE), aber auch des Materialkontrasts (mittels BSE) eingesetzt. Ebenso kann durch eine energiedispersive Röntgenanalyse (kurz EDX) die Elementzusammensetzung der Probensubstanz anhand ihrer charakteristischen Röntgenstrahlung (freigesetzt durch elektronische Übergänge, nachdem kernnahe Elektronen durch den Primärelektronenstrahl ausgeschlagen wurden) charakterisiert werden [182–184].

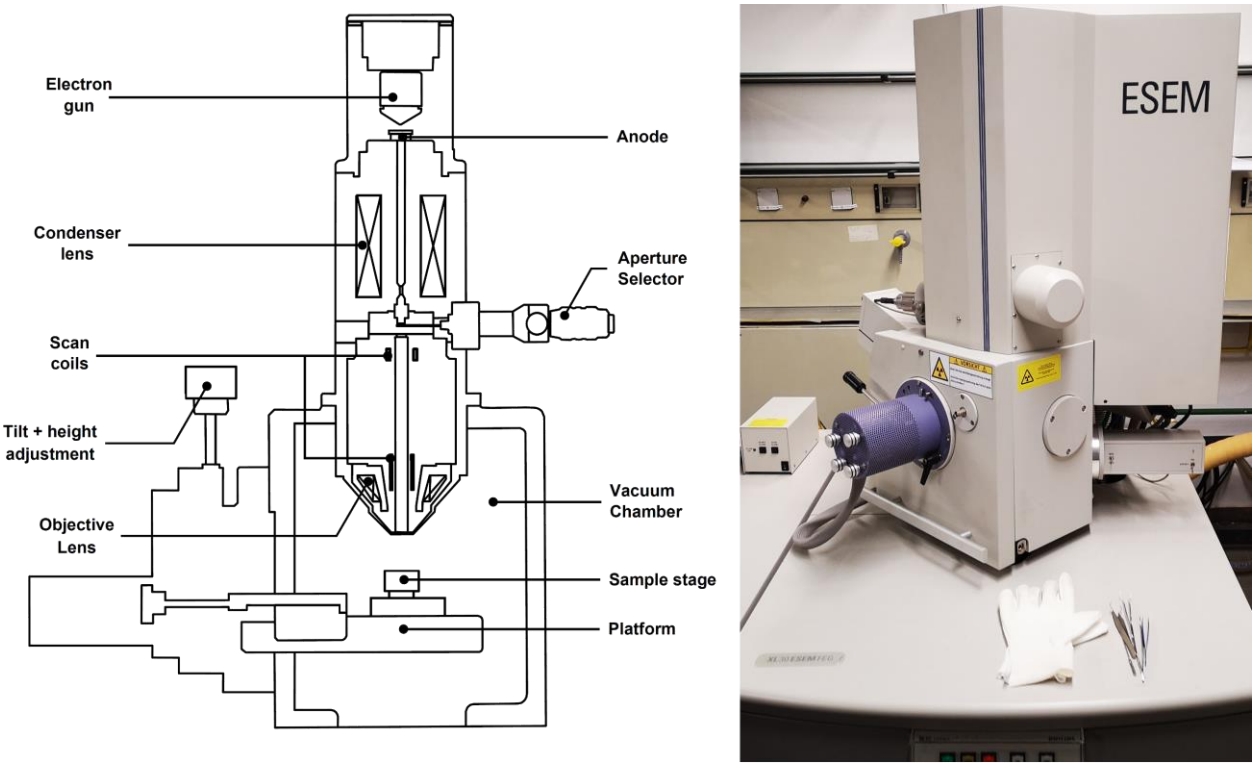

Abbildung 25: Schematischer Aufbau (links) eines Rasterelektronenmikroskops, abgedruckt in veränderter Form mit Genehmigung aus [185], sowie das eingesetzte Modell *FEG XL 30 ESEM* (rechts) der Firma *FEI*.

3. Ergebnisse und Diskussion

Im Folgenden soll ein allgemeiner Überblick über die Vorgehensweise (Meilensteine) der in dieser Arbeit durchgeführten Forschung gegeben werden, deren Ergebnisse in vier Publikationen detailliert beschrieben sind (siehe **Abbildung 26**). Die nachfolgenden **Abbildungen 27 – 30** stellen den wesentlichen Inhalt und die angewendeten Methoden zu den einzelnen Forschungsabschnitten dar. Eine ausführliche Zusammenfassung sowie zusätzliche Informationen zu jeder Publikation sind in den folgenden Unterkapiteln zu finden.

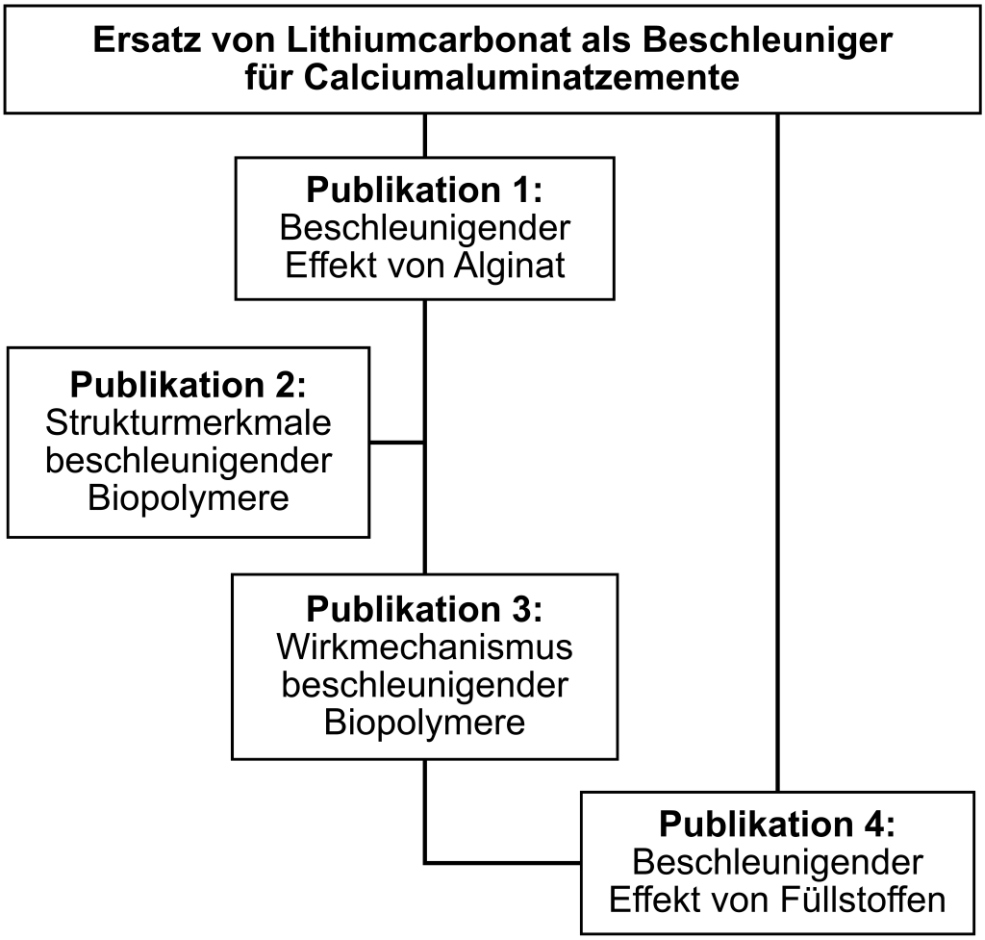

Abbildung 26: Zeitliche Vorgehensweise bei der Erforschung des beschleunigenden Effekts von Alginaten auf CAC.

In einem ersten Schritt wurde die Wirkung von Alginat untersucht (**Abbildung 27**), wobei sowohl Untersuchungen in Zementpaste als auch im Zementmörtel erfolgten. Im Besonderen wurde hier die Effektivität einzelner Alginat-Muster in den verschiedenen Zementen quantifiziert und mit deren Phasenzusammensetzung korreliert. Ebenfalls wurden die physikalisch-chemischen Eigenschaften verschiedener Alginat-Produkte (Molmasse, M/G-Verhältnis und Gegenion) in Bezug auf die Wirksamkeit als

Beschleuniger betrachtet. Zudem wurden erste Ansätze zur mechanistischen Aufklärung mit Fokus auf der Calciumbindefähigkeit des Alginats vorgenommen.

Abbildung 27: Vorgehen bei der Erstuntersuchung zur beschleunigenden Wirkung von Alginaten (**Publikation 1**).

Um den Ursprung dieses ungewöhnlichen beschleunigenden Effekts von Alginat zu ergründen, wurde im nächsten Schritt der Fokus auf die Molekülstruktur des Polymers gelegt (siehe **Abbildung 28**). Hierzu wurden sowohl Alginate unterschiedlichen Ursprungs (extrahiert aus verschiedenen Algenarten) als auch im Labor synthetisierte Derivate des Alginats untersucht. Zur Identifikation wichtiger struktureller Merkmale wurde ebenfalls eine breite Auswahl verschiedener Biopolymere (natürlichen, mikrobiellen und halbsynthetischen Ursprungs) auf ihre Wirkung in CAC getestet.

Im finalen Schritt, der Aufklärung des Wirkmechanismus von Alginat (siehe **Abbildung 29**) wurde die Zementhydratation in Gegenwart des beschleunigenden Polymers betrachtet und die Bildung der Hydratphasen sowohl qualitativ als auch quantitativ analysiert. Die hierbei stattfindenden Prozesse in der Zementporenlösung wurden durch Bestimmung der Ionenkonzentrationen und durch Untersuchung der Wechselwirkung der Ionen mit Alginat näher ermittelt. Basierend auf diesen Informationen konnte ein mechanistisches Modell aufgestellt werden, welches durch elektronenmikroskopische Aufnahmen bestätigt wurde.

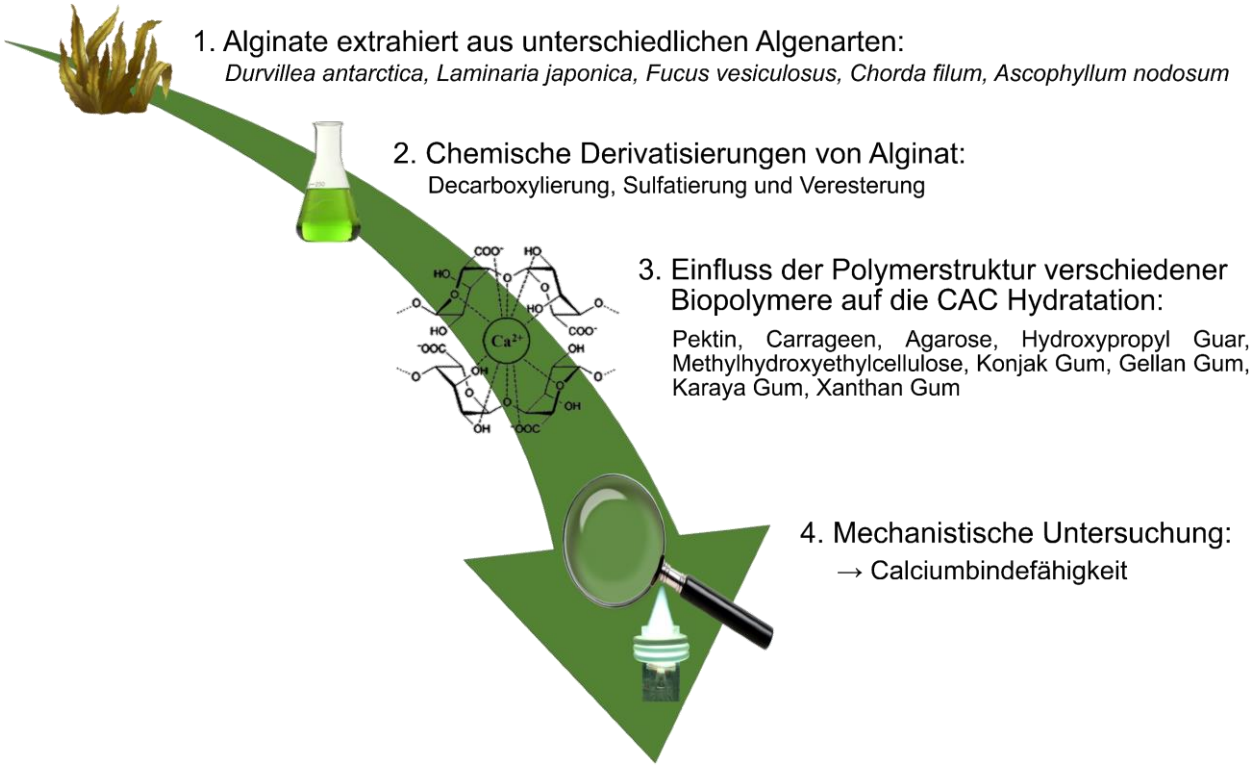

Abbildung 28: Vorgehensweise bei der Untersuchung der Strukturmerkmale in beschleunigenden Biopolymeren (**Publikation 2**).

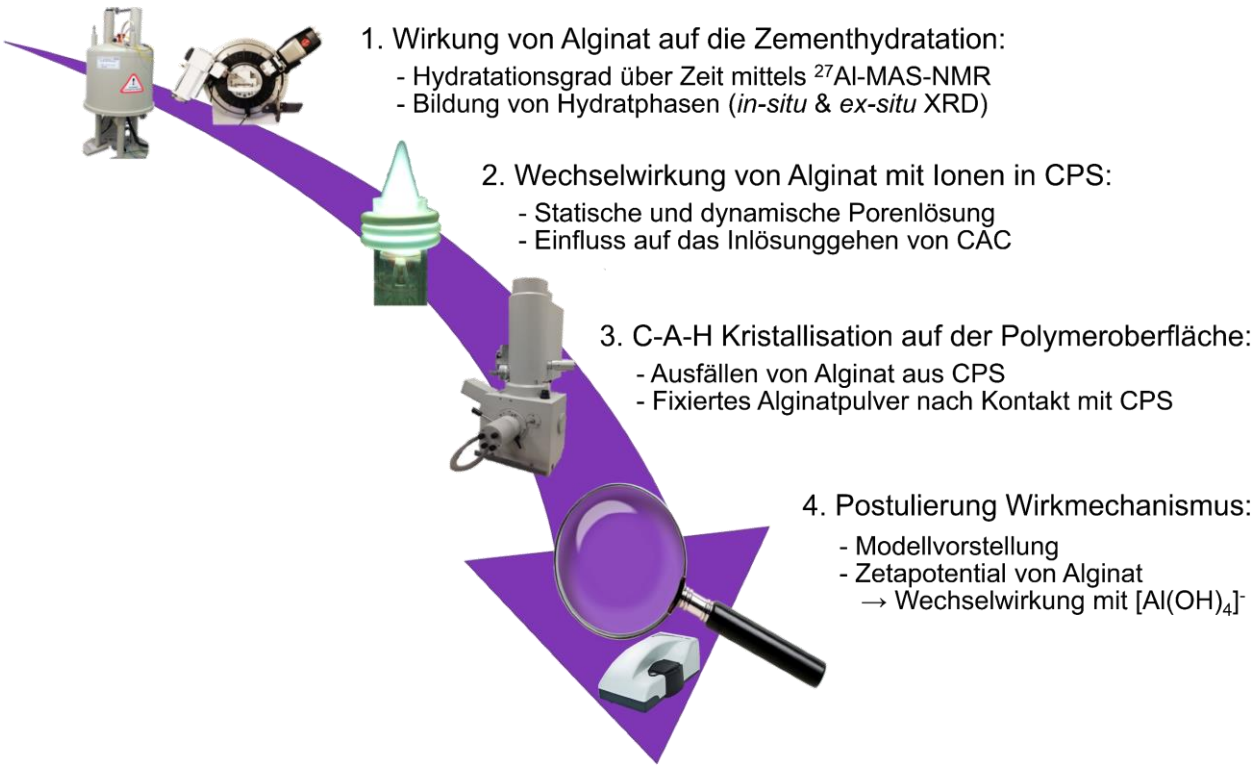

Abbildung 29: Vorgehensweise bei der Ergründung des Wirkmechanismus von Alginat als Hydratationsbeschleuniger (**Publikation 3**).

Da im Rahmen der ersten Publikation Diskrepanzen zwischen den Untersuchungen in Zementpaste und Mörtel festgestellt wurden, wurde dies anschließend näher beleuchtet (siehe **Abbildung 30**). Hierfür wurde im Weiteren die Wirkung unterschiedlicher Füllstoffe (mit diverser chemischer Zusammensetzung und Partikelbeschaffenheit) auf die Hydratation von CAC analysiert. Durch die Erkenntnisse zum Wirkmechanismus des Alginats wurde durch analoge Experimente (Calciumbindefähigkeit, Mikroskopie der Oberfläche bei CPS Kontakt, usw.) das der beschleunigenden Wirkung von feinen Füllstoffen zugrundeliegende Prinzip erkundet, welches dem des Alginats ähnelt.

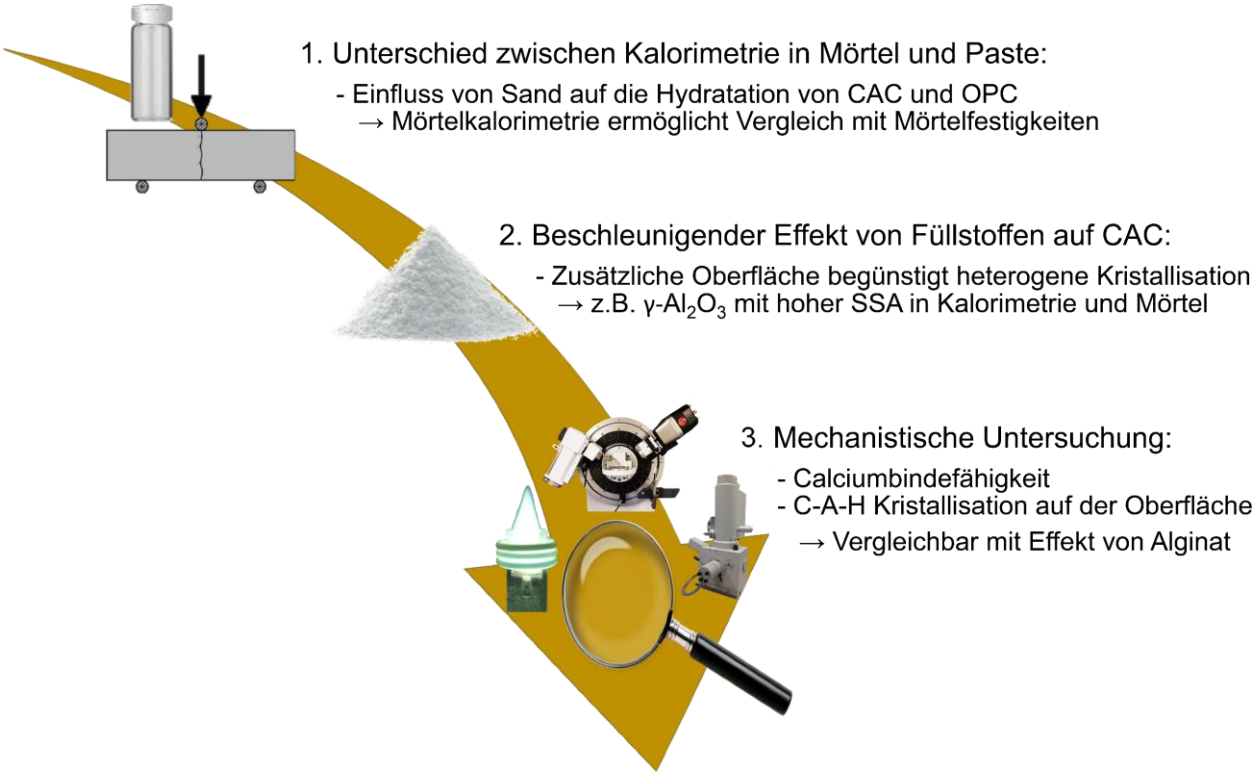

Abbildung 30: Vorgehensweise bei der Untersuchung zur beschleunigenden Wirkung von Sand und feinen Füllstoffen (**Publikation 4**).

3.1 Publikation 1: Beschleunigender Effekt von Alginat in CAC

3.1.1 Zusammenfassung

Wie anfangs beschrieben, werden aktuell Lithiumsalze zur Beschleunigung des Abbindens von Aluminatzement eingesetzt. Der ungewöhnliche Effekt des Alginats, einem Polysaccharid, ebenfalls vorzeitiges Erhärten des Zements hervorzurufen, war völlig überraschend und in der bisherigen Literatur nicht beschrieben. Er war im Rahmen einer früheren Promotionsarbeit am Lehrstuhl für Bauchemie zufällig beobachtet worden [25].

In der hier vorliegenden Studie konnten folgende wichtige Erkenntnisse gewonnen werden:

- Bei Hinzugabe von Alginat zu CAC in der Zementpaste ist ein stark beschleunigender Effekt auf den Hydratationsbeginn zu verzeichnen, wobei die Zeit bis zum Erhärten z.T. halbiert werden konnte.
- Diese Beobachtung erfolgte in verschiedenen Zementen mit einem Al_2O_3-Gehalt zwischen 40 und 80 Gew.%. Hierbei konnte eine individuelle Suszeptibilität für die Wirkung des Alginats auf die verschiedenen Zemente festgestellt werden. Zemente mit besonders reaktiven Klinkerphasen wie $C_{12}A_7$ und C_4AF werden weniger stark beschleunigt.
- Alginate beschleunigen generell nur CACs und nicht z.B. Portlandzement (OPC). Dies ist auf die Bildung von C-A-H-Phasen zurückzuführen, welche jedoch bei der Hydratation von Portlandzement, Calciumsulfoaluminatzement oder ternären Bindemittelsystemen nicht entstehen.
- Der Einsatz verschiedener Alginatproben unterschiedlicher Hersteller zeigte, dass Alginate generell eine beschleunigende Wirkung aufweisen. Der Grad der Beschleunigung kann jedoch variieren.
- Das M/G-Verhältnis (bestimmt mittels IR-Spektroskopie) und das Gegenion im Alginat haben keinen nennenswerten Einfluss auf den beschleunigenden Effekt.
- Entscheidend für die Wirkung des Alginats ist dessen Molmasse, welche u.a. die Viskosität des Polymers in Lösung beeinflusst. Beschleunigende Alginate besitzen einen M_w von 10^5 - 10^6 Da, wohingegen für Alginate mit einer Molmassen von 10^4 Da ein verzögernder Effekt festgestellt wurde.

- Es ist möglich, Lithiumsalze bis zu einer gewissen Dosierung durch Kombination mit Alginat zu ersetzen, um den Lithium-Verbrauch zu reduzieren.
- Die Zugabe von Alginat zu einem Mörtel führte ebenso wie in Zementpaste zu einer erhöhten Frühfestigkeit. So konnte beispielsweise im CAC „*Secar 712“* durch Zugabe von Alginat nach 16 Stunden bereits eine Druckfestigkeit von 33 N/mm^2 erreicht werden, gegenüber 16 N/mm^2 ohne Alginatzugabe.
- Dieser positive Effekt ging aber mit einer schlechteren Verarbeitbarkeit (bedingt durch das hohe Wasserbindevermögen des Biopolymers) einher. Durch Zugabe von PCE-basierten Fließmitteln kann der Viskositätsanstieg durch das Alginat jedoch beseitigt werden.
- Spektrometrische (ICP-OES) Konzentrationsbestimmung von Calcium und Aluminium der Zementporenlösung zeigte, dass Alginat Calcium bindet. Die Menge an freiem Calcium war um bis zu 50 % reduziert. Dies ging mit einer Erhöhung der Aluminium-Konzentration einher, indem weiterer Zementklinker in Lösung geht, um das Lösungsgleichgewicht bzgl. Calcium wieder aufzufüllen.
- Da eine Verringerung der Ca^{2+}-Konzentration in Zementen üblicherweise zu einer Verzögerung führt, ist der beschleunigende Effekt von Alginat außerordentlich unerwartet und erstaunlich.
- Die Kombination von Alginat mit einem Ca^{2+}-komplexierendem Verzögerer (Citrat bzw. Tartrat) ergab erneut eine starke Abnahme der Menge an Calcium sowie zusätzlich an Aluminium in der Porenlösung, dennoch blieb die beschleunigende Wirkung des Alginats erhalten.
- Daraus wurde gefolgert, dass das Alginat die Kristallisation der C-A-H-Phasen auf eine bestimmte, noch aufzuklärende Weise begünstigt und die Ionenkonzentrationen in der Porenlösung dabei keine Rolle spielt.

3.1.2 Veröffentlichung

The effect of alginates on the hydration of calcium aluminate cement

Engbert A., Gruber S., Plank J.

Carbohydrate Polymers, 2020, 236, 116038.

https://doi.org/10.1016/j.carbpol.2020.116038

Carbohydrate Polymers 236 (2020) 116038

Contents lists available at ScienceDirect

Carbohydrate Polymers

journal homepage: www.elsevier.com/locate/carbpol

The effect of alginates on the hydration of calcium aluminate cement

Alexander Engbert, Stefanie Gruber, Johann Plank*

Technische Universität München, Chair for Construction Chemistry, Lichtenbergstr. 4, 85747 Garching, Germany

ARTICLE INFO

Keywords:
Polysaccharide
Alginate
Calcium aluminate cement
Accelerator
Hydration
Calcium complexation

ABSTRACT

The hydration of calcium aluminate cement (CAC) in the presence of sodium alginate which is known to slightly retard Portland cement, was studied using heat flow calorimetry and mortar strength testing. Most surprisingly, addition of alginate resulted in an earlier occurrence of the maximal heat release as well as an increased early strength, thus confirming that in CAC alginate acts as accelerator. The thickening effect of alginate was effectively compensated using a superplasticizer while retaining its accelerating property. An investigation of the pore solution composition indicated that in the presence of alginate the concentration of calcium ions was reduced. Such effect normally causes retardation of cement hydration and should delay the formation of C-A-H phases. Apparently, the strong calcium ion complexing ability of alginate promotes the formation of C-A-H via e.g. a templating effect. A combined application of alginates and lithium salts presents a viable option to reduce the lithium consumption in CAC acceleration.

1. Introduction

Calcium aluminate cements (CACs) have unique properties that include quick high early strength (faster strength development than from Portland cement) and a high acid and abrasion resistance. This makes CAC the cement of choice where those properties are required. Alumina cements are produced at higher temperatures than Ordinary Portland cement (OPC) because of their high content of Al_2O_3 and are sintered or molten at 1450 °C and 1650 °C, respectively (Bensted, 2002). Commercial products normally have an Al_2O_3 content of 35–85 wt.% depending on their field of application. The common hydraulic clinker phases of CACs include CA, CA_2, $C_{12}A_7$, C_4AF and C_2S. By mass, monocalcium aluminate is the most relevant phase present in calcium alumina cement. Hydration of the aluminous clinker phases proceeds via a dissolution and precipitation mechanism from solution. In the pore solution, Ca^{2+} and Al^{3+} are present at a molar ratio of about 0.55 - 0.6 which leads to the crystallisation and precipitation of metastable C-A-H phases (CAH_{10}, C_4AH_{13} or C_4AH_{19} and C_2AH_8/$C_2AH_{7.5}$) of which C_2AH_x is most important for the setting of CAC (Lothenbach, Pelletier-Chaignat, & Winnefeld, 2012; Scrivener & Capmas, 2003). Depending on the temperature, after months or years all metastable hydrates transform into the stable hydrogarnet C_3AH_6 phase (katoite). At low temperatures (< 15 °C) and room temperature (15–25 °C), the hydration of CAC either progresses through the formation of CAH_{10} (I) at first, followed by its transformation to C_2AH_8 (II), or by direct formation of C_2AH_8 (III) (Scrivener & Capmas, 2003).

$$CA + 10\ H \rightarrow CAH_{10} \quad (1)$$

$$2\ CAH_{10} \rightarrow C_2AH_8 + AH_3 + 9\ H \quad (2)$$

$$2\ CA + 11\ H \rightarrow C_2AH_8 + AH_3 \quad (3)$$

In CAC, most commonly lithium salts are used to accelerate its hydration. In particular, Li_2CO_3 is applied at dosages between 0.005 and 0.1 wt.-%, depending on the application and specific binder system. Lithium produces a strong accelerating effect in pure aluminate cement and in combinations with calcium sulphates (binary / ternary systems). According to a model presented by *Goetz-Neunhoeffer*, Li^+ ions accelerate the hydration of the aluminate phases through six pathways: (1) improved dissolution of CA through an increased permeability of the aluminum hydroxo hydrate layer; (2) the thus increased Ca^{2+}/Al^{3+} ratio in solution thermodynamically promotes the formation of C_2AH_8; (3) formation of $[Li_2Al_4(OH)_{12}](OH)_2 \cdot 3\ H_2O$ layered double hydroxide (LDH) compound as seeding material which decreases the activation energy necessary for the crystallisation of C_2AH_8; (4) Li^+ ions are then continuously exchanged and replaced by Al^{3+} ions which then (5) reduces the Al^{3+} concentration in solution and (6) further foster the dissolution of CA by the lower Al^{3+} content in solution (Götz-Neunhoeffer, 2005).

However, the availability of lithium salts in general and for construction applications in particular is becoming increasingly

Abbreviations: C, CaO; A, Al_2O_3; S, SiO_2; H, H_2O; F, Fe_2O_3; T, TiO_2; M, MgO

* Corresponding author at: Chair for Construction Chemistry, Technische Universität München, Lichtenbergstr. 4, 85747 Garching bei München, Germany.
E-mail address: sekretariat@bauchemie.ch.tum.de (J. Plank).

https://doi.org/10.1016/j.carbpol.2020.116038
Received 5 November 2019; Received in revised form 20 January 2020; Accepted 18 February 2020
Available online 20 February 2020

problematic because of the high demand for lithium ion batteries. The fast growing market for mobile phones and electric cars drastically affected the price and the supply security for lithium compared in recent years (Speirs & Contestabile, 2018). Considering the key role which lithium is expected to play in future electromobility it appears to be irresponsible to use up such a precious element in flooring compounds and other CAC-based systems. Hence, a replacement for Li is highly needed.

In the context of another study, we observed an unexpected behaviour of alginates when tracking the hydration of alumina cement via heat flow calorimetry (de Reese, Sperl, Schmid, Sieber, & Plank, 2015). Most surprisingly it was found that alginates act as accelerator for CAC by prematurely triggering its hydration. This effect was not expected, because so far polysaccharides were only known to retard cement hydration.

Alginates are biopolymers composed of mannuronic (M) and guluronic (G) acid that are glycosidically connected via α-1→4 and β-1→4 linkages, forming linear copolymers with average molecular weights between 10,000 and 600,000 Da. The carbohydrate monomer units (M and G) can be linked in different tactical sequences such as MM, GM and GG which leads to different steric arrangements (Fig. 1, top). The ratio between those blocks and the molecular weight (~ viscosity) are mostly responsible for the properties (gel strength/syneresis) of aqueous solutions of the polymer. Furthermore, it is known that especially GG blocks are essential for the strong ionotropic gelling properties of alginate in the presence of divalent cations, like e.g. Ca^{2+} (Imeson, 2011; Plank, 2003). Due to its characteristic appearance, this complexation mode with Ca^{2+} is generally referred to as the "egg-box" model (Fig. 1, bottom), first introduced by Grant, Morris, Rees, Smith, and Thom (1973).

Alginates are biopolymers of natural origin and are harvested via extraction from brown algae *Phaeophyceae*. Depending on the species of algae, their growth conditions and processing after harvest, their chemical composition and molecular weight can vary.

The aim of this research was to investigate and understand this unusual property of alginate in CAC. In order to elucidate the effect of alginates of diverse natural origin, a series of commercial sodium alginate products exhibiting different properties were received from different companies and tested. Additionally, their accelerating effect on alumina cements of various Al_2O_3 contents was examined. This program was developed because CACs can exhibit different mineralogical compositions resulting mainly from the ratio of $CaO/Al_2O_3/Fe_2O_3$ present in the raw meal for CAC production. In order to compensate for the loss of workability resulting from the thickening effect of the biopolymer a superplasticizer was used. Moreover, the accelerating mechanism of the alginate was investigated by applying pore solution analysis.

2. Experimental

2.1. Cement samples

A variety of calcium aluminate cements (*Ciment Fondu, Secar 41, Secar 51, Secar 71, Secar 712, Secar 80 as well as Ternal SE, Ternal LC and Ternal EP*) produced by *Imerys Aluminates* were utilised. Their oxide composition (Table S-1 in supporting information) was determined using XRF (*Axios*, PANalytical, Kassel, Germany) while their mineralogical composition (Table 1) was investigated using XRD (*D8 advance*, Bruker AXS, Karlsruhe, Germany). Average particle size was analysed by laser granulometry (*Cilas 1064*, Cilas Instruments, Orleans, France). Here, particle size was measured three times after complete dispersion in isopropanol using ultrasonic, and the mean value was calculated. The specific surface area was determined according to *Blaine's* method.

2.2. Chemicals

In all experiments deionised water obtained from a *Barnstead Nanopore Diamond Water purification system* (*Werner Reinstwassersysteme*, Leverkusen, Germany) was used. As reference accelerator lithium carbonate (*Chemetall*) and as retarders trisodium citrate (*Merck*) as well as potassium sodium tartrate (Rochelle salt, *Jungbunzlauer*) were utilised. Li_2CO_3 (< 40 µm) was pre-blended at 1/40 wt./wt. ratio with calcium carbonate (≈ 14 µm, *Merck*) to ensure accurate dosing.

2.2.1. Alginates

Over thirty alginate samples were provided by *KIMICA, Eurogum, FMC* (through *IMCD*), *Roeper, Cargill, Danisco* and *Polygal*. Those varied

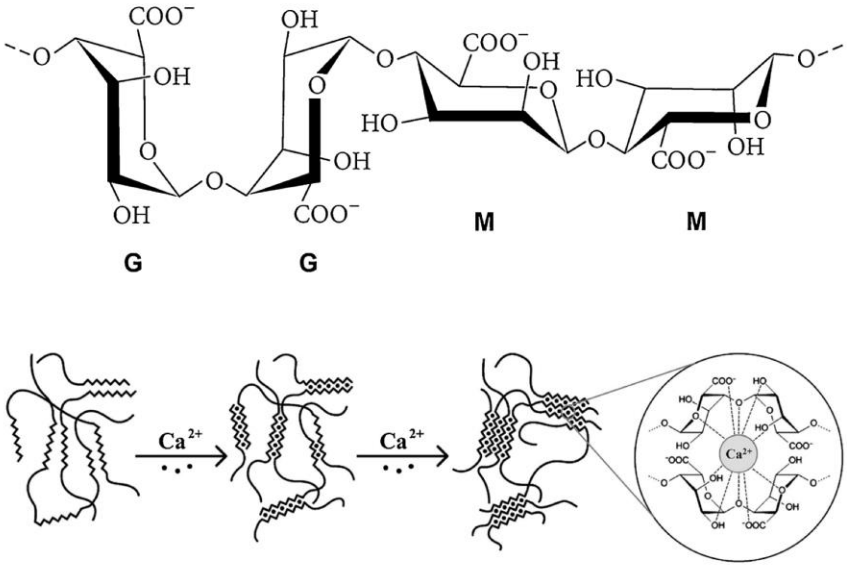

Fig. 1. Top: General chemical structure of the alginate molecule composed of guluronic (G) and mannuronic (M) acid as building blocks; Bottom: Complexation of calcium ions by alginate molecules ("egg-box" model) resulting in gel formation (adapted from Stolarz (2003) and Pistone, Qoragllu, Smistad, and Hiorth, (2015)).

Table 1
Typical contents (wt.%) of hydraulic clinker phases in alumina cement samples used in the study, according to quantitative X-ray diffraction analysis including Rietveld refinement performed by TUM in conjuncture with reported literature values.

	CAC sample (wt.%)					
Phase	Ternal EP	Ciment Fondu Ternal SE	Secar 41	Secar 51 Ternal LC	Secar 71 Secar 712	Secar 80
CA	1–5[1]	47–57[1,2]	54–66[1]	64–74[1,2,3,4,5]	54–64[1,2,7]	35–45[1,7]
CA_2	*n.d.*	*n.d.*	*n.d.*	*n.d.*	36–44[1,7]	22–30[1,7]
C_2AS	*n.d.*	1–10[1]	10–22[1]	18–22[1,3,4,5]	< 1[1,7]	*n.d.*
C_4AF	10–20[1]	10–20[1]	*n.d.*	*n.d.*	*n.d.*	*n.d.*
C_2S	10–20[1]	1–10[1]	1–10 [1]	1–5[1,3,4,5]	*n.d.*	*n.d.*
$C_{12}A_7$	55– 65[1]	1–5[1,2]	1–5[1]	< 1[1,3,5]	< 1[1,7]	< 1[1,7]
other	C_3A, CT	C_3FT, $C_{20}A_{13}M_3S_3$[6]	CT, C_3FT, $C_{20}A_{13}M_3S_3$	CT, C_3FT	α-Al_2O_3[1,7] (< 2)	α-Al_2O_3[1,7] (35 - 45)

[1] Own analysis.
[2] Data from Parr, Bin, Alt, and Wohrmeyer (2006).
[3] Data from Puerta-Falla et al. (2015).
[4] Data from Bizzozero, Gosselin, and Scrivener (2014).
[5] Data from Gosselin and Scrivener (2008).
[6] Data from Touzo, Gloter, and Scrivener (2001).
[7] Data from Ostrander and Schmid (2015).

in purity (food grade or technical grade), particle size, viscosity grade and M/G ratio. In the following work, the commercial alginate products *XEA 5036* (*Eurogum*), *ALGIN (KIMICA)*, *S 900 NS* (*Cargill*), FD 170 (*Danisco*) and *Protanal LF 200 FTS* (*FMC*) were utilised (properties shown in Table 3).

The ratio between mannuronic and guluronic acid was determined via IR spectroscopy. From commercial samples of known composition a calibration curve between the M/G ratio and the ratio of the IR absorptions at about 1025 cm^{-1} and 1085 cm^{-1} was established (Sellimi et al., 2015) (see Table S-2 and Figure S-1 in supporting information). The investigated samples had M/G ratios in the range between 0.4 and 1.6, according to our analysis.

2.2.2. PCE superplasticizer

A polycarboxylate (PCE) superplasticizer based on ω-methoxy poly (ethylene oxide) methacrylate and methacrylic acid was utilised to reduce the viscosity and water demand of the CAC pastes. It was self-prepared via aqueous free radical copolymerisation at 80 °C as described in literature (Plank, Zouaoui, Andres, & Schaefer, 2014). In the PCE copolymers, the molar ratio of the monomers was 6 : 1 (MAA : Ester) and the side chain was composed of 114 ethylene oxide units. Molecular properties of the PCE sample was collected by GPC analysis which revealed a macromonomer conversion of 95 %, resulting in a copolymer with a mass average molecular weight of 33,800 Da and a PDI of 2.26.

2.3. Experimental methods

2.3.1. Isothermal heat-flow calorimetry

Calorimetry was performed following DIN EN 196-11 (2019). Four gram of cement were filled into sealable 10 mL glass ampules and dry-blended with previously placed alginate powder until a homogenous mixture was achieved. This blend was mixed with deionised water at room temperature and homogenised with a vortex mixer *VWT 1419* (*VWR*, Ismaning, Germany) for two minutes. The ampoule was placed in an isothermal conduction calorimeter *TAM air model 3116-2* (*Thermometric*, Järfälla, Sweden) for monitoring of the heat flow. Measurements were conducted at 20 °C until heat evolution was concluded and repeated at least twice.

2.3.2. Mortar tests

Mortar testing was conducted according to DIN EN 196-1 (2016) and strength values were determined at different times of hydration using a *ToniNORM* instrument setup (*Toni Technik*, Berlin, Germany). The mortar was composed of three parts of norm sand and one part of cement which was pre-blended with the alginate powder. Using a *ToniMIX* eccentric agitator (*Toni Technik*, Berlin, Germany) the mortar was automatically prepared whereby the water containing the superplasticizer as well as one drop of defoamer (Dowfax DF 141, *Dow Chemical*) was first placed in the mixer cup. The mortar prisms (4 × 4 × 16 cm) were compacted using a *ToniVib* vibrating table (*Toni Technik*, Berlin, Germany), stored at 20 °C / 90 % relative humidity and demolded 10 min prior to measuring their compressive and tensile strength. Mortar density was calculated from the size and weight of the prisms. Mortar tests were performed from the same shipment of each cement and the prisms were produced in one test series. This precaution was taken because CAC is quite sensitive to ageing.

2.3.2.1. Mortar spread flow. The spread flow of the mortar was determined according to DIN EN 1015-3 (2007). First, the mortar was added in two steps into a Vicat cone (height 40 mm, top diameter 70 mm, bottom diameter 80 mm) and slightly compacted. Each layer was compacted 10 times with a tamping rod. Thereafter, the cone was removed vertically and the flow table was lifted up 40 mm and then dropped 15 times, causing the mortar to spread out. The resulting spread was measured twice, the second measurement being at a 90° angle to the first and averaged to report the mean value.

2.3.2.2. Compressive and tensile strengths. Compressive and tensile strengths were determined according to DIN EN 196-1. For measurement of the tensile strength, three specimens of each sample were used and the average was calculated. The compressive strength was assessed using the broken specimens from the tensile strength testing. The mean value for the compressive strength was calculated from the measured results of the six pieces. Measurements were performed on a *ToniNORM powerbox model 2010* equipped with two load frames *model 1543* and *model 1544*.

2.4. Analytical methods

2.4.1. FT-IR spectroscopy

Infrared spectra of the polymers were measured with an attenuated total reflectance Fourier transform spectrophotometer (ATR-FTIR) (*Vertex 70*, Bruker Optics, Karlsruhe, Germany). It was acquired in transmittance mode on a Diamond ATR crystal cell (*MPV-Pro*, Harrich Scientific Products, Pleasantville, USA) by accumulation of 20 scans with a resolution of 0.5 cm^{-1} and a spectral range of 2000–650 cm^{-1}. Evaluation of the spectra was performed using Bruker's *OPUS 6.5* software after background correction and normalization.

2.4.2. Ion concentrations via ICP-OES

Inductively coupled plasma atomic emission (ICP-OES) spectroscopy was performed on a *series 700* apparatus (*Agilent Technologies*, Santa Clara, CA, USA). The cement paste was prepared by admixing e.g. 20 g Ciment Fondu blended with 0.1 wt.% alginate in a centrifuge tube and subsequent homogenisation for two minutes utilizing a vortex mixer *VWT 1419* (*VWR*, Ismaning, Germany). The cement paste was centrifuged (8500 rpm, 15 min) and the supernatant pore solution was filtrated using a 0.2 µm PES membrane filter. The resulting solution was diluted accordingly (1/30) and automatically measured five times to capture the Ca^{2+} and Al^{3+} content in the pore solution. Calibration was performed at concentrations of 1, 10 and 50 mg/L using an ICP multi-element standard (standard IV, *Merck*) and data was collected at several wavelengths. Results were averaged and deviation was calculated including an additional methodical error of 1 % to account for errors resulting from e.g. weighting and pipetting.

3. Results and discussion

3.1. Effect of alginate on CAC hydration

As is generally known, the addition of various polysaccharides to CAC including Xanthan gum, Welan gum etc. normally results in a retardation of cement hydration. In the course of this study, we surprisingly found that only a few specific polysaccharides (e.g. Gellan Gum or Karaya Gum) have no retarding effect or even produce a weak acceleration under specific circumstances. In contrast to those polymers, an alginate sample was found to strongly accelerate alumina cement. Moreover, other randomly selected sodium alginates showed similar accelerating properties.

In the following, the accelerating effect of four randomly selected alginate samples with different properties on the hydration of a commercial CAC is presented (Fig. 2). Of those samples shown only #1 (XEA 5036) is used in the further study for mortar tests and investigations on the working mechanism. According to the results from heat flow calorimetry, addition of 0.1 wt.% of sodium alginates can reduce the time until maximum heat release is recorded by up to 50 % (Table 2), suggesting that the dormant period is reduced significantly.

For Secar 51, as an example, the point of maximum heat release was detected about 4 h earlier when alginate was added. This corresponds to an acceleration of 45 % of hydration time for sodium alginate XEA 5036 (9.2 h for the reference as compared to 4.9 h upon addition of 0.1 wt.% alginate). To probe whether the effect of the alginate is dependent on the w/b ratio, CAC pastes with w/b ratios of between 0.4 and 0.7 were prepared. No difference between them relative to the general trend was found.

Extensive testing employing CACs of different phase compositions revealed that the accelerating effect occurred in all CAC pastes, but significantly differed with phase composition and particle size of the CAC sample (Table 1 and Table S-1 in supporting information). This can be explained by the clinker phase composition of the cements. Ternal EP (mainly $C_{12}A_7$), Ciment Fondu and Ternal SE (both with an high amount of C_4AF and traces of $C_{12}A_7$) have an inherent high reactivity because of the calcium rich clinker composition and are thus less influenced by alginate. Especially Secar 80 shows a minor acceleration by alginate, which can be attributed to an extremely high fineness which already provides fast hydration (*Blaine* value of Secar 80 is 10,600 cm^2/g as compared to 3,000–4,000 cm^2/g for the other cements).

Table 2
Acceleration of cement hydration in percent measured for different CAC samples (w/b = 0.62) upon addition of alginate sample XEA 5036, calculated from the time periods to reach peak heat release in heat flow calorimetry (see Table S-3 in supporting information).

CAC	+ 0.1 wt.% Alginate	+ 0.2 wt.% Alginate
Fondu	≈ 20 %	≈ 20 %
Secar 41	≈ 20 %	≈ 25 %
Secar 51	≈ 45 %	≈ 50 %
Secar 71	≈ 45 %	≈ 50 %
Secar 712	≈ 50 %	≈ 60 %
Secar 80	≈ 5 %	≈ 15 %
Ternal EP	≈ 15 %	≈ 30 %
Ternal SE	≈ 20 %	≈ 25 %
Ternal LC	≈ 45 %	≈ 50 %

Furthermore, the effect of this specific alginate sample XEA 5036 on the hydration of other binders including Portland cement, calcium sulfoaluminate (CSA) cement, anhydrite or a ternary binder system (OPC / CAC / AH) was probed. There no acceleration was detected, instead consistently no effect or a minor retardation occurred. This allows to conclude that the alginate specifically promotes the hydration of alumina cement only.

3.2. Influence of molecular properties of the alginates on acceleration

In the next step, the impact of the molecular properties of alginate samples on their accelerating effect was studied. Three key molecular parameters were considered: (1) the cation (e.g. Na^+, K^+ and NH_4^+) balancing the anionic charge; (2) the M/G ratio which impacts viscosity and strength gel; and (3) the degree of polymerisation which directly correlates to viscosity and molecular weight, respectively.

(1) When comparing the accelerating effectiveness of for example a sodium and an ammonium alginate, no specific effect of the cation was found (see Figure S-2 in supporting information), thus indicating that the cation plays no role here.

(2) The monomeric composition of alginates which is expressed by the ratio of mannuronic to guluronic acid incorporated, was also found

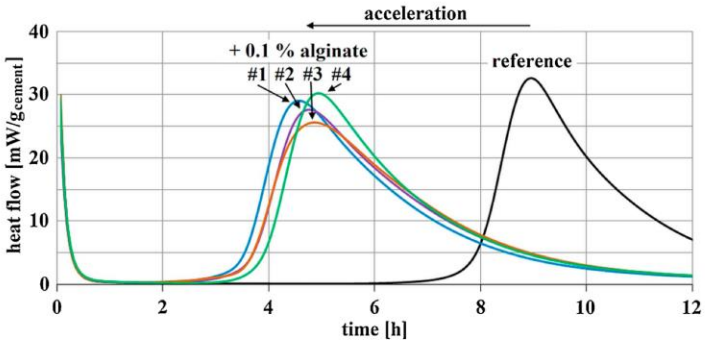

Fig. 2. Accelerating effect of four different alginate samples on CAC added at a dosage of 0.1 wt.%, as determined via heat-flow calorimetry (Secar 51, w/b = 0.5 ; #1 XEA 5036, #2 FD 170, #3 Manucol DH, #4 Protanal LF 200 FTS).

Table 3
Properties of four sodium alginate samples of different M/G-ratio (top) and properties of three sodium alginates of different viscosity grade (bottom), according to suppliers' specifications (viscosity, particle size) and own analysis (M/G ratio).

Alginate sample	Viscosity of a 1 % solution (20 °C)	Particle size	M/G ratio measured
Protanal LF 200 FTS	200–400 mPa s	< 200 µm	0.46 ± 0.04
XEA 5036	300–600 mPa s	< 180 µm	0.82 ± 0.04
FD 170	20–50 mPa s	< 100 µm	1.08 ± 0.05
Satialgine S 900 NS	350–550 mPa s	< 125 µm	1.46 ± 0.05

Alginate sample	Viscosity of a 1 % solution (20 °C)	Viscosity of a 10 % solution (20 °C)	Particle size	M/G ratio measured
ALGIN IL-2	20–50 mPa s	–	< 180 µm	1.49 ± 0.06
ALGIN ULV-1	< 1 mPa s	100–200 mPa·s	< 180 µm	1.31 ± 0.05
ALGIN ULV-L3	–	20–50 mPa·s	< 180 µm	1.16 ± 0.08

to be of no significant impact on the acceleration. To demonstrate, the accelerating effect of four alginates exhibiting very different M/G ratios, as shown in Table 3 (top), was assessed by heat-flow calorimetry (results displayed in Fig. 2). There, no noticeable difference related to the specific composition (M/G ratio) could be observed. The product samples tested exhibited M/G ratios between 0.4 and 1.6.

(3) Opposite to this, the viscosity grade of the alginate samples was found to be most critical for their accelerating effect. Using three samples of different viscosity grade, but of similar particle size and M/G ratio (Table 3, bottom), a comparison was performed. At decreasing viscosity, the acceleration observed via heat-flow calorimetry (Fig. 3) became less and even changed to retardation for ultra-low viscosity grades. Whereas for all alginate samples of high or very-high viscosity grade, no adverse effect could be observed.

Generally, the viscosity of an alginate solution is strongly influenced by the molecular weight of the polymer. This relationship is used in the Mark–Houwink equation to calculate the viscosity average molar mass from the intrinsic viscosity of a solution.

The correlation between the molecular weight and the viscosity grade of different sodium alginate samples was established based on existing literature (see Figure S-3 and S-4 in supporting information). There, for ultra-low viscosity grade alginate samples molecular weights (M_w) in the order of 10^4 Da are reported. It has to be noted that because of their natural origin, alginates exhibit a broad molecular weight distribution. The PDIs (determined by the ratio of M_w/M_n) of commercial products are reported to be as high as four (Fu et al., 2010). Accordingly, even sodium alginates with a higher molecular weight of e.g. 200 kDa (DP > 1000) can contain a noticeable fraction of low molecular (DP ≈ 250 at 50 kDa) alginate polymer. Moreover, low molecular weight samples may contain fractions with M_w as low as 10^3 Da. Those short-chain polysaccharides or even oligomeric components which often originate from the isolation process of the alginate (alkaline extraction and to some extent heat treatment for depolymerisation) seem to cause the retarding effect commonly observed for polysaccharides.

According to this analysis, it is recommendable to use alginates with a M_w of at least 10^5 Da or even higher molecular weight to achieve an accelerating effect.

3.3. Comparison of acceleration from alginates and lithium salts

As mentioned in the introduction, lithium salts are generally used to accelerate alumina cements. In order to check on the substitution potential of lithium via addition of alginates, respective systems and combinations were tested. The results of these experiments are displayed in Fig. 4.

First, it becomes clear that the alginate can achieve a comparable acceleration than lithium carbonate, albeit at a significantly higher dosage only. Furthermore, a combination of Li_2CO_3 and alginate produces an even stronger acceleration, thus demonstrating that both products can be combined well. Accordingly alginate can be used to save the precious lithium compound while keeping the same performance with respect to setting and hardening behavior of this cement. Similar results were obtained in other CAC samples.

3.4. Strength development of alginate treated CAC mortar

To probe further into the accelerating effect of the alginate, mortar testing was conducted using three different CAC samples of distinctly different composition and reactivity. The aim was to affirm the previous results from heat flow calorimetry.

In Ciment Fondu (≈ 38 % Al_2O_3), which exhibits a relatively fast setting, addition of the alginate XEA 5036 at a dosage of 0.1 wt.%

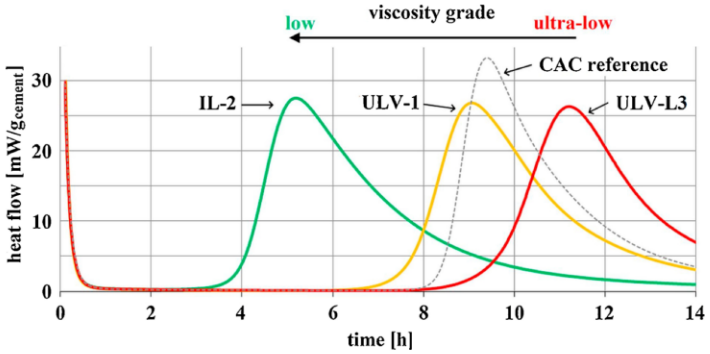

Fig. 3. Accelerating effect of three alginate samples of different viscosity on CAC added at a dosage of 0.1 wt.%, as determined via heat-flow calorimetry (Secar 51, w/b = 0.5).

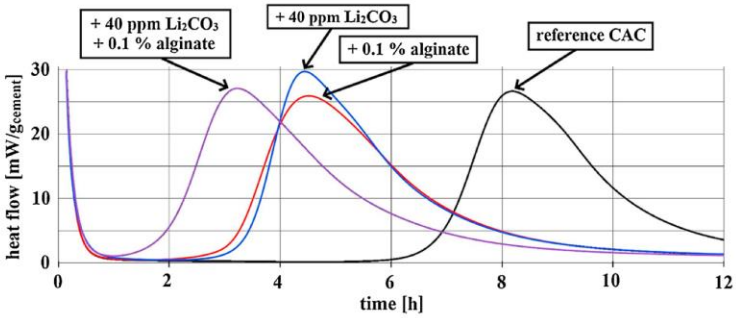

Fig. 4. Accelerating properties of a lithium salt, alginate XEA 5036 and a combination of both on CAC (Secar 71), as determined via heat-flow calorimetry (w/b = 0.62).

accelerates compressive strength development by ≈ ½ hour. Demolding of the specimens (at a compressive strength > 1 N/mm^2) in the presence of alginates was possible earlier compared to the reference.

For Ternal LC cement (≈ 52 % Al_2O_3) similarly an increase in early strength was observed upon addition of alginate. Here the strength increase after 6 hours of curing was 75 % (9.7 N/mm^2 → 17.2 N/mm^2; see Table S-3 in supporting information). Like in Ciment Fondu, addition of the biopolymer (dosage 0.1 wt.% XEA 5036) decreased the workability of the mortar because of its viscosifying property, resulting from a strong gelation in the presence of Ca^{2+} ions as was mentioned in the introduction. This undesired effect necessitates additional treatment with a PCE superplasticizer to achieve good workability. When Li_2CO_3 is used, no such extra treatment with a superplasticizer is required.

In the CA_2 rich Secar 712 (≈ 69 % Al_2O_3), which shows a long dormant period because of a surface modification of the clinker, the improvement in early strength was more pronounced. For example, after 16 hours of curing the compressive strength of the mortar was increased by 110 % upon addition of 0.1 wt.% XEA 5036 alginate (15.8 N/mm^2 → 33.4 N/mm^2 ; see Table 4). Moreover, after 12 hours of ageing the mortar from neat Secar 712 still had not hardened, whereas the sample containing alginate already had developed 11.5 N/mm^2 of compressive strength. This value is comparable to the strength of the neat cement after 16 h of curing, thus indicating an acceleration of about four hours.

3.5. Combination of alginate with PCE superplasticizers

Combination of alginate with PCE superplasticizer can effectively compensate the observed loss of workability owed to the water-binding and viscosifying properties of alginate. However, for PCEs has been shown before that they can induce severe retardation on calcium aluminate cements. Though this effect is much dependent on the specific molecular structure, particularly the side chain length and charge density of the PCE. Moreover, PCEs possessing short side chains and high anionic charge have proven to be almost ineffective in CAC because of chemical absorption (intercalation) into the structure of the C-A-H phases (Plank, Keller, Andres, & Dai, 2006; Ng, Metwalli, Müller-Buschbaum, & Plank, 2013; Assis, Parr, & Hu, 2008).

Here, a PCE possessing long side chains and a low anionic charge was selected for combination with alginate XEA 5036, to offset the viscosifying effect of the biopolymer. As can be seen from Table 4 this PCE effectively restores the fluidity of CAC pastes treated with alginate. Moreover, the retarding effect of the PCE is well compensated by the alginate. Similar results were obtained in other CAC samples.

Thus, this series of tests allows to conclude that CAC paste of high fluidity can be obtained even when alginate is used as accelerator.

4. Mechanistic study

The unexpected accelerating behaviour of alginate which moreover seems to be specific for CAC cements prompted an investigation into the mechanism underlying this effect. As a first step, a study was conducted by analysing the pore solution of the CAC in order to examine the influence of alginates on the ion concentrations shortly after preparing the cement paste.

4.1. Interaction of alginate with ions present in CAC pore solution

As mentioned in the introduction, alginates can interact with a variety of cations. Especially divalent cations such as Ca^{2+} are strongly complexed by the GG blocks of the alginate, leading to an ionotropic gelation. Alginate also shows a strong complexation with Sr^{2+} and Ba^{2+}, while on the other hand Mg^{2+} produces a weak gelation because

Table 4
Mortar properties for Secar 712 (w/b = 0.5) after 16 h of hydration, with and without addition of alginate XEA 5036 and in combination with PCE superplasticizer 114PC6.

Secar 712 16 h of curing	Reference	+ Alginate 0.1 %	+ PCE 0.02 % + Alginate 0.1 %	+ PCE 0.02 %
compressive strength (N/mm^2)	15.8 ± 1.5	33.4 ± 1.6 → 110 % increase	36.9 ± 1.3 → 135 % increase	5.2 ± 1.1 → 70 % decrease
tensile strength (N/mm^2)	2.1 ± 0.3	4.4 ± 0.4 → 110 % increase	4.4 ± 0.4 → 110 % increase	0.8 ± 0.2 → 65 % decrease
mortar density (g/L)	2240 ± 10	2,230 ± 5	2,290 ± 10	2,300 ± 5
spread flow (cm)	19.7 ± 0.1	17.8 ± 0.2	21.3 ± 0.1	24.0 ± 0.1

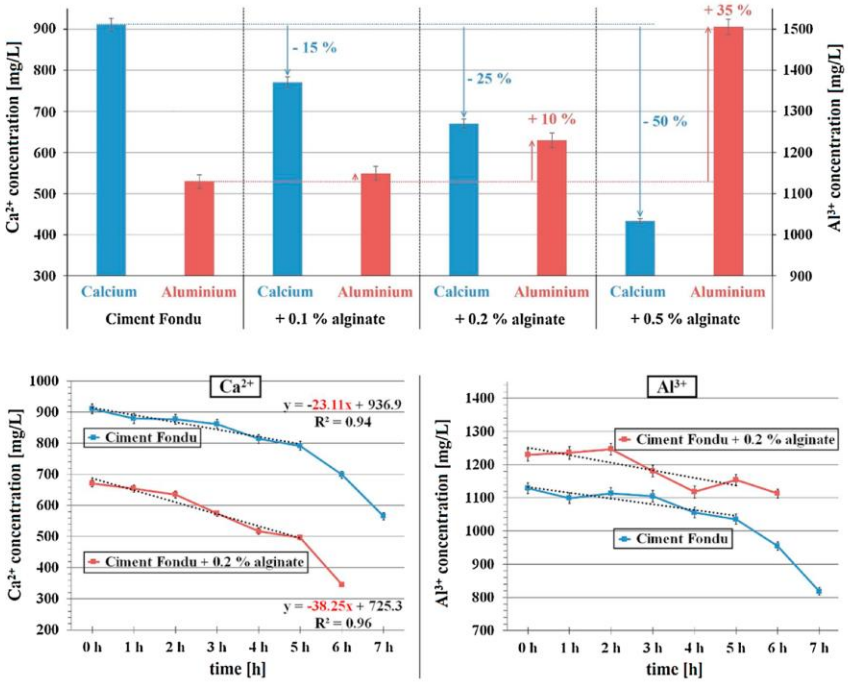

Fig. 5. Top: Ion concentrations of Ca^{2+} and Al^{3+} dissolved in the pore solution of Ciment Fondu (w/b = 0.5), treated without and with increasing dosages of alginate XEA 5036, as determined by ICP-OES; Bottom: Time dependent ion concentrations of Ca^{2+} (left) and Al^{3+} (right) in the pore solution of Ciment Fondu (w/b = 0.5), in the absence and presence of 0.2 wt.% alginate XEA 5036, determined via ICP-OES.

only a diffuse bonding takes place between magnesium and the alginate (Topuz, Henke, Richtering, & Groll, 2012).

According to Mignon et al. (2016), when sodium alginates are dissolved in ordinary portland cement paste, about 85 % of the sodium will be exchanged against calcium, leading to the formation of a viscous hydrogel. In our study, likewise an uptake of Ca^{2+} from pore solution of CAC (Ciment Fondu) upon addition of 0.1 wt.% alginate XEA 5036 was detected, whereby the concentration of Ca^{2+} in the CAC pore solution is decreased by 15 % compared to the neat cement paste (Fig. 5, top). At higher alginate dosages the Ca^{2+} binding capacity becomes even more pronounced and increases to 50 % of the free calcium which is removed from the solution. Such a strong reduction and complexation of the Ca^{2+} ion concentration normally comes with a strong retardation, such as is well-known from trisodium citrate or Rochelle salt. Hence it is most surprising that alginate, inspite of its pronounced calcium complexation ability as is demonstrated here, acts as an accelerator, and not as a retarder.

Theoretically, complexation of Fe^{3+} or Al^{3+} ions by the carboxylate groups present in the alginate is also possible, but because of the alkaline pH (≈ 12) in CAC pore solution those ions will form either $[Al(OH)_4]^-$ or insoluble hydroxides (e.g. $Fe(OH)_3$). As such, an interaction with the negatively charged carboxylate groups is unlikely. Interestingly, the Ca^{2+} chelating effect of the alginate fosters an increase in the concentration of Al^{3+} in the pore solution. The increased solubility of Al^{3+} can be explained by the decreased Ca^{2+} concentration, which promotes the dissolution of the aluminate from the clinker and might this way promote favourable conditions for the earlier formation of CAH phases.

This analysis signifies that if the accelerating effect of the alginate would increase with higher dosage, then its strong calcium complexing ability which favours the dissolution of the aluminate phases would be the key property responsible for its accelerating effect. However, the accelerating effect reaches a plateau at about 0.1 wt.% dosage and increases only marginally at higher dosages. Hence, an influence of the alginate on the solubility and dissolution of the clinker as it is proposed for lithium compounds can be excluded and does not present the mechanism behind its unusual accelerating effect. Furthermore, lithium carbonate, the classical CAC accelerator, was found to increase the concentration of both calcium and aluminium ions in the pore solution of CAC paste simultaneously by 5–10 % (Li_2CO_3 dosage of 25–100 ppm), thus signifying that lithium compounds work according to a completely different mechanism of acceleration, compared to alginate.

To further study the ion binding capability of alginate, the time dependent evolution of the Ca^{2+} concentration in cement paste with and without 0.2 wt.% of alginate was assessed (Fig. 5, bottom). Here, a gradual decrease of Ca^{2+} concentration with time was observed for both systems, but the decline was much more pronounced when alginate was present. In the presence of the biopolymer, the amount of free calcium in solution decreases considerably faster than in the neat cement. This implies an earlier formation of C-A-H phases which is consistent with the calorimetric tests (Fig. 2) and the results on strength development (Table 4). On the other hand, in the presence of alginate the concentration of aluminium ions is substantially higher than in the neat cement, thus confirming its increased solubility in the presence of alginate.

4.2. Interaction of alginate with common retarders

This reduction in Ca^{2+} ion concentration in pore solution as described above is most surprising for an accelerator, as this behaviour is characteristic for retardation. Therefore, the question arose how alginate would behave in combination with known retarders. Here, it would be expected to find an increased retardation as the amount of free calcium would be reduced severely by the combined calcium complexing ability. To investigate, combinations of alginate with Na_3-citrate and KNa-tartrate were tested. The calorimetric results are displayed in Fig. 6 (top).

At first it becomes obvious that in CAC citrate and tartrate develop their well-known retarding effect. However, when combined with them, alginate still accelerates and is able to not only compensate their retarding effect, but even produce a significant acceleration, inspite of the

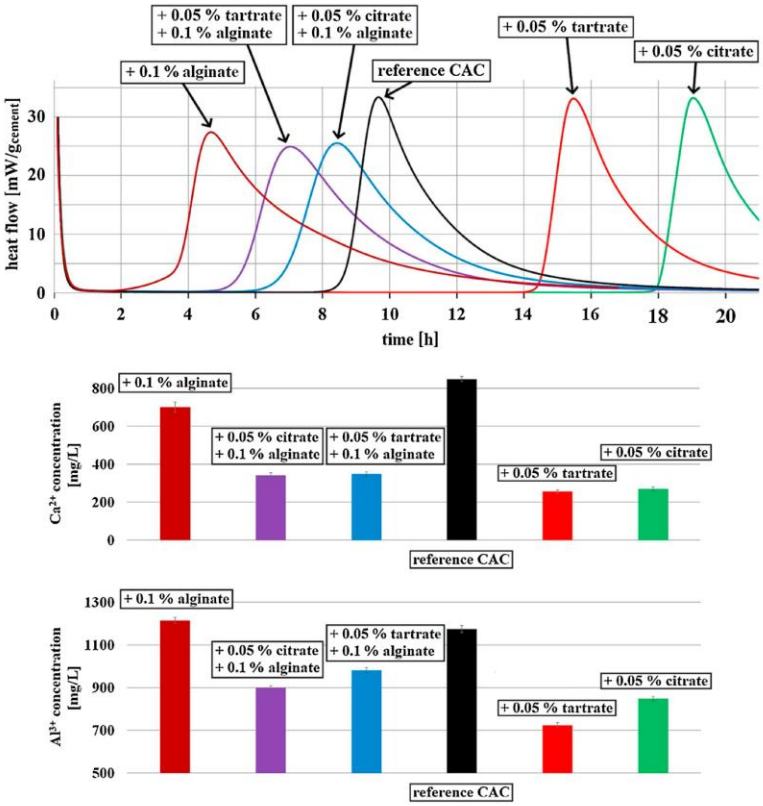

Fig. 6. Comparison of heat release and development of Ca^{2+} and Al^{3+} ion concentrations in CAC pore solution (Secar 51, w/b = 0.5, in the presence of the citrate and tartrate retarders, alginate XEA 5036 and combinations thereof), as determined by ICP-OES.

free calcium concentration in the pore solution being even substantially lower (≈ 40 % of the amount present in the neat cement paste) than in the presence of the alginate only (Fig. 6, bottom). Furthermore, the amount of aluminium ions in the pore solution was also reduced upon presence of the retarders in the CAC paste. Therefore should be expected that for the observed free ion concentrations of Ca^{2+} and Al^{3+}, the crystallisation of the CAH phases from the pore solution to be less favourable and result in a retardation.

Based upon these findings the question arises whether the decreased Ca^{2+} and Al^{3+} concentrations in fact accelerate the formation of C-A-H phases.

5. Conclusion

Our study demonstrates that alginates present a novel accelerator for aluminate cements, as is evidenced by heat-flow calorimetry and strength tests of mortar samples. Addition of this biopolymer seems to shorten the dormant period and therefore shifts the beginning of the hydration reaction to earlier times and results in noticeably higher early strengths. In comparison to lithium salts such as Li_2CO_3, alginate requires higher dosages and the addition of a superplasticizer to counteract its viscosifying effect. Moreover, a combination of alginate with lithium salts presents a viable option to reduce the consumption of precious lithium compounds in construction.

A first mechanistic study revealed that alginates reduce the concentration of free calcium ions present in the pore solution up to 50 %. This effect is owed to the well-known high calcium complexing ability of alginates as described by the “egg box” model. This result is most remarkable, because a chelation of Ca^{2+} is characteristic for common cement retarders. On the other hand, lithium compounds were found to increase the calcium as well as the aluminium ion concentrations which is caused by increased dissolution of the clinker. The experiments on alginates however clearly suggest, that the accelerating mechanism of lithium compounds does not apply to alginates. Consequently, a completely different mechanism is at work when alginates are added to CAC.

In future studies, further investigations on the accelerating mechanism involving XRD and solid state ^{27}Al MAS NMR spectroscopy are planned in order to observe the formation of the hydrate phases under these unusual conditions.

Acknowledgement

The authors are most grateful to *Imerys Aluminates* (formerly *Kerneos*) for the generous supply of aluminate cement over the years (especially Mr. A. Eisenreich and Mr. R. Kwasny-Echterhagen). Our thanks also go to *KIMICA* (especially M. Ishihara), *Eurogum*, *FMC*, *Roeper*, *Cargill*, *Danisco* and *Polygal* for providing different alginates samples. S. Gruber wishes to thank the Jürgen Manchot Foundation for generously providing a scholarship to finance her Ph.D. study at TU München.

The authors are most grateful to Deutsche Forschungsgemeinschaft, Bonn, Germany (DFG) for financing this project under the grant PL-472/13-1.

Appendix A. Supplementary data

Supplementary material related to this article can be found, in the online version, at doi: https://doi.org/10.1016/j.carbpol.2020.116038.

References

Assis, G., Parr, C., & Hu, C. (2008). *Technical paper 75: Improved additive systems for low cement, high purity castables.* France: Kerneos.

Bensted, J. (2002). *Calcium aluminate cementsStructure and performance of cements* (Second edition). Boca Raton, USA: CRC Press114–138.

Bizzozero, J., Gosselin, C., & Scrivener, K. L. (2014). Expansion mechanisms in calcium aluminate and sulfoaluminate systems with calcium sulfate. *Cement and Concrete Research, 56*, 190–202.

de Reese, J., Sperl, N., Schmid, J., Sieber, V., & Plank, J. (2015). Effect of biotechnologically modified alginates on LDH structures. *Bioinspired, Biomimetic and Nanobiomaterials, 4*(3), 174–186.

DIN EN 1015-3 (2007). *Methods of test for mortar for masonry – Part 3: Determination of consistence of fresh mortar (by flow table).* German version EN 1015-3.

DIN EN 196-1 (2016). *Methods of testing cement – Part 1: Determination of strength.* German version EN 196-1.

DIN EN 196-11 (2019). *Methods of testing cement – Part 11: Heat of hydration – Isothermal Conduction Calorimetry method.* German version EN 196-11.

Fu, S., Thacker, A., Sperger, D. M., Boni, R. L., Velankar, S., Munson, E. J., et al. (2010). Rheological evaluation of inter-grade and inter-batch variability of sodium alginate. *AAPS PharmSciTech, 11*(4), 1662–1674.

Gosselin, C., & Scrivener, K. L. (2008). *Microstructure development of calcium aluminate cement accelerated with lithium sulphate. Proceedings of Calcium Aluminate Cement, the Centenary Conference (Fentiman CH, Mangabhai, RJ and Scrivener KL).* Bracknell, UK: IHS BRE Press109–122.

Götz-Neunhoeffer, F. (2005). Kinetics of the hydration of calcium aluminate cement with additives. *ZKG International, 58*(4), 65–72.

Grant, G. T., Morris, E. R., Rees, D. A., Smith, P. J., & Thom, D. (1973). Biological interactions between polysaccharides and divalent cations: The egg-box model. *FEBS Letters, 32*(1), 195–198.

Imeson, A. P. (2011). *Food stabilisers, thickeners and gelling agents.* Hoboken - New Jersey, USA: Wiley Blackwell.

Lothenbach, B., Pelletier-Chaignat, L., & Winnefeld, F. (2012). Stability in the system $CaO–Al_2O_3–H_2O$. *Cement and Concrete Research, 42*(12), 1621–1634.

Mignon, A., Snoeck, D., D'Halluin, K., Balcaen, L., Vanhaecke, F., Dubruel, P., et al. (2016). Alginate biopolymers: Counteracting the impact of superabsorbent polymers on mortar strength. *Construction and Building Materials, 110*, 169–174.

Ng, S., Metwalli, E., Müller-Buschbaum, P., & Plank, J. (2013). Occurrence of intercalation of PCE superplasticizers in calcium aluminate cement under actual application conditions, as evidenced by SAXS analysis. *Cement and Concrete Research, 54*, 191–198.

Ostrander, D., & Schmid, M. (2015). *U.S. Patent No. 9,193,626.* Washington, DC: U.S. Patent and Trademark Office.

Parr, C., Bin, L., Alt, C., & Wohrmeyer, C. (2006). *Technical paper 54: Interactions between silica fume and CAC and methods to optimise castable placing properties.* France: Kerneos.

Pistone, S., Qoraglu, D., Smistad, G., & Hiorth, M. (2015). Formulation and preparation of stable cross-linked alginate–zinc nanoparticles in the presence of a monovalent salt. *Soft Matter, 11*(28), 5765–5774.

Plank, J. (2003). *Applications of biopolymers in construction engineering. Biopolymers: Vol. 10 General aspects and special applications.* Weinheim, Germany: Wiley-VCH29–95.

Plank, J., Keller, H., Andres, P. R., & Dai, Z. (2006). Novel organo-mineral phases obtained by intercalation of maleic anhydride–allyl ether copolymers into layered calcium aluminum hydrates. *Inorganica Chimica Acta, 359*(15), 4901–4908.

Plank, J., Zouaoui, N., Andres, P. R., & Schaefer, C. (2014). PCE superplasticizer - chemistry, application and perspectives. *ZKG International, 67*, 48–59.

Puerta-Falla, G., Kumar, A., Gomez-Zamorano, L., Bauchy, M., Neithalath, N., & Sant, G. (2015). The influence of filler type and surface area on the hydration rates of calcium aluminate cement. *Construction and Building Materials, 96*, 657–665.

Scrivener, K. L., & Capmas, A. (2003). *Calcium aluminate cementsLea's chemistry of cement and concrete* (Fourth edition). Oxford, UK: Butterworth-Heinemann713–782.

Sellimi, S., Younes, I., Ayed, H. B., Maalej, H., Montero, V., Rinaudo, M., et al. (2015). Structural, physicochemical and antioxidant properties of sodium alginate isolated from a Tunisian brown seaweed. *International Journal of Biological Macromolecules, 72*, 1358–1367.

Speirs, J., & Contestabile, M. (2018). *The future of lithium availability for electric vehicle batteries. Behaviour of lithium-ion batteries in electric vehicles.* Cham, Switzerland: Springer35–57.

Stolarz, R. (2003). *Product brochure – Alginates.* FMC Biopolymers.

Topuz, F., Henke, A., Richtering, W., & Groll, J. (2012). Magnesium ions and alginate do form hydrogels: A rheological study. *Soft Matter, 8*(18), 4877–4881.

Touzo, B., Gloter, A., & Scrivener, K. L. (2001). Mineralogical composition of Fondu revisited. *Proceedings of the International Conference on Calcium Aluminate Cement (CAC) (Mangabhai, RJ and Glasser FP)* (pp. 129–138).

Publikation 1:

Carbohydrate Polymers, 2020, 236.

Supporting information

The Effect of Alginates on the Hydration of Calcium Aluminate Cement

Alexander Engbert, Stefanie Gruber, Johann Plank*

Technische Universität München, Chair for Construction Chemistry, Lichtenbergstr. 4, 85747 Garching, Germany

*Corresponding author:

Prof. Dr. Johann Plank

Chair for Construction Chemistry

Technische Universität München

Lichtenbergstr. 4

85747 Garching bei München, Germany

Tel.: +49 (0) 89 289 13 151

Fax: +49 (0) 89 289 13 152

E-Mail: sekretariat@bauchemie.ch.tum.de

ORCID (Johann Plank): 0000-0002-4129-4784

2.1 Cement samples

Table S-1: Oxide composition (only contents ≥ 0.3 wt.-% are shown) and physical properties of the alumina cement samples.

Oxide / property	Ciment Fondu	Secar 51	Secar 71	Secar 712
	contents in wt.%			
Al_2O_3	38.7	51.6	69.4	68.8
CaO	37.5	36.8	29.3	29.0
Fe_2O_3	15.2	2.1	-	-
SiO_2	4.4	5.2	0.5	0.3
TiO_2	2.8	2.2	-	-
MgO	0.5	0.5	-	0.3
Blaine [cm^2/g]	2,810	3,880	3,570	3,370
d_{50} [µm]	18.1 ± 0.3	10.1 ± 0.5	12.8 ± 0.2	13.4 ± 0.2
Reactivity w/water	fast	medium	medium	slow

Oxide / property	Ternal EP	Ternal SE	Secar 41	Ternal LC	Secar 80
	contents in wt.%				
Al_2O_3	36.6	39.9	44.5	51.2	80.7
CaO	47.7	36.7	37.6	37.9	16.6
Fe_2O_3	7.0	15.2	7.2	1.7	-
SiO_2	4.6	4.5	5.6	5.3	0.3
TiO_2	1.9	1.8	2.2	2.5	-
MgO	0.3	0.5	0.3	0.4	0.3
Blaine [cm^2/g]	3,140	3,650	3,580	3,330	10,600
d_{50} [µm]	17.1 ± 0.2	11.2 ± 0.2	15.6 ± 0.2	15.9 ± 0.3	7.4 ± 0.5
Reactivity w/water	fast	fast	fast	medium	medium

2.2.1 Alginates

The linear correlation between the M/G-ratio and the relative intensity of the IR band with an R factor of > 0.9 is shown in **Figure S-1**. The high variation in the M/G ratio of the individual alginate samples is a result of the literature values [S1-S14] reported (**Table S-2**).

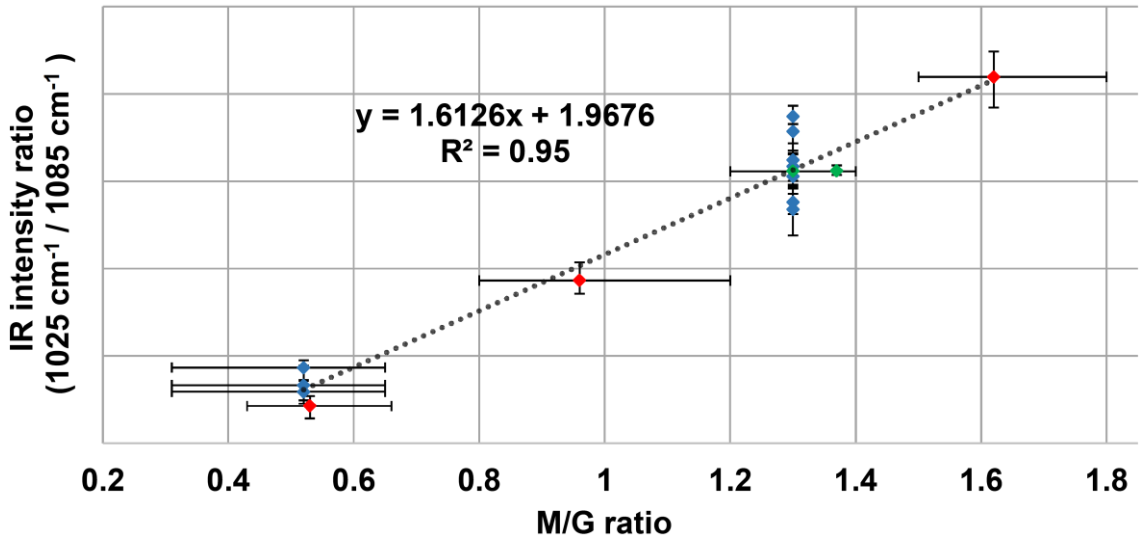

Figure S-1: Correlation between the M/G-ratio and the relative intensity of the IR bands for various alginates which are shown in the following table (blue = KIMICA, red = FMC, green = other).

Table S-2: Properties of different sodium alginates, according to suppliers' specifications, literature [S1-S14] and analysis by TUM

	Viscosity of a 1 % solution (20 °C)	Particle size	M/G ratio (literature)	M/G ratio measured
KIMICA ALGIN high-G	various	< 180 µm	≈ 0.52 [S1 – S3]	0.5 - 0.6
FMC Protanal LF 200 FTS	200 - 400 mPa·s	< 200 µm	≈ 0.53 [S4 - S6]	0.46 ± 0.04
FMC Scogin MV	350 - 500 mPa·s	< 710 µm	≈ 0.96 [S4, S7, S8]	0.91 ± 0.05
KIMICA ALGIN	various	< 180 µm	≈ 1.30 [S1, S2]	1.1 – 1.5
Sigma Aldrich W201502	5 - 40 mPa·s	-	≈ 1.30 [S9 - S11]	1.29 ± 0.04
Cargill Satialgine S 60 NS	20 - 50 mPa·s	< 125 µm	≈ 1.37 [S12]	1.30 ± 0.02
FMC Manucol DH	40 - 90 mPa·s	< 250 µm	≈ 1.62 [S4, S13, S14]	1.63 ± 0.1

3.1 Effect of alginate on CAC hydration

Table S-3: Time periods to reach the peak of heat release in heat flow calorimetry for different CAC samples upon addition of alginate sample XEA 5036 (w/b = 0.62).

CAC	neat	+ 0.1 wt.% Alginate	+ 0.2 wt.% Alginate
Fondu	4.1 ± 0.3	3.0 ± 0.2	2.9 ± 0.1
Secar 41	6.5 ± 0.2	5.1 ± 0.3	4.9 ± 0.2
Secar 51	9.1 ± 0.3	4.9 ± 0.2	4.6 ± 0.2
Secar 71	8.0 ± 0.2	4.3 ± 0.1	4.2 ± 0.1
Secar 712	18.8 ± 0.3	9.6 ± 0.2	7.9 ± 0.2
Secar 80	5.7 ± 0.2	5.3 ± 0.1	4.8 ± 0.1
Ternal EP	4.6 ± 0.1	3.8 ± 0.2	3.3 ± 0.4
Ternal SE	4.7 ± 0.3	3.7 ± 0.2	3.5 ± 0.1
Ternal LC	9.1 ± 0.3	4.7 ± 0.2	4.5 ± 0.2

3.2 Influence of molecular properties of the alginate on acceleration

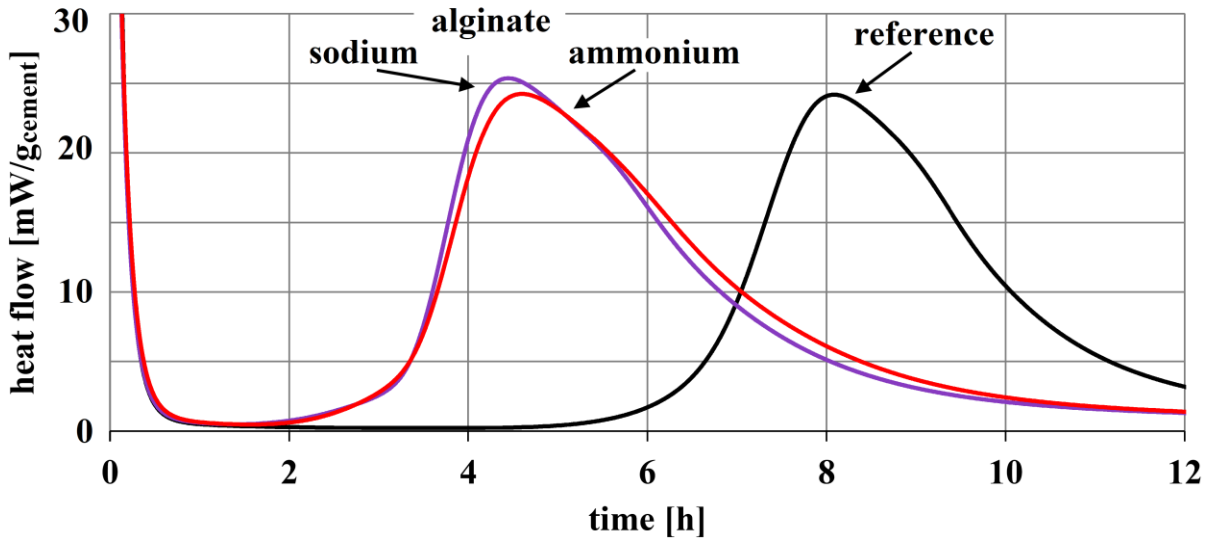

Figure S-2: Comparison of the accelerating effect of ammonium alginate (KIMICA ALGIN NH-3) and sodium alginate (Eurogum XEA 5036) on CAC, as determined via heat-flow calorimetry (Secar 71, w/b = 0.6, alginate dosage 0.1 wt.%).

The correlation between the viscosity of an alginate and its molecular weight is depicted in **Figures S-3** for a wide range of viscosities. The low and ultra-low viscosity range are depicted separately in **Figure S-4** for better distinction.

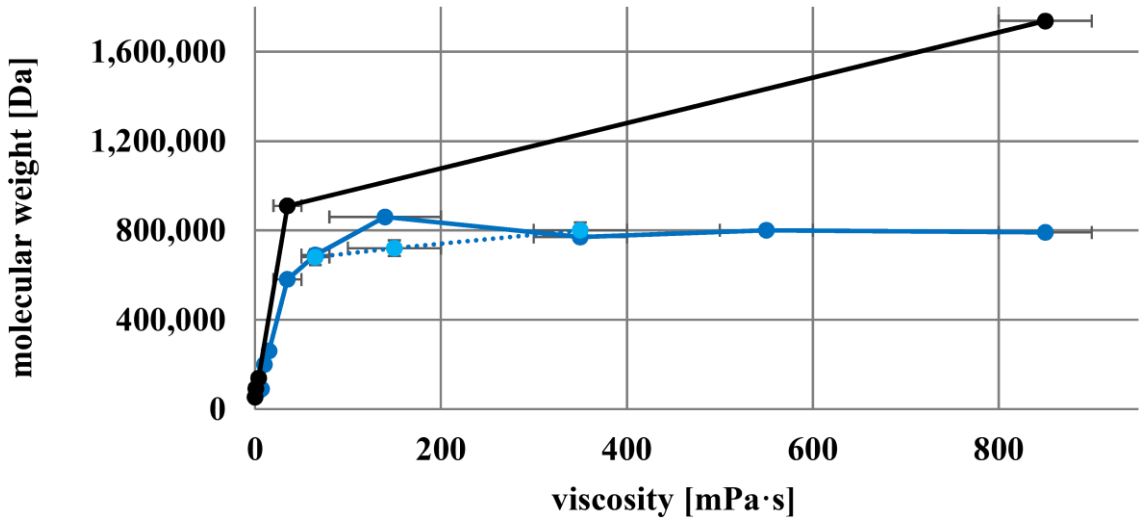

Figure S-3: Correlation between the molecular weight and the viscosity (1 % solution, 20 °C) for various alginates from KIMICA according to literature [S15, S16] (blue = ALGIN from [S15], light-blue = ALGIN high-G from [S15] and black = ALGIN from [S16]).

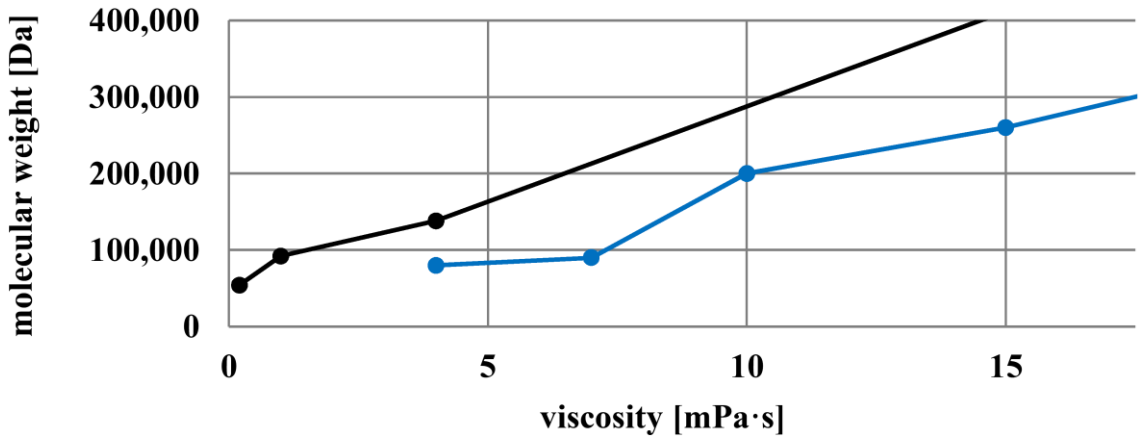

Figure S-4: Correlation between the molecular weight and the viscosity (1 % solution, 20 °C) at low viscosity grade for various alginates from KIMICA according to literature [S15, S16] (blue = ALGIN from [S15] and black = ALGIN from [S16]).

3.4 Strength development of alginate treated CAC mortar

Table S-4: Mortar properties for Ternal LC (w/b = 0.5) after 6 h of hydration with and without addition of 0.1 wt.% alginate sample XEA 5036.

Ternal LC 6 h of curing	**Reference**	**+ Alginate 0.1 %**
compressive strength (N/mm^2)	9.7 ± 1.0	17.2 ± 0.8 **→ 75 % increase**
tensile strength (N/mm^2)	1.4 ± 0.1	2.5 ± 0.2 **→ 80 % increase**
mortar density (g/L)	2,320 ± 5	2,300 ± 5
spread flow (cm)	24.1 ± 0.2	18.8 ± 0.1

Literature

[S1] Sakai, S., Ono, T., Ijima, H., Kawakami, K., *Permeability of alginate/sol–gel synthesized aminopropyl-silicate/alginate membrane templated by calcium-alginate gel*, Journal of membrane science, *205*(1-2), **2002**, p. 183-189.

[S2] Kakita, H., Kamishima, H., *Some properties of alginate gels derived from algal sodium alginate*, In Nineteenth International Seaweed Symposium, p. 93-99, **2008**, Springer, Dordrecht.

[S3] Karakasyan, C., Mathos, J., Lack, S., Davy, J., Marquis, M., Renard, D., *Microfluidics-assisted generation of stimuli-responsive hydrogels based on alginates incorporated with thermo-responsive and amphiphilic polymers as novel biomaterials*, Colloids and Surfaces B: Biointerfaces, *135*, **2015**, p. 619-629.

[S4] Rynka, S., personal correspondence, **2017**.

[S5] Mottet, L., Le Cornec, D., Noël, J. M., Kanoufi, F., Delord, B., Poulin, P., Bibette, J., Bremond, N., *A conductive hydrogel based on alginate and carbon nanotubes for probing microbial electroactivity*, Soft matter, *14*(8), **2018**, p. 1434-1441.

[S6] Schweizer, D., Schönhammer, K., Jahn, M., Göpferich, A., *Protein–polyanion interactions for the controlled release of monoclonal antibodies*, Biomacromolecules, 14(1), **2012**, p. 75-83.

[S7] Gao, C., Pollet, E., Avérous, L., *Properties of glycerol-plasticized alginate films obtained by thermo-mechanical mixing*, Food hydrocolloids, *63*, **2017**, p. 414-420.

[S8] García-Astrain, C., Avérous, L., *Synthesis and evaluation of functional alginate hydrogels based on click chemistry for drug delivery applications*, Carbohydrate polymers, *190*, **2018**, p. 271-280.

[S9] Stößlein, S., Grunwald, I., Stelten, J., Hartwig, A., *In-situ determination of time-dependent alginate-hydrogel formation by mechanical texture analysis*, Carbohydrate polymers, 205, **2019**, p. 287-294.

[S10] Rhein-Knudsen, N., Ale, M. T., Ajalloueian, F., Meyer, A. S., *Characterization of alginates from Ghanaian brown seaweeds: Sargassum spp. and Padina spp*, Food Hydrocolloids, 71, **2017**, p. 236-244.

[S11] Mohammed, A., Bissoon, R., Bajnath, E., Mohammed, K., Lee, T., Bissram, M., John, N., Jalsa, N.K., Lee, K.-Y., Ward, K., *Multistage extraction and purification of waste Sargassum natans to produce sodium alginate: An optimization approach*, Carbohydrate polymers, 198, **2018**, p. 109-118.

[S12] Martins, E., Poncelet, D., Marquis, M., Davy, J., Renard, D., *Monodisperse core-shell alginate (micro)-capsules with oil core generated from droplets millifluidic*, Food hydrocolloids, *63*, **2017**, p. 447-456.

[S13] Horniblow, R. D., Latunde-Dada, G. O., Harding, S. E., Schneider, M., Almutairi, F. M., Sahni, M., Bhatti, A., Ludwig, C., Norton, I. T., Iqbal, T. H. Tselepis, C., *The chelation of colonic luminal iron by a unique sodium alginate for the improvement of gastrointestinal health*, Molecular nutrition & food research, 60(9), **2016**, p. 2098-2108.

[S14] Chan, E. S., Lim, T. K., Voo, W. P., Pogaku, R., Tey, B. T., Zhang, Z., *Effect of formulation of alginate beads on their mechanical behavior and stiffness*, Particuology, 9(3), **2011**, p. 228-234.

[S15] Fukuda, T., Tamura, H., *Adhesion preventing material*, U.S. Patent No. 9,901,662, **2018**.

[S16] Takahashi, Y., *Physiologically active complex comprising protamine and/or salt therefor and an acidic macromolecular substance, and use thereof*, U.S. Patent No. 8,399,014, **2013**.

3.1.3 Addendum

Zusätzlich zu den in der Publikation dargestellten Ergebnissen wurden noch weiterführende Untersuchungen durchgeführt, welche im Folgenden erläutert werden:

Im Rahmen der Publikation wurde die Wirksamkeit von Alginat bei w/z-Verhältnissen von 0,4 bis 0,7 getestet. In weiteren Versuchen, die nicht in der Publikation beschrieben sind, wurde durch Zugabe von PCE-Fließmitteln der w/z-Wert auf 0,3 gesenkt. Weil Aluminatzemente unter diesen Bedingungen zur Sedimentation neigen, musste dem Referenzsystem zusätzlich ein Stabilisierer (Celluloseether) zugesetzt werden. Bei Verwendung von Alginat konnte auf den Einsatz des Celluloseethers verzichtet werden, da das Alginat bereits dessen stabilisierende Funktion übernimmt. Bei diesen Experimenten mittels Wärmeflusskalorimetrie, dargestellt in den **Abbildungen A1** und **A2** (in **Abschnitt 7.1** des Anhangs), wurde festgestellt, dass Alginat auch bei niedrigem w/z-Wert und hoher Fließmitteldosierung einen beschleunigenden Effekt auf den CAC ausübt.

Näher untersucht wurde weiterhin der Einfluss der mineralogischen Zusammensetzung des CAC auf die Wirksamkeit von Alginat. Hierzu ist der beschleunigende Effekt auf einzelne Klinkerphasen, die sowohl selbst synthetisiert als auch bereits am Lehrstuhl vorhanden waren, betrachtet worden. Alginat wirkte gleichwohl auf $C_{12}A_7$, CA und CA_2 als Beschleuniger, wobei dessen Effektivität von der jeweiligen Klinkerphase, deren Reinheit und Herstellungsmethode beeinflusst wurde. Details hierzu können dem Anhang (**Abschnitt 7.2**) entnommen werden. Generell zeigte das Alginat die stärkste Wirkung auf CA.

Ebenfalls wurden Mörtelfestigkeiten in *„Secar 71“* ergänzend zu den Experimenten im Kalorimeter durchgeführt, um den Einfluss der Molmasse des Alginats auf dessen Wirksamkeit auch im Mörtel zu bestimmen. Die gemessenen Druckfestigkeiten nach 4 Stunden waren 4.4 N/mm^2 mit einem Alginat von besonders niedriger Viskosität und 12,5 N/mm^2 für ein Alginat mit mittlerer Viskosität im Vergleich zum reinen CAC mit 4,7 N/mm^2. Sie bestätigten die an CAC-Pasten im Kalorimeter beobachtete Abhängigkeit der beschleunigenden Wirkung von der Viskosität bzw. Molmasse des Alginats. Eine mögliche Erklärung für den Verlust der Beschleunigung bei niedrigem M_w liefert *Kohn (1975)* [186], welcher die Aktivitätskoeffizienten der oligomeren Uronsäuren mit Ca^{2+}-Ionen bestimmt hat. Hierbei wurde für Mannuronat, Guluronat und Galakturonat experimentell festgestellt, dass erst ab einem Polymerisationsgrad von 13 - 30 eine starke Wechselwirkung mit Calcium auftritt. Dies führt zu einer sinkenden Löslichkeit des

Alginat-Calcium-Komplexes und dessen Gelierung. Daher könnte der Verlust der Wirkung niedermolekularer Alginate mit der Löslichkeit der Oligomer-Komplexe begründet sein. Gelöste Calcium-Alginat-Komplexe stehen für den Wirkmechanismus, wie er in **Publikation 3** vorgeschlagen wurde, nicht zur Verfügung. Des Weiteren postulieren *Fang et al. (2007)* [115] eine unterschiedliche molekulare Anordnung von Ca^{2+}-Alginat-Komplexen in Abhängigkeit von der Molmasse des Alginats. Der von diesen Autoren vorgeschlagene Mechanismus für ein niedermolekulares Alginat mit einer Molmasse von 35 kDa bzw. ein hochmolekulares Alginat mit 404 kDa ist in **Abbildung 31** illustriert.

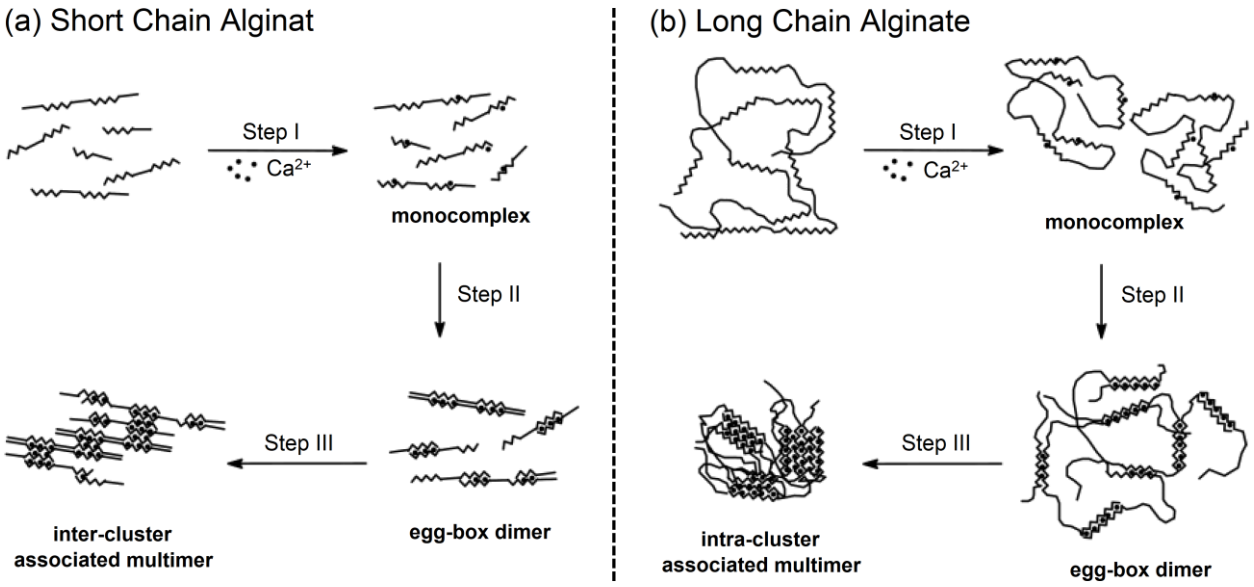

Abbildung 31: Komplexierung eines Calcium-Alginat-Hydrogels für ein Alginat mit hoher bzw. niedriger Molmasse, abgedruckt in bearbeiteter Form mit Genehmigung aus [115].

3.2 Publikation 2: Strukturmerkmale beschleunigender Biopolymere

3.2.1 Zusammenfassung

Nach den in der vorherigen Publikation dargelegten Ergebnissen sind die Eigenschaften des Alginats, insbesondere die Calciumbindefähigkeit und das Molgewicht, für dessen Wirkung ausschlagend.

In der nachfolgenden Studie konnten folgende weitere Erkenntnisse gewonnen werden:

- „Sortenreine“ Alginate, extrahiert aus einer spezifischen Spezies, Genus und Ordnung der Braunalge, wurden erworben und auf ihre Effektivität als Beschleuniger getestet. Dabei wurde kein nennenswerter Unterschied festgestellt. Demnach zeigen Alginate unabhängig von ihrer Herkunft (diese beeinflusst das M/G-Verhältnis und die Monomer-Blockstruktur) eine beschleunigende Wirkung.
- Propylenglykolalginat, ein kommerziell verfügbares propoxyliertes Alginat-Derivat, sowie weitere selbst synthetisierte veresterte Alginate zeigten infolge einer Blockierung der Carboxylatgruppen sowie einer Abschirmung durch Seitenketten einen reduzierten beschleunigenden Effekt.
- Reduktion der Carboxylatgruppe im Alginat zu einer Hydroxylgruppe (= geringere anionische Ladung) oder Sulfatierung des Alginats (= Erhöhung der anionischen Ladung) führten in beiden Fällen zu einer Abnahme der beschleunigenden Wirkung.
- Weitere hochmolekulare Biopolymere (natürlicher, mikrobieller und semi-synthetischer Herkunft) mit ähnlichen Strukturmerkmalen zeigten ebenfalls beschleunigende Wirkung auf die CAC-Hydratation. Carrageen (κ und ι) und Pektin wurden als weitere Polymere, die einen mit Alginat vergleichbar starken beschleunigenden Effekt auf das Abbinden von CAC zeigen, identifiziert.
- Der Vergleich von Alginat, Pektin und Carrageen ergab, dass die anionische Ladung sowie ein weiteres gemeinsames Strukturmerkmal, welches hohes Komplex-bindungsvermögen für Kationen aufweist, entscheidend für die beschleunigende Wirkung ist.
- Eine weitere Gemeinsamkeit aller beschleunigenden Biopolymere ist die Fähigkeit, Calcium-Ionen aus der Zementporenlösung stark zu binden, wie mittels ICP-OES festgestellt werden konnte.

- Allerdings besitzen auch niedermolekulare Alginate, welche die CAC-Hydratation verzögern, eine starke Calciumbindefähigkeit. Demnach wird für die Beschleunigung ein komplexes Wechselspiel aus unterschiedlichen Strukturmerkmalen benötigt.

3.2.2 Veröffentlichung

Identification of Specific Structural Motifs in Biopolymers That Effectively Accelerate Calcium Alumina Cement

Engbert A., Plank J.

Industrial & Engineering Chemistry Research, 2020, 59(26), 11930–11939.

https://doi.org/10.1021/acs.iecr.0c01620

I&EC research
Industrial & Engineering Chemistry Research
pubs.acs.org/IECR
Article

Identification of Specific Structural Motifs in Biopolymers That Effectively Accelerate Calcium Alumina Cement

Alexander Engbert and Johann Plank*

Cite This: *Ind. Eng. Chem. Res.* 2020, 59, 11930−11939
Read Online
ACCESS | Metrics & More | Article Recommendations | Supporting Information

ABSTRACT: Following a previous study where we presented on the surprising accelerating effect of alginates on calcium aluminate cement (CAC), we now systematically screened specific groups of biopolymers, hoping to identify other polysaccharides that also can accelerate CAC. Testing of pure, noncompounded alginates from different species/genera of algae revealed comparable strong acceleration, while chemical modification via esterification, decarboxylation, or sulfatation reduced the accelerating effect, thus highlighting the importance of high anionic charge and the presence of carboxylate groups as key structural features. Furthermore, biopolymers possessing a "cavity" that effectively can chelate and capture Ca^{2+}, such as alginate, were found as another key structural unit; hence, pectin and *ι*- as well as *κ*-carrageenan were identified as biopolymers that possess a similar accelerating effect to alginate. Among other natural, synthetic, or semisynthetic biopolymers, karaya, gellan, and xanthan gum as well as agarose produced a slight accelerating effect, whereas konjac gum, hydroxypropyl guar, and methyl hydroxyethyl cellulose ether either perform neutral or retard CAC hydration. A preliminary mechanistic study revealed that effective accelerators reduce the concentration of free Ca^{2+} present in the cement pore solution and that a combination of high anionic charge, presence of a Ca^{2+} capturing cavity, and a high M_w is required for a biopolymer to act as an accelerator in CAC. Our concept of using biopolymers such as alginate allows us to replace at least partially lithium salts (e.g., Li_2CO_3), which are currently applied to accelerate CAC but are much needed for the production of Li-ion batteries that are necessary for widespread electromobility.

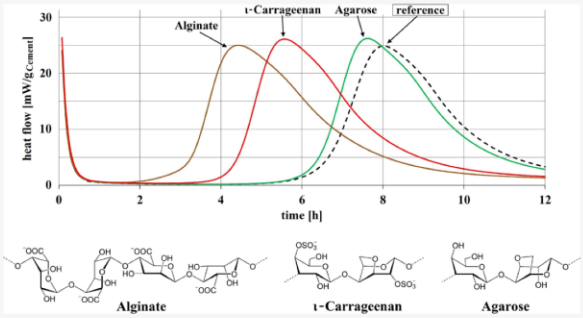

1. INTRODUCTION

In a previous study, we reported on the surprising accelerating effect of randomly selected alginates on the hydration of calcium alumina cement (CAC).[1] Alumina cements mainly consist of monocalcium aluminate, which reacts with water via a dissolution and precipitation process to form calcium aluminate hydrate (C−A−H) phases, such as $[Ca_2Al(OH)_6]^+[Al(OH)_4\cdot xH_2O]^-$ and $CaAl_2(OH)_8(H_2O)_2\cdot xH_2O$. Interestingly, the accelerating effect of alginates was observed for only CAC and did not occur in other binders such as ordinary Portland cement (OPC) or calcium sulfoaluminate cement (CSA). Furthermore, a preliminary study on the mechanism of acceleration induced by alginate surprisingly revealed that the biopolymer reduces the free calcium concentration present in the pore solution. Such behavior is characteristic of hydration retarders[2] and to our knowledge so far has never been reported for accelerators. Especially, for a polysaccharide, such an effect is unusual because, for example, monosaccharides including gluconate or galactose present strong hydration retarders. In view of this unusual accelerating behavior, the question arose whether other biopolymers possessing structural motifs similar to those of alginates, such as carrageenans and pectins, can also accelerate CAC.

Alginates are copolymers composed of guluronic (G) and mannuronic (M) acids that are glycosidically connected at the *α*-1 → 4 and *β*-1 → 4 positions to form a linear polymer with an average molecular weight between 10 000 and 600 000 Da.[3] The carbohydrate monomer units G and M can be linked in different tactical sequences like GG, GM, and MM, thus producing different steric arrangements. Apart from the molecular weight (which defines the chain length and viscosity of the polymer), the ratio between these blocks is mostly responsible for the properties of the polymer. In the presence of divalent cations such as Ca^{2+}, the GG blocks facilitate the formation of a highly viscous gel, commonly described by the "egg-box" model.[4] There, a "cavity" containing several oxygen atoms chelates these cations, which are also coordinated to the carboxylate group (see Figure 1).

Received: March 30, 2020
Revised: June 5, 2020
Accepted: June 5, 2020
Published: June 17, 2020

https://dx.doi.org/10.1021/acs.iecr.0c01620
Ind. Eng. Chem. Res. 2020, 59, 11930−11939

Industrial & Engineering Chemistry Research pubs.acs.org/IECR Article

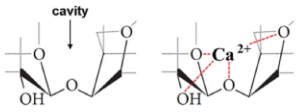

Figure 1. Illustration of the cavity that presents a common characteristic structural feature in alginates and carrageenans, and the coordination to cations (e.g., Ca^{2+}).

Commercial pectin is mainly composed of linearly homopolymerized galacturonic acid with some residues of rhamno galacturonan, which forms side chains made up of neutral sugars like galactose and arabinose. Pectins possess a cavity that is very similar to that present in alginates and are distinguished by their degree of esterification (DE). High methoxylation (DE = 55−75%) or low methoxylation (DE = 20−45%) of the carboxylate groups strongly influences the gelling properties of pectins. Of interest is low methoxy pectin (LM pectin) that in the presence of Ca^{2+} ions forms a gel according to a similar mechanism as described by the egg-box model for alginates. It is worth noting that relative to their structures, polygalacturonic acid (pectin) and polyguluronic acid (alginate) structurally are almost mirror images of each other.[3,5,6]

Carrageenans are composed of galactose and 3,6-anhydro galactose, which are linked at the α-1 → 4 and β-1 → 3 positions to form a copolymer. Typical molecular weights range between 200 000 and 800 000 Da. Kappa (κ)- and iota (ι)-carrageenan differ by the degree of sulfatation, while the lambda (λ) modification exhibits a structural modification and thus shows different behavior in solution as well as relative to its interaction with ions. κ- and ι-carrageenan also possess a cavity and can form a gel in the presence of specific cations (e.g., Ca^{2+}) by bridging with the sulfate groups, as illustrated in Figure 2.[3,5]

Alginates, pectins, and carrageenans are biopolymers of natural origin, which are produced by extraction from brown algae (Phaeophyceae), citrus/malus fruits, and red algae (Rhodophyceae), respectively.[3]

In the present study, the potential accelerating effect on CAC of commercial pristine and chemically modified alginate samples as wells as other biopolymers exhibiting similar structural motifs to alginate was assessed and their behavior was compared with that of a reference alginate with the aim to identify the structural motifs that are responsible for the accelerating effect. First, alginates from different algae species were probed to clarify whether the accelerating effect presents a general feature of alginates or is specific to an individual genus. Additionally, chemically derivatized alginates (esterified, decarboxylated, or sulfated ones) were procured or self-synthesized to investigate the role of the carboxylate functionality present in alginates. Moreover, biopolymers possessing a similar cavity to that present in alginates (namely, pectin and carrageenans) were tested for their accelerating potential. Also, natural (karaya and konjac gum), microbial (xanthan and gellan gum), and semisynthetic biopolymers (cellulose and guar ether) were screened. From these investigations, it was hoped to identify the key structural motif that enables a biopolymer to successfully accelerate CAC. Finally, to understand the mechanism underlying the accelerating effect, the concentration of free Ca^{2+} ions present in the pore solution of CAC admixed with these biopolymers was determined via Inductively coupled plasma atomic emission spectroscopy (ICP-OES) measurements.

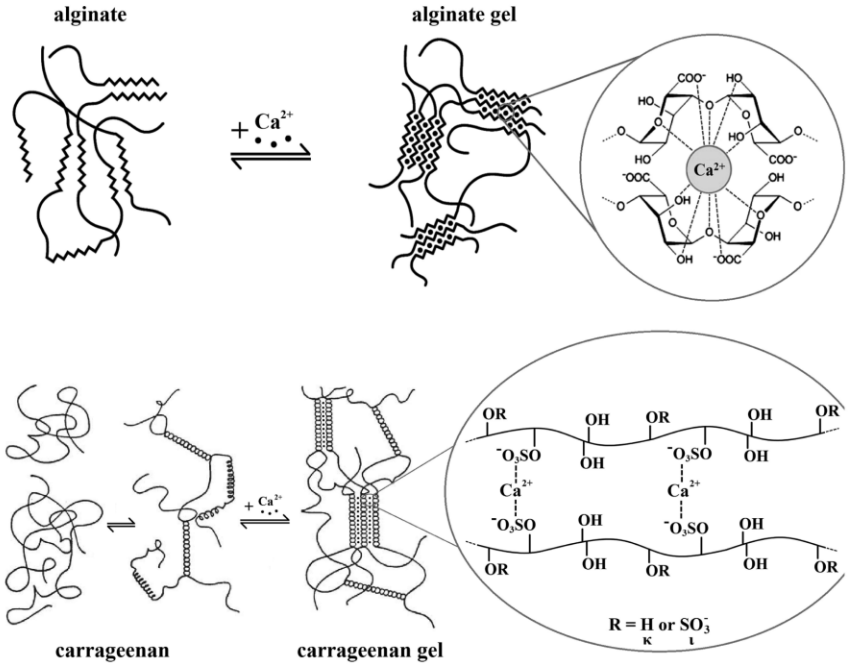

Figure 2. Mechanism of Ca^{2+}-induced complexation of alginate (top, adopted from ref 1 Copyright 2020 Engbert, Gruber, Plank, published by Elsevier Ltd.) and carrageenan (bottom, adapted from ref 3 Copyright 2009 John Wiley and Sons).

https://dx.doi.org/10.1021/acs.iecr.0c01620
Ind. Eng. Chem. Res. 2020, 59, 11930−11939

2. EXPERIMENTAL SECTION

2.1. Cement Samples. Different calcium aluminate cements (Ciment Fondu, Secar 41, Secar 51 and Secar 71, produced by Imerys Aluminates, France) were utilized. Their mineralogical composition (see Table 1) was determined via X-ray diffraction (XRD) (D8 Advance instrument, Bruker AXS, Karlsruhe, Germany) using Rietveld refinement, while their oxide composition (see 1) was analyzed using XRF (Axios, PANalytical, Kassel, Germany).

Table 1. Typical Phase Composition (wt %) of the CAC Samples Used in the Study[a]

	CAC sample (wt %)			
Phase	Ciment Fondu	Secar 41	Secar 51	Secar 71
CA	47−57	54−66	64−74	54−64
CA_2	n.d.	n.d.	n.d.	36−44
C_2AS	1−10	10−22	18−22	<1
C_4AF	10−20	n.d.	n.d.	n.d.
C_2S	1−10	1−10	1−5	n.d.
$C_{12}A_7$	1−5	1−5	<1	<1
other	C_3FT, $C_{20}A_{13}M_3S_3$	CT,C_3FT, $C_{20}A_{13}M_3S_3$	CT, C_3FT	α-Al_2O_3 (<2)

[a]Adapted from ref 1 Copyright 2020 Engbert, Gruber, Plank, Published by Elsevier Ltd.

2.2. Materials. Deionized water obtained from a Barnstead Nanopore Diamond Water purification system (Werner Reinstwassersysteme, Leverkusen, Germany) was used in all experiments. Methoxy polyethylene glycol (M-PEG)/PEG macromonomers for grafting were provided by Clariant (Burgkirchen, Germany). *p*-Toluenesulfonic acid, 1-ethyl-3-(3-dimethylamino-propyl) carbodiimide, $NaNO_2$, and $NaHSO_3$ were bought from Merck (Darmstadt, Germany), and sodium borohydride was supplied by Acros Organics (New Jersey).

2.2.1. Biopolymers. The commercial biopolymer products Eurogel XEA 5036 (sodium alginate, Eurogum, Herlev, Denmark), Gelcarin GP 379 NF (*ι*-carrageenan, FMC BioPolymer, Philadelphia), CU 701 (LM pectin, Herbstreith & Fox, Neuenbürg, Germany), and K3B426 (propylene glycol alginate, FMC BioPolymer, Philadelphia) are key materials utilized in this study. Their properties are presented in Table 2.

Table 2. Properties of Key Biopolymer Samples Used in the Study

sample	biopolymer	properties
XEA 5036	sodium alginate	M/G ratio ≈ 0.8[1]
GP 379	*ι*-carrageenan	M_w ≈ 271 kDa[7]
CU 701	LM pectin	GalA content ≈ 91%, DE ≈ 31%, M_w ≈ 320 kDa, M_n ≈ 63 kDa[8]
K3B426	propylene glycol alginate	DE ≈ 55%, M/G ratio ≈ 1.6[9]

Furthermore, several "pure" alginates (samples ALG100−ALG104) extracted from specific algae species and focuidan (FUC400, a sulfated polymer extracted from brown algae) were purchased from Elicityl (Crolles, France). Additionally, several *κ*-carrageenans (Cerogel SRC K4100, Roeper; Gelcarin PH812/GP911, FMC), xanthan gum (CX900, Cargill), gellan gum (type 700 low acyl, Roeper), agarose (Biozyme LE, Biozym Scientific), hydroxypropyl guar gum (Galactasol 474, Ashland), karaya gum (Ceroka Nr.1, Roeper), konjac gum (Cerokon CKHY 1240, Roeper), methyl hydroxyethyl cellulose ether (MHB 10000 P2, SE Tylose), and *λ*-carrageenan (Viscarin GP 209 NF, FMC) were also investigated. Their individual chemical structures are presented later in the sections describing their performance.

2.2.2. Chemical Modification of Alginate. To elucidate the specific structural motifs that are responsible for the accelerating effect of alginate, several modifications were also undertaken in our lab. Those included (1) esterification of the carboxylate groups with methoxy polyethylene glycol (M-PEG) or polyethylene glycol (PEG) of variable chain lengths (M_w), (2) reduction of the carboxylate group to an alcohol, and (3) sulfatation of the hydroxyl groups. A schematic presentation of the individual reaction patterns is provided later in Scheme 1 (see Section 3.1.2).

Esterification was performed in accordance with the procedure utilized in the preparation of M-PEG polycarboxylate comb polymers.[10] Here, alginate, water, and M-PEG or PEG were heated up to 95 °C until all components form a homogeneous solution. After the addition of *p*-toluenesulfonic acid as a grafting catalyst, water was removed through vacuum distillation (0.01 mbar, 120 °C) and the temperature was set to 175 °C to start the grafting. After about 4 h, the esterification was complete, and the product was cooled to ambient and then purified via dialysis.

Reduction of the carboxylate groups was carried out as described by Taylor and Conrad.[11] First, the alginate was coupled with EDC·HCl (1-ethyl-3-(3-dimethylamino-propyl) carbodiimide) at an acidic pH (≈4.75 using HCl, 2 h, room temperature) to obtain the amide. Afterward, the reduction was carried out at room temperature by dropwise addition of the sodium borohydride solution. The pH was continuously adjusted to 7 using dilute hydrochloric acid. The product was purified via dialysis.

Sulfatation was achieved using the following procedure:[13] $NaHSO_3$ is dissolved in water and heated up to 90 °C. Next, an aqueous solution of $NaNO_2$ is added dropwise to the $NaHSO_3$ solution. After stirring for 1.5 h, the mixture is cooled to 40 °C and then alginate is added. The mixture is agitated for 4 h, and the resulting sulfated alginate was purified via dialysis.

2.3. Experimental Methods. *2.3.1. Isothermal Heat Flow Calorimetry.* Paste calorimetry was performed according to DIN EN 196−11.[12] Four grams of cement was filled in sealable 10 mL glass ampoules and dry-blended with a previously placed polymer powder. This blend was then mixed with deionized water and homogenized for 2 min using a vortex mixer VWT 1419 (VWR, Ismaning, Germany). The ampoules were placed in an isothermal heat flow conduction calorimeter, TAM air model 3116-2 (Thermometric, Järfälla, Sweden), for monitoring the heat flow. Measurements were repeated at least twice and conducted at 20 °C until heat evolution ceased.

All calorimetric tests were performed using the same shipment of each cement because CAC is very sensitive to aging (uptake of moisture and CO_2). It was observed that results can vary depending on the age and storage conditions of different batches from the same cement.

2.3.2. Ion Concentrations via ICP-OES. Inductively coupled plasma atomic emission (ICP-OES) spectroscopy was conducted on a series 700 model (Agilent Technologies, Santa Clara, CA). The cement paste was prepared by admixing 20 g of Ciment Fondu dry-blended with 0.1 wt % polymer in a

https://dx.doi.org/10.1021/acs.iecr.0c01620
Ind. Eng. Chem. Res. 2020, 59, 11930−11939

Industrial & Engineering Chemistry Research pubs.acs.org/IECR Article

Scheme 1. Structures and Synthesis Routes for the Preparation of Chemically Modified Alginate Samples Used in the Tests

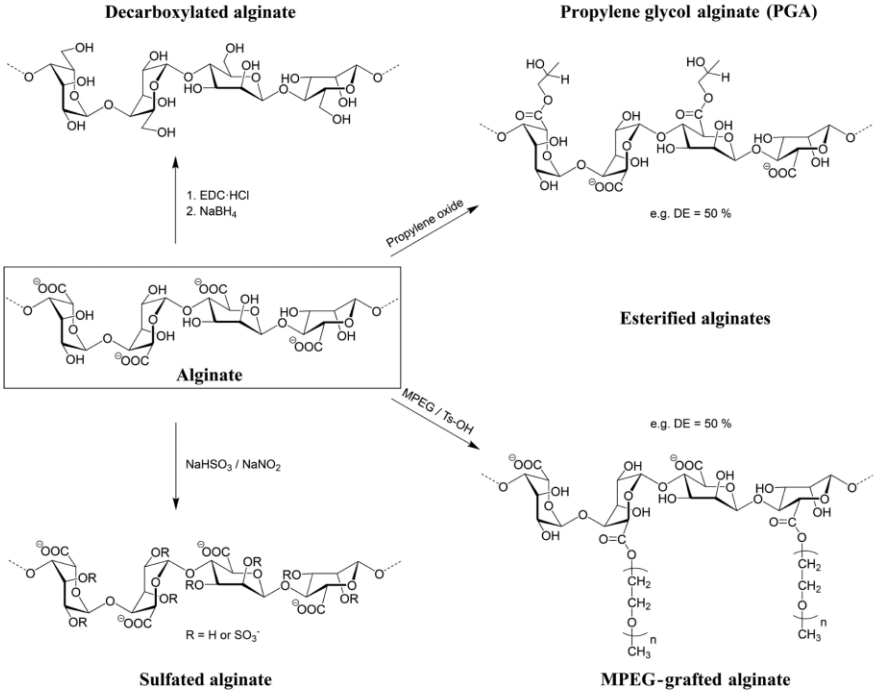

centrifuge tube and subsequent homogenization for 2 min utilizing a vortex mixer (VWR, Ismaning, Germany). The paste was centrifuged (8500 rpm, 15 min), and the supernatant pore solution filtrated using a membrane filter (0.2 μm PES). The resulting solution was diluted (1/30 v/v) and measured five times to capture the Ca^{2+} content. Calibration was carried out at different Ca^{2+} concentrations (1, 10, and 50 mg/L) utilizing an ICP multielement standard (standard IV, Merck), and data were recorded at several wavelengths. Results were averaged, and the deviation was calculated including an additional methodical error of 1% to account for deviations resulting from, e.g., pipetting and weighting.

3. RESULTS AND DISCUSSION

3.1. Investigation of the Structural Motifs Responsible for Acceleration. *3.1.1. Alginates.* In our previous investigations, commercial bulk products of alginates exhibiting different molecular weights and ratios between mannuronic and guluronic acid were utilized.[1] However, commercial products often present a blend of different algae harvests and/or algae species/genera, which are then compounded to obtain batches of consistent property. Still, the accelerating effect of alginate was found for a broad variety of randomly selected product samples from different suppliers. To clarify whether the effect is independent of the algae source, here, pure alginates extracted from specific species and genus of algae were procured. They were taken from *Durvillea antarctica*, *Laminaria japonica*, *Fucus vesiculosus*, *Chorda filum*, and *Ascophyllum nodosum* (properties of all samples are displayed in Table S1 in the Supporting Information). These samples were chosen because of the different conditions in their biosynthesis and growth, which made us expect notable differences in their molecular weight, M/G ratio, and especially the monomer sequence (block structure). Thus, if these samples would show severe differences in acceleration, then not every alginate would be suitable for CAC. However, a comparison of their effect via heat flow calorimetry revealed no significant difference regarding their accelerating property. All of these pure alginates perform similar to the commercial (blended) products and reduce the hydration time of, e.g., Secar 71 by 2.9−3.6 h as compared to that of the neat cement (see Figure 3). The results allow us to conclude that alginates generally display an accelerating effect on alumina cement, independent of the algae species/genus.

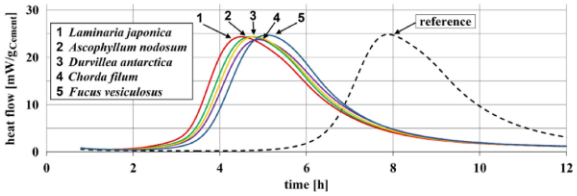

Figure 3. Effect of pure alginate samples on CAC hydration, as determined via heat flow calorimetry (Secar 71, w/b = 0.5, alginate dosage 0.1 wt %).

3.1.2. Chemically Derivatized Alginates. Natural, non-modified alginates strongly accelerate CAC hydration, as has been demonstrated before. To pin down specific structural features that are responsible for the accelerating effect, chemically derivatized alginates were also probed. For this purpose, a commercially available esterified derivate, namely, hydroxypropyl alginate (also denominated as propylene glycol alginate or, in short, PGA), self-prepared M-PEG/PEG esters of alginate exhibiting various side chains, a decarboxylated alginate, and a sulfated alginate were probed. The chemical structures of these derivatives are shown in Scheme 1.

https://dx.doi.org/10.1021/acs.iecr.0c01620
Ind. Eng. Chem. Res. 2020, 59, 11930−11939

Table 3. Comparison of Specific Molecular Characteristics of Different Biopolymers Featuring a Cavity

biopolymer	alginate	pectin	carrageenan	agarose	fucoidan
product name	XEA 5036	CU 701	GP 379 (ι)	Biozyme LE	FUC400
cavity	yes	yes	yes	yes	no
charge per monosaccharide	1	≈0.7	0.5−1 ($\kappa - \iota$)		≈1
anionic functionality	carboxylate	carboxylate	sulfate	none	sulfate

Heat flow calorimetry revealed that the commercial alginate ester (PGA) accelerates CAC hydration slightly less compared to the nonmodified alginate (see Table S2 in the Supporting Information). We attribute this behavior to the blocking of the carboxylate groups via esterification (DE > 50%), which seems to be important for the accelerating property of the polymer. Removal of a major portion of the anionic charge notably weakens the accelerating potency. Nevertheless, PGA still strongly accelerates CAC hydration, which we attribute to the hydrolysis of the ester under the alkaline conditions of the cement pore solution (pH ≈ 12) that leads to carboxylate groups. This assumption is supported by literature that reports that PGA ester is subject to saponification already at pH values as low as 10.[14]

Based on the observation that derivatization of the carboxylate group reduces the acceleration effectiveness, M-PEG and PEG esters of alginate with varying degree of esterification (DE) and side-chain length were self-synthesized and studied. Here, either through increasing the DE or in the presence of longer side chains the acceleration was reduced further until no acceleration was detected anymore (see Table S3 in supporting information). Therefore, a high amount of free carboxylate groups as well as the accessibility of the cavity for Ca^{2+} ions (shielding of the backbone through the side chains) was identified as important for the accelerating property.

As shown above, the anionic charge of the biopolymer presented by the carboxylate groups seems to be vital for the effect. Therefore, as a next step, the anionic carboxylate group was removed via $NaBH_4$ reduction to affirm its necessity for acceleration. Using an amide intermediate, the carboxylate groups were converted to hydroxyl groups and thus into neutral functionalities.[11] The resulting polymer that only retained a minor amount of carboxylate groups no longer accelerated the hydration of CAC (see Table S4 in the Supporting Information). Instead, even a retarding effect was observed for the decarboxylated alginate, thus again pointing toward the anionic charge being crucial for the working mechanism of alginates.

In the next step, another chemical modification of the alginate was performed by further increasing its anionic charge through sulfatation. Here, the hydroxyl groups were converted to sulfate groups and the resulting carboxylated/sulfated alginate possessing extra-high anionicity was tested for its accelerating property. Interestingly, calorimetry revealed a reduced accelerating effect of the sulfated alginate as compared to the neat alginate (see Table S4 in the Supporting Information). Apparently, even higher anionic charge does not further increase its effectiveness, indicating that a certain degree of anionic charge is sufficient to achieve the accelerating effect of alginate.

3.1.3. Other Biopolymers Possessing a Cavity. To find out which structural units are responsible for this effect, we then focussed on biopolymers that possess a cavity including several oxygen atoms for potential coordination to cations, as occurring in alginates (see Figure 1). These comparative biopolymers included pectin, carrageenan, and agarose. The properties of these biopolymer samples are listed in Table 3, and their chemical structures are shown in Figure 4. In the following, the impact of these biopolymers on the hydration of a CAC containing 70% Al_2O_3 was studied via heat flow calorimetry.

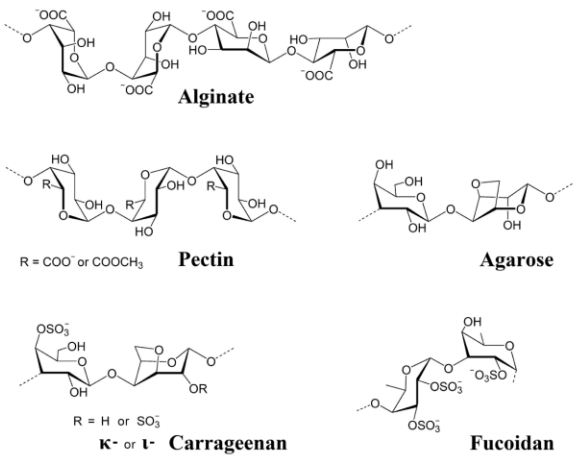

Figure 4. Repeating structural units present in alginate, pectin, carrageenan, agarose, and fucoidan.

According to Figure 5, all of these biopolymer samples except fucoidan accelerate CAC hydration. However, clear

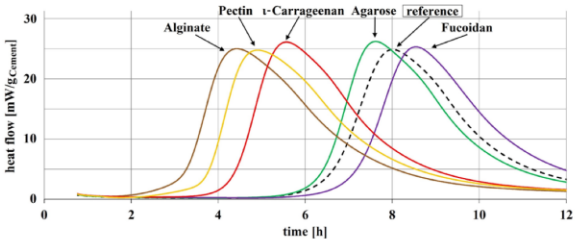

Figure 5. Effect of different polysaccharide samples admixed at a dosage of 0.1 wt % on CAC hydration in comparison to neat cement (dashed line), as determined via heat flow calorimetry (CAC, Secar 71; w/b = 0.5).

differences can be observed between them. Especially, carrageenan and pectin stand out because of their comparatively stronger accelerating effect, which is quite close to that of the alginate. Similar pronounced accelerating effects were obtained in other CAC samples (results displayed in Table S2 in the Supporting Information), thereby confirming their generally strong accelerating effect on CACs.

The effectiveness of pectin in comparison to alginate was lightly less. The reason for this difference can be attributed to a

https://dx.doi.org/10.1021/acs.iecr.0c01620
Ind. Eng. Chem. Res. 2020, 59, 11930−11939

Table 4. Comparison of Specific Molecular Features in Different Biopolymers

biopolymer	karaya gum	konjac gum	gellan gum	xanthan gum	guar ether	cellulose ether
product name	Ceroka Nr.1	Cerokon CKHY 1240	Ceroga type 700	CX900T	Galactasol 474	MHB 10000 P2
cavity	no	no	no	no	no	no
charge per monosaccharide	≈0.4	neutral	0.25	0.2−0.25	neutral	neutral
anionic functionality	carboxylate	none	carboxylate	carboxylate	none	none

different interaction with Ca^{2+}. Even though pectin and alginate are structurally quite similar (see Figure 4), their interaction with calcium and the accompanying ionotropic gelation differ. Various investigations on the interaction between Ca^{2+} and pectate indicated a weaker interaction compared to alginate which results in a different gelation mechanism.[6,15−17] For pectin, the junction zone (site of interaction polymer-cation) of the polymer cannot be described by the egg-box model, even though it appears to be similar.

Unexpected was the accelerating property of ι- and κ-carrageenan because of their significant structural difference to alginate (see Figure 4) expressed by their sulfate groups instead of the carboxylate groups found in alginate and pectin. Nevertheless, alginates as well as κ- and ι-carrageenan exhibit one common structural element, namely, the cavity (see Figure 1), which allows complexation of cations. Studies on the interaction of carrageenan with cations such as Ca^{2+} indicate only weak gelation. Carrageenans are assembled in a helix, which aggregates through interaction with ions.[18−20] In carrageenans, the cations only bridge and gel the helices (see Figure 2), but they are not essential to form the helix. Therefore, carrageenan exhibit a very different gelling mechanism with Ca^{2+} as compared to pectin and alginate. Because carrageenans show a weaker accelerating effect than alginate, we contemplate that the sulfate group presents the major factor for the loss of potency, as sulfate groups complex calcium ions not as effectively as carboxylate groups. It should be noted here that λ-carrageenan, which exhibits only a partial cavity including sulfate groups, does not accelerate CAC hydration comparably.

Similar to the alginates, the molecular weight of carrageenans also seems to be relevant for their accelerating properties. This was confirmed when comparing the accelerating properties of several κ-carrageenan samples from different suppliers. For instance, one κ-carrageenan accelerated CAC hydration, while another retarded the hydration. The analysis revealed a M_w on the order of 10^4 Da for the retarding carrageenan, while the accelerating sample exhibited a molecular weight on the order of 10^5−10^6 Da. These values are consistent with our previous findings for alginates and confirm the requirement for a high molecular weight of the polymer to achieve the accelerating effect in CAC.[1]

Agarose is structurally very similar to carrageenan and likewise possesses a cavity (Figure 4). In contrast to carrageenan, however, agarose is a neutral polysaccharide composed of galactose and anhydro galactopyranose and does not contain a sulfate group. Calorimetry revealed a weak accelerating effect, resulting in a minor shift of the heat release to earlier times only (Figure 5). Obviously, the accelerating effect not only derives from the cavity but also requires a certain anionicity of the biopolymer. As such, a combination of high anionic charge, the presence of a cavity, and a high molecular weight may provide optimal acceleration.

To check on the relevance of the cavity, we tested fucoidan, which is a biopolymer similar to carrageenans and alginate (Figure 4). Fucoidan also possesses a higher M_w and contains anionic sulfate groups but lacks the cavity, which is characteristic for all accelerating biopolymers identified so far. Fucoidan belongs to the group of sulfated fucose-based polysaccharides and has no definite composition. In fucoidan, also carbohydrates like, e.g., xylose, glucose, or uronic acid can be incorporated.[21] Interestingly, calorimetry revealed a retarding effect of fucoidan on CAC hydration (Figure 5), thus implying that anionic charge and high molecular weight alone do not guarantee an accelerating behavior.

To summarize, compared to the strong effect of alginate, pectin, and κ-/ι-carrageenan, agarose provides a weaker accelerating effect. Still, all five biopolymer samples, which possess a cavity, promote CAC hydration. Thus, it is demonstrated that the cavity presents a crucial structural element for biopolymers to accelerate CAC hydration.

3.1.4. Further Polysaccharides (Natural, Microbial, and Semisynthetic). To gain a broader perspective, additional samples of natural (karaya and konjac gum), microbial (xanthan and gellan gum), and semisynthetic (HP guar and cellulose ethers) biopolymers were tested in comparison to alginate. All of these polymers do not possess a cavity and are either anionic or nonionic. Their characteristic properties are presented in Table 4. These biopolymers are commonly utilized as thickening agents in food preparations. Their effect on CAC hydration was studied using heat flow calorimetry (Figure 6) and discussed for each polymer in the following.

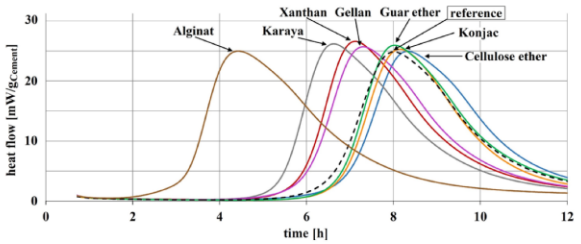

Figure 6. Effect of different polysaccharide samples on CAC hydration admixed at a dosage of 0.1 wt % compared to neat cement (dashed line), as determined via heat flow calorimetry (CAC, Secar 71; w/b = 0.5).

3.1.4.1. Natural Biopolymers (Karaya and Konjac Gum). Karaya gum, also known as sterculia gum, is a complex, branched polymer of high molecular weight and composed of galactose, rhamnose, and—most importantly—glucuronic and galacturonic acid. It is negatively charged, even though not as high as alginate or pectin. On the other hand, konjac gum is a linear glucomannan of high M_w and exhibits partial acetylation. It consists of mannopyranose and glucopyranose units and holds no ionic charge. The molecular structures of karaya and konjac gum are displayed in Figure 7[3,22]

https://dx.doi.org/10.1021/acs.iecr.0c01620
Ind. Eng. Chem. Res. 2020, 59, 11930−11939

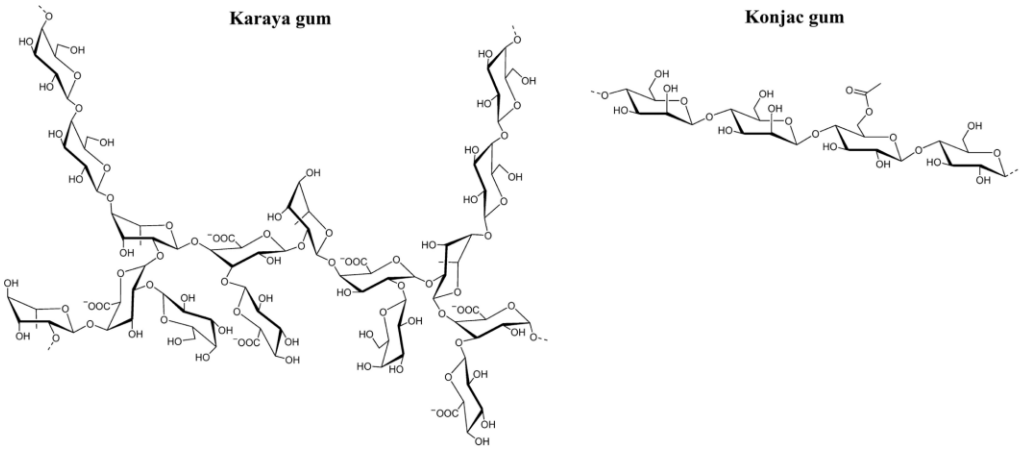

Figure 7. Molecular structures of karaya gum and konjac gum.

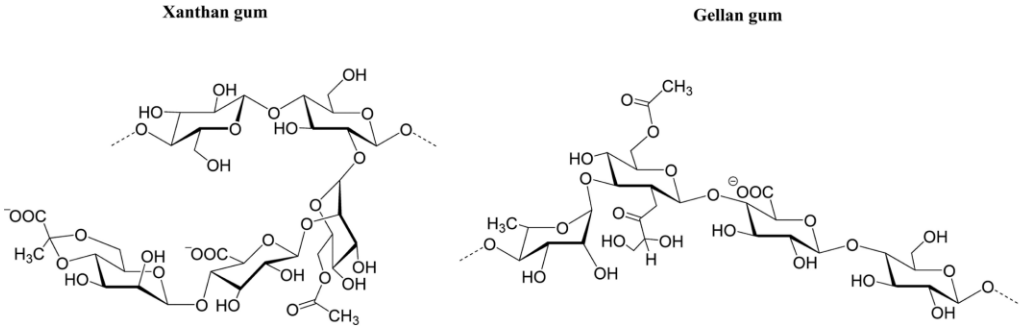

Figure 8. Molecular structures of xanthan gum and gellan gum.

According to heat flow calorimetry, konjac gum shows a very minor retarding effect, while karaya gum shows a medium-strong accelerating effect (Figure 6), which however is much less compared to that of alginate (only about one-third of alginate). The retarding effect of konjac gum was expected, while it was quite unexpected for karaya gum to accelerate. The latter shows a comparatively high anionic charge compared to the other polymers (see Table 4) and features galacturonic acid units, which are also incorporated in pectin. This high amount of uronic acids in karaya gum has been reported to facilitate a significant calcium-binding capacity.[23] Compared to alginate, however, the Ca^{2+} binding ability of karaya gum still is less pronounced. This explains why this polysaccharide shows a weaker accelerating effect, and it highlights the importance of the anionic charge for the accelerating effect.

3.1.4.2. Microbial Biopolymers (Xanthan and Gellan Gum). Furthermore, the microbial biopolymers gellan gum and xanthan gum that are produced via fermentation using bacteria were investigated regarding their effect on CAC hydration.

Xanthan gum is a comb polymer with a backbone consisting of glucose units, similar to those in cellulose. The side chains include trisaccharides composed of a mannose (partially acetylated), a glucuronic acid, and a terminal mannose unit that is partially pyruvated.[3] On the other hand, gellan gum presents a linear terpolymer made up of glucose, rhamnose, and glucuronic acid units. It can be acylated with acetate or glycerate on the glucose unit. The molecular structures of these gums are displayed in Figure 8.

Both biopolymers, xanthan gum and gellan gum, produced an accelerating effect which is almost comparable to that of karaya gum (Figure 6). Thus, surprisingly, even though structurally very dissimilar, those anionic and high molecular weight polysaccharides produce an accelerating effect, although weak. This allows us to conclude that a high anionic charge is very important for the accelerating effect.

3.1.4.3. Semisynthetic Biopolymers (Cellulose and Guar Ethers). To further investigate the influence of the anionic charge we selected two nonionic biopolymers without cavity for investigation. If the charge was indeed crucial for the effect, then no acceleration, but instead retardation should be recorded.

Here, methyl hydroxyethyl cellulose (commonly denominated as MHEC) and a hydroxypropyl guar gum (HPG) composed of galactose and mannose units were utilized. The molecular structures of these biopolymer derivatives are displayed in Figure 9.

As expected, both polymers did not accelerate the CAC hydration (Figure 6). While guar gum produced no noticeable effect, the cellulose ether resulted in slight retardation. For cellulose ethers, such behavior has been reported before from studies on CAC and Portland cement.[24,25]

3.1.5. Dosage Dependence of the Accelerating Effect. As it is well established in OPC systems that the retarding effect of polymers is highly dosage-dependent, the accelerating effect of karaya gum on CAC hydration was probed at different addition rates of 0−0.4 wt %. The results of this test series conducted

https://dx.doi.org/10.1021/acs.iecr.0c01620
Ind. Eng. Chem. Res. 2020, 59, 11930−11939

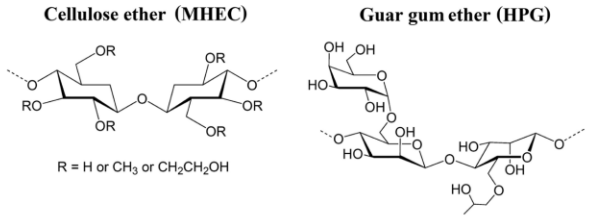

Figure 9. Molecular structures of the semisynthetic ethers MHEC and HPG.

with a CAC sample Secar 41 (45% Al_2O_3) are displayed in Figure 10.

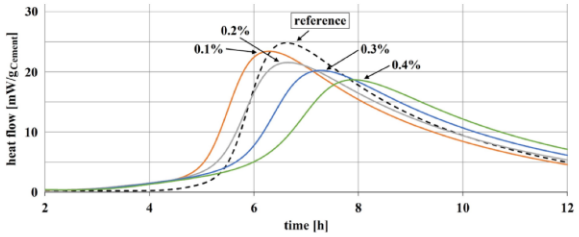

Figure 10. Dosage-dependent effect of karaya gum on CAC hydration compared to neat cement, as determined via heat flow calorimetry (CAC, Secar 41; w/b = 0.6).

There, it becomes evident that karaya gum promotes CAC hydration only at the lowest dosage of 0.1 wt %. At increased additions, its effect reverses to retardation, and this trend increases with increasing dosage. Hence, biopolymers exhibiting a minor accelerating effect at low dosage may not present accelerators at higher addition rates. Such dosage-dependent reversal of the accelerating effect has not been observed for pectin and alginate.[1]

3.2. Mechanistic Investigation. For alginates, we have already reported that they reduce the free calcium concentration existing in the pore solution of CAC.[1] This observation was quite surprising for an accelerator because a reduced Ca^{2+} concentration normally results in retardation of cement hydration, as the system is starved from Ca^{2+} needed to form the hydrate phases. To confirm that the decrease of the Ca^{2+} concentration was not specific only for alginates but presents a general mechanistic feature of biopolymers that accelerates CAC hydration, the pore solution composition of CAC in the presence of ι-carrageenan and pectin was determined.

Also here, a reduction of the free calcium concentration was observed upon the addition of these biopolymers to CAC (Figure 11), thus corroborating that calcium complexation presents a vital step in the accelerating mechanism of the biopolymers. Interestingly, the calcium-binding capacity at a given dosage correlates well with the accelerating effectiveness. Carrageenan exhibits the lowest calcium-binding capacity (reduction in Ca^{2+} concentration vs reference, $\Delta Ca^{2+} \approx 5\%$ at 0.1 wt % dosage) and accelerating effectiveness, while pectin ($\Delta Ca^{2+} \approx 10\%$ at 0.1 wt % dosage) provides a stronger acceleration. This compares with a 15% decrease of the free Ca^{2+} concentration for alginate at 0.1 wt % dosage.[1] Unsurprisingly, alginate presents the strongest accelerator amongst the three biopolymers (Figure 5). Even higher reductions in the concentration of free Ca^{2+} ions were observed at increased dosages of carrageenan and pectin (Figure 11), thus confirming their stronger accelerating effect at higher addition rates.

To summarize, the calcium-complexing ability of biopolymers seems to be crucial for their accelerating effectiveness; however, it does not represent the one and only structural characteristic for a biopolymer to act as an accelerator. For example, carboxymethyl cellulose also reduces the amount of free Ca^{2+} but clearly retards CAC hydration. Similarly, alginates or carrageenans of low M_w do not accelerate CAC, although they show the same high calcium-binding capacity as their high M_w counterparts. This points to the fact that the accelerating effect of biopolymers on CAC is the result of a complex interplay of different structural features and properties. Further studies are required to gain more insight into this unusual behavior.

4. CONCLUSIONS

Following our previous study on the unusual accelerating behavior of alginate, the screening of various additional biopolymers resulted in the identification of two more species that also exhibit strong accelerating properties, namely, pectin and carrageenan. Both polymers share a similar structural feature with alginate represented by a cavity and high anionic charge (even though carrageenan carries a sulfate group compared to the carboxylate of the alginate). All three polymers exhibit a strong binding capacity for dissolved Ca^{2+} ions present in the cement pore solution.

An investigation on the structural motif responsible for the acceleration revealed that high anionic charge, presence of a

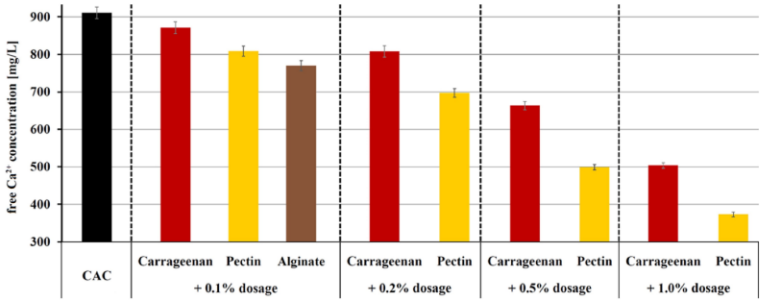

Figure 11. Concentration of free Ca^{2+} present in the pore solution of CAC (Ciment Fondu, w/b = 0.5), neat and admixed with increasing dosages of ι-carrageenan (GP 379) and pectin (CU 701), as compared to alginate (XEA 5036), measured via ICP-OES.

https://dx.doi.org/10.1021/acs.iecr.0c01620
Ind. Eng. Chem. Res. 2020, 59, 11930−11939

cavity capable to capture free Ca^{2+} ions, and a high molecular weight present the key molecular features to provide a strong accelerating effect. Only a combination of all of these features guarantees such promotion of CAC hydration, while the absence of any of these properties typically results in retardation.

Still, the overall underlying mechanism of CAC acceleration by specific biopolymers remained unclear and therefore will be the subject of another separate study utilizing XRD, ^{27}Al MAS NMR spectroscopy, and scanning electron microscopy (SEM) imaging. However, the results presented here and in our previous work clearly suggest that the accelerating mechanism of the biopolymers here is totally different from the working principle of the known accelerators for CAC, for example, lithium salts, especially Li_2CO_3, which currently presents the most widely used accelerator for CAC. They operate via a complex cation-specific effect involving multiple steps.[26−29]

In view of the strongly increasing demand for Li in lithium-ion batteries, which present the key to enabling electromobility and the limited availability of this relatively rare element, the biopolymers highlighted in this paper (alginate, pectin, and carrageenan) present a viable substitute for lithium. Furthermore, lithium salts are well known to be pharmaceuticals and applied in refractory systems where unfortunately they decrease the melting point of refractories. Compared to Portland cement for which a broad portfolio of accelerators including Ca and Al salts as well as nucleation-promoting (seeding) materials can be utilized, CAC currently solely depends on Li salts, thus emphasizing the need for alternatives.

■ ASSOCIATED CONTENT

Supporting Information

The Supporting Information is available free of charge at https://pubs.acs.org/doi/10.1021/acs.iecr.0c01620.

Properties of the alginate samples extracted from specific algae, accelerating effect of various biopolymers on three different alumina cements, effect of different esterification grades of M-PEG alginate esters on CAC hydration, and effect of decarboxylated and sulfated alginate on CAC hydration (PDF)

■ AUTHOR INFORMATION

Corresponding Author

Johann Plank − *Technische Universität München, Chair for Construction Chemistry, 85747 Garching, Germany;* orcid.org/0000-0002-4129-4784; Phone: +49 (0) 89 289 13 151; Email: sekretariat@bauchemie.ch.tum.de; Fax: +49 (0) 89 289 13 152

Author

Alexander Engbert − *Technische Universität München, Chair for Construction Chemistry, 85747 Garching, Germany*

Complete contact information is available at: https://pubs.acs.org/10.1021/acs.iecr.0c01620

Notes

The authors declare no competing financial interest.

■ ACKNOWLEDGMENTS

The authors are most grateful to Imerys Aluminates (formerly Kerneos) for the generous supply of aluminate cement over the years (especially A. Eisenreich and Dr. R. Kwasny-Echterhagen). Our gratitude also goes to Eurogum, FMC, and Herbstreith & Fox for providing biopolymer samples, and personal thanks go to the students Luis Schnürer and Richard Foja for their assistance in some of the tests. Moreover, the authors are most grateful to Deutsche Forschungsgemeinschaft, Bonn, Germany (DFG) for financing this project under grant PL-472/13-1 ("Investigation on the replacement of lithium carbonate as an accelerator for calcium aluminate cements and its underlying working mechanism").

■ ABBREVIATIONS USED

C CaO
A Al_2O_3
S SiO_2
H H_2O
F Fe_2O_3
T TiO_2
M MgO

■ REFERENCES

(1) Engbert, A.; Gruber, S.; Plank, J. The Effect of Alginates on the Hydration of Calcium Aluminate Cement. *Carbohydr. Polym.* **2020**, No. 116038.

(2) Bensted, J. Calcium aluminate cements. In *Structure and Performance of Cements*, 2nd ed.; Bensted, J.; Barnes, P., Eds.; CRC Press: Boca Raton, 2002; pp 114−138.

(3) Imeson, A. P. *Food Stabilisers, Thickeners and Gelling Agents*; Wiley Blackwell: Hoboken - New Jersey, 2011.

(4) Grant, G. T.; Morris, E. R.; Rees, D. A.; Smith, P. J.; Thom, D. Biological interactions between polysaccharides and divalent cations: the egg-box model. *FEBS Lett.* **1973**, *32*, 195−198.

(5) Plank, J. Applications of biopolymers in construction engineering. In *Biopolymers*; Steinbüchel, A., Ed.; Wiley-VCH Weinheim, 2003; Vol. *10*, pp 29−95.

(6) Morris, E. R.; Powell, D. A.; Gidley, M. J.; Rees, D. A. Conformations and interactions of pectins: I. Polymorphism between gel and solid states of calcium polygalacturonate. *J. Mol. Biol.* **1982**, *155*, 507−516.

(7) Barahona, T.; Prado, H. J.; Bonelli, P. R.; Cukierman, A. L.; Fissore, E. L.; Gerschenson, L. N.; Matulewicz, M. C. Cationization of kappa- and iota-carrageenan − Characterization and properties of amphoteric polysaccharides. *Carbohydr. Polym.* **2015**, *126*, 70−77.

(8) Borisenkov, M. F.; Karmanov, A. P.; Kocheva, L. S.; Markov, P. A.; Istomina, E. I.; Bakutova, L. A.; Litvinets, S. G.; Martinson, E. A.; Durnev, E. A.; Vityazev, F. V.; Popov, S. V. Adsorption of β-glucuronidase and estrogens on pectin/lignin hydrogel particles. *Int. J. Polym. Mater. Polym. Biomater.* **2016**, *65*, 433−441.

(9) Mao, S.; Guan, J.; Helgerud, T.; Zhang, Y. Nanosuspension Formulation. U.S. Patent 15/525,1732015.

(10) Pickelmann, J.; Li, H.; Baumann, R.; Plank, J. A ^{13}C NMR spectroscopic study on the preparation of acid and ester groups in MPEG type PCEs prepared via radical copolymerization and grafting techniques. *ACI Special Publication* **2015**, *302*, 25−38.

(11) Taylor, R.; Conrad, H. E. Stoichiometric depolymerization of polyuronides and glycosamino-glycuronans to monosaccharides following reduction of their carbodiimide-activated carboxyl group. *Biochemistry* **1972**, *11*, 1383−1388.

(12) Methods of testing cement − Part 11: Heat of hydration − Isothermal Conduction Calorimetry method *DIN EN 196-11:2019-03*; German version EN 196-11:2018, 2018.

(13) Fan, L.; Jiang, L.; Xu, Y.; Zhou, Y.; Shen, Y.; Xie, W.; Long, Z.; Zhou, J. Synthesis and anticoagulant activity of sodium alginate sulfates. *Carbohydr. Polym.* **2011**, *83*, 1797−1803.

(14) Kennedy, J. F.; Griffiths, A. J.; Philp, K.; Stevenson, D. L.; Kambanis, O.; Gray, C. J. Characteristics and distributions of ester groups in propylene glycol alginates. *Carbohydr. Polym.* **1989**, *11*, 1−22.

https://dx.doi.org/10.1021/acs.iecr.0c01620
Ind. Eng. Chem. Res. 2020, 59, 11930−11939

(15) Walkinshaw, M. D.; Arnott, S. Conformations and interactions of pectins: II. Models for junction zones in pectinic acid and calcium pectate gels. *J. Mol. Biol.* **1981**, *153*, 1075−1085.
(16) Braccini, I.; Pérez, S. Molecular basis of Ca^{2+}-induced gelation in alginates and pectins: the egg-box model revisited. *Biomacromolecules* **2001**, *2*, 1089−1096.
(17) Assifaoui, A.; Lerbret, A.; Uyen, H. T.; Neiers, F.; Chambin, O.; Loupiac, C.; Cousin, F. Structural behaviour differences in low methoxy pectin solutions in the presence of divalent cations (Ca^{2+} and Zn^{2+}): a process driven by the binding mechanism of the cation with the galacturonate unit. *Soft Matter* **2015**, *11*, 551−560.
(18) Arnott, S.; Scott, W. E.; Rees, D. A.; McNab, C. G. A. ι-Carrageenan: Molecular structure and packing of polysaccharide double helices in oriented fibres of divalent cation salts. *J. Mol. Biol.* **1974**, *90*, 253−267.
(19) Morris, E. R.; Rees, D. A.; Robinson, G. Cation-specific aggregation of carrageenan helices: domain model of polymer gel structure. *J. Mol. Biol.* **1980**, *138*, 349−362.
(20) Hermansson, A. M.; Eriksson, E.; Jordansson, E. Effects of potassium, sodium and calcium on the microstructure and rheological behaviour of kappa-carrageenan gels. *Carbohydr. Polym.* **1991**, *16*, 297−320.
(21) Yuan, Y.; Macquarrie, D. Microwave assisted extraction of sulfated polysaccharides (fucoidan) from Ascophyllum nodosum and its antioxidant activity. *Carbohydr. Polym.* **2015**, *129*, 101−107.
(22) Bie, Y.; Yang, J.; Nuli, Y.; Wang, J. Natural karaya gum as an excellent binder for silicon-based anodes in high-performance lithium-ion batteries. *J. Mater. Chem. A* **2017**, *5*, 1919−1924.
(23) Ha, Y. W.; Thomas, R. L.; Dyck, L. A.; Kunkel, M. E. Calcium binding of two microalgal polysaccharides and selected industrial hydrocolloids. *J. Food. Sci.* **1989**, *54*, 1336−1340.
(24) Wang, Z.; Zhao, Y.; Zhou, L.; Xu, L.; Diao, G.; Liu, G. Effects of hydroxyethyl methylcellulose ether on the hydration and compressive strength of calcium aluminate cement. *J. Therm. Anal. Calorim.* **2020**, *140*, 545−553.
(25) Müller, I. Influence of cellulose ethers on the kinetics of early Portland cement hydration. Ph.D. Thesis; Westfälische Wilhelms-Universität Münster: Germany, 2006.
(26) Rodger, S. A.; Double, D. D. The chemistry of hydration of high alumina cement in the presence of accelerating and retarding admixtures. *Cem. Concr. Res.* **1984**, *14*, 73−82.
(27) Matusinović, T.; Čurlin, D. Lithium salts as set accelerators for high alumina cement. *Cem. Concr. Res.* **1993**, *23*, 885−895.
(28) Damidot, D.; Rettel, A.; Capmas, A. Action of admixtures on Fondu cement: Part 1 Lithium and sodium salts compared. *Adv. Cem. Res.* **1996**, *8*, 111−119.
(29) Goetz-Neunhoeffer, F. Kinetics of the hydration of calcium aluminate cement with additives. *ZKG Int.* **2005**, *58*, 65−72.

https://dx.doi.org/10.1021/acs.iecr.0c01620
Ind. Eng. Chem. Res. 2020, 59, 11930−11939

Publikation 2:

Industrial & Engineering Chemistry Research, 2020, 59(26).

Supporting information

Identification of Specific Structural Motifs in Biopolymers That Effectively Accelerate Calcium Alumina Cement

Alexander Engbert, Johann Plank*

Technische Universität München, Chair for Construction Chemistry, Lichtenbergstr. 4, 85747 Garching, Germany

*Corresponding author:

Prof. Dr. Johann Plank

Chair for Construction Chemistry

Technische Universität München

Lichtenbergstr. 4

85747 Garching bei München, Germany

Tel.: +49 (0) 89 289 13 151

Fax: +49 (0) 89 289 13 152

E-Mail: sekretariat@bauchemie.ch.tum.de

ORCID (Johann Plank): 0000-0002-4129-4784

Table S1: Properties of the alginate samples extracted from specific algae, data provided by the supplier.

Alginate, extracted from	M_w	M/G
Durvillea antarctica	180,000	-
Laminaria japonica	-	1.40
Fucus vesiculosus	100,000	2.00
Chorda filum	75,000	1.84
Ascophyllum nodosum	300,000	-

Table S2: Accelerating effect of various biopolymers on three different alumina cements (w/b = 0.62), as determined via heat flow calorimetry (alginate samples XEA 5036, PGA K3B426; ι-carrageenan sample GP 379; and pectin sample CU 701).

CAC	0.1 % alginate	0.1 % PGA	0.1 % ι-carrageenan	0.1 % pectin
Secar 41	≈ 20 %	≈ 15 %	≈ 15 %	≈ 15 %
Secar 51	≈ 45 %	≈ 35 %	≈ 35 %	≈ 40 %
Secar 71	≈ 45 %	≈ 35 %	≈ 35 %	≈ 40 %

Table S3: Effect of different esterification grades (based on educt ratio) of MPEG alginate esters on CAC hydration, as determined via calorimetry (Secar 51, w/b = 0.62, polymer dosage 0.2 wt.%).

sample	neat CAC	alginate	MPEG 1000 esterification grade			
			40 %	60 %	80 %	100 %
time upon maximum heat flow	8.6	4.6	5.7	6.1	6.6	8.3

Table S4: Effect of decarboxylated and sulphated alginate on CAC hydration, as determined via calorimetry (Secar 51, w/b = 0.62).

sample	neat CAC	alginate 0.2%	decarboxylated alginate 0.1%	sulfated alginate 0.2%
time upon maximum heat flow	8.6	4.6	10.5	7.0

3.2.3 Addendum

Zusätzlich zu den in der Publikation dargestellten Ergebnissen wurden noch weiterführende Untersuchungen durchgeführt, welche im Folgenden erläutert werden:

Im Rahmen der Publikation wurden Pektin und Carrageen als weitere Biopolymere mit einem beschleunigenden Effekt mittels Wärmeflusskalorimetrie identifiziert. Die Wirkung dieser beiden Polymere im Vergleich zu Alginat und der Referenz wurden, wie in **Tabelle 3** zu erkennen ist, zusätzlich in einem CAC Mörtel verifiziert, was in der Publikation nicht beschrieben ist.

Tabelle 3: Eigenschaften und Festigkeiten eines „*Secar 71“* Mörtels (w/b = 0,5; 0,2 M.% PCE Fließmittel 114PC6) nach 4 Std. Hydratation in Gegenwart verschiedener Biopolymere (Alginat *XEA 5036*, ι-Carrageen *GP 379* und Pektin *CU 701*).

Secar 71 nach 4h Hydratation	**Referenz**	**+ 0,1 % Alginat**	**+ 0,2 % ι-Carrageen**	**+ 0,2% Pektin**
Druckfestigkeit (N/mm^2)	2,6	12,7	9,8	9,9
Biegezugfestigkeit (N/mm^2)	0,7	2,5	2,1	2,1
Mörteldichte (kg/m^3)	2210	2200	2200	2200
Ausbreitmaß (cm)	18,2	14,6	14,7	17,4

Dabei zeigte sich, dass alle Polymere die Festigkeit erheblich steigern, wobei der Effekt beim Alginat am stärksten und bei Carrageen sowie Pektin geringer, aber vergleichbar ist. Interessanterweise verdickt Pektin den Mörtel nur geringfügig, was für die praktische Anwendung sehr vorteilhaft ist, wohingegen Alginat und Carrageen die Verarbeitbarkeit stark reduzieren.

Außerdem wurde die Wirkung aller Biopolymere in einer zweiten Charge von *„Secar 71“* Zement erneut bestimmt (siehe **Tabelle 4**). Dabei war zu erkennen, dass der Effekt einzelner Polymere (v.a. Guar und Xanthan gum) je nach Zement-Charge unterschiedlich ausfällt. Dies betrifft jedoch nicht die Polymere Alginat, Pektin und ι-Carrageen mit einer stark beschleunigenden Wirkung.

Tabelle 4: Vergleich der Wirkung diverser Biopolymere auf die Hydratation zweier unterschiedlicher Chargen von „*Secar 71“* (Charge 1 produziert 2018, Charge 2 produziert 2019), ermittelt durch Wärmeflusskalorimetrie.

Polymer	Alginat	Pektin	ι-Carrageen	Agarose	Fucoidan
Produktname	*XEA 5036*	*CU 701*	*GP 379*	*Biozyme LE*	*FUC400*
Charge 1	**++**	**++**	**++**	**+**	**-**
Charge 2	**++**	**++**	**++**	**+**	**--**

Guar Gum	Gellan Gum	Xanthan Gum	Karaya Gum	Konjac Gum	Celluloseether
Galactasol 474	*type 700*	*CX900T*	*Ceroka Nr.1*	*Cerokon CKHY 1240*	*MH 300 P2*
-	**+**	**+**	**+**	**-**	**-**
+	**+**	**-**	**+**	**--**	**-**

++ stark beschleunigend, + schwach beschleunigend, - kein Effekt / schwach verzögernd, -- stark verzögernd

3.3 Publikation 3: Wirkmechanismus beschleunigender Biopolymere

3.3.1 Zusammenfassung

Abschließend wurde der Wirkmechanismus beschleunigender Biopolymere am Beispiel des Alginats näher untersucht. Dabei konnten folgende wichtige Erkenntnisse gesammelt werden, um den Wirkmechanismus zu postulieren:

- Der Einfluss des Polymers auf die Zementhydratation wurde mittels ^{27}Al-Festkörper-NMR-Spektroskopie untersucht, um den Reaktionsfortschritt des CAC zu quantifizieren. Es zeigte sich, dass die dormante Phase der Abbindereaktion durch Zugabe des Alginats deutlich verkürzt wird, wodurch die Bildung der Hydratphasen in der Akzelerationsphase früher einsetzte.
- Zusätzliche *in-situ* und *ex-situ* XRD-Untersuchungen bestätigten in Gegenwart von Alginat ebenfalls eine vorzeitige Bildung der Hydratphasen. Bei der Identifikation der Hydratationsprodukte konnte kein Auftreten zusätzlicher Reaktionsprodukte wie Polymer-LDH-Interkalationsverbindungen beobachtet werden.
- Beim Betrachten der Wechselwirkung des Alginats mit den Ionen in der Zementporenlösung zeigte sich, dass Alginat die freie Calcium- und Aluminium-Konzentration deutlich reduziert.
- Da in der Porenlösung aufgrund des hohen alkalischen pH-Werts das Aluminium als $[Al(OH)_4]^-$-Anion vorliegt, sollte es eigentlich zwischen Alginat und dem ebenfalls anionischen Aluminat-Ion zu keiner direkten Wechselwirkung kommen. Dass dennoch eine Wechselwirkung stattfindet, wurde durch Bestimmung des Zeta-Potentials (Oberflächenladung) des Alginat-Moleküls aufgeklärt. Demnach nimmt Alginat Ca^{2+}-Ionen an den negativ geladenen Carboxylatgruppen auf, wodurch seine negative Ladung reduziert wird. Mit den an der Polymeroberfläche komplex gebundenen Ca^{2+}-Ionen interagieren im Folgenden die $[Al(OH)_4]^-$-Anionen und werden dann entlang der Molekülkette fixiert.
- Diese kombinierte Bindung von Calcium (als Ca^{2+}) und Aluminium (als $[Al(OH)_4]^-$) aus der CPS erklärt das unterschiedliche Verhalten von Alginat gelöst in CPS im Vergleich zu den einzelnen Ionen. In Folge dessen führt die Zugabe von Alginat zu CPS innerhalb weniger Stunden zu einer merklichen Trübung der Lösung. Aus dieser flockt das Alginat anschließend aus.

- Mittels Rasterelektronenmikroskopie wurde festgestellt, dass die Ausflockung des Biopolymers durch Kristallisation von C-A-H-Phasen auf der Polymeroberfläche hervorgerufen wird.
- Die Bildung von CAC-Hydratphasen auf der Alginatoberfläche wurde auch bei weiteren REM-Untersuchungen beobachtet, in denen eine Alginat-Probe für eine definierte Zeit mit CPS in Kontakt gebracht wurde (siehe **Abbildung 24** in Kapitel 2.4.4).
- Basierend auf diesen Erkenntnissen wurde als Wirkmechanismus des Alginats die Schaffung einer heterogenen Kristallisationsoberfläche erkannt, auf der weitere Nukleation und Kristallwachstum von C-A-H-Phasen stattfindet.

3.3.2 Veröffentlichung

Templating effect of alginate and related biopolymers as hydration accelerator for calcium alumina cement - A mechanistic study

Engbert A., Plank J.

Materials & Design, 2020, 195, 109054.

https://doi.org/10.1016/j.matdes.2020.109054

Materials and Design 195 (2020) 109054

Contents lists available at ScienceDirect

Materials and Design

journal homepage: www.elsevier.com/locate/matdes

Templating effect of alginate and related biopolymers as hydration accelerators for calcium alumina cement - A mechanistic study

Alexander Engbert, Johann Plank *

Technische Universität München, Lichtenbergstr. 4, 85747 Garching, Germany

HIGHLIGHTS

- Proposed mechanism behind the accelerating effect of alginate on CAC hydration was assembled through in-depth investigation.
- Addition of alginate shortens the induction period of the hydration reaction which prompts earlier formation of C-A-H phases.
- Alginate sorbs high amount of Ca^{2+} as well as $[Al(OH)_4]^-$ ions, thus reducing concentration of free ions in pore solution.
- C-A-H phases form via deposition of Ca^{2+} / $[Al(OH)_4]^-$ onto the biopolymer, thereby generating a heterogeneous nucleation surface

GRAPHICAL ABSTRACT

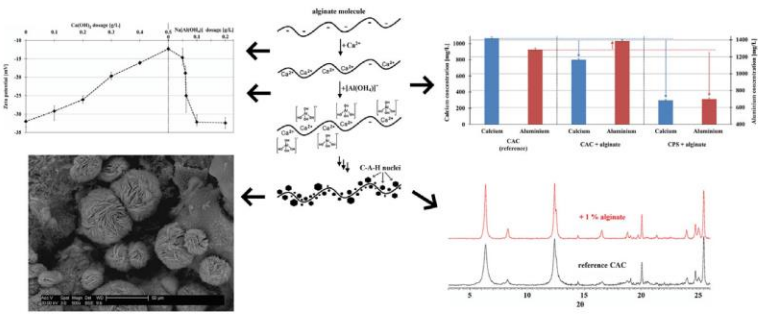

ARTICLE INFO

Article history:
Received 4 May 2020
Received in revised form 17 July 2020
Accepted 8 August 2020
Available online 10 August 2020

Keywords:
Biopolymer
Calcium aluminate cement
Hydration
Mechanism
Crystallization

ABSTRACT

In earlier publications it has been demonstrated that alginate and similarly structured biopolymers unexpectedly accelerate the hydration of calcium alumina cement. Here, this effect is investigated by applying ^{27}Al MAS NMR spectroscopy and XRD technique to track the hydration reaction and identify the hydration products. In the presence of these biopolymers an earlier consumption of clinker phases was observed indicating a shortened induction period. The subsequent formation of hydration products occurs earlier, resulting in the formation of C-A-H phases (CAH_{10} and C_2AH_8). No further reaction products like intercalation compounds were detected. An in-depth mechanistic study revealed that alginate does not adsorb on cement, but captures Ca^{2+} ions from the pore solution, thus resulting in a positively charged biopolymer chain which then attracts $[Al(OH)_4]^-$ ions to its surface. Through this binding of calcium and aluminate ions and alignment to the alginate molecule, a precursor for calcium aluminate hydrates is formed which acts as a nucleation seed and triggers continued growth into large C-A-H crystals, similar as in related biotemplating processes which are known for calcite or brushite formation.

1. Introduction

Previous studies [1,2] have reported the surprising accelerating effect of alginate or pectin on the hydration of calcium alumina cement (CAC). This effect solely occurs in CAC and was not observed for silicate- or sulfoaluminate-based binders (OPC, CSA). Alumina cements

Abbreviations: C=, CaO; A =, Al_2O_3; S =, SiO_2; H =, H_2O; F =, Fe_2O_3; T =, TiO_2; M =, MgO.

* Corresponding author at: Technische Universität München, Munich, Lichtenbergstr. 4, 85747 Garching bei München, Germany.
E-mail address: sekretariat@bauchemie.ch.tum.de (J. Plank).

https://doi.org/10.1016/j.matdes.2020.109054

are mainly composed of monocalcium aluminate which hydrates according to a dissolution and precipitation mechanism. There, C-A-H phases such as e.g. CAH_{10} ($CaAl_2(OH)_8(H_2O)_2 \cdot xH_2O$) and C_2AH_8 ($[Ca_2Al(OH)_6]^+[Al(OH)_4 \cdot xH_2O]^-$) are formed via homogeneous and heterogeneous nucleation. Hydration of the clinker at room temperature precedes as described by the following reaction equation, where the formation of CAH_{10} (predominately below 15 °C) and C_2AH_8 (starting at about 15 °C) as well as the conversion to the latter is shown:

$$CA + 10\,H \rightarrow CAH_{10}$$

$$2\,CAH_{10} \rightarrow C_2AH_8 + AH_3 + 9\,H$$

$$2\,CA + 11\,H \rightarrow C_2AH_8 + AH_3$$

Lithium salts (e.g. Li_2CO_3) are commonly applied to accelerate the reaction of CAC with water in order to achieve rapid strength development after casting, e.g. in self-levelling underlayments (SLU) and flooring compounds. The mechanism behind this specific effect of the Li^+ cation still is under discussion. It was first addressed by *Rodger and Double* [3] in 1984 and additional work was published by *Matusinovic* [4,5], *Damidot* [6] and more recently by *Goetz-Neunhoeffer* [7]. The latter presented that Li^+ ions accelerate the hydration of the aluminate phases (CA, $C_{12}A_7$ etc.) through six interconnected pathways: (1) increased dissolution of the clinker via an improved permeability of the blocking aluminium hydroxo hydrate layer; (2) formation of $[LiAl_2(OH)_6]_2^+$ $[(OH)_2 \cdot x\,H_2O]^{2-}$ layered double hydroxide (LDH) as seeding material which decreases the Gibbs free activation energy ΔG which needs to be overcome to form C_2AH_8 clusters of a size larger than the critical nucleus; (3) this increases the Ca^{2+} / Al^{3+} ratio in solution which thermodynamically promotes the formation of C_2AH_8; (4) Li^+ ions are continuously recycled for binding of Al^{3+} ions which (5) reduces the Al^{3+} concentration in solution and (6) further triggers continued the dissolution of clinker as a result of the decreased Al^{3+} content in solution. In a recent publication by *Manninger* et al. [8], however, the mechanism in step (4) which is crucial for the accelerating effect was questioned. The authors observed that in a CAC/calcite mixture, a decrease of the Li^+ concentration present in the cement pore solution was observed without replenishment.

In the case of alginate or pectin, a mechanism similar to that of Li salts would be quite unlikely. A first investigation into the mechanism revealed a strong calcium binding capability of the biopolymer, resulting in a reduction of the free calcium ion concentration in the pore solution [1]. Here, a link between the calcium binding capacity and the accelerating effectiveness was observed, whereat alginate came out on top [2]. Such a calcium binding effect normally is observed for retarding admixtures [9] and not for accelerators. To the best of our knowledge, no such calcium binding effect has been reported for accelerators so far. Obviously, a completely different mechanism as compared to that of Li^+ comes into play when biopolymers such as alginate or pectin are admixed to alumina cement. (Bio)polymers on the other hand were generally found to retard the hydration of CAC with the exemption of anionic polymers of high molecular weight, which possess a favourable structure to effectively complex calcium ions [1,2].

Alginate and pectin (see Fig. 1) are natural biopolymers produced by extraction from brown algae (*Phaeophyceae*) and *Citrus* / *Malus* fruits, respectively. Their structural characteristics are as follows: Alginates are copolymers comprised of guluronic (G) and mannuronic (M) acid, with an average molecular weight between 10,000 and 600,000 Da. The monosaccharide units (M and G) are linked in different sequences such as GM, GG and MM, this way producing different steric arrangements as illustrated in Fig. 1. Especially the GG blocks are vital for the ionotropic gelling effect observed in the presence of divalent cations like Ca^{2+}, as described by the 'egg box' model (Fig. 2) [10–12]. Commercial pectin is comprised of a linear

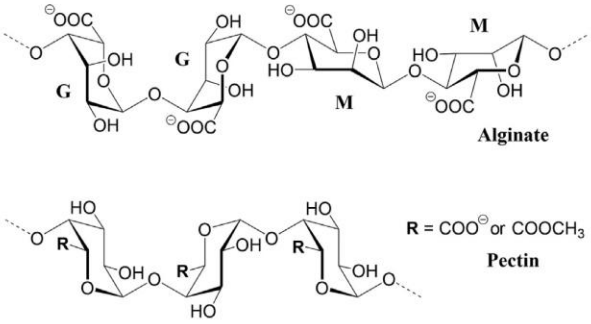

Fig. 1. Comparison of the molecular structures of alginate and pectin.

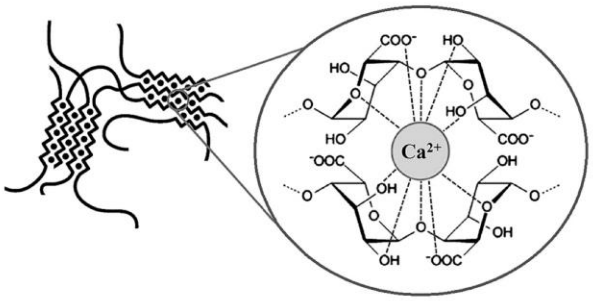

Fig. 2. Schematic representation of the Ca^{2+} induced complexation and gelation of alginate (adapted from [1]).

homopolymer of galacturonic acid (see Fig. 1) containing minor residues of rhamno galacturonan in the form of side chains composed of neutral sugars like arabinose and galactose. Pectins are distinguished by their degree of esterification (DE, ratio of methoxylate to carboxylate groups) and classified as high methoxylated (DE = 55–75%) or low methoxylated (DE = 20–45%) variant. The DE is crucial for its gelling properties. Only low methoxy pectin (LM pectin) gels in the presence of Ca^{2+} ions in a similar way as described by the "egg-box" model [10].

In the work presented here, mainly alginate was used in the investigations, because of its superior effectiveness. First, the impact of the polymer on the hydration of CAC was studied via ex-situ ^{27}Al MAS NMR spectroscopy and tracked the degree of hydration over time (0 −12h). Moreover, the formation of hydration products was monitored using ex-situ and in-situ XRD technique. Finally, the interaction of alginate with ions present in the pore solution (Ca^{2+} and $[Al(OH_4]^-$) was elucidated and based on those findings, a model for the working mechanism of accelerating biopolymers such as alginate was developed.

2. Experimental

2.1. Cement samples

Various calcium alumina cements containing different Al_2O_3 contents (*Ciment Fondu, Secar 51 and Secar 71*, supplied by *Imerys Aluminates, France)* were utilized in this study. Their mineralogical composition (Table 1) was analysed via XRD (*D8 advance* instrument, Bruker AXS, Karlsruhe, Germany) including *Rietveld* refinement (software *Topas 4.0*, Bruker AXS) and their oxide contents (values see [1]) were captured by XRF analysis (*Axios*, PANalytical, Kassel, Germany).

Table 1
Phase contents of the calcium alumina cement samples used in the study [1].

Phase	CAC sample (wt%) Ciment Fondu	Secar 51	Secar 71
CA	47–57	64–74	54–64
CA_2	*n.d.*	*n.d.*	36–44
$C_{12}A_7$	1–5	< 1	< 1
C_4AF	10–20	*n.d.*	*n.d.*
C_2AS	1–10	18–22	< 1
C_2S	1–10	1–5	*n.d.*
Other	C_3FT, $C_{20}A_{13}M_3S_3$	CT, C_3FT	α-Al_2O_3 (< 2)

2.2. Materials

Deionised water was obtained from a *Barnstead Nanopore Diamond Water purification system* (*Werner Reinstwassersysteme*, Leverkusen, Germany) and was used in all experiments. Calcium hydroxide (*EMSURE*, > 99.7%) was procured from *Merck KGaA* (Darmstadt, Germany), while a sodium aluminate solution was prepared by reacting aluminium powder (1.35 g) in a sodium hydroxide (150 mL 1 M NaOH) solution followed by filtration.

2.2.1. Biopolymers

Two commercial biopolymer products, alginate sample *XEA 5036* (*Eurogum*) and pectin sample *CU 701* (*Herbstreith & Fox*), were utilized. Their characteristic properties are displayed in Table 2.

2.3. Experimental methods

2.3.1. Isothermal heat-flow calorimetry

Paste calorimetry was performed following DIN EN 196–11 [14] using sealable 10 mL glass ampoules. For testing, biopolymer powder was placed in the ampoule and dry-blended with four grams of cement. Deionised water was added to this blend and the paste was homogenised for two minutes via a vortex blender (*VWR*, Ismaning, Germany). The heat flow was monitored by placing the ampoules into an isothermal conduction calorimeter *TAM air model 3116–2* (*Thermometric*, Järfälla, Sweden) at 20 °C until heat evolution ceased.

2.3.2. Electrical conductivity

Following established methods [15,16], electrical conductivity of cement pastes was determined by using a self-built setup containing a *Qcond 2200* conductivity meter (*VWR International GmbH*, Germany). Here, the dissolution of the cement clinker phases as well as their interaction with admixtures can be observed via electrical conductivity which is linked to the amount of dissolved ions and species in the pore solution.

For this purpose, into a 5 L plastic beaker the cement (700 g of Secar 71), neat or dry-blended with e.g. 0.2 wt% alginate, was placed. Submerged into the cement powder were a stirrer (Eurostar KPG stirrer, *IKA-Werke*, Germany) with propeller shaped blades (4-leaf) and the conductivity probe. Then the stirrer was started, and water (490 g, w/c = 0.7) was added in one step. Conductivity values were recorded at ten-second intervals as soon as a homogeneous cement paste was obtained. Measurements were performed at 20 °C and recorded until the rate of conductivity increase dropped. Thereafter, values were taken at larger intervals, depending on the development of conductivity.

Table 2
Properties of the alginate and pectin samples used in the study.

Biopolymer	Product name	Properties
Sodium alginate	XEA 5036	M/G-ratio ≈ 0.8 [1]
LM-pectin	CU 701	$M_w \approx 320$ kDa, $M_n \approx 63$ kDa, GalA content ≈ 91%, DE ≈ 31% [13]

2.3.3. SEM imaging

SEM images were taken on a *XL–30 FEG* microscope (*FEI*, Eindhoven, Netherlands) using a secondary electron and backscattered electron detector. Magnifications ranged between 100× and 40,000×, and the accelerating voltage was between 4.0 kV and 30.0 kV. Samples were fixated on the sample holder stub with *Leit Adhesive Carbon Tabs* (*PLANO*, Wetzlar, Germany). After drying, the sample was sputtered with gold for improved conductivity. Alginate hydrogels were either dried through solvent exchange or freeze dried after gentle freezing with liquid N_2.

2.3.4. Zeta potential of cement pastes

The zeta potential of CAC paste was determined on a model *DT-300 Electroacoustic Spectrometer* (*Dispersion Technology Inc.*, Bedford Hills, New York). First, the ionic background of the cement pore solution was determined and subtracted from the zeta potential value obtained during titration of the biopolymer samples to the cement paste. To capture the dosage dependent zeta potential of CAC pastes, an aqueous alginate solution (0.25 wt%, pH = 7) was added stepwise (0.5 mL increments) to the cement slurry. The zeta potential of the cement paste was then recorded as a function of the biopolymer dosage.

2.3.5. Electrical charge of alginate

The electrical charge of alginate was determined in aqueous solution at 25 °C via laser Doppler micro-electrophoresis using a *Zetasizer* model *Nano ZS* (*Malvern Instruments*, UK). For this purpose, an alkaline alginate solution (0.15 wt% polymer; pH = 12, adjusted with NaOH) was investigated and the changes in the electrical charge of the polymer were monitored in dependence of the ionic composition of the polymer solution. Ascending concentrations of (1) calcium hydroxide or (2) the combination of an increasing concentration of sodium aluminate with a fixed amount of $Ca(OH)_2$ were added to the alginate solution and the zeta potential was determined for each system. For this purpose, in a centrifuge tube 10 mL samples were prepared by first placing 1 mL alginate solution (1.5 g/L). Then water was added, followed by the aluminate solution (0.9 g/L) and the calcium hydroxide solution (1.7 g/L). The sample was homogenised for approximately two minutes via shaking and placing in an ultrasonic bath (3 x 10s). Measurements were taken automatically after two minutes of thermal equilibration using a *Folded Capillary Zeta Cell*.

2.4. Analytical methods

2.4.1. Ion concentrations via ICP-OES

Inductively coupled plasma atomic emission (ICP-OES) spectrometry was conducted on a *series 700* instrument (*Agilent Technologies*, Santa Clara, CA, USA). The cement paste was prepared in a centrifuge tube by mixing e.g. 20 g Ciment Fondu dry-blended with 0.2 wt% biopolymer and subsequently homogenised for two minutes using a vortex mixer (*VWR*, Ismaning, Germany) after 10 mL of water had been added. The resulting paste was centrifuged (15 min at 8500 rpm) and the supernatant pore solution was filtrated via a membrane filter (0.2 µm PES). The solution was diluted at 1:30 (v/v) and the concentrations of Ca^{2+} and Al^{3+} in the pore solution were determined five times. Measurements were collected at several wavelengths and the resulting values were averaged. Deviation was calculated including an additional methodical error of 1% to account for inaccuracies resulting from e.g. pipetting and weighting.

2.4.2. X-ray diffraction

In-situ XRD was performed by placing the cement paste onto the sample holder and covering the paste with a *Kapton*® polyimide foil

(*VHG Labs*, Manchester, UK). Diffraction patterns were captured over 12 h every 30 min on a *D8 advance* instrument (*Bruker AXS*, Karlsruhe, Germany) equipped with a *VÅNTEC-1* detector (5–40° 2θ, 40 kV, 30 mA, 0.025° step, $t = 0.6$ s, fixed 0.5° divergence slit, *Bragg-Brentano* geometry and Cu Kα source). Because of the heat generated by the x-ray tube, the temperature in the chamber of the XRD rose to ≈ 27.5 °C during the in-situ measurements. Powder diffraction patterns were measured on the same *D8 advance* instrument (3–50° 2θ, 35 kV, 40 mA, 0.017° step, $t = 0.8$ s, variable divergence slit V6). Evaluation and processing of the diffraction patterns was performed using Bruker's *EVA V2* software.

2.4.3. ^{27}Al MAS NMR spectroscopy

Solid-state NMR experiments were performed on an *Advance 300* instrument (*Bruker BioSpin*, Karlsruhe, Germany) possessing a magnetic field strength of 7.0455 T and a ^{27}Al resonance frequency of 78.1 MHz. Chemical shifts were recorded relative to the external standard Al $(NO)_3 \cdot 9\,H_2O$.

Samples were prepared ex-situ by mixing cement, biopolymer and water in a centrifuge tube or a sealable glass ampule and subsequent storage at 20 °C for different periods of reaction time. Non-hardened samples were quenched with acetone and freeze-dried. Hardened samples were ground in a mortar and measured immediately. Samples were

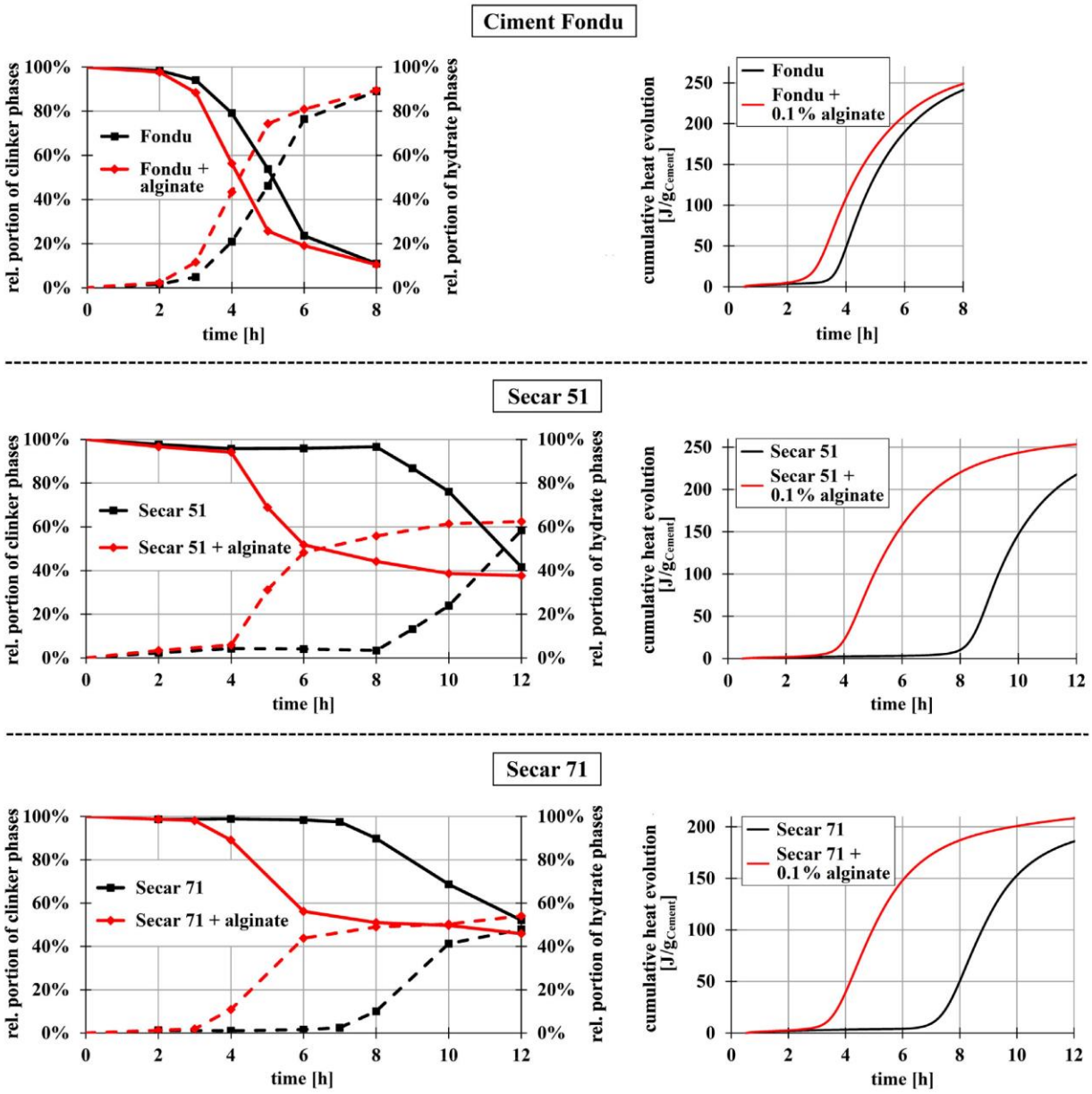

Fig. 3. Ex-situ ^{27}Al MAS NMR spectroscopic measurements (left) monitoring the time-dependent hydration of different CAC samples (w/b = 0.5) in the absence and presence of alginate (sample XEA 5036; bold line = clinker and dashed line = hydrate) and cumulative heat evolution of the corresponding samples (right).

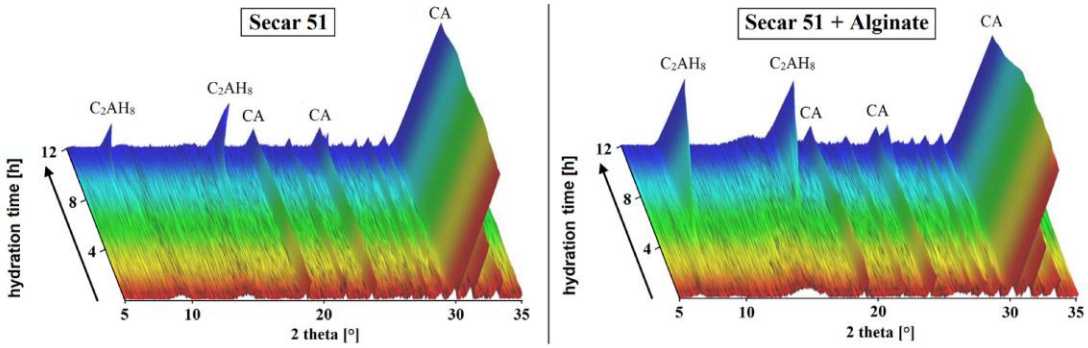

Fig. 4. In-situ XRD measurements monitoring the hydration of a CAC sample (Secar 51, w/b = 0.45, T ≈ 27.5 °C) over 12 h in the absence and presence of alginate sample XEA 5036.

filled into 4 mm zirconia rotors and rotated at 15 kHz. Single-pulse technique was used with a pulse width of 3 milliseconds. Repetition time was 2 s and the number of scans was 1000. Deconvolution and integration of the signals was performed after phase and background correction using *MNova 12* software (*Mestrelab Research*, Spain).

3. Results and discussion

Following the discovery of the accelerating effect of alginate and few other similarly structured polysaccharides [1,2], the working mechanism behind this unusual property still remained unclear. In order to investigate into this complex subject, at first the course of cement hydration was studied by tracking the time-dependent degree of the hydration and by analysing the hydration products formed. ^{27}Al MAS NMR spectroscopy was used to quantify the degree of hydration as a function of reaction time and ex-situ as well as in-situ XRD techniques were applied to identify the phases formed.

3.1. Tracking CAC hydration via ^{27}Al MAS NMR spectroscopy

The progress of hydration of an alumina cement can be quantified via ^{27}Al solid state NMR spectroscopy, as was reported by various authors before [e.g. 17]. The signals obtained from the clinker phases which contain tetrahedrally coordinated aluminium (Al-IV) and from the hydration products which contain octahedrally coordinated aluminium (Al-VI) can be integrated and express the degree of hydration of the cement. Here, the time dependent course of the hydration was studied ex-situ in cement pastes, neat as well as admixed with alginate (see exemplary NMR spectra for Secar 51 in Fig. S1 in supporting information). As cements, three mineralogically different CAC samples possessing Al_2O_3 contents between 45 and 70 wt% were utilized. According to the results exhibited in Fig. 3, two significant observations were made for all cements tested:

First, in the presence of alginate the induction period of CAC (represented by the portion of clinker which remained unreacted in the first hours after contact with water) is shortened as compared to the neat cement (black vs. red curve in Fig. 3, left). This effect is more pronounced in less reactive alumina cements with an increased Al_2O_3 content. Second, the observation of earlier hydration corresponds well with results obtained from heat flow calorimetry, as is shown in Fig. 3 (right). These observations are in accordance with literature reports for CAC hydration and comparable to the effect of lithium [17,18].

For example, in the paste holding Ciment Fondu within the first 8 h of hydration nearly all Al-IV reacts to Al-VI, whereas for the Secar 51 and Secar 71 pastes a consumption of only about 60% Al-IV is recorded over the first 12 h. This difference in hydration kinetics is caused by the different phase compositions of the cement samples. As such, Ciment Fondu which mainly contains CA and C_4AF (see Table 1) hydrates much faster than Secar 51 (main phases: CA and C_2AS) and Secar 71 (main phases: CA and CA_2) which hydrate slower because of their significant contents of gehlenite and grossite, respectively. At room temperature, gehlenite reacts only slowly over several weeks to form strätlingite [19], while it has been reported that grossite hydration begins only after the CA hydration decelerates [20]. Thus, the progress of hydration in the first 12 h for Secar 51 and Secar 71 is mainly dominated by the amount of CA contained in the clinker, and CACs holding higher

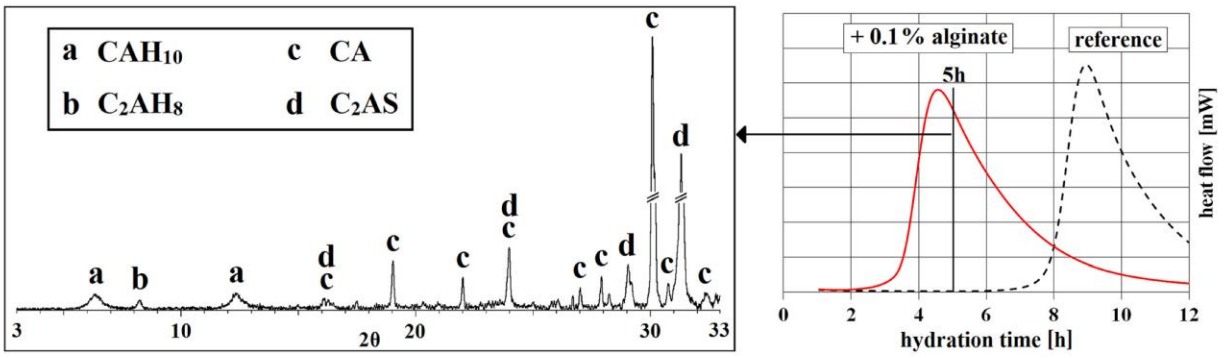

Fig. 5. X-Ray diffractogram (left) of ground CAC cement sample (Secar 51, w/b = 0.5) after five hours of hydration in the presence of 0.1 wt% alginate XEA 5036; and heat flow diagram (right) illustrating the time-dependent progress of hydration.

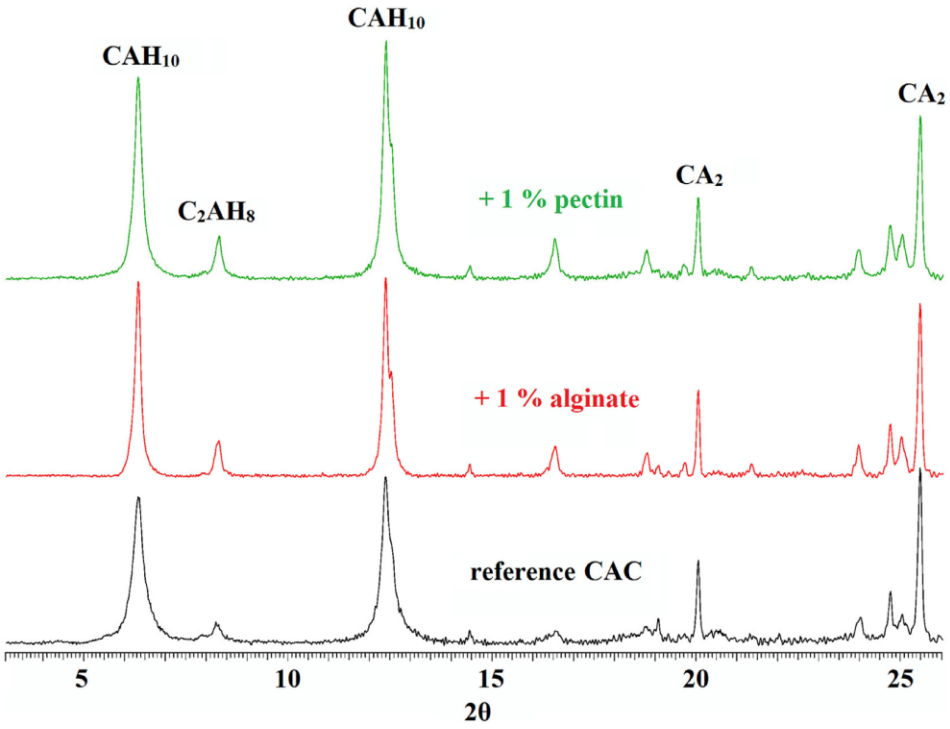

Fig. 6. XRD analysis of ground cement samples (Secar 71, w/b = 1, 20 °C) after 24 h of hydration in the absence or presence of 1 wt% alginate (sample XEA 5036) or pectin (sample CU 701).

amounts of this phase respond stronger to the alginate's accelerating effect.

3.2. Formation of hydrate phases tracked via XRD

Following the NMR investigation, hydration of the cement samples was also studied using X-ray diffraction in order to identify the specific hydrate phases (e.g. CAH_{10}, C_2AH_8, C_4AH_{13}, C_3AH_6) formed during the reaction with water.

First, in-situ XRD measurements were performed to monitor the time-dependent phase development of a Secar 51 sample in the absence and presence of alginate. There, it became obvious that in the presence of alginate, C_2AH_8 which presents the main hydration product of a CAC under those conditions, crystallizes earlier (shorter induction period) and thus in larger quantity (Fig. 4). The fact that only C_2AH_8 and no CAH_{10} was detected is explained in earlier literature [9]. According to these studies, when a transparent polymer foil (e.g. *Mylar* or *Kapton*) is used for in-situ measurements, as is the case here, then the water is retained in the sample which favours the formation of C_2AH_8. Furthermore, the formation of C_2AH_8 is also promoted by the increased temperature in the diffractometer under in-situ conditions. Because temperature influences the formation of hydrate phases thermodynamically, further ex-situ measurements of CAC hydrated at a definite temperature were conducted. Thus, for example at 10 °C only formation of CAH_{10} was detected.

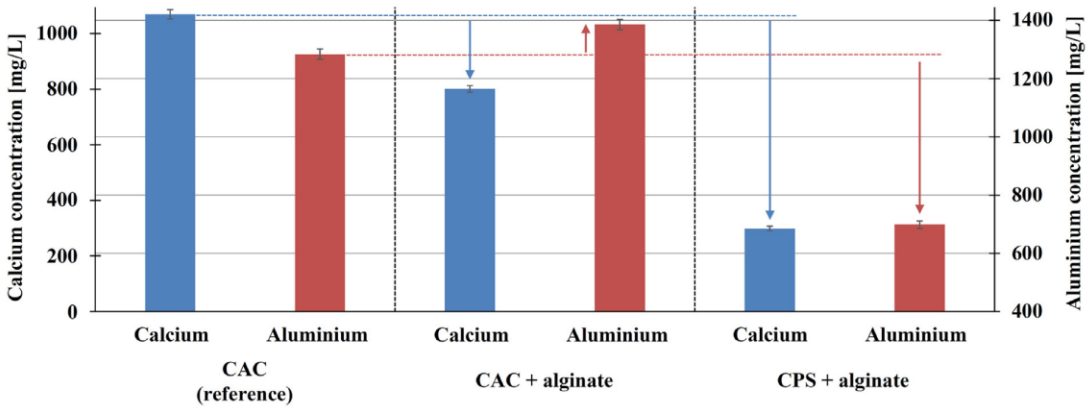

Fig. 7. Ca^{2+} and Al^{3+} ion concentrations in the pore solution (CPS) of Ciment Fondu (w/b = 0.5) after addition of 0.2 wt% alginate to the CAC paste or the CPS.

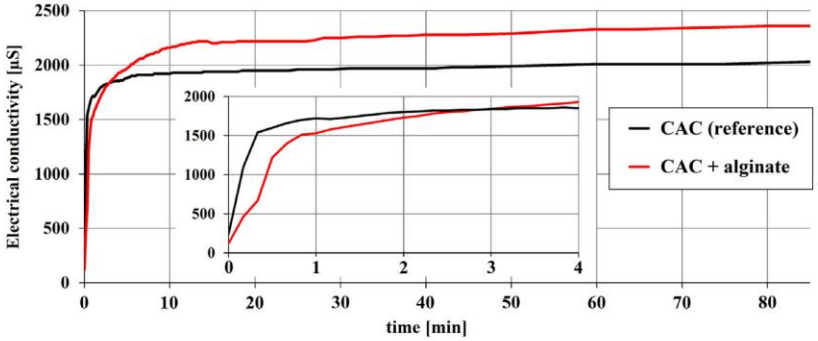

Fig. 8. Electrical conductivity of a CAC paste, neat and admixed with alginate (Secar 71, w/b = 0.7; 0.2 wt% alginate sample XEA 5036).

Furthermore, the early phase development after 5 h of hydration ($T = 20$ °C) was studied using powder XRD of a ground solidified sample (Fig. 5, left). Here, for the sample admixed with alginate, at the peak of the acceleration period the appearance of both C_2AH_8 as well as CAH_{10} was observed. Moreover, in accordance with the results from heat flow calorimetry (see Fig. 5, right) it was also noticed that after five hours of hydration the cement paste without alginate still was liquid while the paste containing the biopolymer already had stiffened and begun to harden. Apparently, alginate induces an earlier formation of C-A-H phases which results in an earlier strength development [1].

It is well established that hydrating alumina cement can chemically intercalate anionic polymers into the interlayer space of hydrates, thereby forming layered organo-mineral phases of the hydrocalumite type, abbreviated as Ca-Al-polymer-LDH [21]. These intercalation compounds are isostructural with the main hydration products of CAC (e.g. C_2AH_8) and therefore could act as a seeding and nucleation enhancing material and thus play a major role in the accelerating effect of the biopolymers. For this reason, their potential formation in the systems studied here was investigated.

The diffractograms presented above (Figs. 4 and 5) do not show any reflection at low 2θ angles (e.g. 2–5°) which are characteristic for such intercalation compounds [22]. However, considering the low addition rate of alginate in this experiment (0.1 wt%), the formation of such a by-product cannot be ruled out completely, because signal intensity for these organo-mineral phases might be too low. Thus, in order to clarify the potential formation of such Ca-Al-biopolymer LDHs, additional tests at significantly higher dosages of up to 1 wt% were performed by admixing either alginate or pectin to Secar 71. Even at such high additions, no occurrence of reflections characteristic for these intercalates was observed at 2θ angles <5°. As an example, the XRD diffractograms of the pastes holding 1 wt% of alginate or pectin are displayed in Fig. 6 (an overlap of the diffraction patterns is shown in Fig. S2 in the

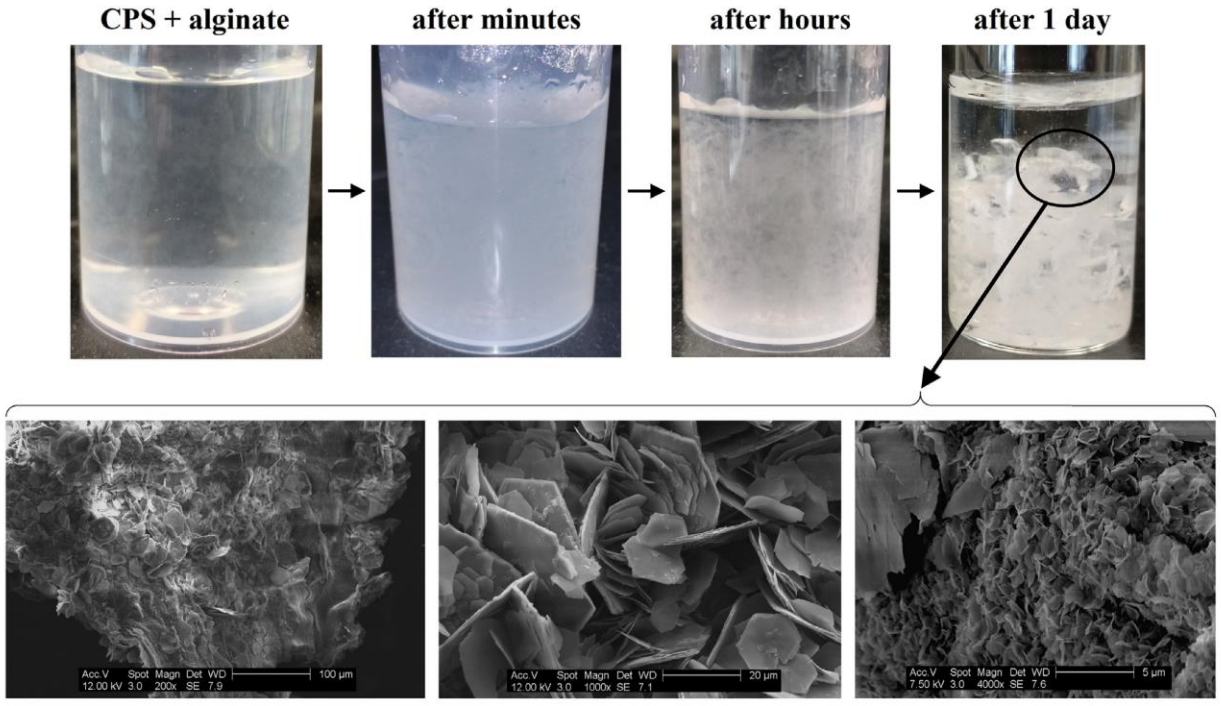

Fig. 9. Time-dependent behavior of alginate in CPS (top) and SEM images of the precipitated particles (bottom); magnifications (from left to right): 200×, 1000×, 4000×.

supplementary information). There, more intense peaks representing the hydrates C_2AH_8 and CAH_{10} were recorded when the biopolymers were present, thus confirming the accelerating effect of the polysaccharides.

Based upon these findings it can be concluded that different to the previously mentioned mechanism for Li-Al-LDH compounds [4–8], here the formation of biopolymer-containing Ca-Al-LDH intercalation compounds does not occur and hence plays no role in the accelerating effect of these polysaccharides. The absence of Ca-Al-biopolymer-LDHs can be explained with the strong interaction of these biopolymers with calcium ions in solution whereby after contact with Ca^{2+} the alginate molecule becomes much less anionic which significantly decreases its quality as guest molecule for intercalation into the LDH host structure.

To further study the interaction of the biopolymers with CAC the zeta potential of cement pastes which were stepwise admixed with alginates (sample XEA 5036 and a low M_w alginate, KIMICA ULV-L3 - properties see [1]) or pectin (sample CU 701) was measured. There, no change in the surface charge of the cement particles was detected, thus ruling out adsorption of the biopolymers on CAC. Thus, it can be assumed that the accelerating effect of the biopolymers only involves processes which occur in the pore solution and not on the surface of cement or its hydrates.

3.3. Interaction with ions in the pore solution

In the following, the interaction of alginate with Ca^{2+} and $[Al(OH)_4]^-$ ions present in the cement pore solution (pH ≈ 12) was investigated. At first, the ion concentrations in the pore solution of Ciment Fondu were determined. For this purpose, the cement was mixed for 2 min with water (w/c = 0.5), then centrifuged, filtered off and the resulting cement pore solution (CPS) was analysed for its content of Ca^{2+} and Al^{3+}, respectively using ICP-OES. As displayed in Fig. 7 (left), the initial concentration of Ca^{2+} was 1069 mg/L while Al^{3+} was present at 1284 mg/L in the CPS.

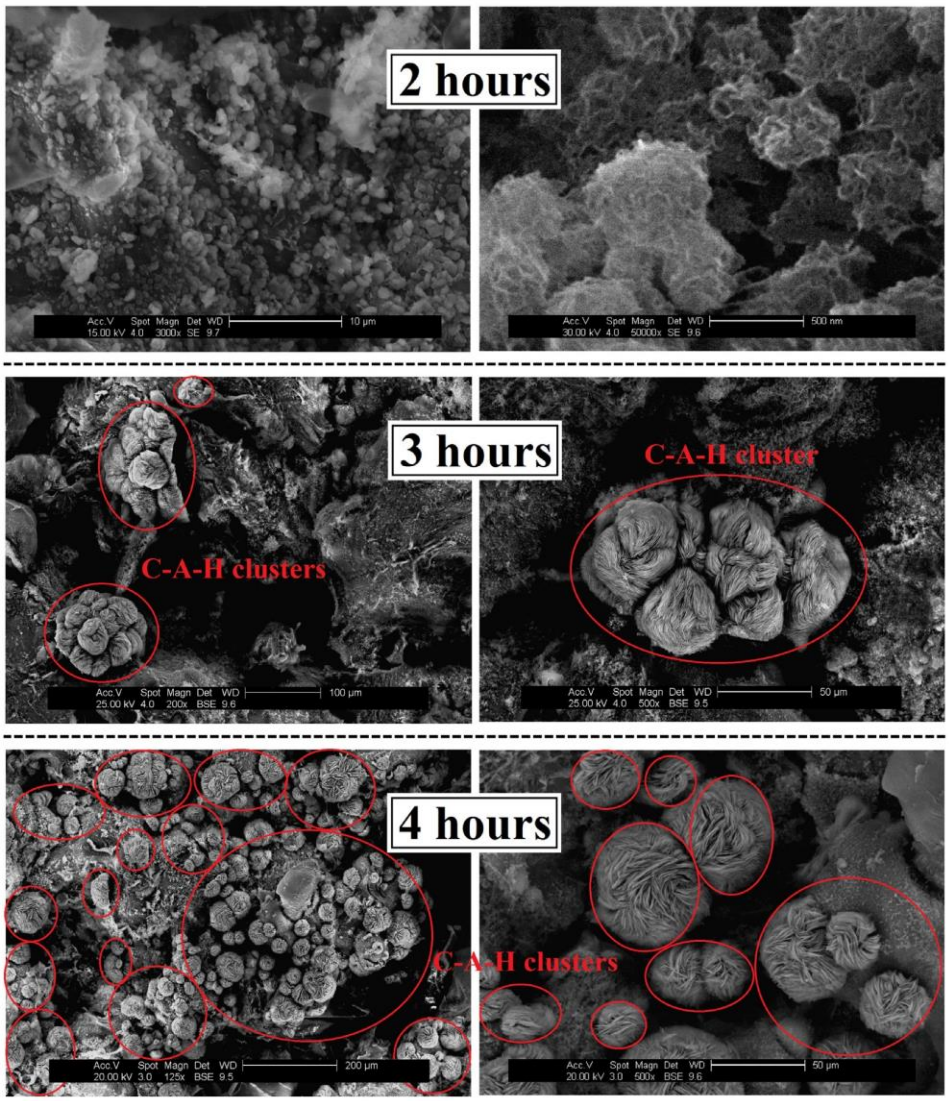

Fig. 10. Surfaces of freeze-dried alginate hydrogel submerged in CPS after various times of imbibition, as observed via SEM (magnification increasing from left to right).

To probe the impact of alginate on the ion concentrations, in the next step the same cement slurry was prepared, however 0.2 wt% of alginate were dry-blended into the cement. As can be seen from Fig. 7 (middle), in this case the concentration of Ca^{2+} is reduced from 1069 mg/L (in the neat paste) to 801 mg/L when the alginate is present. Contrary to this trend, the concentration of Al^{3+} increases from 1284 mg/L (for the neat paste) to 1386 mg/L in the presence of alginate. The same increase for Al^{3+} has been observed for Secar 51 and Secar 71 cement, respectively when alginate was admixed to them. There as well a reduction in the Ca^{2+} concentration and an increase in the Al^{3+} concentration was monitored.

The results can be interpreted as follows: alginate captures significant amounts of Ca^{2+} in its molecular cavity, as is well established and described by the 'egg-box' model [12]. As a consequence of the reduced Ca^{2+} concentration and stimulated by the solution equilibrium, more of the CA phase dissolves to replenish the Ca^{2+} which was taken up by the biopolymer. Consequently, the concentration of Al^{3+} rises above its initial value. The elevated aluminate concentrations could promote the formation of aluminate hydrates such as e.g. CAH_{10}. This mechanism of replenishment for Ca^{2+} could well explain why a polymer which captures Ca^{2+} can accelerate and not retard the hydration of CAC.

In order to confirm this model, a pore solution of neat Ciment Fondu was extracted and the CPS was treated with 0.2 wt% alginate (related to the mass of the cement), mixed for 2 min and after centrifugation and filtration was analysed for the ion contents. As is shown in Fig. 7 (right), there both the Ca^{2+} as well as the Al^{3+} concentrations drop significantly. Also, for Ca^{2+} the reduction is much more pronounced (from 1069 mg/L to 299 mg/L) than for Al^{3+} (1284 mg/L to 698 mg/L). This experiment confirms the preferred Ca^{2+} binding capacity of alginate, but also hints to an interaction of the biopolymer with the aluminate ion.

The latter was investigated further by mixing the same amount of alginate with a sodium aluminate solution of defined concentration (900 mg/L) and monitoring the Al^{3+} content, as it has been reported that in CPS sugars can form complexes with metal hydroxides [23–26]. Here, however, only a very minor decrease of ≈ 30 mg/L which is close to the margin of error was observed, thus indicating that a more complex mechanism is at work here.

These findings on the dissolution and complexing processes were further supported by conductivity measurements. Here, CAC pastes with and without alginate were continuously stirred and the electrical conductivity of the pore solution which directly correlates to the dissolved ions in the CPS was tracked. For this purpose, a CAC sample with 70% Al_2O_3 (Secar 71) was used because of its slower dissolution rate which allows for a better investigation of the early minutes of interaction with water and potentially alginate.

As displayed in Fig. 8, over the first three minutes alginate decreases the electrical conductivity, presumably as a result of the uptake of cations, especially Ca^{2+}, and the concomitant reduction in the charge of the biopolymer. However, thereafter this trend is reversed, and the conductivity of the paste admixed with alginate becomes higher than that of the neat paste, owed to increased clinker dissolution and the resulting higher aluminate concentration.

To conclude, the conductivity measurements support the previous finding from the pore solution analysis that alginate essentially triggers an increased dissolution of the clinker phases and especially increases

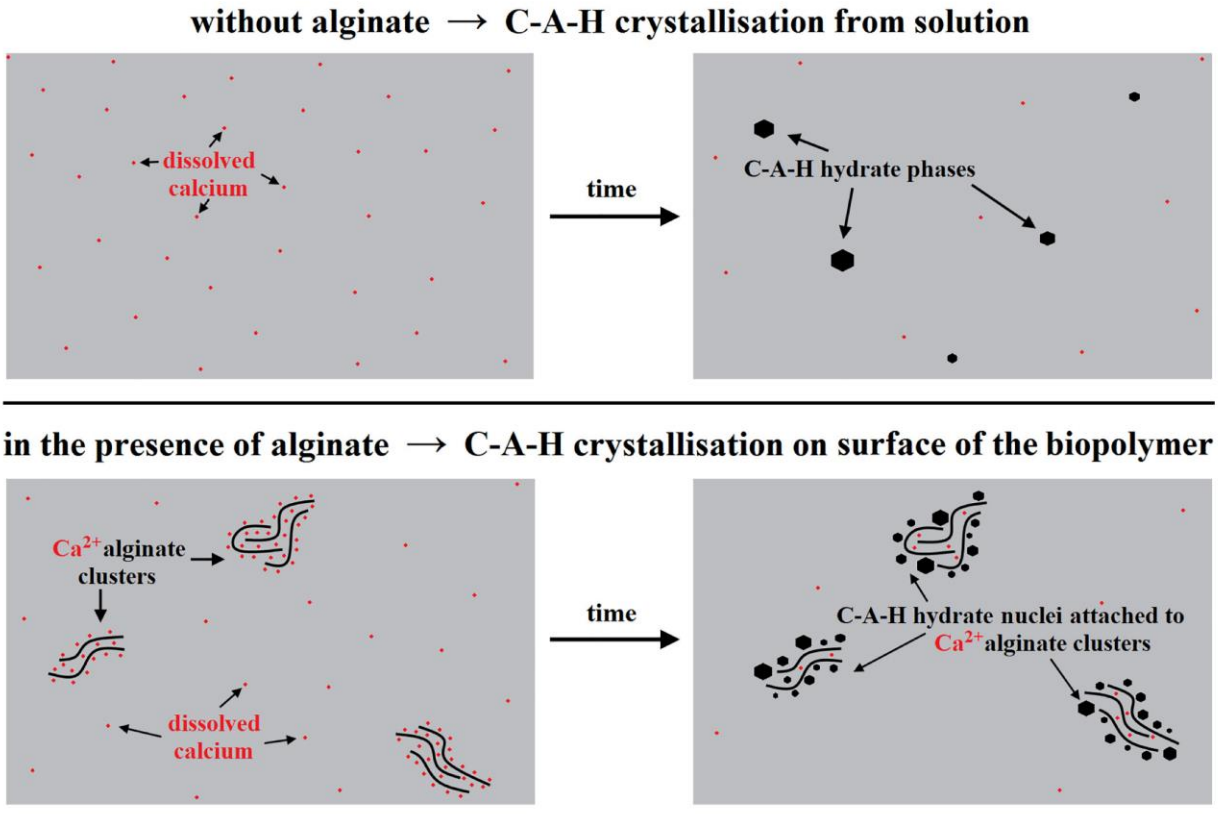

Scheme 1. Models for the C-A-H crystallization from neat CPS (top) and in the presence of alginate (bottom), where a templating effect involving the alignment of Ca^{2+} ions along the biopolymer chain takes place.

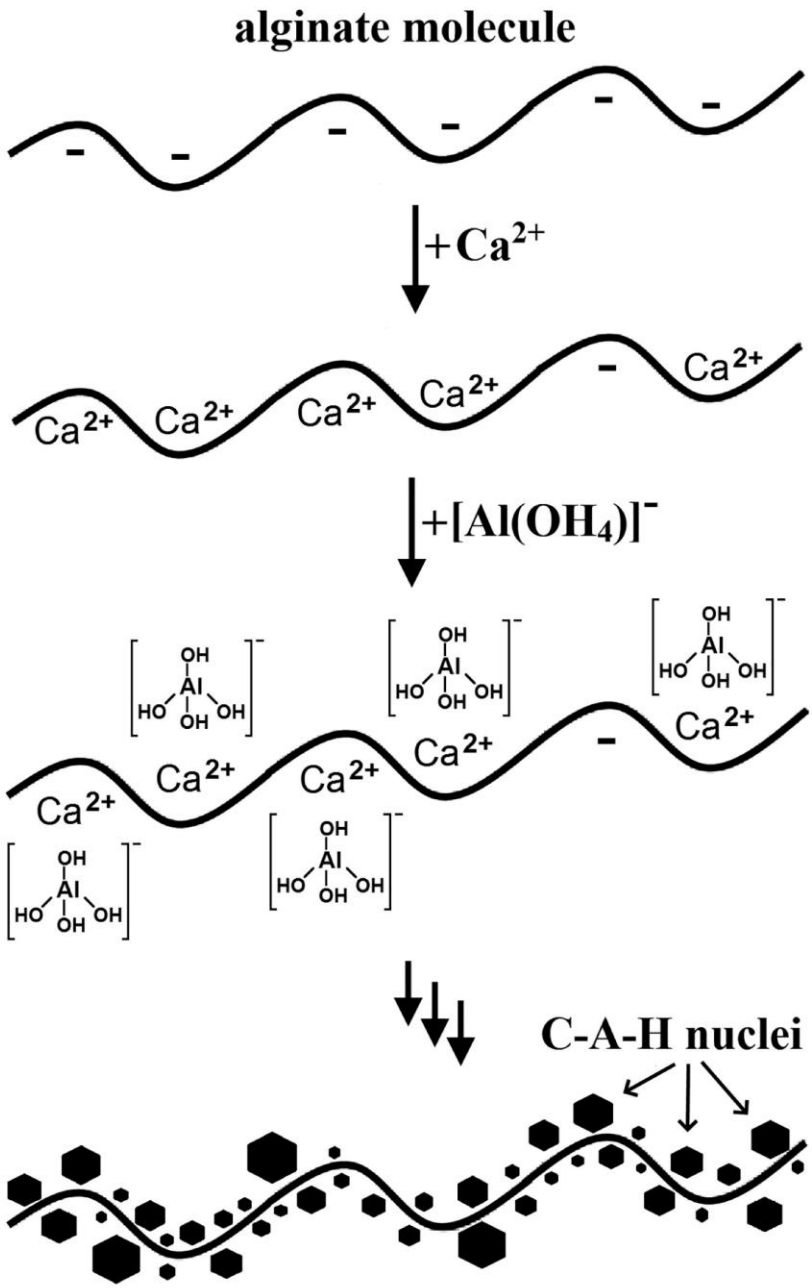

Scheme 2. Schematic illustration of the proposed interaction mechanism between alginate and Ca^{2+} as well as $[Al(OH)_4]^-$ ions in cement pore solution, leading to the formation of C-A-H phases.

the aluminate content in the resulting pore solution which might promote the precipitation of calcium aluminate hydrates, as observed in the XRD analysis before (see Figs. 4 and 5).

4. Proposed working mechanism for alginate

The investigations conducted so far can be summarized as follows:

- The accelerating effect is specific for alumina cements and differs with their reactivity which is dependent on their CA and $C_{12}A_7$ content. The more reactive a cement, the less effective is alginate [1].
- ^{27}Al solid state NMR spectroscopy and XRD confirm earlier formation of C-A-H phases and corresponding consumption of clinker phases in the presence of alginate (Figs. 3 and 4).
- Alginate does not intercalate or adsorb onto the surface of CAC or its hydrates. Hence, its accelerating effect derives from processes occurring in the pore solution.
- Alginate reduces the concentration of free Ca^{2+} in the pore solution through complexation via its 'cavity'. Furthermore, it also reduces

the amount of aluminate in solution (Fig. 7). Because aluminate ions cannot be chelated in the cavity like Ca^{2+}, it can be hypothesized that $[Al(OH)_4]^-$ ions coordinate with positively charged parts of the alginate resulting from Ca^{2+} uptake.

- Even in the presence of retarders such as e.g. citrate and tartrate, alginates still accelerate, in spite of significantly reduced concentrations of dissolved calcium and aluminate [1].

In consideration of this, still the question remains whether Ca^{2+} which has been captured by the alginate is irreversibly bound there or might be released to be incorporated into hydrate phases. Various literature reports (e.g. [27]) present that Ca^{2+} is in fact removed from the biopolymer when stronger chelators such as EDTA, sodium citrate or tartrate are added. Therefore, it can be assumed that at first calcium is extracted from the pore solution, but later is released to contribute to the formation of C-A-H phases. As such, by attracting and locally enriching Ca^{2+} ions along the molecule chain, alginate presents a heterogeneous crystallization surface, thus creating a reservoir and a template from which an initial cluster can nucleate and grow into a crystallite.

In order to verify the proposed mechanism, it was further studied whether C-A-H indeed crystallizes on the surface of the biopolymer chain. To investigate, at first a small amount of sodium alginate solution (2 wt%) was mixed with CPS (extracted from Ciment Fondu). Here, immediately upon addition formation of a slightly opaque hydrogel is observed, thus confirming abundant Ca^{2+} complexation. Furthermore, within a few hours the gel becomes increasingly cloudy and finally distinct particles precipitate from the solution (Fig. 9, top). This effect does not occur in Ca-alginate hydrogels, but only in CPS-alginate hydrogels, thus indicating that the combination of ions in CPS interact differently with alginate than individual Ca^{2+} or $[Al(OH)_4]^-$. Using SEM imaging the particles were identified as alginate polymer encrusted with platy C-A-H crystals (Fig. 9, bottom). Similar observations were also made for mixtures of pectin with CPS.

To further confirm this co-precipitation mechanism of alginate encrusted with C-A-H phases, alginate powder fixed to a sample holder or parts of a calcium alginate hydrogel were submerged in CPS and stored over up to four hours. For the alginate powder placed on the SEM sample holder, after 3 h the first C-A-H clusters were observed on the polymer surface, and after 4 h had covered most of the surface, as is displayed in Fig. 10.

Such templating effect of alginate, pectin and similarly structured biopolymers in biomineralization of e.g. $CaCO_3$ or brushite has been observed before by several authors [28–32]. For example, Ni-Al-LDH which is isostructural to several of the C-A-H phases can be prepared hydrothermally via a "facile biopolymer-assisted" crystallization process using alginate [33]. The proposed mechanism underlying this synthesis (Ni-Al-LDH nucleates and crystallizes along the alginate molecule) follows a similar pattern as the working mechanism which was proposed above for the accelerating effect of alginate on CAC hydration: In the following scheme, the templating effect which triggers C-A-H nucleation via initial interaction of alginate with Ca^{2+} ions is illustrated (Scheme 1). Thus, the proposed mechanism for the behavior of alginate in cement pore solution is supported by processes already known from comparable bio-based systems.

Still, this model does not yet explain the role of aluminate ions which when alginate is present in CPS also significantly decreases in concentration (see Fig. 7). We assume its behavior as follows: the interaction of Ca^{2+} with alginate results in a biopolymer chain exhibiting positive charges along its backbone (Scheme 2). To these sites, negatively charged $[Al(OH)_4]^-$ is attracted. Other authors have reported that while in aqueous solution alginate exhibits a negative electrical charge / zeta potential. In the presence of cations like Ca^{2+} or of cationic polymers (e.g. chitosan), the charge decreases and approaches zero [34,35]. Furthermore, it was found that in case of a layer-by-layer deposition of anionic alginate and cationic chitosan onto a planar surface, a charge reversal occurs with each additional layer ($Algi^- \rightarrow Chit^+ \rightarrow Algi^- \ldots$) [36].

In order to verify that a similar layer-by-layer deposition mechanism is at work here, the zeta potential of alginate in the presence of increasing dosages of calcium ions was determined. Here, the initially highly negative electrical charge of alginate was found to decrease from −32 mV to −12 mV (Fig. 11), similar as has been reported by [34,35], thus confirming the chelation of Ca^{2+} cations by the polysaccharide chain. Next, an increasing dosage of aluminate ions was fed into the alginate solution in combination with a fixed amount (0.5 g/L) of $Ca(OH)_2$. Interestingly, in the presence of $[Al(OH)_4]^-$ the trend for the charge reversed, and with increasing $Na[Al(OH)_4]$ concentration the zeta potential became more negative (from −12 mV to −32 mV, see Fig. 11). This observation confirms our concept that at first Ca^{2+} and in a second step $[Al(OH)_4]^-$ is attracted to the alginate molecule and coordinate to the biopolymer chain whereby at the high pH Ca-Al-OH clusters form which through continued uptake of Ca^{2+} and $[Al(OH)_4]^-$ ions from the pore solution grow into critical clusters and ultimately form the characteristic large, platy crystals of C-A-H phases (Scheme 2).

This mechanistic model combines all previous findings and can well explain why the accelerating effect (1) is absolutely specific for biopolymers possessing high Ca^{2+} capturing capability and (2) why this mechanism cannot work in OPC which does form C-A-H phases during its hydration.

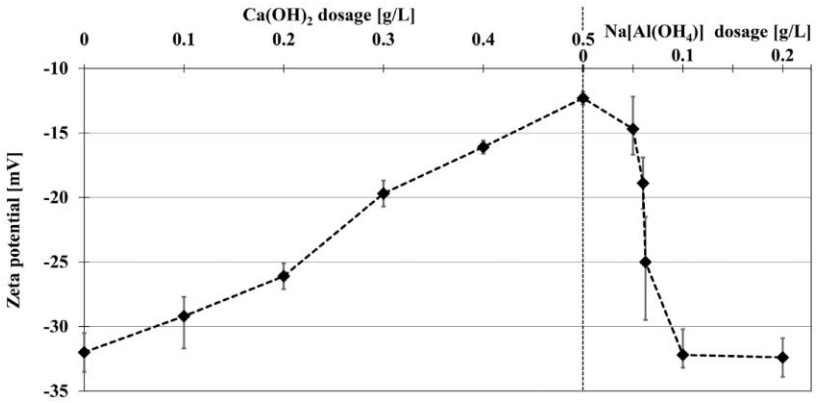

Fig. 11. Zeta potential of aqueous alginate solution (0.15 wt%, pH >12) as a function of increasing Ca^{2+} concentration (left) and $Na[Al(OH)_4]$ addition (right).

5. Conclusion

This study investigated the mechanism underlying the unexpected accelerating effect of alginates and similarly structured biopolymers on alumina cements by first using ^{27}Al MAS NMR spectroscopy to determine the degree of hydration and, second, XRD analysis to monitor hydrate phase development. From these experiments a shortening of the induction period during CAC hydration was evidenced via an earlier commencement of clinker dissolution. Obviously, in the presence of alginate the formation of hydrate phases starts earlier. Such promotion of C-A-H formation leads to an earlier strength development [1].

In order to elucidate the working mechanism which is responsible for this accelerating effect, the interaction between alginate and the ions present in the CAC pore solution was studied. Here, not only a strong complexation of calcium ions through the carboxylate groups in the 'cavity' of the biopolymer, but also an interaction with aluminate ions was found. These results suggested that a bi-layer is formed along the biopolymer chain whereby initially Ca^{2+} ions are captured by the alginate and subsequently aluminate anions are then aligned along the molecule chain, thus templating the essential constitutional part in calcium aluminate hydrates, the Ca-Al-OH building block, and triggering their nucleation and subsequent growth.

Based upon these finding a model is proposed for the mode of action of alginate as an accelerator in CAC. According to this, in CPS the alginate molecule provides a heterogeneous crystallization surface by generating favourable conditions for the very first nucleation and growth of C-A-H phases. This biotemplated process was substantiated by SEM images confirming the earlier nucleation and growth of C-A-H crystals on the surface of the biopolymer.

Currently, lithium salts such as Li_2CO_3 present the only viable accelerator for CAC. Due to the increased demand for lithium ion batteries in electromobility and the relatively limited availability of this element, the substitution of lithium salts in CAC applications appears to be highly urgent and almost compulsory. Biopolymers such as alginate or pectin which present green and renewable materials seem to offer an attractive alternative to replace the precious lithium compounds in calcium aluminate cements.

Declaration of Competing Interest

Funding was provided by Deutsche Forschungsgemeinschaft, Germany (DFG) under the grant PL-472/13-1 ("*Investigation on the replacement of lithium carbonate as accelerator for calcium aluminate cements and its underlying working mechanism*").

The authors wish to declare that no conflicts of interest or competing interests exists.

Acknowledgement

The authors are most grateful to *Imerys Aluminates* (formerly *Kerneos*) for the generous supply of aluminate cement samples. Especially Mr. A. Eisenreich and Dr. R. Kwasny-Echterhagen are thanked for their support. Our gratitude also goes to *Eurogum* and *Herbstreith & Fox* for providing the biopolymer samples. Moreover, the authors are most grateful to Deutsche Forschungsgemeinschaft, Bonn, Germany (DFG) for financing this project under the grant PL-472/13-1 ("*Investigation on the replacement of lithium carbonate as accelerator for calcium aluminate cements and its underlying working mechanism*"). Finally, the support of T. Burger (Chair for Technical Chemistry, TUM) for conducting the ICP-OES measurements is also acknowledged.

Appendix A. Supplementary data

Supplementary data to this article can be found online at https://doi.org/10.1016/j.matdes.2020.109054.

References

[1] A. Engbert, S. Gruber, J. Plank, The effect of alginates on the hydration of calcium aluminate cement, Carbohydr. Polym. 236 (2020) 116038.
[2] A. Engbert, J. Plank, Identification of specific structural motifs in biopolymers that effectively accelerate calcium alumina cement, Ind. Eng. Chem. Res. 59 (26) (2020) 11930–11939.
[3] S.A. Rodger, D.D. Double, The chemistry of hydration of high alumina cement in the presence of accelerating and retarding admixtures, Cem. Concr. Res. 14 (1) (1984) 73–82.
[4] T. Matusinović, D. Čurlin, Lithium salts as set accelerators for high alumina cement, Cem. Concr. Res. 23 (4) (1993) 885–895.
[5] T. Matusinovic, N. Vrbos, D. Čurlin, Lithium salts in rapid setting high-alumina cement materials, Ind. Eng. Chem. Res. 33 (11) (1994) 2795–2800.
[6] D. Damidot, A. Rettel, A. Capmas, Action of admixtures on Fondu cement: part 1 Lithium and sodium salts compared, Adv. Cem. Res. 8 (31) (1996) 111–119.
[7] F. Goetz-Neunhoeffer, Kinetics of the hydration of calcium aluminate cement with additives, ZKG Int. 58 (4) (2005) 65–72.
[8] T. Manninger, D. Jansen, J. Neubauer, F. Goetz-Neunhoeffer, Accelerating effect of Li_2CO_3 on formation of monocarbonate and Al-hydroxide in a CA-cement and calcite mix during early hydration, Cem. Concr. Res. 126 (2019) 105897.
[9] J. Bensted, Calcium aluminate cements, Structure and Performance of Cements, Second editionCRC Press, Boca Raton, USA 2002, pp. 114–138.
[10] A.P. Imeson, Food stabilisers, thickeners and gelling agents, Wiley Blackwell, Hoboken - New Jersey, USA, 2011.
[11] J. Plank, Applications of biopolymers in construction engineering, Biopolymers: Vol. 10 General Aspects and Special Applications, Wiley-VCH, Weinheim, Germany 2003, pp. 29–95.
[12] G.T. Grant, E.R. Morris, D.A. Rees, P.J. Smith, D. Thom, Biological interactions between polysaccharides and divalent cations: the egg-box model, FEBS Lett. 32 (1) (1973) 195–198.
[13] M.F. Borisenkov, A.P. Karmanov, L.S. Kocheva, et al., Adsorption of β-glucuronidase and estrogens on pectin/lignin hydrogel particles, Int. J. Polym. Mater. Polym. Biomater. 65 (9) (2016) 433–441.
[14] DIN EN 196-–11, Methods of testing cement – part 11: heat of hydration – isothermal conduction Calorimetry method, German Version EN (2019) (196–11).
[15] A. Bier, A. Mathieu, B. Espinosa, J.P. Bayoux, Technical Paper 1: The Use of Conductimetry to Characterize the Reactivity of High Alumina Cements, Kerneos, France, 1993.
[16] C.D. Parr, C. Revais, H. Fryda, Technical Paper 18: The Nature of Chemical Reactions that Occur during Castable Installation and Analytical Techniques Used to Follow these Reactions, Kerneos, France, 1999.
[17] X. Cong, R.J. Kirkpatrick, Hydration of calcium aluminate cements: a solid state ^{27}Al NMR study, J. Am. Ceram. Soc. 76 (2) (1993) 409–416.
[18] T. Luong, H. Mayer, H. Eckert, T.I. Novinson, In situ ^{27}Al NMR studies of cement hydration: the effect of lithium-containing setting accelerators, J. Am. Ceram. Soc. 72 (11) (1989) 2136–2141.
[19] C. Gosselin, Microstructural Development of Calcium Aluminate Cement Based Systems With and Without Supplementary Cementitious Materials, Ph.D. thesis École Polytechnique Fédérale de Lausanne, Switzerland, 2009.
[20] S.R. Klaus, J. Neubauer, F. Goetz-Neunhoeffer, Hydration kinetics of CA_2 and CA - investigations performed on a synthetic calcium aluminate cement, Cem. Concr. Res. 43 (2013) 62–69.
[21] S. Ng, E. Metwalli, P. Müller-Buschbaum, J. Plank, Occurrence of intercalation of PCE superplasticizers in calcium aluminate cement under actual application conditions, as evidenced by SAXS analysis, Cem. Concr. Res. 54 (2013) 191–198.
[22] J. Plank, Z. Dai, N. Zouaoui, Novel hybrid materials obtained by intercalation of organic comb polymers into Ca–Al–LDH, J. Phys. Chem. Solids 69 (5–6) (2008) 1048–1051.
[23] J.F. Young, A review of the mechanisms of set-retardation in Portland cement pastes containing organic admixtures, Cem. Concr. Res. 2 (4) (1972) 415–433.
[24] T. dos Santos, C.I. Pereira, R. Gonçalves, et al., Gluconate action in the hydration of calcium aluminate cements: theoretical study, processing of aqueous suspensions and hydration reactivation, J. Eur. Ceram. Soc. 39 (8) (2019) 2748–2759.
[25] A. Pallagi, Interaction of Calcium With Sugar Type Ligands in Solutions Related to the Bayer Process, Ph.D. thesis University of Szeged, Hungary, 2012.
[26] F.R. Venema, J.A. Peters, H. Van Bekkum, Multinuclear magnetic resonance study of the coordination of aluminium (III) aldarate complexes with calcium (II) in aqueous solution, Recueil des Travaux Chimiques des Pays Bas 112 (7–8) (1993) 445–450.
[27] M. Kobašlija, D.T. McQuade, Removable colored coatings based on calcium alginate hydrogels, Biomacromolecules 7 (8) (2006) 2357–2361.
[28] M. Díaz-Dosque, P. Aranda, M. Darder, et al., Use of biopolymers as oriented supports for the stabilization of different polymorphs of biomineralized calcium carbonate with complex shape, J. Cryst. Growth 310 (24) (2008) 5331–5340.
[29] R. Fried, Y. Mastai, The effect of sulfated polysaccharides on the crystallization of calcite superstructures, J. Cryst. Growth 338 (1) (2012) 147–151.
[30] M.F. Butler, W.J. Frith, C. Rawlins, et al., Hollow calcium carbonate microsphere formation in the presence of biopolymers and additives, Crystal Growth Des. 9 (1) (2008) 534–545.
[31] S. Ucar, S.H. Bjørnøy, D.C. Bassett, et al., Nucleation and growth of Brushite in the presence of alginate, Cryst. Growth Des. 15 (11) (2015) 5397–5405.
[32] Z. Schnepp, Biopolymers as a flexible resource for nanochemistry, Angew. Chem. Int. Ed. 52 (4) (2013) 1096–1108.

[33] H. Wang, G. Fan, C. Zheng, et al., Facile sodium alginate assisted assembly of Ni—Al layered double hydroxide nanostructures, Ind. Eng. Chem. Res. 49 (6) (2010) 2759–2767.
[34] M. Cegnar, J. Kerč, Self-assembled polyelectrolyte Nanocomplexes of alginate, chitosan and ovalbumin, Acta Chim. Slov. 57 (2) (2010).
[35] L. Miao, C. Wang, J. Hou, et al., Effect of alginate on the aggregation kinetics of copper oxide nanoparticles (CuO NPs): bridging interaction and heteroaggregation induced by Ca^{2+}, Environ. Sci. Pollut. Res. 23 (12) (2016) 11611–11619.
[36] A. Acevedo-Fani, L. Salvia-Trujillo, R. Soliva-Fortuny, O. Martín-Belloso, Layer-by-layer assembly of food-grade alginate/chitosan nanolaminates: formation and physicochemical characterization, Food Biophys. 12 (3) (2017) 299–308.

Publikation 3:

Materials & Design, 2020, 195, 109054.

Supporting information

Templating Effect of Alginate and Related Biopolymers as Hydration Accelerators for Calcium Alumina Cement - A Mechanistic Study

Alexander Engbert, Johann Plank*

Technische Universität München, Chair for Construction Chemistry, Lichtenbergstr. 4, 85747 Garching, Germany

*Corresponding author:

Prof. Dr. Johann Plank

Chair for Construction Chemistry

Technische Universität München

Lichtenbergstr. 4

85747 Garching bei München, Germany

Tel.: +49 (0) 89 289 13 151

Fax: +49 (0) 89 289 13 152

E-Mail: sekretariat@bauchemie.ch.tum.de

ORCID (Johann Plank): 0000-0002-4129-4784

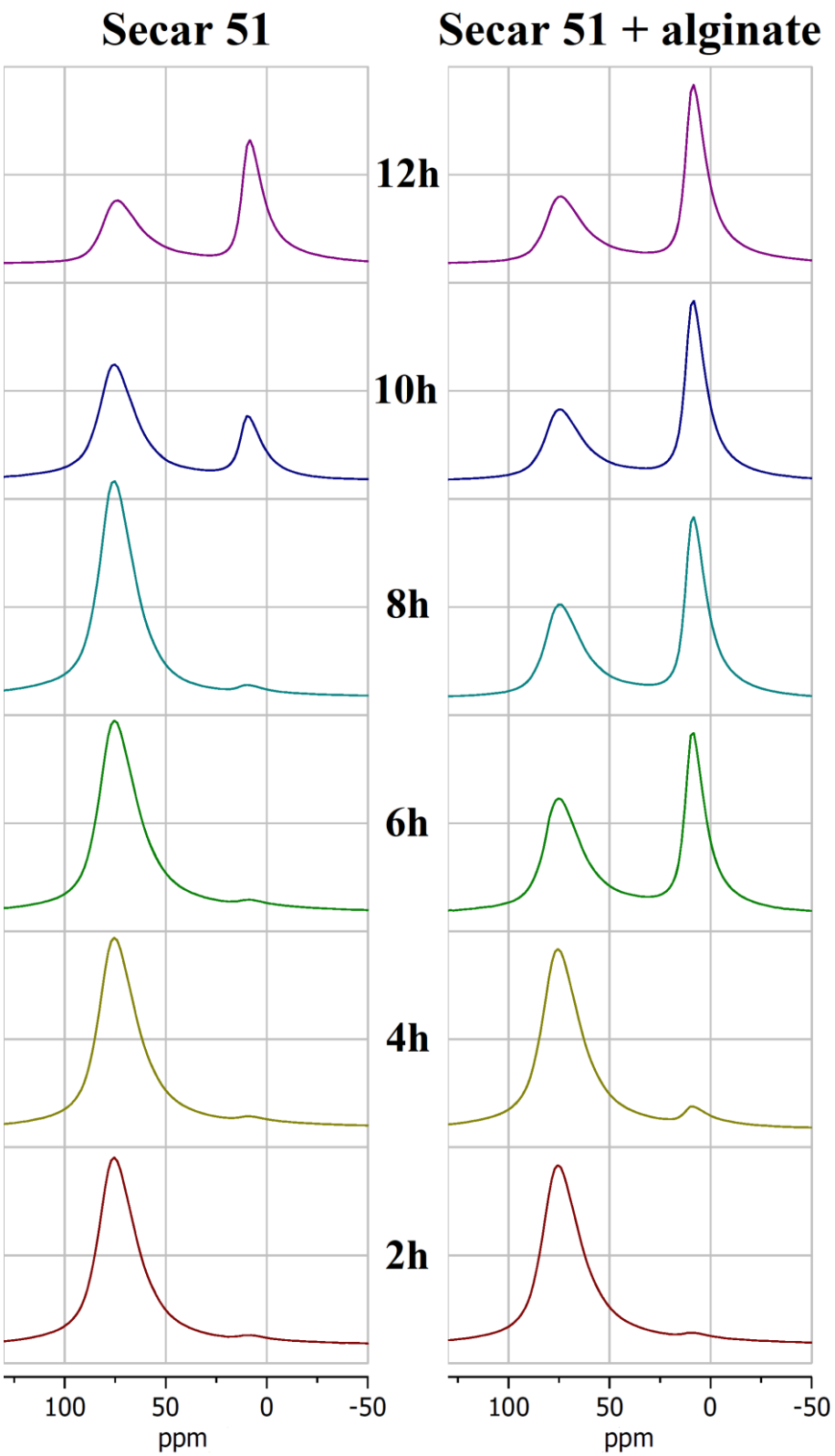

Figure S1: ^{27}Al MAS NMR spectroscopic measurements of CAC sample Secar 51 (w/b = 0.5) in the absence and presence of alginate (sample XEA 5036) after different hydration periods.

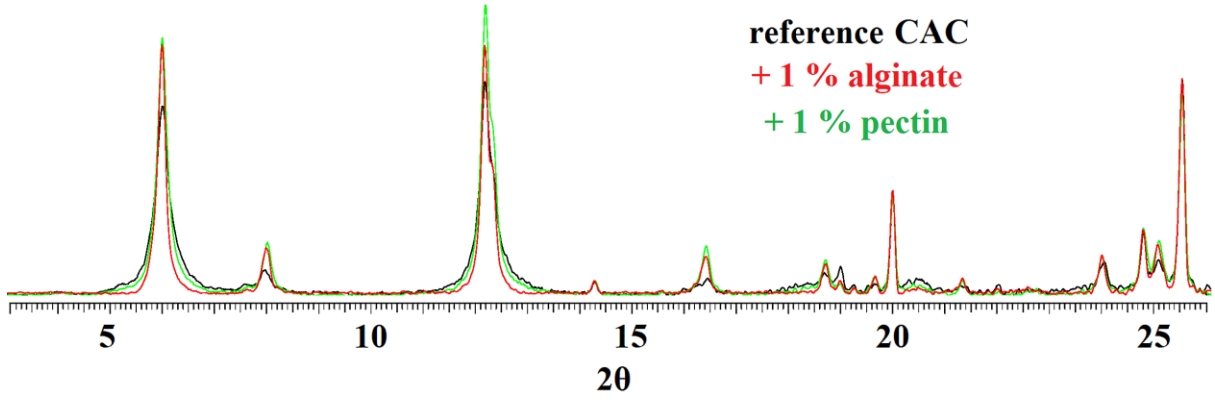

Figure S2: Overlap of the XRD diffractograms of ground cement samples (Secar 71, w/b = 1, 20 °C) after 24 hours of hydration in the absence or presence of 1 wt.% alginate (sample XEA 5036) or pectin (sample CU 701).

3.3.3 Addendum

Zusätzlich zu den in der Publikation dargestellten Ergebnissen wurden noch weiterführende Untersuchungen durchgeführt, welche im Folgenden erläutert werden:

Im Rahmen der Publikation wurde die Bildung von Hydratationsprodukten mittels *ex-situ* XRD bei 20 °C betrachtet. Da ein häufiger Anwendungsbereich von Aluminatzementen unter anderem die Zementierung bei niedrigen Temperaturen ist, wurde darüberhinaus das Abbindeverhalten und die hierbei entstehenden Hydratphasen bei unterschiedlichen Temperaturen untersucht. Bei niedrigen Temperaturen von 5 und 10 °C wurde lediglich die Bildung von CAH_{10} festgestellt, wobei Alginat weiterhin einen beschleunigenden Effekt auf die Hydratation zeigte. Dieser fiel aber im Vergleich zu 20 °C geringer aus, aufgrund der bekannt schnelleren Hydratation von CAC bei niedrigen Temperaturen. Auch bei erhöhten Temperaturen (> 20 °C) wurde eine geringere Beschleunigung festgestellt. Generell zeigen Aluminatzemente im Temperaturbereich von 25 – 35 °C aufgrund der thermodynamisch ungünstigen Kristallisationsbedingungen eine deutlich verlängerte dormante Phase. Während Lithiumcarbonat dort weiterhin einen stark beschleunigenden Effekt zeigt, folgt Alginat dem Trend verlängerter Abbindezeiten mit steigender Temperatur. Bei 40 °C zeigte die Analyse der gebildeten Hydratphasen AH_3, C_2AH_8 und C_3AH_6, sowie bei 70 °C AH_3 und C_3AH_6. Details hierzu sind dem Anhang in **Abschnitt 7.3** zu entnehmen.

Nachdem mittels REM-Untersuchungen eine heterogene Bildung von C-A-H-Phasen auf der Polymer-Oberfläche festgestellt wurde, erfolgte im Weiteren der Versuch, derartige auf dem Alginat gebildeten Kristalle mittels Röntgendiffraktometrie zu erfassen und zu charakterisieren. Hierfür wurde ein Probenträger analog zur Herstellmethode für die Elektronenmikroskopie (siehe **Abbildung 24** in Kapitel 2.4.4) mit Alginatpulver in CPS gelagert und die gefriergetrocknete Probe vermessen. Das erhaltene Diffraktogramm (siehe Anhang **Abschnitt 7.4**) zeigte Reflexe, welche den Ca-Al-LDH Phasen C_2AH_8, C_4AH_{19} sowie den Dehydratationsprodukten C_2AH_5 bzw. C_2AH_4 zugeordnet werden konnten [61,66].

Weitere REM Aufnahmen der in der Publikation gezeigten C-A-H-Alginat-Proben (siehe **Abbildungen A15** und **A16**) sowie Aufnahmen vorheriger Untersuchungen mit alternativen Probenpräparationsmethoden (siehe **Abbildung A18 – A20**) sind in **Abschnitt 7.5** des Anhangs beigefügt. Im Rahmen letztgenannter Experimente wurden ebenfalls C-A-H-Carrageen- und C-A-H-Pektin-Proben mikroskopiert (siehe **Abbildung A21**).

3.4 Publikation 4: Beschleunigender Effekt von Füllstoffen auf CAC

3.4.1 Zusammenfassung

Bei genauerer Betrachtung der in **Publikation 1** gefundenen Ergebnisse zur Beschleunigung von CAC durch Alginat ist zu erkennen, dass sich die Wirksamkeit des Alginats in der Zementpaste (Kalorimetrie) und in den Mörtelfestigkeiten deutlich unterscheidet.

Dieses Phänomen wurde in der hier vorliegenden Studie betrachtet, wobei folgende wichtige Erkenntnisse gewonnen wurden:

- Die Abbindereaktion wurde anhand ihrer Wärmefreisetzung in Zementpaste sowie in einer Mörtelmischung (Zement + Normsand) mittels isothermer Kalorimetrie untersucht. Dabei wurde festgestellt, dass der „inerte“ Füllstoff Sand einen nennenswerten Einfluss auf die Hydratation von CAC hat, wobei diese früher einsetzt.
- Kalorimetrische Messungen an Mörteln zeigten eine deutlich bessere Korrelation mit den Ergebnissen der Druckfestigkeitstests als die kalorimetrischen Messungen in Zementpaste. Demnach ermöglichen kalorimetrische Messungen mit Mörteln eine bessere Abschätzung der tatsächlichen Festigkeitsentwicklung.
- Durch die vom Sand eingebrachte zusätzliche heterogene Kristallisationsoberfläche tritt ein vorzeitiges Abbinden des Mörtels im Vergleich zur Zementpaste ein. Dieser beschleunigende Einfluss des Füllstoffs überdeckt den Effekt von Alginat als Beschleuniger und lässt seine Wirksamkeit geringer erscheinen.
- Da dieser Effekt bereits bei Normsand (0 – 2 mm) zu beobachten war, wurden weitere Füllstoffe mit zunehmender Feinheit und BET-Oberfläche getestet. Hier zeigte sich ein mit abnehmender Partikelgröße bzw. zunehmender SSA verstärkt beschleunigender Einfluss auf die Hydratation von CAC.
- Dies ermöglichte im Mörtel eine beachtliche Steigerung der Frühfestigkeit über einen anteiligen Ersatz des Normsandes durch feine Füllstoffe. So konnte in einem Mörtel mit dem CAC „*Secar 51“* eine Festigkeit von 29 N/mm^2 (gegenüber 2 N/mm^2 bei der Referenz) erreicht werden, indem 50 g der 1,35 kg des Sandes durch γ-Al_2O_3 (d_{50} 30 µm, BET 75 m^2/g) ersetzt wurden.

- Eine mechanistische Betrachtung der beschleunigenden Wirkung der Füllstoffe α- und γ-Al_2O_3 durch Analyse der Zementporenlösung zeigte analog zum Alginat eine ausgeprägte Calciumbindefähigkeit, was ein vergleichbares Wirkprinzip zu den beschleunigenden Biopolymeren impliziert.
- Die Untersuchung der Füllstoffoberfläche durch Rasterelektronenmikroskopie nach Kontakt mit CPS wies einen kristallinen Überwuchs der γ-Al_2O_3 Partikel mit Hydratationsprodukten auf und bestätigte die Wirkung als heterogene Kristallisationsoberfläche, ähnlich wie bei Alginat.

3.4.2 Veröffentlichung

Impact of Sand and Filler Materials on the Hydration Behavior of Calcium Aluminate Cement

Engbert A., Plank J.

Journal of the American Ceramic Society, 2020.

https://doi.org/10.1111/jace.17505

Received: 26 May 2020 | Revised: 13 August 2020 | Accepted: 12 September 2020

DOI: 10.1111/jace.17505

ORIGINAL ARTICLE

Journal of the American Ceramic Society

Impact of sand and filler materials on the hydration behavior of calcium aluminate cement

Alexander Engbert | **Johann Plank**

Chair for Construction Chemistry, Technische Universität München, Garching bei München, Germany

Correspondence
Prof. Dr. Johann Plank, Chair for Construction Chemistry, Technische Universität München, Lichtenbergstr. 4, 85747 Garching bei München, Germany.
Email: sekretariat@bauchemie.ch.tum.de

Funding information
Funding was provided by Deutsche Forschungsgemeinschaft, Germany (DFG) under the grant PL-472/13-1 ("Investigation on the replacement of lithium carbonate as accelerator for calcium aluminate cements and its underlying working mechanism"). Open access funding enabled and organized by Projekt DEAL.

Abstract

In earlier work, we have observed discrepancies relating to the early hydration of calcium aluminate cement (CAC) when comparing data from heat flow calorimetry of CAC paste with results from mortar strength tests using the crushing method. Here, we investigated on this phenomenon and found that the sand which is used as a filler exerts a major influence on CAC hydration resulting in acceleration. Furthermore, in particular fine filler materials such as, for example, microsilica, fine limestone powder, and especially α- and γ-Al_2O_3 also produced a strong hydration accelerating effect which is dependent on their specific surface area. The mechanism underlying the acceleration is that under alkaline conditions their negative surface charge attracts calcium ions as was confirmed via inductively coupled plasma atomic emission measurements. Such a layer generates favourable conditions for the nucleation of CAC hydration products (C-A-H phases). The resulting crystalline hydrates which form on the surface of the filler particles submerged in CAC cement pore solution were visualized via SEM imaging. This way, specifically selected fillers can significantly accelerate CAC hydration and save precious lithium salts which are commonly used to boost the early strength of CAC.

KEYWORDS

acceleration, calcium aluminate cement, filler materials, hydration, mortar calorimetry

1 | INTRODUCTION

The set behavior of cements such as ordinary Portland cement (OPC) or calcium aluminate cement (CAC) in the presence of various admixtures like superplasticizers,[1-3] latex polymers,[4,5] retarders,[6,7] or accelerators including nano C-S-H[8,9] or biopolymers, for example, alginate[10-12] has been investigated extensively. Most often, heat flow calorimetry in cement paste and mortar strength tests are applied to study the impact of admixtures on the hydration reaction of the binder.

It is generally known that heat flow calorimetry only presents insight into exothermic hydration reactions which are not necessarily linked to the strength development of the binder. One such example is the so-called "sulfate depletion peak."[13,14] This reaction which includes the conversion of ettringite to monosulfoaluminate does not much contribute to the specimen's strength which mostly originates from C-S-H formation. Another observation is that calorimetric results from cement pastes often do not match with data on actual strength development of mortar or concrete obtained from

Abbreviations: A, Al2O3; C, CaO; F, Fe2O3; H, H2O; M, MgO; S, SiO2; T, TiO2.

TABLE 1 Physical properties of different filler materials (particle size, Brunauer-Emmett-Teller-Analysis (BET) value, alkali content and *Blaine* value according to supplier's information)

	APYRAL	ACTILOX	NABALOX	NABALOX	NABALOX	SILMIKRON	AEROXIDE	PRECARB	MILLISIL	QUARZ-SAND
Product name	**200SM**	**200SM**	**NO 221-30**	**NO 783**	**NO 784**	**805/10-1**	**P25**	**100**	**W 12**	**F 36**
Filler material	$Al(OH)_3$	AlO(OH)	γ-Al_2O_3	α-Al_2O_3	α-Al_2O_3	SiO_2	TiO_2	$CaCO_3$	SiO_2	SiO_2
Purity (wt%)	99.3	98.5	>99	≥99.7	≥99.8	99	≥99.5	99	99	99.3
Alkali content (wt%)	≥0.04	—	—	≤0.3	≤0.1	0.4	—	—	0.3	—
d_{10} (µm)	0.3	0.2	—	0.4	0.4	0.2	0.2[a]	—	—	—
d_{50} (µm)	0.4	0.3	30	0.8	0.8	0.5	2.7[a]	1.0	16	160
d_{90} (µm)	0.8	0.6	50	2.0	2.0	1.0	9.2[a]	—	—	—
BET (m^2/g)	15	17	75	12	7	20	50	9	0.9	—
Blaine (cm^2/g)	39 500[a]	—	3700[a]	23 500[a]	—	—	—	—	3800	—

Values were determined by ourselves using a *Blaine* instrument or a laser granulometer model *1064* (CILAS Instruments).[a]

crushing tests. This discrepancy has been addressed for example by *Cottin and George* when investigating the setting time of a CAC paste as compared to a CAC concrete.[15] The authors report a difference for the initial setting time of up to 5 hours between both systems, depending on the reaction temperature.

In previous works, we have investigated the accelerating effect of alginate and similarly structured biopolymers on CAC.[10,11] As working mechanism for these unusual accelerators, we proposed a heterogeneous surface crystallization process facilitated by alternating layers of Ca^{2+} und $[Al(OH)_4]^-$ ions deposited along the molecular chain of the biopolymers.[12] Furthermore, in this study a discrepancy between heat flow calorimetry using paste and strength data collected from mortar was observed. For example, calorimetry suggested that in the presence of alginate the maximum heat release occurs 20%-50% earlier as in the neat cement paste. In the case of one cement sample (Ternal LC), this presented a reduction of the induction period of ≈ 4.5 hours (max. heat release of neat cement at 9.1 hours vs 4.7 hours in the presence of alginate).[10] However, mortar strength testing using this cement revealed that after 6 hours of curing the neat mortar already had developed ≈ 10 N/mm^2 of compressive strength.[10] Whereas, according to the calorimetry performed in paste, the neat mortar should not yet have hardened at 6 hours after preparation.

In the work presented here, we investigated upon this discrepancy between results obtained from paste and mortar, and probed into the cause behind this effect. At first, the heat release in calorimetry was determined in cement paste as well as in mortar, especially taking into account the impact of admixtures like, for example, alginate. Thereafter, the relationship between calorimetric data obtained from mortar calorimetry and actual mortar strength development was qualitatively correlated. Furthermore, in the next step, the impact of sand and filler materials in general on the setting behaviour and strength development of CAC was investigated via calorimetry and compressive strength testing of mortar specimens. Finally, a mechanistic study was conducted to further elucidate the role of sand and fillers in CAC hydration by analyzing the cement pore solution composition via ICP-OES and characterization of the filler particle surface after imbibition in cement pore solution via Scanning electron microscopy (SEM) imaging.

2 | EXPERIMENTAL PROCEDURE

2.1 | Cement samples

Different CACs (*Secar 51*, *Secar 71*, and *Secar 712*, produced by Imerys Aluminates) and an ordinary Portland cement (CEM I 52.5 N, *HeidelbergCement*, Milke plant) were

utilised in this study. Information regarding their mineralogical phase composition, particle size, and *Blaine* value has been provided previously.[10,16]

2.2 | Materials

Different filler materials ($CaCO_3$, SiO_2, TiO_2, Al_2O_3, AlO(OH) and $Al(OH)_3$) were supplied by *Nabaltec*, *Quarzwerke*, *Schaefer Kalk,* and *Evonik*. Their chemical composition, alkali/earth alkali content (Na_2O, K_2O, CaO, and MgO), particle size and specific surface area (SSA) are display in Table 1.

In all experiments, deionised water obtained from a *Barnstead Nanopore Diamond* purification system (Werner Reinstwassersysteme) was used. Mortars were prepared using European Committee for Standardization (Comité Européen de Normalisation) standard sand (Normensand GmbH).

Alginate sample *XEA 5036* (Eurogum; for properties refer to[10]) was used as accelerator for CAC while anhydrous citric acid (≥99.5 wt%, Bernd Kraft GmbH) was added as retarder for OPC. As superplasticizer, an MPEG-type Polycarboxylate ester (PCE) exhibiting high anionic character and possessing a long side chain was utilized. Its properties are described in.[10]

2.3 | Experimental methods

2.3.1 | Isothermal heat-flow calorimetry

Paste calorimetry was performed in accordance with DIN EN 196-11[17] using sealable 10 mL glass ampules. Four grams of cement were filled into the ampoule and dry-blended with previously placed alginate powder, solid citric acid, or filler material.

Mortar calorimetry was conducted utilizing sealable 20 mL glass ampules. First, alginate or citric acid were placed into the ampoule, followed by precisely four grams of cement and the norm sand/filler material (s + f = 12 g).

Deionised water was added to the mixture, the ampoule was sealed and homogenized for 2 minutes using a vortex mixer (VWR) before placement into an isothermal heat flow conduction calorimeter *TAM air model 3116-2* (Thermometric). Measurements were conducted at 20°C until heat evolution ceased.

2.3.2 | Mortar tests

Mortar testing was conducted according to DIN EN 196-1[18] (strength testing) and DIN EN 1015-3[19] (workability). Strength values were determined using a *ToniNORM* instrument setup (Toni Technik) consisting of a *powerbox model 2010* equipped with two load frames (*model 1543* and *model 1544*). Using a *ToniMIX* eccentric agitator (Toni Technik), the mortar was automatically prepared whereby the water containing the superplasticizer as well as one drop of defoamer (Dowfax DF 141; Dow Chemical) were first placed in the mixer cup. The mortar prisms (4 × 4 × 16 cm) were compacted using a *ToniVib* vibrating table (Toni Technik) and stored at 20°C until demoulding. Mortar density was calculated from the size and weight of the prisms.

Mortar tests were performed using the same shipment of each cement and the prisms were produced in one test series. This precaution was taken because CAC is quite sensitive to aging.

2.4 | Analytical methods

2.4.1 | Ion concentrations via inductively coupled plasma atomic emission

Extraction of a cement pore solution for analysis was performed via centrifugation (10 000 *g*, 15 minutes) of the cement paste which was prepared by admixing, for example, 20 g of Secar 51 dry-blended with 20 wt% filler in a centrifuge tube and subsequent homogenisation for 2 minutes utilizing a vortex mixer. The supernatant pore solution was filtrated using a 0.2 µm Polyethersulfone membrane filter, diluted 1:30 using an acidified (hydrochloric acid) solution and analyzed via inductively coupled plasma atomic emission spectroscopy on a *series 700* apparatus (Agilent Technologies). Resulting data were averaged and reported including an additional methodical error of 1% to account for deviations in sample preparation.

2.4.2 | SEM imaging

Sample material was fixated to the sample holder stub with *Leit Adhesive Carbon Tabs* (PLANO) and was sputtered with gold for improved conductivity after freeze-drying. SEM imaging was performed on a *XL–30 FEG* microscope (FEI) equipped with secondary and backscattered electron detectors at 15 or 25 kV accelerating voltage at a working distance of 10 mm.

2.4.3 | X-ray diffraction

Powder diffraction patterns were captured on a *D8 advance* instrument (Bruker AXS) equipped with a *VÅNTEC-1* detector (3° - 45° 2θ, 30 kV, 35 mA, 0.008° step, variable

divergence slit V6, *Bragg-Brentano* geometry and Cu Kα source). Evaluation and processing of the diffraction patterns was performed using Bruker's *EVA V2* software.

3 | RESULTS AND DISCUSSION

3.1 | Hydration of cement paste and mortar investigated via calorimetry

As described in the introduction, in our previous investigation[10] the results on the accelerating effect of alginate in CAC obtained from calorimetry using cement paste did not match with those from mortar strength testing. Therefore, either calorimetry in general or calorimetry performed using cement paste seems to be inappropriate to produce data which are representative of the setting behavior of mortar. To investigate on this subject, heat flow calorimetry was conducted by employing a CAC mortar consisting of three quarters of sand (12 g) and one quarter of cement (4 g). This approach of using a mortar containing sand for calorimetric measurements is not described in the standard DIN EN 169-11 which focuses on paste only.[17]

The results from this experiment are displayed in Figure 1. There, the heat flow curves from paste (top) and mortar (bottom) based on a neat CAC sample (Secar 71), admixed with or without 0.1 wt% of alginate are presented.

As is evident from the graphs, the setting behaviour (as expressed by the heat released during hydration) of a CAC paste or mortar diverge significantly. The system accelerated by alginate yields comparable results while the neat paste and mortar exhibit a difference of nearly 3 hours for the time until maximum heat release occurs. Obviously, the addition of norm sand shifts the beginning of the acceleration period to a much earlier time, resulting in faster hardening of the mortar. This effect of sand needs to be taken into account and thus well explains the discrepancy observed in our previous investigations.

To check whether such an effect is specific only for aluminate cement, also an OPC was investigated via calorimetry (see Figure 2). Again, results achieved in paste as well as in mortar were compared, and the system without or admixed with 0.1 wt% of citric acid retarder were looked at. Also here, as was noticed in the case for CAC before, an accelerating effect of the norm sand regarding the time of maximum heat release was observed which however was less pronounced than in CAC, but still significant enough.

To validate mortar calorimetry as a method which better represents the actual hydration behaviour and strength development of CAC mortar, additional tests were performed employing two different CAC samples and comparing the results from mortar heat flow calorimetry with those from mortar strength testing. As CAC samples, one exhibiting a long induction period (Secar 712) and one possessing a short induction period (Ternal LC) were probed. Moreover the mortars were admixed with biopolymer accelerator (alginate or carrageenan). In the case of Secar 712, a PCE superplasticizer was admixed to improve workability of the mortar.

As is evident from Figure 3, mortar calorimetry produces results which qualitative match the strength development of the

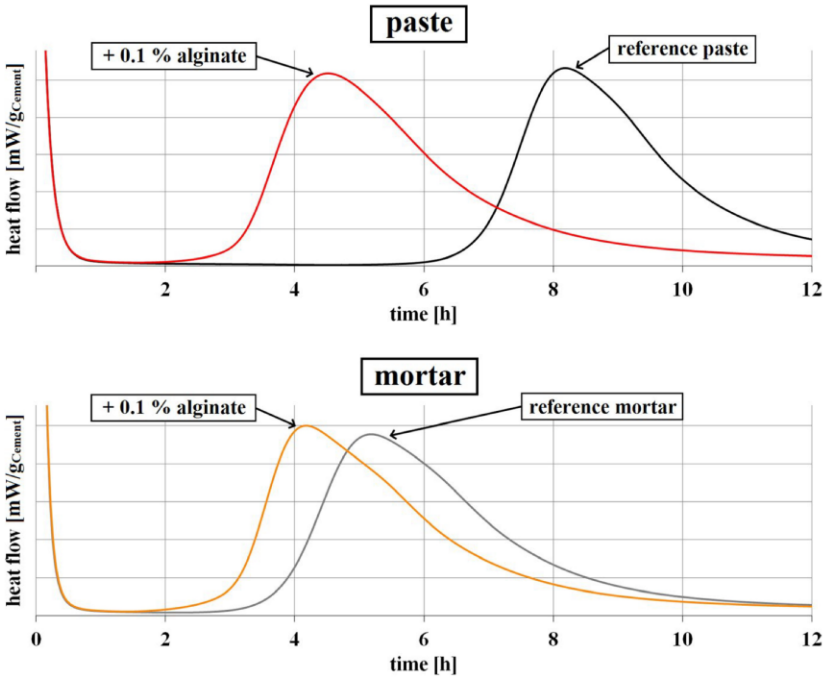

FIGURE 1 Comparison of heat evolution from cement paste (top, w/c = 0.5) or mortar (bottom, w/c = 0.55) of a calcium aluminate cement sample (Secar 71), neat or admixed with 0.1 wt.% alginate (sample XEA 5036)

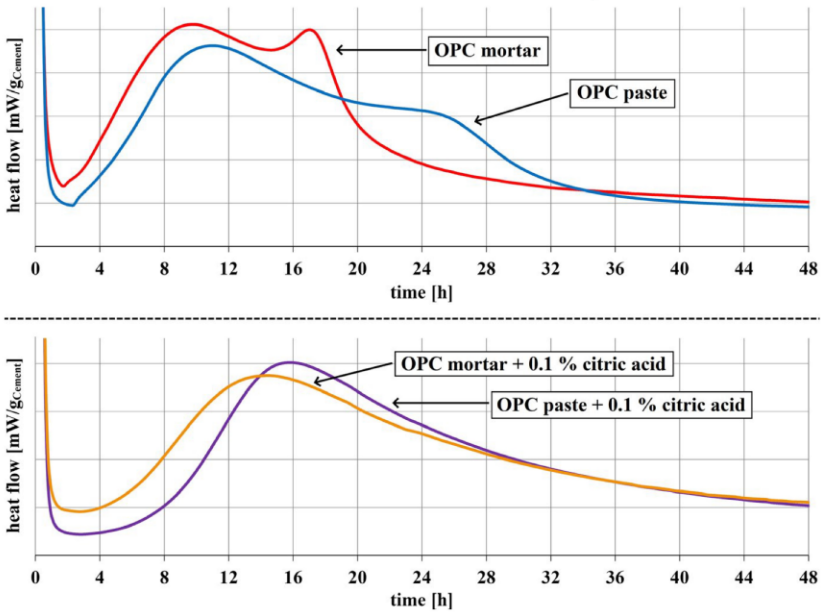

FIGURE 2 Comparison of heat evolution from cement paste or mortar of an ordinary Portland cement (OPC) sample (CEM I 52.5 N, w/c = 0.5), neat (top) or in the presence of 0.1 wt% citric acid retarder (bottom)

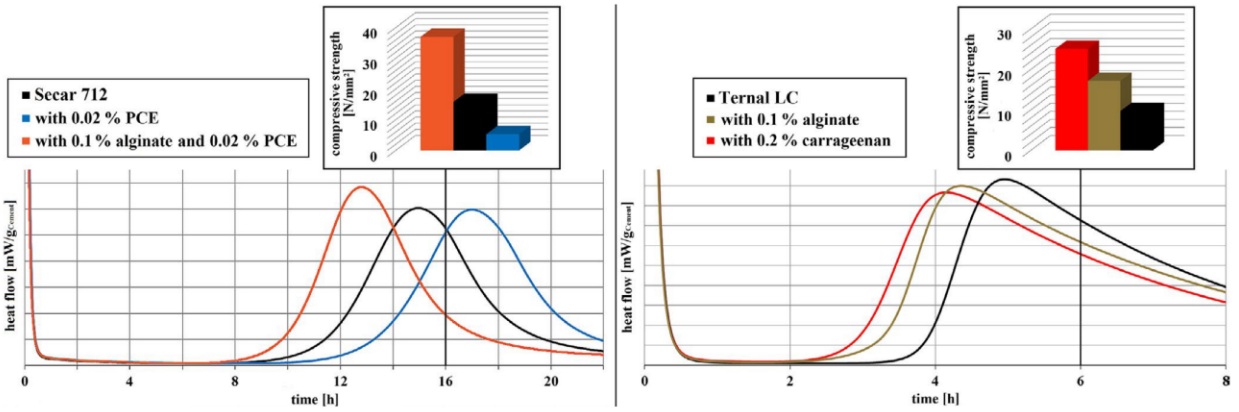

FIGURE 3 Comparison of compressive strength development of mortar (w/c = 0.5) and mortar heat flow monitored via calorimetry (w/c = 0.55) of calcium aluminate cement sample Secar 712 (left) and Ternal LC (right), neat and admixed with biopolymers (alginate or carrageenan) and/or a PCE superplasticizer

mortar at a given time and can be utilized to make a rule of thumb estimate. This is observed in the presence of the accelerating biopolymers as well of the retarding PCE superplasticizer, and also for a combination of these admixtures. Therefore, we conclude that mortar calorimetry presents a more reliable method to monitor actual hardening and strength development of CAC mortar then calorimetry in cement paste. In addition, we observed here that the accelerating effect of alginate which is based on providing a heterogeneous crystallization surface for C-A-H phases by attracting Ca^{2+} and $[Al(OH)_4]^-$ ions and enriching them along the biopolymer's chain,[12] is still visible albeit less pronounced as compared to the effect recorded in CAC paste.[10] This hints to a specific impact which presumably is owed to the sand particles.

In order to further investigate the impact of norm sand on the hydration behaviour of CAC as well as the associated reduced effectiveness of alginate as accelerator, the general influence of filler materials on CAC hydration was probed in-depth whereby the cement was partially replaced by different kinds of fillers.

3.2 | Accelerating effect of fine fillers

A similar accelerating effect as observed before for the norm sand was recorded on addition of quartz sand (Millisil W12 or Frechen F36) to a CAC paste. Addition of 20 or 40 wt% of such fine sands (these portions only present a fraction of what is present in a norm mortar which contains as much as 75 wt% sand and 25 wt% cement) already resulted in an earlier maximum for the heat release. Moreover the addition of submicron filler particles (primary crystal and/or particle

size in the nanometer range) to the CAC paste strongly promoted the hydration to much earlier times (see Figure 4; Table 2). The effect clearly increases with increasing SSA of various filler materials which are tabulated in Table 2 along with the particle size and chemical composition of the product samples. The effectiveness of selected accelerating filler samples is presented in Figure 4. There, $Al(OH)_3$ exhibiting a d_{50} value of 0.4 μm was identified as the most effective accelerator.

In a next step, the dosage dependence of the accelerating effect of all fillers listed in Table 1 was probed. There, substitution rates for CAC by filler of 0 - 75 wt% were studied. The results are tabulated in Table 2. It was found that (a) the accelerating effect of a filler clearly depends on its particle size/SSA (ie the smaller the particle or the higher the SSA, the stronger is the effect); and (b) higher addition rates of the fine fillers instigate a more pronounced acceleration (see Table 2).

The results from Table 2 suggest that the chemical composition of the filler material is less important than particle size and SSA. Only in the case of $Al(OH)_3$ another factor comes into play which is represented by the solubility of the submicron powder. An increased $[Al(OH)_4]^-$ content in the pore solution presumably promotes nucleation and crystal growth of C-A-H phases and this way accelerates CAC hydration. Furthermore, the nanoscale $Al(OH)_3$ might also act as nucleation seed for hydration products.

To further confirm the accelerating effect of fine fillers, mortar calorimetry using γ-Al_2O_3 and $Al(OH)_3$ as accelerator (see Figure S1, top) and mortar strength testing was performed on specimens holding γ-Al_2O_3 (sample NO 221-30, d_{50} 30 μm, 75 m^2/g, primary crystal size 10 - 50 nm) which was found to present the best filler regarding dosage effectiveness (see Table 2). By using this filler, substitution of a small amount only of the norm sand with this filler resulted in a nine-fold increase of the early strength of Secar 71 mortar cured for 4 hours, and a 15-fold increase for Secar 51 mortar cured for 5 hours (see Tables S1 and S2).

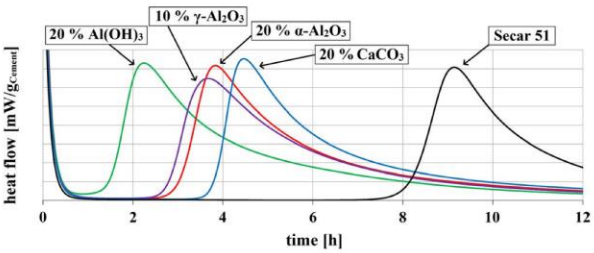

FIGURE 4 Accelerating effect of submicron filler particles on calcium aluminate cement (CAC) paste hydration, as determined via heat flow calorimetry of a mixture of cement (Secar 51, w/c = 0.6, 3.2 or 3.6 g CAC) substituted with 10 or 20 wt% (0.4 or 0.8 g) filler and compared to the neat CAC (4 g). $Al(OH)_3$ = APYRAL 200SM, γ-Al_2O_3 = NO 221-30, α-Al_2O_3 = NO 783, and $CaCO_3$ = PRECARB 100

The acceleration caused by fillers can well explain another observation which we previously had made when testing the alginate in CAC sample Secar 80.[10] There, surprisingly we noticed only a minor accelerating effect of the biopolymer in this CAC. It is important to know that Secar 80 presents a formulated CAC which holds about 40 wt% α-Al_2O_3 and possesses a *Blaine* value of ≈ 10 600 cm^2/g. Thus, to obtain a similar mixture as in Secar 80, we blended Secar 71 with fine α-Al_2O_3 (sample NO 783). Note that Secar 80 exhibits a similar clinker composition relative to the ratio of CA/CA_2 as is present in Secar 71,[10] it only differs in that it is formulated with aluminium oxide. Already at a 20 wt% replacement of the cement with this fine filler, a major reduction in the time until maximum heat release occurred was found (Figure 5). Moreover, upon addition of alginate as an accelerator to this mixture, only minor effectiveness of the biopolymer was recorded. Therefore, we contemplate that the accelerating effect of fine filler materials is almost comparable to that of the accelerating biopolymer admixture. This explains why alginate is relatively less effective in such CAC formulated with a fine filler. Furthermore, it suggests that incorporation of expensive accelerating admixtures (e.g. lithium salts) can be reduced by pre-formulating the CAC with simple inorganic fillers such as silica or limestone powder (see Figure S1).

4 | MECHANISTIC STUDY

In a series of previous studies employing fine Al_2O_3 and SiO_2 Gessner et al[20-23] already noticed that the addition of a fine filler material "…changes the nucleation mechanism…" and in CAC hydration produces "…a preferential nucleation of the hydration products…"[22] They also identified the influence of the SSA, the Na_2O content as well as the concentration of acid sites on aluminium oxide as relevant parameters with respect to the acceleration. Similar observations were made by other researchers.[24-26] In particular, Puerta-Falla et al showed "…that the number of product nuclei, formed at the end of the induction period, is linearly proportional to the additional surface area provided by the fillers. This suggests that CAC hydrated is enhanced by the provision of additional solid surface area for the heterogeneous nucleation of products. …"[25]

Our results fully confirm these previous findings and directed us to further investigate the working mechanism of these fine fillers, specifically taking into account the model proposed for the accelerating effect of alginate.[12] According to this, the negative charge along the alginate polymer chain attracts Ca^{2+} ions which are then bound and chelated by the biopolymer in a molecular cavity holding carboxylate groups. This way, the electric charge of the alginate reverses

TABLE 2 Time period until the maximum of heat release is achieved in a paste (w/c = 0.6, 4 g CAC fixed) prepared from CAC cement (Secar 51) dry-blended with different filler materials

Material	Product name	d_{50} (µm)	BET (m^2/g)	Time until max. heat release at substitution rate (wt%) of cement by filler				
				5%	10%	20%	40%	75%
SiO_2	CEN standard sand	700	—	—	—	—	—	5.0 h
SiO_2	QUARZSAND F 36	160	—	—	—	7.2 h	6.6 h	4.9 h
SiO_2	MILLISIL W 12	16	0.9	—	—	6.9 h	6.0 h	—
α-Al_2O_3	NABALOX NO 784	0.8	7	—	6.3 h	4.8 h	3.2 h	—
$CaCO_3$	PRECARB 100	1	9	—	5.9 h	4.5 h	2.6 h	—
SiO_2	SILMIKRON 805	0.5	20	—	5.1 h	4.2 h	—	—
α-Al_2O_3	NABALOX NO 783	0.8	12	—	4.9 h	3.8 h	—	—
$Al(OH)_3$	APYRAL 200SM	0.4	15	5.6 h	4.4 h	**2.3 h**	—	—
AlO(OH)	ACTILOX 200SM	0.3	17	5.3 h	4.2 h	**3.0 h**	—	—
γ-Al_2O_3	NABALOX NO 221-30	**30**	**75**	**4.5 h**	**3.6 h**	**3.4 h**	—	—
TiO_2	AEROXID P25	2.7	50	3.9 h	3.0 h	—	—	—

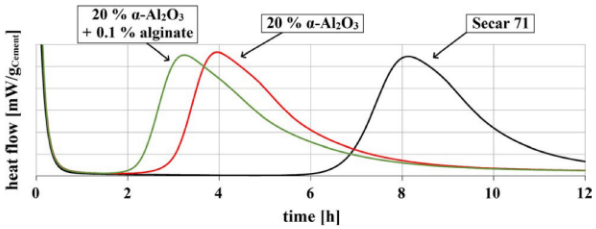

FIGURE 5 Heat release from neat calcium aluminate cement (CAC) (Secar 71, 4 g, w/c = 0.62) compared to a paste (w/(c + f) = 0.62) prepared from CAC (3.2 g) and fine α-Al_2O_3 (sample NO 783, 0.8 g), admixed with alginate (sample XEA 5036)

from negative to positive and now is capable of attracting $[Al(OH)_4]^-$ anions. Through this biotemplating effect involving alternating layers of calcium and aluminate ions, the alginate becomes a heterogeneous crystallization surface for C-A-H nuclei. This was further proven by SEM imaging of alginate which was imbibed into CAC pore solution. There, a much enhanced growth of C-A-H clusters on the surface of the biopolymer became visible.[12]

Relative to the fillers studied here, it is generally known that in alkaline medium Al_2O_3, SiO_2, TiO_2 and $CaCO_3$ exhibit negative zeta potentials (surface charges).[27,28] Moreover in the presence of Ca^{2+} ions these cations can adsorb onto the surfaces of these fillers which—as is the case for alginates—leads to a reversal of the surface charge from negative to positive.[27-29] For Al_2O_3, this interaction with calcium causes an ion binding that has been reported to be proportional to the BET surface area.[30]

To elucidate the interactions occurring in the presence of our fillers, we investigated the ionic composition of the pore solution of pastes from CAC sample Secar 51 dry-blended with two different fillers, namely α-Al_2O_3 (BET surface area 12 m^2/g) and γ-Al_2O_3 (BET surface area 75 m^2/g). The results are presented in Figure 6.

According to the results, a binding of calcium by the Al_2O_3 is clearly observed. For example, in the case of the γ-Al_2O_3 filler possessing a high SSA (75 m^2/g) the concentration of initial free calcium decreases by ≈ 30% (from 842 to 612 mg/L). This decrease in the Ca^{2+} concentration further fosters dissolution of the CA phase as a consequence of the solution equilibrium, resulting in higher Al^{3+} concentrations

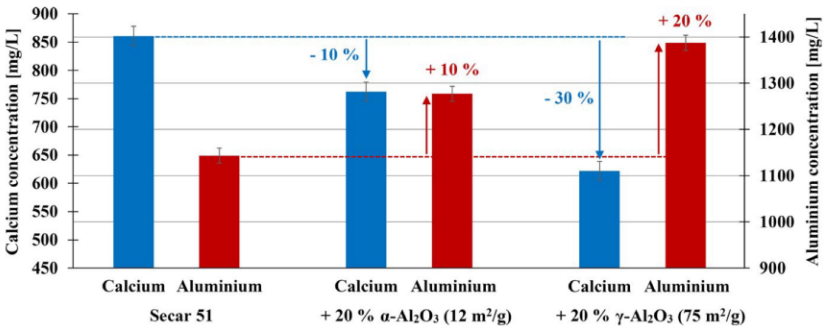

FIGURE 6 Ca^{2+} and Al^{3+} ion concentrations present in the pore solution of a calcium aluminate cement paste prepared from Secar 51 (20 g, w/c = 0.7), neat and dry-blended with additional 20 wt.% (4 g) of α-Al_2O_3 (NO 783) or γ-Al_2O_3 (NO 221-30)

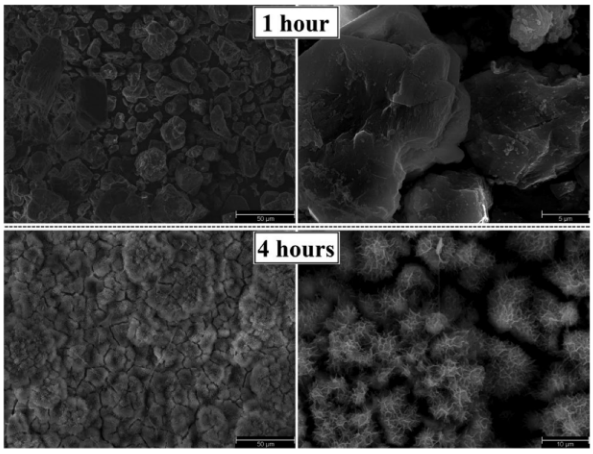

FIGURE 7 Surfaces of γ-Al_2O_3 submerged in calcium aluminate cement pore solution after 1 or 4 h of imbibition, as observed via SEM (left: magnification 500×; SE detector; right: magnifications 4000× [top], 2000× [bottom]; Secondary electron (SE) [top], Backscattered electron (BSE) [bottom] detectors)

in the pore solution. A similar behaviour was observed for the working mechanism of alginate accelerator. Hence, it can be postulated that on the surface of the filler particles an electrochemical double layer composed of Ca^{2+} at first and a second layer of aluminate ions is formed, similar to the mechanism found for alginate. There, formation of C-A-H nuclei along the alginate molecular chains could be visualized via SEM imaging.

To investigate whether a similar layer of hydrate phases forms on the surface of the filler particles, γ-Al_2O_3 powder was fixed to a SEM sample holder, submerged in CPS and then analysed via SEM imaging. There, after 4 hours of contact time, massive overgrowth of the surface with crystalline cement hydration products exhibiting the characteristic morphology of C-A-H was observed, as is displayed in Figure 7. A more detailed image of these early C-A-H phases recorded at higher magnification is presented in Figure S2.

Furthermore, XRD analysis of the hydration products was performed on CAC paste samples hardened over 20 hours at 20 °C. There, in the presence of fillers (e.g. α-Al_2O_3 sample NO 783) formation of a C-A-H phase (CAH_{10}) as early hydration product was observed (sample diffractograms for Al_2O_3 and $CaCO_3$ fillers shown in Figure S3). No other hydration products were observed which would indicate a different path of hydration taking place. These findings are consistent with previous reports on the application of accelerating filler materials on CAC hydration conducted via XRD and SEM analysis.[21,25,31,32]

5 | CONCLUSION

Heat flow calorimetry using cement paste can produce results which are not consistent with actual mortar strength development data from mortars. This effect is particularly pronounced for CACs. Their strength development is significantly impacted when heterogeneous crystallization surfaces are present. Utilizing heat flow calorimetry of a mortar instead of cement paste can mitigate this problem and produce a correlation between the time at which peak heat release occurs and mortar strength, the reason being that sand provides a heterogeneous crystallization surface.

Probing of different filler materials including SiO_2, $CaCO_3$, α-/γ-Al_2O_3, AlO(OH), $Al(OH)_3$, and TiO_2 on CAC hydration affirmed the role of the specific surface area of the fillers, with high surface area prompting earlier hydration. For example, a γ-Al_2O_3 sample exhibiting a high BET surface (75 m^2/g) was found to significantly accelerate CAC hydration.

A mechanistic study involving pore solution analysis and SEM imaging revealed that the accelerating effect of the fillers is based on a similar mechanism as was proven before for alginate. In CAC pore solution, the initially negatively charged filler particles first adsorb Ca^{2+} ions which induces a charge reversal. Onto these layers of cations, another layer of $[Al(OH)_4]^-$ anions is deposited. This electrochemical double layer presents the template for continued crystal growth of C-A-H phases which provide the strength to CAC.

Our study suggests that the dosages of accelerating admixtures such as lithium salts or alginates can be reduced substantially by formulating the CAC binder with suitable inorganic nano fillers (see Figure S1) while still achieving exceptionally high early strength values. However, these fine materials also actively promote the formation of C-A-H, the term "filler" might describe their function only partially as it usually refers to inert materials.

ACKNOWLEDGMENT

The authors are most grateful to *Imerys Aluminates* (formerly *Kerneos*) for the generous supply of calcium aluminate cement over the years (especially Mr A. Eisenreich and Mr R. Kwasny-Echterhagen). Furthermore, the authors thank *Nabaltec* (especially Dr C. Dünzen), *Quarzwerke* and *Schaefer Kalk* for supplying the filler materials. The authors also thank Deutsche Forschungs-gemeinschaft, Bonn, Germany (DFG) for financing this project under the grant PL-472/13-1 ("Investigation on the replacement of lithium carbonate as accelerator for calcium aluminate cements and its underlying working mechanism"). Open access funding enabled and organized by Projekt DEAL.

CONFLICT OF INTEREST

The authors wish to declare that no conflicts of interest or competing interests exists.

ORCID

Alexander Engbert https://orcid.org/0000-0003-4104-8492
Johann Plank https://orcid.org/0000-0002-4129-4784

REFERENCES

1. Robeyst N, De Schutter G, Grosse C, De Belie N. Monitoring the effect of admixtures on early-age concrete behaviour by ultrasonic, calorimetric, strength and rheometer measurements. Mag Concr Res. 2011;63(10):707–21.
2. Ukrainczyk N. Effect of polycarboxylate superplasticiser on properties of calcium aluminate cement mortar. Adv Cem Res. 2015;27(7):388–98.
3. Alonso MDM, Palacios M, Puertas F. Effect of polycarboxylate–ether admixtures on calcium aluminate cement pastes. Part 2: hydration studies. Ind Eng Chem Res. 2013;52(49):17330–40.
4. Baueregger S, Perello M, Plank J. Impact of carboxylated styrene–butadiene copolymer on the hydration kinetics of OPC and OPC/CAC/AH: the effect of Ca^{2+} sequestration from pore solution. Cem Concr Res. 2015;73:184–9.
5. Ukrainczyk N, Rogina A. Styrene–butadiene latex modified calcium aluminate cement mortar. Cem Concr Compos. 2013;41:16–23.
6. Zhang X, He Y, Lu C, Huang Z. Effects of sodium gluconate on early hydration and mortar performance of Portland cement-calcium aluminate cement-anhydrite binder. Constr Build Mater. 2017;157:1065–73.
7. Bensted J. Some applications of conduction calorimetry to cement hydration. Adv Cem Res. 1987;1(1):35–44.
8. Nicoleau L, Gädt T, Chitu L, Maier G, Paris O. Oriented aggregation of calcium silicate hydrate platelets by the use of comb-like copolymers. Soft Matter. 2013;9(19):4864–74.
9. Kanchanason V, Plank J. Effect of calcium silicate hydrate–polycarboxylate ether (CSH–PCE) nanocomposite as accelerating admixture on early strength enhancement of slag and calcined clay blended cements. Cem Concr Res. 2019;119:44–50.
10. Engbert A, Gruber S, Plank J. The effect of alginates on the hydration of calcium aluminate cement. Carbohydr Polym. 2020;236:116038.
11. Engbert A, Plank J. Identification of specific structural motifs in biopolymers which allow to effectively accelerate calcium alumina cement. Ind Eng Chem Res. 2020;59(26):11930–9.
12. Engbert A, Plank J. Templating effect of alginate and related biopolymers as hydration accelerators for calcium alumina cement—a mechanistic study. Mater Des. 2020;109054.
13. Frølich L, Wadsö L, Sandberg P. Using isothermal calorimetry to predict one day mortar strengths. Cem Concr Res. 2016;88:108–13.
14. Jansen D, Naber C, Ectors D, Lu Z, Kong XM, Götz-Neunhoeffer F, et al. The early hydration of OPC investigated by in-situ XRD, heat flow calorimetry, pore water analysis and ^{1}H NMR: learning about adsorbed ions from a complete mass balance approach. Cem Concr Res. 2018;109:230–42.
15. Scrivener K. Chapter 2: calcium aluminate. In: Newman J, Choo BS, editor. Advanced Concrete Technology—Constituent Materials. 2003; Amsterdam, the Netherlands: Elsevier, 13 pp.
16. Stecher J, Plank J. Novel concrete superplasticizers based on phosphate esters. Cem Concr Res. 2019;119:36–43.
17. DIN EN 196-11:2019-03. Methods of testing cement – part 11: heat of hydration – Isothermal Conduction Calorimetry method. German version EN 196–11: 2018.
18. DIN EN 196-1:2016-11. Methods of testing cement – part 1: determination of strength. German version EN 196–1: 2016.
19. DIN EN 1015–3:2007–05. Methods of test for mortar for masonry – part 3: determination of consistence of fresh mortar (by flow table); German version EN 1015–3: 1999.
20. Rettel A, Seydel R, Gessner W, Bayoux JP, Capmas A. Investigations on the influence of alumina on the hydration of monocalcium aluminate at different temperatures. Cem Concr Res. 1993;23(5):1056–64.
21. Gessner W, Möhmel S, Bier TA. Effects of the alumina quality on hydration and thermal behaviour of calcium aluminate/alumina mixes. In: RJ Mangabhai, FP Glasser, editor. Proceedings of the International Conference on Calcium Aluminate Cement (CAC). London, UK: IOM Communications Ltd, 2001.
22. Möhmel S, Gessner W. The influence of alumina reactivity on the hydration behaviour of mono calcium aluminate. Solid State Ion. 1997;101:937–43.
23. Möhmel S, Gessner W, Bier TA, Parr C. The influence of microsilica on the course of hydration of monocalcium aluminate. In: RJ Mangabhai, FP Glasser, editor. Proceedings of the International Conference on Calcium Aluminate Cement (CAC). London, UK: IOM Communications Ltd, 2001.
24. Parr C, Spreafico E, Bier TA, Mathieu A. Technical paper 6: calcium aluminate cements for monolithic refractories. Dunkirk, France: Kerneos; 1997.
25. Puerta-Falla G, Kumar A, Gomez-Zamorano L, Bauchy M, Neithalath N, Sant G. The influence of filler type and surface area on the hydration rates of calcium aluminate cement. Constr Build Mater. 2015;96:657–65.
26. Klaus SR, Neubauer J, Götz-Neunhoeffer F. Influence of the specific surface area of alumina fillers on CAC hydration kinetics. Adv Cem Res. 2016;28(1):62–70.
27. Lowke D, Gehlen C. The zeta potential of cement and additions in cementitious suspensions with high solid fraction. Cem Concr Res. 2017;95:195–204.
28. Zhu S, Avadiar L, Leong YK. Yield stress-and zeta potential-pH behaviour of washed α-Al_2O_3 suspensions with relatively high Ca (II) and Mg (II) concentrations: hydrolysis product and bridging. Int J Miner Process. 2016;148:1–8.
29. Huang CP, Stumm W. Specific adsorption of cations on hydrous γ-Al_2O_3. J Colloid Interface Sci. 1973;43(2):409–20.
30. Bier A, Mathieu A, Espinosa B, Bayoux JP. Technical Paper 1: the use of conductimetry to characterize the reactivity of high alumina cements. Dunkirk, France: Kerneos; 1993.
31. Gosselin C. Microstructural development of calcium aluminate cement based systems with and without supplementary cementitious materials. Ph.D. thesis, École Polytechnique Fédérale de Lausanne, Switzerland. 2009.
32. Shang X, Ye G, Zhang Y, Li H, Hou D. Effect of micro-sized alumina powder on the hydration products of calcium aluminate cement at 40°C. Ceram Int. 2016;42(13):14391–4.

SUPPORTING INFORMATION

Additional supporting information may be found online in the Supporting Information section.

How to cite this article: Engbert A, Plank J. Impact of sand and filler materials on the hydration behavior of calcium aluminate cement. *J Am Ceram Soc*. 2020;00:1–9. https://doi.org/10.1111/jace.17505

Publikation 4:

Journal of the American Ceramic Society, 2020.

Supporting information

Impact of Sand and Filler Materials on the Hydration Behavior of Calcium Aluminate Cement

Alexander Engbert, Johann Plank*

Technische Universität München, Chair for Construction Chemistry, Lichtenbergstr. 4, 85747 Garching, Germany

*Corresponding author:

Prof. Dr. Johann Plank

Chair for Construction Chemistry

Technische Universität München

Lichtenbergstr. 4

85747 Garching bei München, Germany

Tel.: +49 (0) 89 289 13 151

Fax: +49 (0) 89 289 13 152

E-Mail: sekretariat@bauchemie.ch.tum.de

ORCID (Johann Plank): 0000-0002-4129-4784

Table S1: Mortar properties after 4 h of hydration for Secar 71 (450 g cement, w/c = 0.5, 0.02 wt.% MPEG PCE 114PC6), neat and at partial replacement of the norm sand with γ-Al_2O_3 filler (sample NO 221-30); 45 g filler (10 wt.% relative to CAC) and 1305 g norm sand.

Secar 71 properties after 4 h of curing	**Reference**	**with 10 % γ-Al_2O_3**
compressive strength (N/mm^2)	2.6 ± 0.4	24.2 ± 0.5 **→ ninefold increase**
tensile strength (N/mm^2)	0.7 ± 0.1	4.0 ± 0.2 **→ sixfold increase**
mortar density (g/L)	2,210	2,210
spread flow (cm)	18.2 ± 0.3	13.7 ± 0.2

Table S2: Mortar properties after 5 h of hydration for Secar 51 (500 g cement, w/c = 0.45, 0.02 wt.% MPEG PCE 114PC6), neat and at partial replacement of the norm sand with γ-Al_2O_3 filler (sample NO 221-30); 50 g filler (10 wt.% relative to CAC) and 1300 g norm sand.

Secar 51 properties after 5 h of curing	**Reference**	**with 10 % γ-Al_2O_3**
compressive strength (N/mm^2)	1.9 ± 0.5	28.8 ± 1.2 **→ fifteenfold increase**
tensile strength (N/mm^2)	0.4 ± 0.1	3.9 ± 0.4 **→ tenfold increase**
mortar density (g/L)	2,340	2,310
spread flow (cm)	27.4 ± 0.5	25.3 ± 0.5

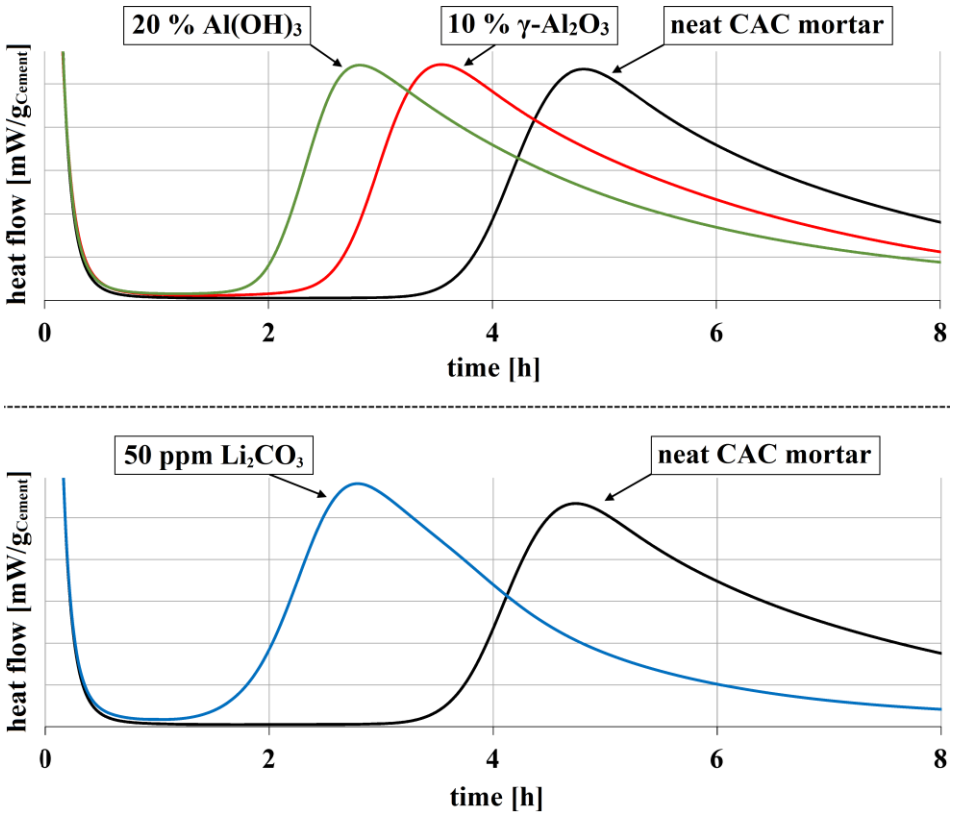

Figure S1: Accelerating effect of submicron fillers (top) compared to Li_2CO_3 (bottom) on CAC mortar hydration, as determined via heat flow calorimetry. Mortar composed of 4 g CAC (sample Secar 51, w/c = 0.55) and 12 g sand/filler mixture (neat: 12 g sand; γ-Al_2O_3: 11.6 g sand + 0.4 g filler NO 221-30; $Al(OH)_3$: 11.2 g sand + 0.8 g filler APYRAL 200SM).

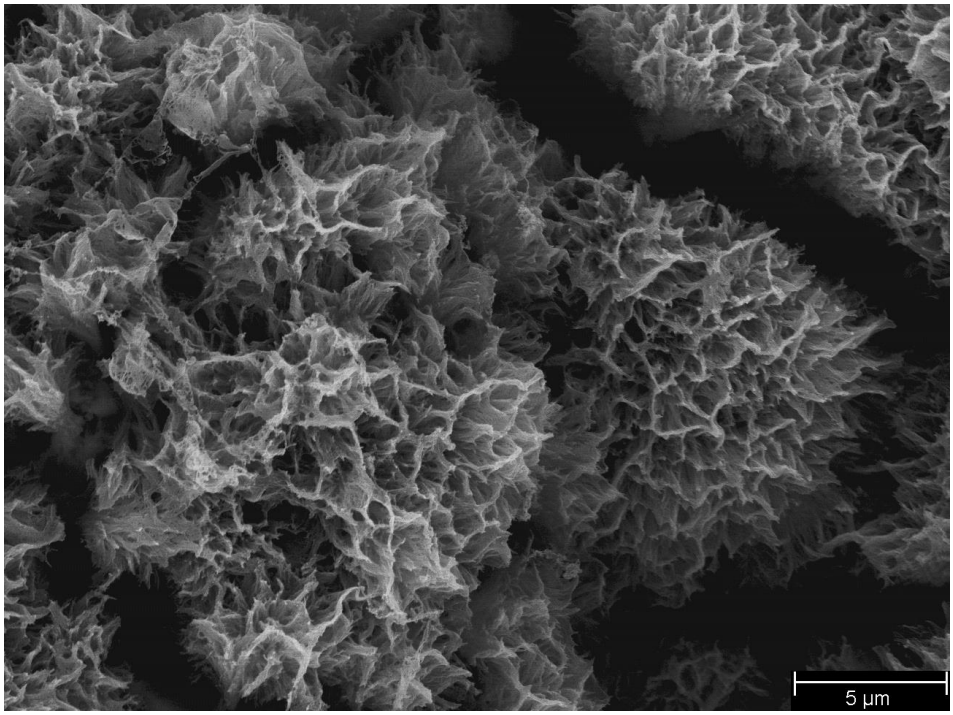

Figure S3: Close-up image of the surface of γ-Al_2O_3 after 4 hours of imbibition in CAC pore solution, as observed via SEM (magnification 4000x, 15 kV accelerating voltage, spot 4, BSE detector).

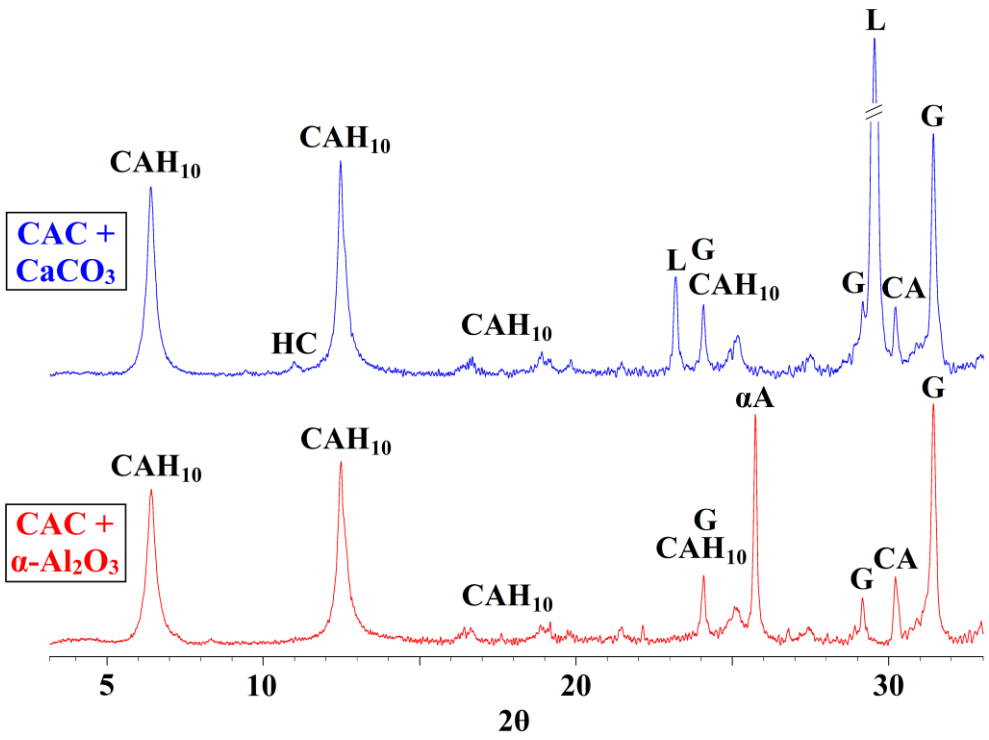

Figure S4: XRD analysis of ground cement samples (Secar 51, w/s = 0.6, 20 °C) after 20 hours of hydration in the presence of 40 wt.% filler (top: limestone powder PRECARB 100, bottom: α-Al_2O_3 NO 783). Abbreviations as follows: HC = Hemicarbonate, L = Limestone, G = Gehlenite, α-A = α-Al_2O_3 and CA = monocalcium aluminate.

3.4.3 Addendum

Zusätzlich zu den in der Publikation dargestellten Ergebnissen wurde ferner die Wirksamkeit des γ-Al_2O_3-Füllstoffs in Gegenwart von Fließmitteln bei niedrigem w/z-Wert (w/z = 0,3) getestet. Aufgrund des bereits in **Abschnitt 3.1.3** erwähnten Sedimentationsverhaltens musste ein Stabilisierer sowohl in der Referenz als auch dem mit γ-Al_2O_3 beschleunigten System zugegeben werden. Bei diesen Experimenten wurde mittels Wärmeflusskalorimetrie (siehe **Abbildungen A1** und **A2** in **Abschnitt 7.1** des Anhangs) festgestellt, dass Füllstoffe ebenfalls bei niedrigem w/z-Wert und hoher Fließmitteldosierung einen beschleunigenden Effekt auf den CAC ausüben.

4. Zusammenfassung und Ausblick

In dieser Arbeit wurden alternative Beschleuniger für Calciumaluminatzemente erforscht, wobei ein besonderes Augenmerk auf dem Einsatz nachhaltiger Substanzen lag. Kommerziell werden derzeit Lithiumsalze, allen voran Li_2CO_3, eingesetzt und somit dem Wertstoffkreislauf durch „Einzementieren“ entzogen. Weitere Beschleuniger wären beispielsweise die korrosiven und alkalischen Verbindungen $Ca(OH)_2$ bzw. NaOH sowie das giftige NaF. Die Aufklärung der beschleunigenden Wirkung von Alginat, einem Polysaccharid extrahiert aus Braunalgen, stellt eine ungewöhnliche, neue Substanzklasse für den Einsatz als Beschleuniger für CAC zur Verfügung. Dies ist insoweit außergewöhnlich, da traditionell hochmolekulare Polymere und im besonderen Polysaccharide als Verdickungs- und Wasserretentionsmittel für Zemente gelten und in der Regel eine verzögernde Wirkung auf die Hydratation ausüben.

Der Einsatz von Alginat als Beschleuniger wurde in Aluminatzementen unterschiedlicher mineralogischer Zusammensetzung sowohl in Zementpaste als auch im Mörtel getestet. Hierbei konnte die ungewöhnliche Wirkung von Alginat bestätigt und mit der inhärenten Reaktivität des CAC in Zusammenhang gebracht werden, d.h. Zemente mit einer kurzen dormanten Phase werden nur geringfügig, Zemente mit einer langen dormanten Phase hingegen stark beschleunigt. Dieser Effekt war bei allen Alginat-Produkten, sofern geeignete Reinheit und Feinheit vorlag, vergleichbar ausgeprägt und unabhängig von der Herkunft des Alginats. Lediglich die Molmasse des Biopolymers ist entscheidend für dessen Wirkung, da sehr niedermolekulare Alginate keine beschleunigende Wirkung hervorrufen. Überraschend war die hohe Calciumbindefähigkeit der Alginate, welche die Konzentration freier Ca^{2+}-Ionen in der Zementporenlösung stark reduziert. Mit einem solchen Effekt wird, wie anfangs beschrieben, traditionell eine verzögernde Wirkung assoziiert.

Die Untersuchung des für den beschleunigenden Effekt verantwortlichen Strukturmerkmals zeigte, dass er auf einem komplexen Zusammenspiel verschiedener Eigenschaften des Alginats beruht. Neben der bereits genannten Molmasse und der Calciumbindefähigkeit wurde als weiteres Strukturmerkmal die Fähigkeit zur effizienten Komplexierung von Kationen identifiziert. Dieses konnte in zwei weiteren Biopolymeren, dem Pektin und dem Carrageen, gefunden werden, welche ebenfalls einen beschleunigenden Effekt zeigen.

Der diesen beschleunigenden Polymeren zugrunde liegende Wirkmechanismus wurde unter Zuhilfenahme diverser analytischer Techniken untersucht. Hierzu wurde der Effekt

einer Alginatzugabe auf die Hydratationsreaktion des CAC mittels *ex-situ* und *in-situ* XRD qualitativ und über ^{27}Al-MAS-NMR quantitativ bestimmt. Die Messungen offenbarten eine deutlich verkürzte dormante Phase der Zementhydratation und ein früheres Einsetzen der Akzelerationsperiode, was zur vorzeitigen Bildung der Hydratphasen führte. Da hier lediglich die Kristallisation bekannter C-A-H-Phasen und keine Bildung von Fremdphasen oder Interkalationsverbindungen zu beobachten war, muss Alginat die Kristallbildung oder das Löslichkeitsverhalten des Zements selbst beeinflussen. Zur weiteren Untersuchung des Wirkmechanismus wurde die Wechselwirkung von Alginat mit den Ionen in der Zementporenlösung genauer betrachtet. Dabei zeigte sich, dass das Biopolymer freies Ca^{2+} aus der Porenlösung bindet, was wiederum das Auflösen weiteren Klinkers begünstigt. Hierdurch wird die Aluminium-Konzentration in der CPS erhöht, was die Hydratphasenbildung begünstigen könnte. Allerdings konnte in einem weiteren Experiment, bei dem Alginat nachträglich zu einer extrahierten Zementporenlösung zugegeben wurde, gezeigt werden, dass das Alginat sowohl Calcium als auch Aluminium bindet. Da bei einem pH-Wert von 12 in der CPS das Aluminium als Aluminat-Anion vorliegt, erscheint eine Wechselwirkung der anionischen Carboxylat-Gruppe mit dem $[Al(OH)_4]^-$-Ion als unwahrscheinlich. Dieses Phänomen konnte jedoch durch Bestimmung des Zeta-Potentials des Polymers in Gegenwart von Ca^{2+}- und $[Al(OH)_4]^-$-Ionen geklärt werden. Demnach bindet Alginat erhebliche Menge an Ca^{2+}, wodurch es zu einer Neutralisierung der Ladung bzw. partieller Umladung des anionischen Biopolymers kommt. Über die Calcium-Ionen an der Oberfläche des Alginats kann nun das Aluminat adsorbieren. Durch diese Anreicherung und Bindung der Ionen entlang der Polymerkette entstehen günstige Bedingungen für die Nukleation und das Wachstum von C-A-H-Hydratphasen.

Im letzten Teil dieser Arbeit wurde basierend auf den Erkenntnissen um das Wirkprinzip des Alginats die beschleunigende Wirkung von feinen Füllstoffen mit einer hohen spezifischen Oberfläche betrachtet. Diese zeigten mit zunehmender Feinheit und SSA eine stärkere Wirkung auf die Hydratation von CAC in Form von heterogener Kristallisation, welche analog wie bei den Alginaten über Calciumbindung abläuft. Durch diesen Effekt werden Messergebnisse zum Abbindeverhalten von Aluminatzement mittels Wärmeflusskalorimetrie beeinflusst. Ein Normmörtel entwickelt durch den hohen Sand-Anteil (75 %) aufgrund des Effekts der feinen Sandfraktionen eine nennenswert höhere Frühfestigkeit als eine Zementpaste.

Abschließend ist festzuhalten, dass Alginat als Beschleuniger für Calciumaluminatzemente geeignet ist und hier in einem gewissen Rahmen als Ersatz für Lithiumsalze eingesetzt bzw. mit diesem kombiniert werden kann. Dies ermöglicht in der Bauindustrie einen reduzierten Einsatz von Lithium, welches für die Herstellung von Akkumulatoren benötigt wird. Inzwischen wurde die positive Wirkung dieser neuen Beschleuniger auch in anwendungsnahen kommerziellen Formulierungen verifiziert [187].

In der Zukunft sollten weitere (Bio)Polymere mit vergleichbarer Struktur untersucht und/oder synthetische Polymere zielgerecht hergestellt werden mit dem Ziel, die Wirksamkeit bezüglich des beschleunigenden Effekts weiter zu verbessern.

Ebenso bleiben für die wichtigen ternären Bindemittelsysteme (OPC/CAC/AH), die häufig im Trockenmörtelbereich eingesetzt werden, Lithiumsalze die wichtigsten Beschleuniger. In diesen zeigen Alginate keine nennenswerte beschleunigende Wirkung, da ihr Abbinden nicht auf C-A-H-Bildung, sondern Ettringit beruht. Einen möglichen alternativen Beschleuniger für ternäre Bindemittelsysteme stellte die Firma *IMCD* kürzlich vor [188]. Bei diesem handelt es sich um Titanylsulfat ($TiOSO_4 \cdot x\ H_2O$), welches eine mit Lithium vergleichbare (molare) Wirksamkeit im ternären Bindemittelsystem aufweisen soll. Veröffentlichungen in Fachzeitschriften sowie Untersuchungen zu dessen Wirkmechanismus sind bis *dato* nicht erfolgt. Eigene Versuche einen Beschleuniger für dieses System zu finden, beispielsweise auf Basis von Impfkristallen aus Nano-Ettringit, waren ohne Erfolg. Diese Untersuchungen sind in dieser Arbeit nicht näher ausgeführt, sie sollten in Zukunft jedoch gezielt fortgeführt werden

5. Summary and Outlook

Within this work alternative accelerators for calcium aluminate cement were investigated and especially the application of sustainable compounds (“green” admixtures such as biopolymers) was taken into account. Up to date, lithium salts such as Li_2CO_3 are used commercially and hence lithium is removed from the circular economy via cementing into building products. Alternatives to lithium compounds include accelerators e.g. the corrosive and alkaline $Ca(OH)_2$ or NaOH as well as the toxic NaF. The unravelling of the accelerating properties of alginate, a polysaccharide extracted from brown algae, presents an unusual albeit novel class of accelerators for CAC. Traditionally, high molecular weight polymers and especially polysaccharides are commonly known to work as thickeners and water retention agents in cement and to induce a retarding effect on the hydration.

Effectiveness of alginate as accelerator was first tested in high-alumina cements of different mineralogical composition and in cement paste as well as in mortar. Here, the unusual effect of alginate was verified and revealed a correlation with the inherent reactivity of CAC, i.e. cements with a short dormant period are only slightly accelerated whereas the hydration of cements with a long dormant period is strongly promoted. The effect is comparable for all alginate products of sufficient purity and fineness, independent of their origin (algae species etc.). Only the molecular weight of the biopolymer is critical for its effectiveness, since alginates of ultra-low molecular weight do not exhibit an accelerating property. Surprisingly, a strong calcium binding property was observed for alginates which reduced the amount of free Ca^{2+} ions in the cement pore solution. Such an effect is commonly associated with a retarding action.

Investigation of the structural motif responsible for the accelerating effect revealed a complex interplay of different molecular properties which are required. Next to the already mentioned molecular weight and calcium binding capacity, another structural motif was identified which comprises the ability to effectively chelate cations. This building block was also observed in two additional biopolymers, namely pectin and carrageenan which likewise exhibit an accelerating effect.

The working mechanism underlying the accelerating effect has been investigated using various analytical techniques. Hereunto, the effect of alginate addition on the hydration reaction was quantified using ^{27}Al-MAS-NMR spectroscopy as well as qualitatively investigated via *ex-situ* and *in-situ* XRD. There, a distinct shortening of the dormant period and earlier onset of the acceleration period was observed which induces an earlier

formation of hydrate phases. Since only crystallization of known C-A-H phases and no formation of unconventional phases or intercalation compounds could be observed, it was concluded that alginate must influence either the crystal formation or the solubility behavior of the cement itself. Thus, further investigations were conducted on the interaction of alginate with the ions present in the cement pore solution. As mentioned before, the biopolymer binds copious amounts of free Ca^{2+} from the pore solution, thereby promoting the dissolution of further clinker. Hence, the aluminum concentration is increased in the CPS which should favor the formation of hydrate phases. However, in another experiment in which alginate was added to an extracted CPS it was shown that the alginate binds both calcium and aluminum. Since at pH 12 the aluminum in CPS exists as aluminate ion, an interaction of the anionic carboxylate groups with the $[Al(OH)_4]^-$ ions can be ruled out. This phenomenon was then explained by determining the zeta potential (charge) of the polymer in the presence of calcium and aluminate ions, where through the binding of Ca^{2+} by the anionic biopolymer a charge neutralization or partial charge reversal was observed. The aluminate ion can now sorb onto the calcium ions on the surface of the alginate, and thus through enriching and binding of ions create a template for the nucleation and growth of C-A-H phases.

In the last section of this work, we investigated the accelerating properties of fine filler materials exhibiting a high SSA. It was observed that with increasing fineness and SSA, these fillers produce an accelerating effect on the hydration of CAC due to heterogeneous crystallization which occurs via binding of calcium analogue to alginates. Thus, when using heat flow calorimetry the result is much influenced depending on whether a paste or a mortar is investigated, because the sand (75 %) present in a standard mortar acts as an accelerating filler and leads to considerably higher early strength.

Finally, it is concluded that alginate is suitable as an accelerator for calcium aluminate cements and can be used to a certain extent as a substitute for lithium salts or combined with them. This enables a reduced use in the construction industry of lithium, which is required for the production of batteries for electrical automobiles. Meanwhile, effectiveness of these new accelerators has been verified in actual commercial formulations [187].

In the future, other (bio)polymers with a comparable structure should be investigated and synthetic polymers should be manufactured with the aim of improving the effectiveness of this accelerating effect.

Still, lithium salts remain the most important accelerators for ternary binder systems (OPC/CAC/AH) that are commonly used in the dry-mix mortar industry. Here, alginates do not show any noteworthy accelerating effect, since these binders do not rely on C-A-H phases, but rather ettringite. Recently, a potential alternate accelerator for ternary binder systems was presented by *IMCD* company [188]. Their product is based on titanyl sulfate ($TiOSO_4$ x H_2O) and should have a similar (molar) effectiveness in the ternary binder system compared to lithium. To the best of our knowledge, no peer-review journal article or study on its effectiveness and mechanism of action has been published. Own attempts to find an accelerator for this system, for example based on seed crystals made from nano-ettringite, were unsuccessful within this Ph.D. work. These investigations are not presented in this dissertation, but definitely should be pursued in the future.

6. Literaturverzeichnis

[1] Stark J., Wicht B. Zement und Kalk, Der Baustoff als Werkstoff. Basel: Birkhäuser Basel; 2000.

[2] Hewlett P.C. (ed.). Lea's chemistry of cement and concrete. 4th ed. Amsterdam: Elsevier/Butterworth Heinemann; 2004.

[3] Kurdowski W. Cement and Concrete Chemistry. Dordrecht: Springer Netherlands; 2014.

[4] Jackson M.D., Landis E.N., Brune P.F., Vitti M., Chen H., Li Q. et al. Mechanical resilience and cementitious processes in Imperial Roman architectural mortar. *Proceedings of the National Academy of Sciences of the United States of America*, 2014, 111(52): S. 18484–18489.

[5] U.S. Geological Survey. Mineral commodity summaries 2020; 2020.

[6] Taylor H.F.W. Cement chemistry. 2nd ed. London: Telford Publ; 2003.

[7] Juenger M.C.G., Winnefeld F., Provis J.L., Ideker J.H. Advances in alternative cementitious binders. *Cement and Concrete Research*, 2011, 41(12): S. 1232–1243.

[8] Gartner E., Sui T. Alternative cement clinkers. *Cement and Concrete Research*, 2018, 114: S. 27–39.

[9] Shi C., Jiménez A.F., Palomo A. New cements for the 21st century: The pursuit of an alternative to Portland cement. *Cement and Concrete Research*, 2011, 41(7): S. 750–763.

[10] Shi C., Qu B., Provis J.L. Recent progress in low-carbon binders. *Cement and Concrete Research*, 2019, 122: S. 227–250.

[11] Newman J.B., Choo B.S. Advanced concrete technology, - Constituent materials. Oxford, England, Burlington, MA: Butterworth-Heinemann; 2003.

[12] Barnes P., Bensted J. Structure and Performance of Cements. Florence: CRC Press; 2001.

[13] Metalary. Durchschnittlicher Preis von Lithiumcarbonat weltweit in den Jahren von 2002 bis 2018 (in US-Dollar je Tonne). In: Statista, Statista GmbH. [abgerufen am: 16.11.2020]; URL: https://de.statista.com/statistik/daten/studie/979746/umfrage/durchschnittlicher-preis-von-lithium-weltweit.

[14] Deutsche Rohstoffagentur. Preismonitor April 2020; 2020.

[15] Nayak P.K., Yang L., Brehm W., Adelhelm P. Von Lithium- zu Natrium-ionenbatterien: Vorteile, Herausforderungen und Überraschendes. *Angewandte Chemie*, 2018, 130(1): S. 106–126.

[16] OICA. Entwicklung der weltweiten Automobilproduktion in den Jahren 2000 bis 2019 (in Millionen). In: Statista, Statista GmbH. [abgerufen am: 16.11.2020]; URL: https://de.statista.com/statistik/daten/studie/151749/umfrage/entwicklung-der-weltweiten-automobilproduktion/.

[17] VDA. Anzahl der produzierten Personenkraftwagen (Pkw) in Deutschland von 1990 bis 2019 (in Millionen). In: Statista, Statista GmbH. [abgerufen am: 16.11.2020]; URL: https://de.statista.com/statistik/daten/studie/75210/umfrage/produktion-von-pkw-in-deutschland-seit-1990/.

[18] Wang Y., Chen R., Chen T., Lv H., Zhu G., Ma L. et al. Emerging non-lithium ion batteries. *Energy Storage Materials*, 2016, 4: S. 103–129.

[19] Rahman A., Wang X., Wen C. High Energy Density Metal-Air Batteries: A Review. *Journal of The Electrochemical Society*, 2013, 160(10): A1759-A1771.

[20] Massé R.C., Uchaker E., Cao G. Beyond Li-ion: electrode materials for sodium- and magnesium-ion batteries. *Science China Materials*, 2015, 58(9): S. 715–766.

[21] Liu Y., Sun Q., Li W., Adair K.R., Li J., Sun X. A comprehensive review on recent progress in aluminum–air batteries. *Green Energy & Environment*, 2017, 2(3): S. 246–277.

[22] Larouche F., Tedjar F., Amouzegar K., Houlachi G., Bouchard P., Demopoulos G.P. et al. Progress and Status of Hydrometallurgical and Direct Recycling of Li-Ion Batteries and Beyond. *Materials*, 2020, 13(3).

[23] Mayyas A., Steward D., Mann M. The case for recycling: Overview and challenges in the material supply chain for automotive li-ion batteries. *Sustainable Materials and Technologies*, 2019, 19: e00087.

[24] Pistoia G., Liaw B. Behaviour of Lithium-Ion Batteries in Electric Vehicles. Cham: Springer International Publishing; 2018.

[25] Reese J. de. Wechselwirkung von Bionanokompositen und Fließmitteln mit zementären Systemen [Dissertation], Technische Universität München; 2016.

[26] Reese J. de, Sperl N., Schmid J., Sieber V., Plank J. Effect of biotechnologically modified alginates on LDH structures. *Bioinspired, Biomimetic and Nano-biomaterials*, 2015, 4(3): S. 174–186.

[27] Peschard A., Govin A., Grosseau P., Guilhot B., Guyonnet R. Effect of polysaccharides on the hydration of cement paste at early ages. *Cement and Concrete Research*, 2004, 34(11): S. 2153–2158.

[28] Peschard A., Govin A., Pourchez J., Fredon E., Bertrand L., Maximilien S. et al. Effect of polysaccharides on the hydration of cement suspension. *Journal of the European Ceramic Society*, 2006, 26(8): S. 1439–1445.

[29] Garci Juenger M.C., Jennings H.M. New insights into the effects of sugar on the hydration and microstructure of cement pastes. *Cement and Concrete Research*, 2002, 32(3): S. 393–399.

[30] Thomas N.L., Birchall J.D. The retarding action of sugars on cement hydration. *Cement and Concrete Research*, 1983, 13(6): S. 830–842.

[31] Young J.F. A review of the mechanisms of set-retardation in portland cement pastes containing organic admixtures. *Cement and Concrete Research*, 1972, 2(4): S. 415–433.

[32] Bishop M., Barron A.R. Cement Hydration Inhibition with Sucrose, Tartaric Acid, and Lignosulfonate: Analytical and Spectroscopic Study. *Industrial & Engineering Chemistry Research*, 2006, 45(21): S. 7042–7049.

[33] Imeson A. (ed.). Food Stabilisers, Thickeners and Gelling Agents. 1st ed. New York, NY: John Wiley & Sons; 2011.

[34] Stephen A.M., Phillips G.O., Williams P.A. Food polysaccharides and their applications. 2nd ed. Boca Raton, FL: CRC/Taylor & Francis; 2006.

[35] Phillips G.O., Williams P.A. (eds.). Handbook of Hydrocolloids. 2nd ed. Cambridge: Woodhead Pub; 2009.

[36] Pöllmann H. Calcium Aluminate Cements - Raw Materials, Differences, Hydration and Properties. *Reviews in Mineralogy and Geochemistry*, 2012, 74(1): S. 1–82.

[37] Parr C., Simonin F., Touzo B., Wöhrmeyer C., Valdelièvre B., Namba A. The impact of calcium aluminate cement hydration upon the properties of refractory castables, Technical Paper – 43, Kerneos. France; 2005.

[38] Touzo B. Ultra-fast setting cement based on amorphous calcium aluminate (FR3021047A1); 2015.

[39] Mahiaoui J., Estival J., Bousseau J.N., Martinet A. Ultra-fast setting cement based on amorphous calcium aluminate comprising a surface treatment (FR3021046A1); 2015.

[40] Parr C., Spreafico E., Bier T.A., Mathieu A. Calcium Aluminate Cements (CAC) for Monolithic Refractories, Technical Paper – 6, Kerneos. France; 1997.

[41] Lamour V.H.R., Monteiro P.J.M., Scrivener K.L., Fryda H. Microscopic studies of the early hydration of calcium aluminate cements. In: Mangabhai R.J., Glasser F.P., editors. Calcium aluminate cements 2001: Proceedings of the International Conference on Calcium Aluminate Cements (CAC) held at Heriot-Watt University Edinburgh, Scotland, UK, 16 - 19 July 2001. London: IOM Communications; 2001.

[42] Gosselin C. Microstructural development of calcium aluminate cement based systems with and without supplementary cementitious materials [Dissertation], EPFL Lausanne; 2009.

[43] Lothenbach B., Pelletier-Chaignat L., Winnefeld F. Stability in the system CaO–Al_2O_3–H_2O. *Cement and Concrete Research*, 2012, 42(12): S. 1621–1634.

[44] Damidot D., Sorrentino D., Guinot D. Factors Influencing the Nucleation and Growth of the Hydrates in Cementitious Systems An Experimental Approach. In: 2nd Int workshop on hydration & setting; 1997.

[45] Parr C., Revais C., Valdelievre B., Namba A. The Effect of Ambient Temperature upon the Placing Properties of Deflocculated Castables, Technical Paper – 19, Kerneos. France; 2000.

[46] Parr C., Wöhrmeyer C., Valdelièvre B., Namba A. Effect of Formulation Parameters upon the Strength Development of Calcium Aluminate Cement Containing Castables, Technical Paper – 34, Kerneos. France; 2002.

[47] Götz-Neunhoeffer F. Kinetics of the hydration of calcium aluminate cement with additives. *ZKG International*, 2005, 58(4).

[48] Götz-Neunhoeffer F. Hydration kinetics of calcium aluminate cement in the presence of Li_2CO_3. In: Fentiman C.H., editor. Calcium Aluminate Cements: Proceedings of the centenary Conference 2008, Palais des Papes, Avignon, France, 30 June - 2.Juli 2008. Norfolk: IHS BRE Press; 2008.

[49] Fujii K., Kondo W., Ueno H. Kinetics of Hydration of Monocaldum Aluminate. *Journal of the American Ceramic Society*, 1986, 69(4): S. 361–364.

[50] Klaus S. Quantification of CA hydration and influence of its particle fineness during early hydration of calcium aluminate cement [Dissertation], Friedrich-Alexander-Universität Erlangen-Nürnberg (FAU); 2015.

[51] Damidot D., Rettel A., Capmas A. Action of admixtures on Fondu cement: Part 1. Lithium and sodium salts compared. *Advances in Cement Research*, 1996, 8(31): S. 111–119.

[52] Ukrainczyk N. Effect of polycarboxylate superplasticiser on properties of calcium aluminate cement mortar. *Advances in Cement Research*, 2015, 27(7): S. 388–398.

[53] Bier T.A., Parr C. Admixtures with Calcium Aluminate Cements and CAC Based Castables, Technical Paper – 5, Kerneos. France; 1996.

[54] Banfill P.F.G. Superplasticizers for Ciment Fondu. Part 2: Effects of temperature on the hydration reactions. *Advances in Cement Research*, 1995, 7(28): S. 151–157.

[55] Edmonds R.N., Majumdar A.J. The hydration of monocalcium aluminate at different temperatures. *Cement and Concrete Research*, 1988, 18(2): S. 311–320.

[56] Bushnell-Watson S.M., Sharp J.H. The effect of temperature upon the setting behaviour of refractory calcium aluminate cements. *Cement and Concrete Research*, 1986, 16(6): S. 875–884.

[57] Bushnell-Watson S.M., Sharp J.H. On the cause of the anomalous setting behaviour with respect to temperature of calcium aluminate cements. *Cement and Concrete Research*, 1990, 20(5): S. 677–686.

[58] Rettel A., Seydel R., Gessner W., Bayoux J.P., Capmas A. Investigations on the influence of alumina on the hydration of monocalcium aluminate at different temperatures. *Cement and Concrete Research*, 1993, 23(5): S. 1056–1064.

[59] Rashid S., Barnes P., Turrillas X. The rapid conversion of calcium aluminate cement hydrates, as revealed by synchrotron energy-dispersive diffraction. *Advances in Cement Research*, 1992, 4(14): S. 61–67.

[60] Rashid S., Barnes P., Bensted J., Turrillas X. Conversion of calcium aluminate cement hydrates re-examined with synchrotron energy-dispersive diffraction. *Journal of Materials Science Letters*, 1994, 13(17): S. 1232–1234.

[61] Ukrainczyk N., Matusinović T., Kurajica S., Zimmermann B., Sipusic J. Dehydration of a layered double hydroxide - C_2AH_8. *Thermochimica Acta*, 2007, 464(1-2): S. 7–15.

[62] Gessner W., Müller D., Behrens H.-J., Scheler G. Zur Koordination des Aluminiums in den Calciumaluminathydraten $2CaO \cdot Al_2O_3 \cdot 8H_2O$ und $CaO \cdot Al_2O_3 \cdot 10\ H_2O$. *Zeitschrift für anorganische und allgemeine Chemie*, 1982, 486(1): S. 193–199.

[63] Guirado F., Galí S., Chinchón S., Rius J. Crystal Structure Solution of Hydrated High-Alumina Cement from X-ray Powder Diffraction Data. *Angewandte Chemie International Edition*, 1998, 37(1-2): S. 72–75.

[64] Rivas Mercury J.M., Pena P., Aza A.H. de, Turrillas X., Sobrados I., Sanz J. Solid-state ^{27}Al and ^{29}Si NMR investigations on Si-substituted hydrogarnets. *Acta Materialia*, 2007, 55(4): S. 1183–1191.

[65] Christensen A.N., Lebech B., Sheptyakov D., Hanson J.C. Structure of calcium aluminate decahydrate ($CaAl_2O_4 \cdot 10D_2O$) from neutron and X-ray powder diffraction data. *Acta crystallographica. Section B, Structural science*, 2007, 63(Pt 6): S. 850–861.

[66] Hüller F., Neubauer J., Kaessner S., Goetz-Neunhoeffer F. Hydration of calcium aluminates at 60°C – Development paths of C_2AH_x in dependence on the content of free water. *Journal of the American Ceramic Society*, 2019, 102(7): S. 4376–4387.

[67] Manninger T., Jansen D., Neubauer J., Götz-Neunhoeffer F. Accelerating effect of Li_2CO_3 on formation of monocarbonate and Al-hydroxide in a CA-cement and calcite mix during early hydration. *Cement and Concrete Research*, 2019, 126: S. 105897.

[68] Manninger T., Jansen D., Neubauer J., Götz-Neunhoeffer F. Phase Solubility Changes during Hydration of Monocalciumaluminate and Calcite-The Influence of Alkali Accumulation. *Materials*, 2020, 13(6).

[69] Duan X., Evans D.G. Layered Double Hydroxides. Berlin Heidelberg: Springer-Verlag GmbH; 2005.

[70] Ng S., Metwalli E., Müller-Buschbaum P., Plank J. Occurrence of intercalation of PCE superplasticizers in calcium aluminate cement under actual application conditions, as evidenced by SAXS analysis. *Cement and Concrete Research*, 2013, 54: S. 191–198.

[71] Plank J., Keller H., Andres P.R., Dai Z. Novel organo-mineral phases obtained by intercalation of maleic anhydride–allyl ether copolymers into layered calcium aluminum hydrates. *Inorganica Chimica Acta*, 2006, 359(15): S. 4901–4908.

[72] Plank J., Dai Z., Zouaoui N. Novel hybrid materials obtained by intercalation of organic comb polymers into Ca–Al–LDH. *Journal of Physics and Chemistry of Solids*, 2008, 69(5-6): S. 1048–1051.

[73] Smith B.J., Rawal A., Funkhouser G.P., Roberts L.R., Gupta V., Israelachvili J.N. et al. Origins of saccharide-dependent hydration at aluminate, silicate, and aluminosilicate surfaces. *Proceedings of the National Academy of Sciences of the United States of America*, 2011, 108(22): S. 8949–8954.

[74] Nalet C., Nonat A. Effect of the Stereochemistry of Polyols on the Hydration of Cement: Influence of Aluminate and Sulfate Phases. *ACI Symposium Publication*, 302.

[75] dos Santos T., Pereira C.I., Gonçalves R., Salvini V.R., Zetterström C., Wöhrmeyer C. et al. Gluconate action in the hydration of calcium aluminate cements: Theoretical study, processing of aqueous suspensions and hydration reactivation. *Journal of the European Ceramic Society*, 2019, 39(8): S. 2748–2759.

[76] Matusinović T., Vrbos N. Alkali metal salts as set accelerators for high alumina cement. *Cement and Concrete Research*, 1993, 23(1): S. 177–186.

[77] Novinson T., Crahan J. Lithium Salts as Set Accelerators for Refractory Concretes: Correlation of Chemical Properties With Setting Times. *ACI Materials Journal*, 85(1).

[78] Duran A., Sirera R., Pérez-Nicolás M., Navarro-Blasco I., Fernández J.M., Alvarez J.I. Study of the early hydration of calcium aluminates in the presence of different metallic salts. *Cement and Concrete Research*, 2016, 81: S. 1–15.

[79] Rodger S.A., Double D.D. The chemistry of hydration of high alumina cement in the presence of accelerating and retarding admixtures. *Cement and Concrete Research*, 1984, 14(1): S. 73–82.

[80] Matusinović T., Čurlin D. Lithium salts as set accelerators for high alumina cement. *Cement and Concrete Research*, 1993, 23(4): S. 885–895.

[81] Matusinović T., Vrbos N., Čurlin D. Lithium Salts in Rapid Setting High-Alumina Cement Materials. *Industrial & Engineering Chemistry Research*, 1994, 33(11): S. 2795–2800.

[82] Damidot D., Rettel A., Sorrentino D., Capmas A. Action of admixtures on fondu cement: II. Effect of lithium salts on the anomalous setting time observed for temperatures ranging from 18 to 35°C. *Advances in Cement Research*, 1997, 9(35): S. 127–134.

[83] Götz-Neunhoeffer F. The function of Li carbonate and tartaric acid in the hydration of mixtures of calcium aluminate cement (CAC) with calcium sulfate hemihydrate. *Cement International*, 2007, 5: S. 90–101.

[84] van Straten H.A., Schoonen M.A.A., Bruyn P.L. de. Precipitation from supersaturated aluminate solutions. III. Influence of alkali ions with special reference to Li^+. *Journal of Colloid and Interface Science*, 1985, 103(2): S. 493–507.

[85] Alt C. Lithium Salts and their Role in Ettringite and Calcium Aluminate Hydration Acceleration. (Vortrag). 3rd Mortar Convention (Live Event Online); 2020.

[86] Khatib L.M.-A., Franceschini A., Taquet P. Lithium: a Booster for Calcium Aluminate Mortars through Massive Hydroxide Ion Supply. In: Leopolder F., editor. Drymix Mortar Yearbook 2020.

[87] Currell B.R., Grzeskowlak R., Mldgley H.G., Parsonage J.R. The acceleration and retardation of set high alumina cement by additives. *Cement and Concrete Research*, 1987, 17(3): S. 420–432.

[88] Müller I. Influence of cellulose ethers on the kinetics of early Portland cement hydration [Dissertation]. Karlsruhe, Universität Karlsruhe; 2006.

[89] Wang Z., Zhao Y., Zhou L., Xu L., Diao G., Liu G. Effects of hydroxyethyl methyl cellulose ether on the hydration and compressive strength of calcium aluminate cement. *Journal of Thermal Analysis and Calorimetry*, 2020, 140(2): S. 545–553.

[90] Plank J. Applications of Biopolymers in Construction Engineering. In: Steinbüchel A., editor. Biopolymers Online. Wiley; 2005.

[91] Hu M., Guo J., Du J., Liu Z., Li P., Ren X. et al. Development of Ca^{2+}-based, ion-responsive superabsorbent hydrogel for cement applications: Self-healing and compressive strength. *Journal of Colloid and Interface Science*, 2019, 538: S. 397–403.

[92] Mignon A., Snoeck D., D'Halluin K., Balcaen L., Vanhaecke F., Dubruel P. et al. Alginate biopolymers: Counteracting the impact of superabsorbent polymers on mortar strength. *Construction and Building Materials*, 2016, 110: S. 169–174.

[93] Sánchez V.E., Bartholomai G.B., Pilosof A.M.R. Rheological properties of food gums as related to their water binding capacity and to soy protein interaction. *LWT - Food Science and Technology*, 1995, 28(4): S. 380–385.

[94] Rhein-Knudsen N., Ale M.T., Meyer A.S. Seaweed hydrocolloid production: an update on enzyme assisted extraction and modification technologies. *Marine drugs*, 2015, 13(6): S. 3340–3359.

[95] Djabourov M., Nishinari K., Ross-Murphy S.B. Ionic gels. In: Djabourov M., Nishinari K., Ross-Murphy S.B., editors. Physical Gels from Biological and Synthetic Polymers. Cambridge: Cambridge University Press; 2013, S. 124–155.

[96] Haug A., Larsen B., Smidsrød O. Uronic acid sequence in alginate from different sources. *Carbohydrate Research*, 1974, 32(2): S. 217–225.

[97] Penman A., Sanderson G.R. A method for the determination of uronic acid sequence in alginates. *Carbohydrate Research*, 1972, 25(2): S. 273–282.

[98] Hecht H., Srebnik S. Structural Characterization of Sodium Alginate and Calcium Alginate. *Biomacromolecules*, 2016, 17(6): S. 2160–2167.

[99] Donati I., Holtan S., Mørch Y.A., Borgogna M., Dentini M., Skjåk-Braek G. New hypothesis on the role of alternating sequences in calcium-alginate gels. *Biomacromolecules*, 2005, 6(2): S. 1031–1040.

[100] Marburger A. Alginate und Carrageenane - Eigenschaften, Gewinnung und Anwendungen in Schule und Hochschule [Dissertation]. Marburg, Philipps-Universität Marburg; 2003.

[101] van den Hoek C., Mann D., Jahns H.M. Algae, An introduction to phycology. Cambridge: Cambridge Univ. Press; 2002.

[102] Wang Z.-Y., Zhang Q.-Z., Konno M., Saito S. Sol-gel transition of alginate solution by the addition of various divalent cations: ^{13}C-nmr spectroscopic study. *Biopolymers*, 1993, 33(4): S. 703–711.

[103] DeRamos C.M., Irwin A.E., Nauss J.L., Stout B.E. ^{13}C NMR and molecular modeling studies of alginic acid binding with alkaline earth and lanthanide metal ions. *Inorganica Chimica Acta*, 1997, 256(1): S. 69–75.

[104] Draget K.I., Skjåk Bræk G., Smidsrød O. Alginic acid gels: the effect of alginate chemical composition and molecular weight. *Carbohydrate Polymers*, 1994, 25(1): S. 31–38.

[105] Harper B.A., Barbut S., Lim L.-T., Marcone M.F. Effect of various gelling cations on the physical properties of "wet" alginate films. *Journal of food science*, 2014, 79(4): E562-7.

[106] Iskandar L., Rojo L., Di Silvio L., Deb S. The effect of chelation of sodium alginate with osteogenic ions, calcium, zinc, and strontium. *Journal of biomaterials applications*, 2019, 34(4): S. 573–584.

[107] Emmerichs N., Wingender J., Flemming H.-C., Mayer C. Interaction between alginates and manganese cations: identification of preferred cation binding sites. *International Journal of Biological Macromolecules*, 2004, 34(1-2): S. 73–79.

[108] Topuz F., Henke A., Richtering W., Groll J. Magnesium ions and alginate do form hydrogels: a rheological study. *Soft matter*, 2012, 8(18): S. 4877.

[109] Grant G.T., Morris E.R., Rees D.A., Smith P.J.C., Thom D. Biological interactions between polysaccharides and divalent cations: The egg-box model. *FEBS Letters*, 1973, 32(1): S. 195–198.

[110] Agulhon P., Markova V., Robitzer M., Quignard F., Mineva T. Structure of alginate gels: interaction of diuronate units with divalent cations from density functional calculations. *Biomacromolecules*, 2012, 13(6): S. 1899–1907.

[111] Braccini I., Pérez S. Molecular basis of Ca^{2+}-induced gelation in alginates and pectins: the egg-box model revisited. *Biomacromolecules*, 2001, 2(4): S. 1089–1096.

[112] Plazinski W. Molecular basis of calcium binding by polyguluronate chains. Revising the egg-box model. *Journal of computational chemistry*, 2011, 32(14): S. 2988–2995.

[113] Wolnik A., Albertin L., Charlier L., Mazeau K. Probing the helical forms of Ca^{2+}-guluronan junction zones in alginate gels by molecular dynamics 1: Duplexes. *Biopolymers*, 2013, 99(8): S. 562–571.

[114] Plazinski W., Drach M. Calcium-α-L-guluronate complexes: Ca^{2+} binding modes from DFT-MD simulations. *The journal of physical chemistry. B*, 2013, 117(40): S. 12105–12112.

[115] Fang Y., Al-Assaf S., Phillips G.O., Nishinari K., Funami T., Williams P.A. et al. Multiple steps and critical behaviors of the binding of calcium to alginate. *The journal of physical chemistry. B*, 2007, 111(10): S. 2456–2462.

[116] Draget K.I., Skjåk-Bræk G., Smidsrød O. Alginate based new materials. *International Journal of Biological Macromolecules*, 1997, 21(1-2): S. 47–55.

[117] Takemasa M., Round A.N., Sletmoen M., Stokke B.T. Bridging the Gap Between Single-Molecule Unbinding Properties and Macromolecular Rheology. In: Kaneda I., editor. Rheology of Biological Soft Matter. Tokyo: Springer Japan; 2017, S. 3–37.

[118] Assifaoui A., Lerbret A., Uyen H.T.D., Neiers F., Chambin O., Loupiac C. et al. Structural behaviour differences in low methoxy pectin solutions in the presence of divalent cations (Ca^{2+} and Zn^{2+}): a process driven by the binding mechanism of the cation with the galacturonate unit. *Soft matter*, 2015, 11(3): S. 551–560.

[119] Huynh U.T.D., Lerbret A., Neiers F., Chambin O., Assifaoui A. Binding of Divalent Cations to Polygalacturonate: A Mechanism Driven by the Hydration Water. *The journal of physical chemistry. B*, 2016, 120(5): S. 1021–1032.

[120] Pistone S., Qoragllu D., Smistad G., Hiorth M. Formulation and preparation of stable cross-linked alginate-zinc nanoparticles in the presence of a monovalent salt. *Soft matter*, 2015, 11(28): S. 5765–5774.

[121] Voragen A.G.J., Coenen G.-J., Verhoef R.P., Schols H.A. Pectin, a versatile polysaccharide present in plant cell walls. *Structural Chemistry*, 2009, 20(2): S. 263–275.

[122] Kyomugasho C., Munyensanga C., Celus M., van de Walle D., Dewettinck K., van Loey A.M. et al. Molar mass influence on pectin-Ca^{2+} adsorption capacity, interaction energy and associated functionality: Gel microstructure and stiffness. *Food Hydrocolloids*, 2018, 85: S. 331–342.

[123] Walkinshaw M.D., Arnott S. Conformations and interactions of pectins:, II. Models for junction zones in pectinic acid and calcium pectate gels. *Journal of Molecular Biology*, 1981, 153(4): S. 1075–1085.

[124] Powell D.A., Morris E.R., Gidley M.J., Rees D.A. Conformations and interactions of pectins:, II. Influence of residue sequence on chain association in calcium pectate gels. *Journal of Molecular Biology*, 1982, 155(4): S. 517–531.

[125] Morris E.R., Powell D.A., Gidley M.J., Rees D.A. Conformations and interactions of pectins:, I. Polymorphism between gel and solid states of calcium polygalacturonate. *Journal of Molecular Biology*, 1982, 155(4): S. 507–516.

[126] Du Maire Poset A., Zitolo A., Cousin F., Assifaoui A., Lerbret A. Evidence for an egg-box-like structure in iron(ii)-polygalacturonate hydrogels: a combined EXAFS and molecular dynamics simulation study. *Physical chemistry chemical physics PCCP*, 2020, 22(5): S. 2963–2977.

[127] Alagna L., Prosperi T., Tomlinson A.A.G., Rizzo R. Extended x-ray absorption fine structure investigation of solid and gel forms of calcium poly(+.alpha.-D-galacturonate). *The Journal of Physical Chemistry*, 1986, 90(26): S. 6853–6857.

[128] Rochas C., Rinaudo M., Landry S. Role of the molecular weight on the mechanical properties of kappa carrageenan gels. *Carbohydrate Polymers*, 1990, 12(3): S. 255–266.

[129] Nickerson M.T., Darvesh R., Paulson A.T. Formation of calcium-mediated junction zones at the onset of the sol-gel transition of commercial kappa-carrageenan solutions. *Journal of food science*, 2010, 75(3): E153-6.

[130] Morris E.R., Rees D.A., Robinson G. Cation-specific aggregation of carrageenan helices: Domain model of polymer gel structure. *Journal of Molecular Biology*, 1980, 138(2): S. 349–362.

[131] Janaswamy S., Chandrasekaran R. Effect of calcium ions on the organization of iota-carrageenan helices: an X-ray investigation. *Carbohydrate Research*, 2002, 337(6): S. 523–535.

[132] Hermansson A.-M., Eriksson E., Jordansson E. Effects of potassium, sodium and calcium on the microstructure and rheological behaviour of kappa-carrageenan gels. *Carbohydrate Polymers*, 1991, 16(3): S. 297–320.

[133] Janaswamy S., Chandrasekaran R. Heterogeneity in iota-carrageenan molecular structure: insights for polymorph II--III transition in the presence of calcium ions. *Carbohydrate Research*, 2008, 343(2): S. 364–373.

[134] Iglauer S., Wu Y., Shuler P., Tang Y., Goddard W.A. Dilute iota- and kappa-Carrageenan solutions with high viscosities in high salinity brines. *Journal of Petroleum Science and Engineering*, 2011, 75(3-4): S. 304–311.

[135] Rochas C., Rinaudo M. Mechanism of gel formation in κ-carrageenan. *Biopolymers*, 1984, 23(4): S. 735–745.

[136] Arnott S., Scott W.E., Rees D.A., McNab C.G.A. i-Carrageenan: Molecular structure and packing of polysaccharide double helices in oriented fibres of divalent cation salts. *Journal of Molecular Biology*, 1974, 90(2): S. 253–267.

[137] Schröfl C., Mechtcherine V., Gorges M. Relation between the molecular structure and the efficiency of superabsorbent polymers (SAP) as concrete admixture to mitigate autogenous shrinkage. *Cement and Concrete Research*, 2012, 42(6): S. 865–873.

[138] Martirena F., Rodriguez-Rodriguez Y., Callico A., Diaz Y., Bracho G., Hereira A. et al. Microorganism-based bioplasticizer for cementitious materials. In: Biopolymers and Biotech Admixtures for Eco-Efficient Construction Materials. Elsevier; 2016, S. 151–171.

[139] Govin A., Bartholin M.-C., Biasotti B., Giudici M., Langella V., Grosseau P. Effect of Guar Gum Derivatives on Fresh State Properties of Portland Cement-Based Mortars. In: Jay S., Kwesi S.-C., editors. Concrete 2015 / RILEM Week - 27th Biennial National Conference of the Concrete Institute of Australia in conjunction with the 69th RILEM Week. Melbourne, Australia: the Concrete Institute of Australia; 2015.

[140] Khayat K.H. Viscosity-enhancing admixtures for cement-based materials — An overview. *Cement and Concrete Composites*, 1998, 20(2-3): S. 171–188.

[141] Ma B., Peng Y., Tan H., Lv Z., Deng X. Effect of Polyacrylic Acid on Rheology of Cement Paste Plasticized by Polycarboxylate Superplasticizer. *Materials*, 2018, 11(7).

[142] Cano-Barrita P.d.J.F., León-Martínez F.M. Biopolymers with viscosity-enhancing properties for concrete. In: Biopolymers and Biotech Admixtures for Eco-Efficient Construction Materials. Elsevier; 2016, S. 221–252.

[143] Li M., Pan L., Li J., Xiong C. Competitive adsorption and interaction between sodium alginate and polycarboxylate superplasticizer in fresh cement paste. *Colloids and Surfaces A: Physicochemical and Engineering Aspects*, 2020, 586: S. 124249.

[144] Schmidt W., Brouwers H.J.H., Kühne H.-C., Meng B. Interactions of polysaccharide stabilising agents with early cement hydration without and in the presence of superplasticizers. *Construction and Building Materials*, 2017, 139: S. 584–593.

[145] León-Martínez F.M., Cano-Barrita P.d.J.F., Lagunez-Rivera L., Medina-Torres L. Study of nopal mucilage and marine brown algae extract as viscosity-enhancing admixtures for cement based materials. *Construction and Building Materials*, 2014, 53: S. 190–202.

[146] Hurnaus T., Plank J. Adsorption of non-ionic cellulose ethers on cement revisited. *Construction and Building Materials*, 2019, 195: S. 441–449.

[147] Willson R.J. Calorimetry. In: Haines P., editor. Principles of Thermal Analysis and Calorimetry. Cambridge: Royal Society of Chemistry; 2002, S. 129–165.

[148] Wadsö L. Isothermal calorimetry for the study of cement hydration. Division of Building Materials, LTH, Lund University; 2001.

[149] Bensted J. Some applications of conduction calorimetry to cement hydration. *Advances in Cement Research*, 1987, 1(1): S. 35–44.

[150] DIN EN 196-11:2019-03, Prüfverfahren für Zement - Teil 11: Hydratationswärme - Isotherme Wärmeflusskalorimetrie-Verfahren; Deutsche Fassung EN 196-11:2018. Berlin: Beuth Verlag GmbH.

[151] Thermometric AB. Instruction manual, Thermometric 3114/3236 TAM Air Isothermal Calorimeter. Version 2.4. Schweden; 2000.

[152] Jansen D., Naber C., Ectors D., Lu Z., Kong X.-M., Götz-Neunhoeffer F. et al. The early hydration of OPC investigated by in-situ XRD, heat flow calorimetry, pore water analysis and ^{1}H NMR: Learning about adsorbed ions from a complete mass balance approach. *Cement and Concrete Research*, 2018, 109: S. 230–242.

[153] Frølich L., Wadsö L., Sandberg P. Using isothermal calorimetry to predict one day mortar strengths. *Cement and Concrete Research*, 2016, 88: S. 108–113.

[154] Smith M.A., Matthews J.D. Conduction calorimetric studies of the effect of sulphate on the hydration reactions of Portland cement. *Cement and Concrete Research*, 1974, 4(1): S. 45–55.

[155] DIN EN 196-1:2016-11, Prüfverfahren für Zement - Teil 1: Bestimmung der Festigkeit; Deutsche Fassung EN 196-1:2016. Berlin: Beuth Verlag GmbH.

[156] Dinnebier R.E., Friese K. Modern XRD methods in mineralogy. *Introduction to the Mineralogical Sciences: Encyclopedia of Life Support Systems (EOLSS)*, 2003.

[157] Spieß L., Teichert G., Schwarzer R., Behnken H., Genzel C. Moderne Röntgenbeugung, Röntgendiffraktometrie für Materialwissenschaftler, Physiker und Chemiker. 3rd ed. Wiesbaden: Vieweg & Teubner; 2018.

[158] Rietveld H.M. A profile refinement method for nuclear and magnetic structures. *Journal of Applied Crystallography*, 1969, 2(2): S. 65–71.

[159] Young R.A. (ed.). The Rietveld method, Product of the International Workshop on the Rietveld Method in Petten, The Netherlands, 13 - 15 June 1989. Oxford: Oxford University Press; 1993.

[160] Canet D. NMR - Konzepte und Methoden. Berlin, Heidelberg: Springer; 1994.

[161] Mason J. (ed.). Multinuclear NMR. Boston, MA: Springer US; 1987.

[162] MacKenzie K.J.D., Smith M.E. Multinuclear Solid-State Nuclear Magnetic Resonance of Inorganic Materials. 1st ed. s.l.: Elsevier textbooks; 2002.

[163] Xu J., Wang Q., Li S.i., Deng F. Solid-State NMR Principles and Techniques. In: Xu J., Wang Q., Li S., Deng F., editors. Solid-State NMR in Zeolite Catalysis. Singapore: Springer Singapore; 2019, S. 1–55.

[164] Kemp W. NMR in Chemistry, A Multinuclear Introduction. London, s.l.: Macmillan Education UK; 1986.

[165] Gonnella N.C. Nuclear Magnetic Resonance. In: Grinberg N., Rodriguez S., editors. Ewing's analytical instrumentation handbook. Boca Raton, FL: CRC Press, Taylor & Francis Group; 2019.

[166] Brown S.P., Emsley L. Solid-State NMR. In: Gauglitz G., Vo-Dinh T., editors. Handbook of spectroscopy. Weinheim: Wiley-VCH; 2005, S. 269–326.

[167] Luong T., Mayer H., Eckert H., Novinson T.I. In Situ ^{27}Al NMR Studies of Cement Hydration: The Effect of Lithium-Containing Setting Accelerators. *Journal of the American Ceramic Society*, 1989, 72(11): S. 2136–2141.

[168] Cong X., Kirkpatrick R.J. Hydration of Calcium Aluminate Cements: A Solid-State ^{27}Al NMR Study. *Journal of the American Ceramic Society*, 1993, 76(2): S. 409–416.

[169] Faucon P., Charpentier T., Bertrandie D., Nonat A., Virlet J., Petit J.C. Characterization of Calcium Aluminate Hydrates and Related Hydrates of Cement Pastes by ^{27}Al MQ-MAS NMR. *Inorganic chemistry*, 1998, 37(15): S. 3726–3733.

[170] Skibsted J., Henderson E., Jakobsen H.J. Characterization of Calcium Aluminate Phases in Cements by ^{27}Al MAS NMR spectroscopy. *Inorganic Chemistry*, 1993, 32(6): S. 1013–1027.

[171] Rawal A., Smith B.J., Athens G.L., Edwards C.L., Roberts L., Gupta V. et al. Molecular silicate and aluminate species in anhydrous and hydrated cements. *Journal of the American Chemical Society*, 2010, 132(21): S. 7321–7337.

[172] Müller D., Rettel A., Gessner W., Scheler G. An application of solid-state magic-angle spinning ^{27}Al NMR to the study of cement hydration. *Journal of Magnetic Resonance (1969)*, 1984, 57(1): S. 152–156.

[173] Doty F.D. Solid State NMR Probe Design. *eMagRes*, 2007.

[174] Wang T. Inductively Coupled Plasma Optical Emission Spectrometry. In: Grinberg N., Rodriguez S., editors. Ewing's analytical instrumentation handbook. Boca Raton, FL: CRC Press, Taylor & Francis Group; 2019.

[175] Rosenberg E., Panne U. Atomic Absorption Spectrometry (AAS) and Atomic Emission Spectrometry (AES). In: Gauglitz G., Vo-Dinh T., editors. Handbook of spectroscopy. Weinheim: Wiley-VCH; 2005, S. 421–496.

[176] Khandpur R.S. Inductively Coupled Plasma Optical Emission Spectrometer (ICP-OES). In: Khandpur R.S., editor. Compendium of Biomedical Instrumentation, Volume 1. Wiley; 2020, S. 1057–1062.

[177] Brennan M. A practical approach to quantitative metal analysis of organic matrices. Chichester, U.K: Wiley; 2008.

[178] Nölte J. ICP-Emissionsspektrometrie für Praktiker, Grundlagen, Methodenentwicklung, Anwendungsbeispiele. Weinheim: Wiley-VCH; 2005.

[179] Müller R.H., Nitzsche R., Paulke B.-R. Zetapotential und Partikelladung in der Laborpraxis, Einführung in die Theorie, praktische Messdurchführung, Dateninterpretation. Stuttgart: Wiss. Verlag-Ges; 1996.

[180] van der Meeren P., Cocquyt J., Vanderdeelen J. Surface Charge Analysis. In: Nollet L.M.L., editor. Handbook of food analysis, 2nd ed. New York, NY: Dekker; 2004.

[181] Malvern Instruments Ltd. Zetasizer Nano User Manual, MAN0485 Issue 1.1; 2013.

[182] Ul-Hamid A. A Beginners' Guide to Scanning Electron Microscopy. Cham: Springer International Publishing; 2018.

[183] Goldstein J.I., Newbury D.E., Michael J.R., Ritchie N.W.M., Scott J.H.J., Joy D.C. Scanning Electron Microscopy and X-Ray Microanalysis. 4th ed. New York, NY: Springer New York; 2018.

[184] Reimer L. Scanning Electron Microscopy, Physics of Image Formation and Microanalysis. Berlin, Heidelberg, s.l.: Springer Berlin Heidelberg; 1998.

[185] Marturi N. Vision and Visual Servoing for Nanomanipulation and Nanocharacterization using Scanning Electron Microscope [Dissertation], Université de Franche-Comté; 2013.

[186] Kohn R. Ion binding on polyuronates - alginate and pectin. *Pure and Applied Chemistry*, 1975, 42(3): S. 371–397.

[187] Plank J. Persönliche Mitteilung; 2020.

[188] Hetche O. Lithium Carbonate Alternatives for fast curing Dry Mix Applications, Präsentation 20.2. Nürnberg; 2019.

[189] Hüller F., Ectors D., Neubauer J., Götz-Neunhoeffer F. Influence of crystallinity and surface area on the hydration kinetics of CA_2. *Cement and Concrete Research*, 2016, 89: S. 136–144.

[190] Raab B. Synthese und Charakterisierung nanoskaliger hydraulisch hochreaktiver Phasen des Portland- und Tonerdezements [Dissertation]. Halle (Saale), Martin-Luther-Universität Halle-Wittenberg; 2010.

[191] Hüller F., Naber C., Neubauer J., Götz-Neunhoeffer F. Impact of initial CA dissolution on the hydration mechanism of CAC. *Cement and Concrete Research*, 2018, 113: S. 41–54.

[192] International Centre for Diffraction Data. Powder Diffraction File (PDF), PDF-2 Release 2010.

7. Anhang

7.1 Wirkung von Alginat und Füllstoff bei niedrigem w/z-Wert

In den **Abbildungen A1** und **A2** ist das Abbindeprofil zweier Calciumaluminatzemente („*Ciment Fondu*“ und „*Secar 71*“) bei einem niedrigen w/z-Wert von 0,3 dargestellt. Deutlich zu erkennen ist die spätere Wärmefreisetzung der Referenz, welche aufgrund des Fließmittels und des Celluloseethers verzögert ist. Durch Zugabe eines beschleunigenden Füllstoffs wie γ-Al_2O_3 oder durch den Einsatz von Alginat anstelle des Celluloseethers findet der Zeitpunkt der Wärmefreisetzung im Kalorimeter aufgrund deren beschleunigenden Eigenschaften erheblich früher statt.

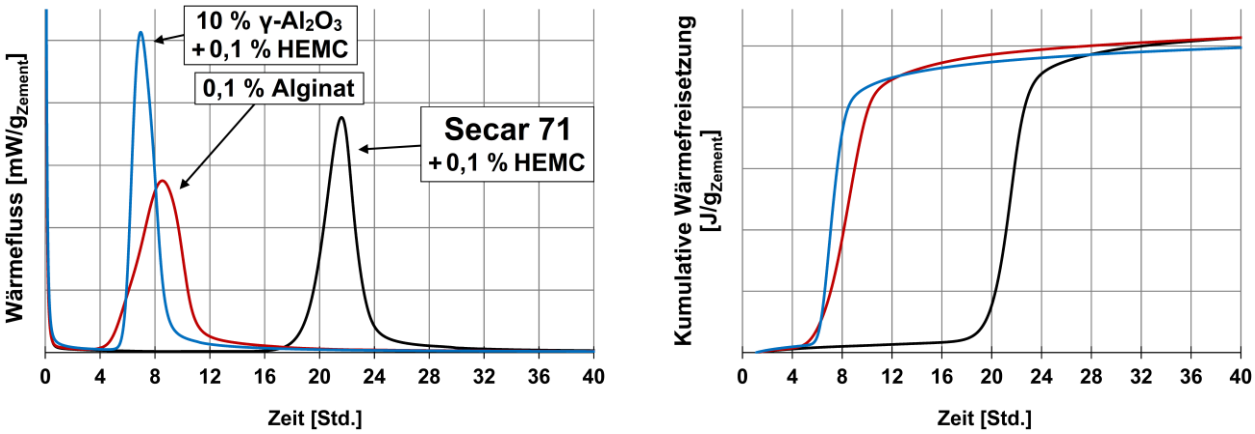

Abbildung A1: Einfluss von Alginat (*XEA 5036*) sowie γ-Al_2O_3 (*NO 221-30*) auf das Abbindeverhalten von CAC (*Secar 71*, w/z = 0,3) stabilisiert mit 0,1 % *MHB 300 P2* (HEMC) in Gegenwart von 0,075 % PCE (*Melflux 2651*) und Triethylenglykol, bestimmt mittels Wärmeflusskalorimetrie in Paste.

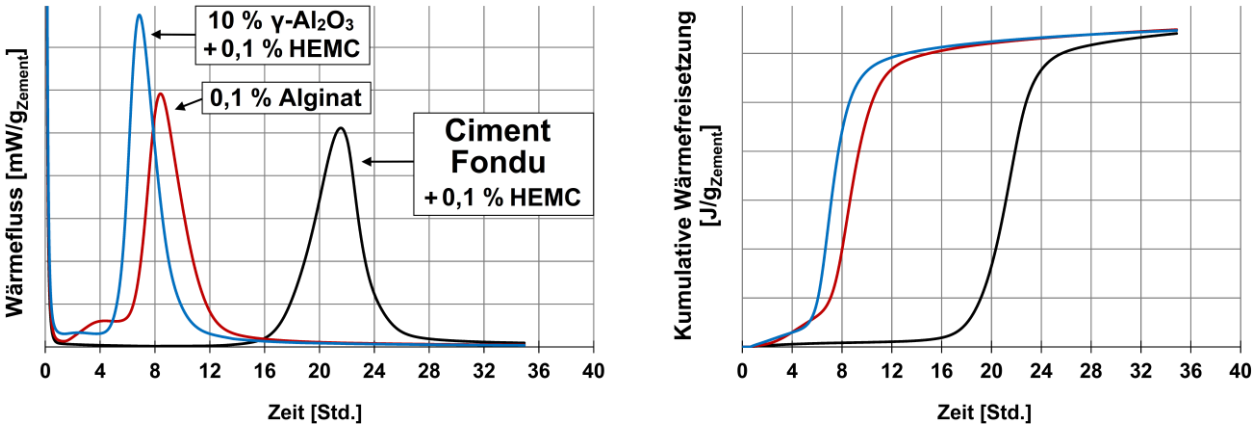

Abbildung A2: Einfluss von Alginat (*XEA 5036*) sowie γ-Al_2O_3 (*NO 221-30*) auf das Abbindeverhalten von CAC (*Ciment Fondu*, w/z = 0,3) stabilisiert mit 0,1 % *MHB 300 P2* (HEMC) in Gegenwart von 0,125 % PCE (*Melflux 2651*) und Triethylenglykol, bestimmt mittels Wärmeflusskalorimetrie in Paste.

7.2 Untersuchungen mit reinen CAC-Klinkerphasen

Die mineralogische Zusammensetzung und das Verhalten von Calciumaluminatzement wird maßgeblich durch die Klinker-Phasen CA, CA_2 und $C_{12}A_7$ bestimmt. Um die beschleunigende Wirkung von Alginat auf verschiedene Zemente besser zu verstehen, wurde die Wechselwirkung einzelner Klinkerphasen mit dem Biopolymer betrachtet.

Hierzu wurden diese Phasen entweder selbst synthetisiert (#1, Syn.) oder sie waren von früheren Arbeiten bereits vorrätig (#2, Vor.) oder wurden von einem externen Partner (#3, Ext.) zur Verfügung gestellt. Mittels Wärmeflusskalorimetrie in Paste wurde die Hydratation der Klinkerphasen sowie der Einfluss der Alginat-Zugabe betrachtet, wobei die beschleunigende Wirkung des Alginats deutlich zu erkennen war. Die Ergebnisse dieser Untersuchungen sind in **Tabelle A1** gelistet.

Tabelle A1: Zeitpunkt der maximalen Wärmefreisetzung verschiedener Klinkerphasen in An- und Abwesenheit von Alginat, bestimmt mittels isothermer Wärmefluss-kalorimetrie in Paste (n.b. = nicht bestimmbar).

System	Zeitpunkt maximaler Wärmefreisetzung [Std.]		
	CA	**CA_2**	**$C_{12}A_7$**
#1 (Syn.)	13,6 ± 0,1	n.b.	5,8 ± 0,5
#1 (Syn.) + 0,1 % Alginat	5,3 ± 0,2	n.b.	4,8 ± 0,6
#1 (Syn.) + 0,2 % Alginat	5,0 ± 0,1	n.b.	4,8 ± 0,2
#2 (Vor.)	20,1 ± 0,4	12,2 ± 0,1	7,6 ± 0,3
#2 (Vor.) + 0,1 % Alginat	7,8 ± 0,5	9,4 ± 0,3	4,9 ± 0,4
#2 (Vor.) + 0,2 % Alginat	4,9 ± 0,1	7,7 ± 0,1	4,4 ± 0,1
#3 (Ext.)	6,3	-	-
#3 (Ext.) + 0,1 % Alginat	3,8	-	-
#3 (Ext.) + 0,2 % Alginat	2,4	-	-

Insbesondere CA wurde durch das Alginat beschleunigt, wobei der Zeitpunkt der maximalen Wärmefreisetzung 40 – 75 % früher auftrat. Die inhärent reaktive Phase $C_{12}A_7$, die für die Reaktivität von Aluminatzementen maßgeblich verantwortlich ist, wurde hingegen nur um 20 – 40 % beschleunigt. Dies spiegelt die Erkenntnisse aus **Publikation 1** wieder, in welcher festgestellt wurde, dass Zemente mit einem hohen Calcium-zu-Aluminium-Verhältnis (z.B. „*Ciment Fondu*“) nur schwach durch das Alginat beschleunigt werden. Die Untersuchung des Hydratationsverhaltens von CA_2 kam hingegen zu keinem eindeutigen Ergebnis. Für CA_2 aus Probe #2 (Vor.) konnte eine beschleunigende Wirkung bezüglich des Auftretens der Wärmefreisetzung festgestellt

werden. Hingegen war bei CA_2 aus Probe #1 (Syn.) keine deutliche Wärmefreisetzung zu erkennen, da die Hydratation stetig ohne definierten Spitzenwert erfolgte. Hier konnte in Gegenwart von Alginat keine Beschleunigung beobachtet werden.

Die unterschiedliche Reaktivität derselben Klinkerphase kann u.a. auf verschiedene Mahlfeinheit zurückgeführt werden, da sie für die Reaktivität der Klinkerphasen ausschlaggebend ist [189–191]. Die Partikelgrößen der unterschiedlichen Klinkerphasen sind zum Vergleich in **Tabelle A2** für die verschiedenen Produkte aufgeführt.

Tabelle A2: Vergleich der Partikelgrößen der unterschiedlichen Klinkerphasen, bestimmt mittels Lasergranulometrie.

Probe/Kornfraktion		Partikelgröße [µm]		
		CA	**CA_2**	**$C_{12}A_7$**
#1 (Syn.)	d_{10}	1,2 ± 0,1	0,9 ± 0,1	1,4 ± 0,1
	d_{50}	21,7 ± 0,3	11,0 ± 0,1	21,2 ± 0,2
	d_{90}	78,4 ± 1,5	47,7 ± 0,9	80,7 ± 1,5
#2 (Vor.)	d_{10}	2,4 ± 0,1	1,1 ± 0,1	5,2 ± 0,1
	d_{50}	29,8 ± 0,2	16,4 ± 0,2	54,9 ± 0,7
	d_{90}	106,7 ± 0,5	73,4 ± 0,1	278,1 ± 6,5
#3 (Ext.)	d_{10}	1,5 ± 0,1		
	d_{50}	14,7 ± 0,2		
	d_{90}	47,7 ± 1,5		

Die Synthese der Klinkerphasen für die Proben #1 (Syn.) erfolgte in einem Hochtemperaturofen *LHT 08/16* der Firma *Nabertherm*. Hierzu wurden Calciumcarbonat (d_{50} 1,6 µm, *Criscal 1*, Firma *Provencale*) und Aluminiumoxid (d_{50} 0,8 µm, *Nabalox 784*, Firma *Nabaltech*) in Wasser unter Rühren suspendiert und anschließend vakuumfiltriert. Der feuchte Filterrückstand wurde bei 100 °C getrocknet und nach kurzem Aufmahlen im Achatmörser in Platintiegel überführt. Für die Synthese wurde innerhalb von 14 Stunden auf 1550 °C erhitzt, wobei Restfeuchte und CO_2 ausgetrieben wurden. Die Temperatur von 1550 °C wurde über vier Stunden gehalten und die Tiegel bei mindestens 1350 °C aus dem Ofen entnommen, um den Klinker abzuschrecken. Das gesinterte Material (CA und CA_2) bzw. Glas ($C_{12}A_7$) wurde manuell zerkleinert, in einer Planetenkugelmühle (*Pulverisette 6*, Firma *Fritsch*) bei einer Mahlgeschwindigkeit von 300 U/min aufgemahlen und die Fraktion < 125 µm durch ein Analysesieb abgetrennt.

Die Reinheit der Klinkerphasen wurde mittels Röntgenpulverdiffraktometrie qualitativ analysiert, wobei mit Ausnahme von Probe CA_2 #2 (Vor.), welche eine geringe Menge Gibbsit enthielt, alle Proben phasenrein waren. Die zugehörigen Diffraktogramme sind in

Abbildung A3 (CA), **Abbildung A4** (CA_2) und **Abbildung A5** ($C_{12}A_7$) dargestellt. Zusätzlich wurden die Hydratationsprodukte nach der Reaktion mit Wasser für die Klinkerphasen der Proben #1 (Syn.) nach mehreren Tagen Hydratation bei 20 °C in An- und Abwesenheit von Alginat mittels XRD bestimmt. Hierbei konnte für $C_{12}A_7$ (CAH_{10} und $C_2AH_{7,5}$) und CA (CAH_{10}) kein Unterschied in der Bildung der C-A-H-Phasen festgestellt werden, wohingegen CA_2 in Gegenwart von Alginat bevorzugt C_2AH_8 bzw. $C_2AH_{7,5}$ ausbildete (siehe **Abbildungen A6 und A7**).

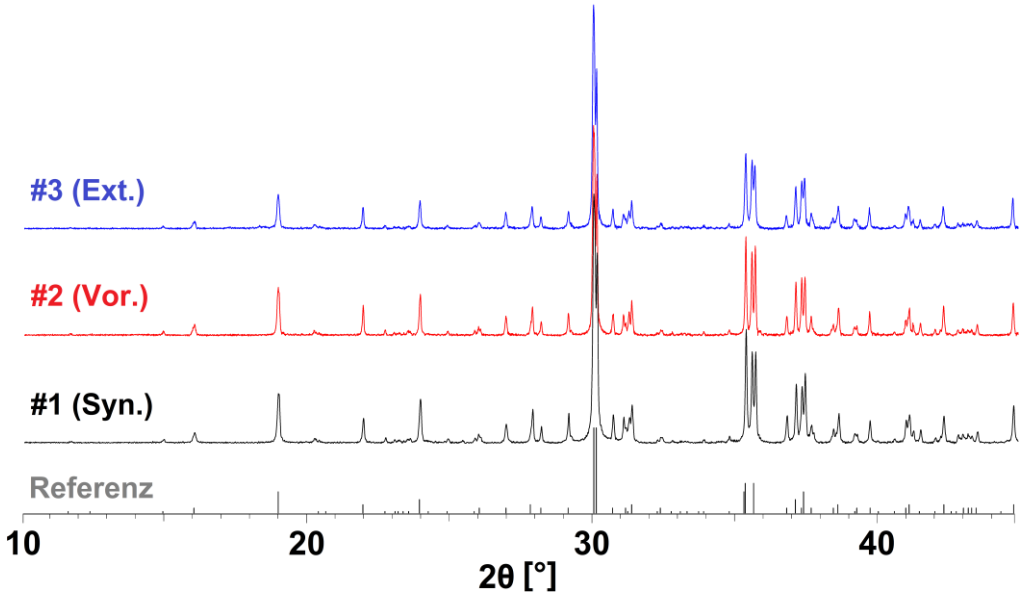

Abbildung A3: XRDs der eingesetzten Proben von CA (Monocalciumaluminat) im Vergleich zu einem Referenzdiffraktogramm (PDF 01-070-0134) [192].

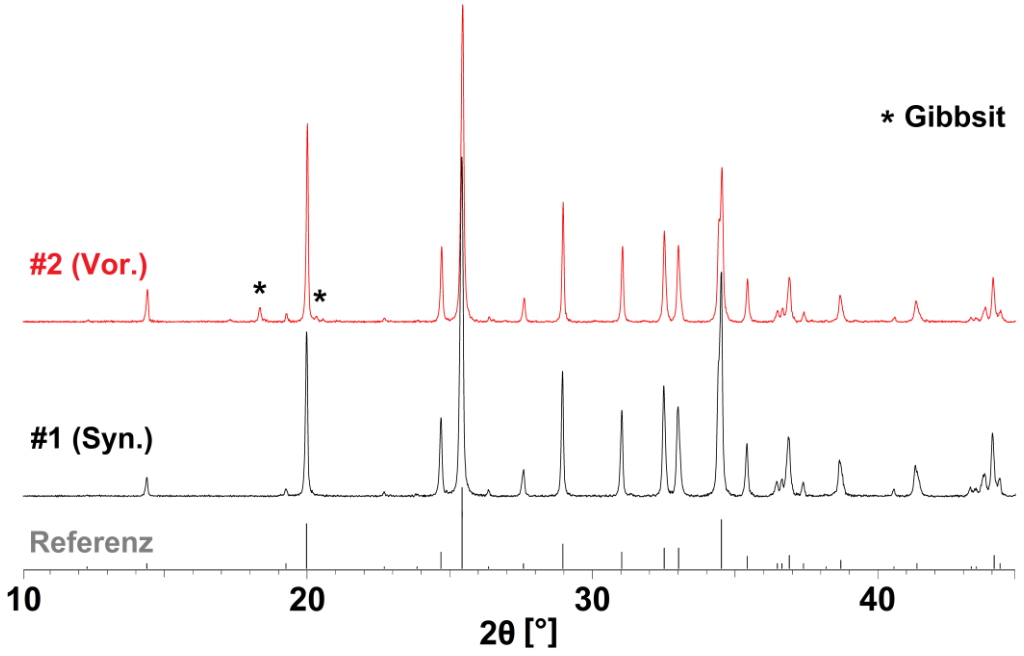

Abbildung A4: XRDs der eingesetzten Proben von CA_2 (Grossit) im Vergleich zu einem Referenzdiffraktogramm (PDF 01-072-0767) [192].

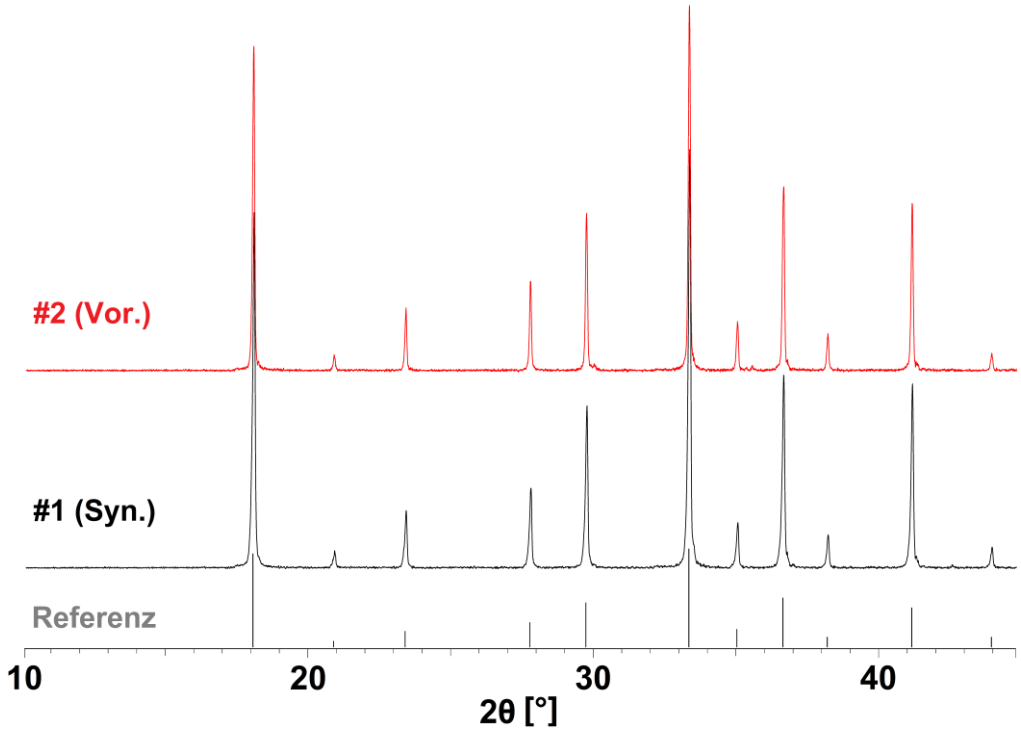

Abbildung A5: XRDs der eingesetzten Proben von $C_{12}A_7$ (Mayenit) im Vergleich zu einem Referenzdiffraktogramm (PDF 00-009-0413) [192].

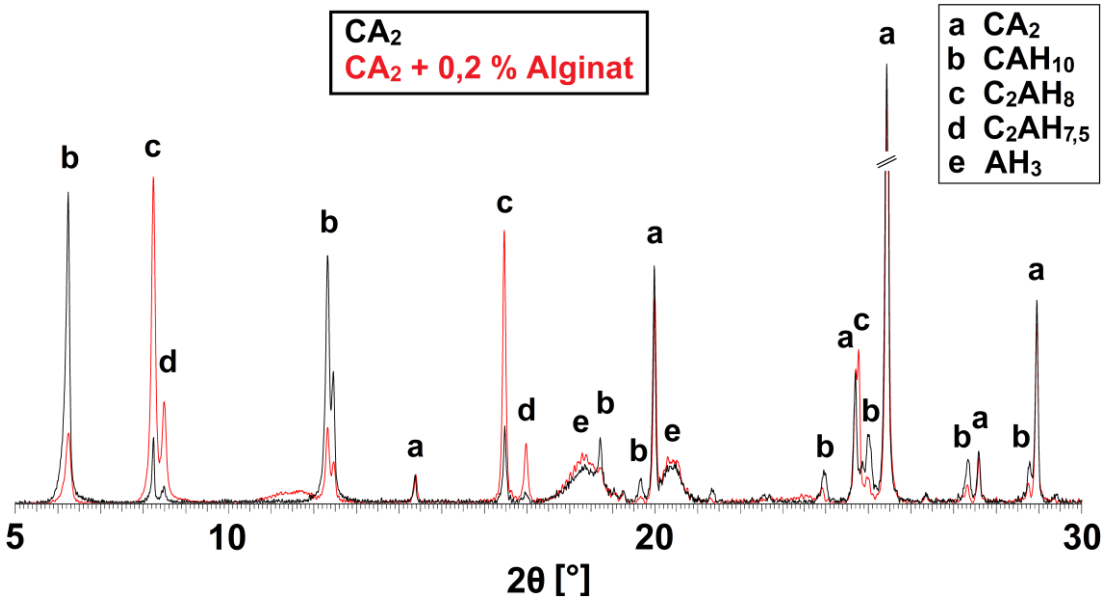

Abbildung A6: XRDs der Hydratationsprodukte von CA_2 (#1, Syn) in Anwesenheit (rot) und Abwesenheit (schwarz) von Alginat nach 10 Tagen Hydratation bei 20 °C.

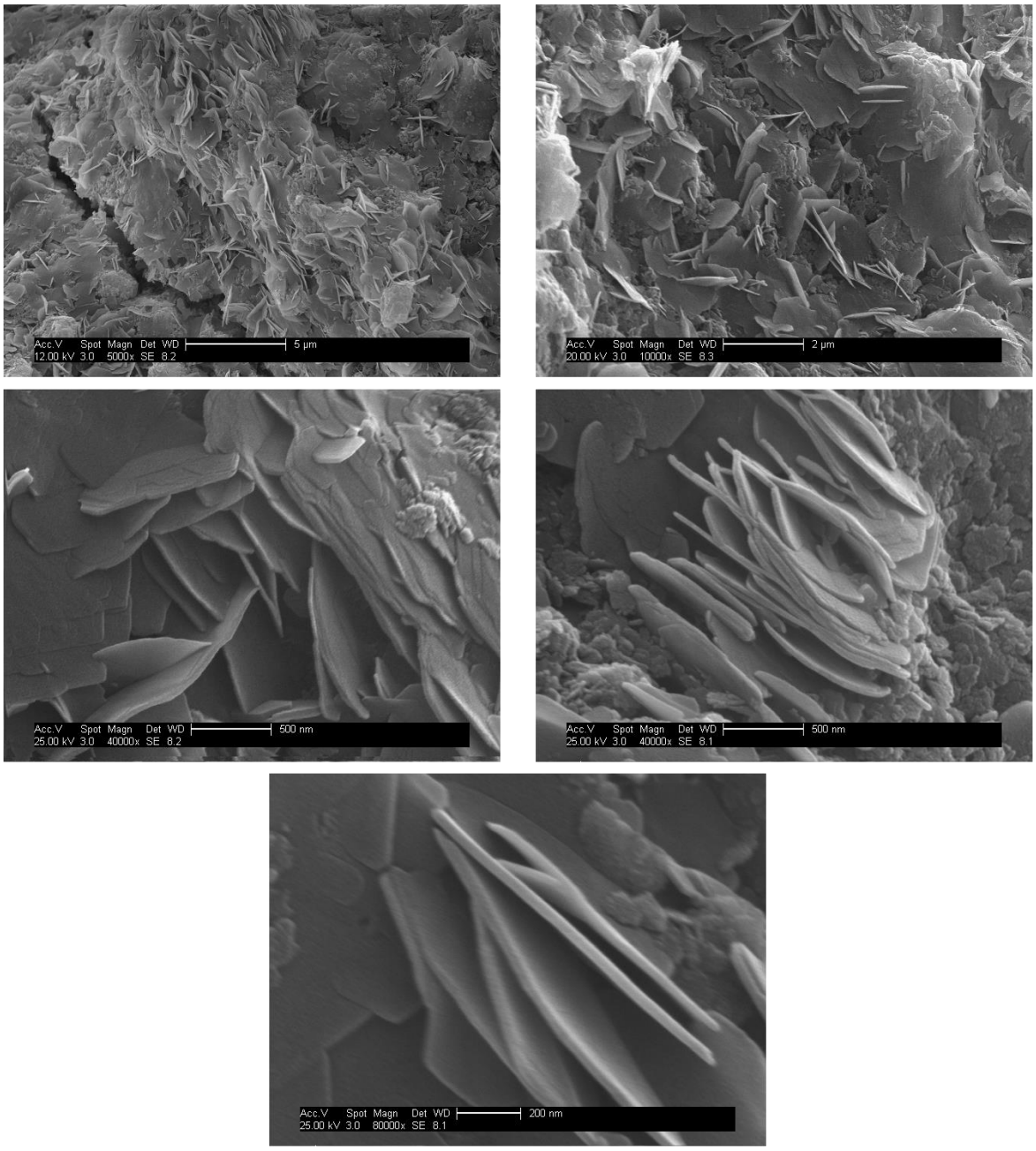

Abbildung A7: Elektronenmikroskopische Aufnahme des Hydratationsprodukts von CA_2 in Gegenwart von Alginat bei 20°C.

7.3 Untersuchungen zum temperaturabhängigen Verhalten

Für die genauere Aufklärung des hydratationsbeschleunigenden Effekts von Alginat auf Calciumaluminatzemente, deren Hydratation sich durch eine ausgeprägte Abhängigkeit von der Reaktionstemperatur auszeichnet (siehe **Abschnitt 2.1**), wurde das Abbindeverhalten (siehe **Abbildungen A8** – **A12**) sowie die Bildung der Hydratphasen (siehe **Abbildung A13**) temperaturabhängig untersucht.

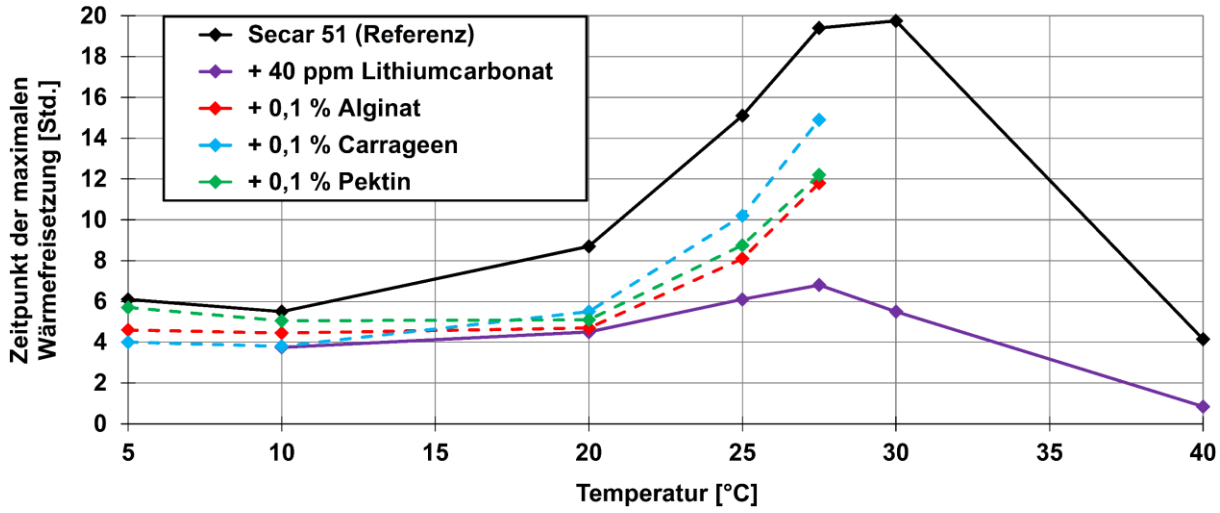

Abbildung A8: Zeitpunkt der maximalen Wärmefreisetzung im Kalorimeter für den Aluminatzement *„Secar 51“* in Abhängigkeit von der Reaktionstemperatur und der Anwesenheit beschleunigender Zusatzmittel (Alginat *XEA 5036*, Carrageen *GP 379* und Pektin *CU 701*).

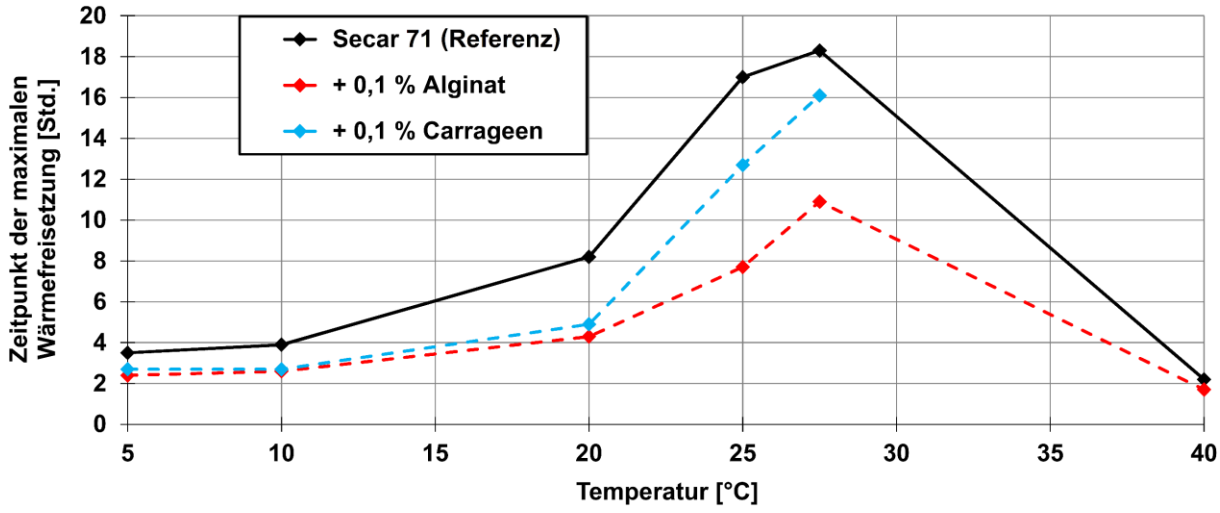

Abbildung A9: Zeitpunkt der maximalen Wärmefreisetzung im Kalorimeter für den Aluminatzement *„Secar 71“* in Abhängigkeit von der Reaktionstemperatur und der Anwesenheit beschleunigender Biopolymere (Alginat *XEA 5036* und Carrageen *GP 379*).

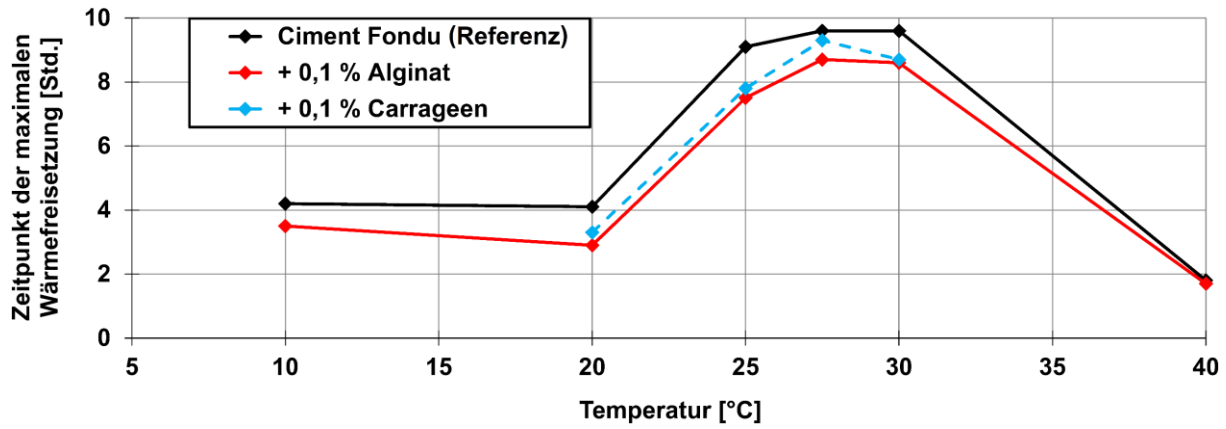

Abbildung A10: Zeitpunkt der maximalen Wärmefreisetzung im Kalorimeter für den Aluminatzement *„Ciment Fondu“* in Abhängigkeit von der Reaktionstemperatur und der Anwesenheit beschleunigender Biopolymere (Alginat *XEA 5036* und Carrageen *GP 379*).

Wie anhand der **Abbildungen A8** – **A10** festgestellt werden kann, zeigen die Biopolymere ein ausgeprägt temperaturabhängiges Beschleunigungsverhalten. Insbesondere im Vergleich zu Li_2CO_3 (siehe **Abbildung A8**) wird der unterschiedliche Wirkmechanismus, der den Biopolymeren zugrunde liegt, sehr deutlich.

Der Einfluss des Alginats führt insbesondere bei Temperaturen ab 30 °C in *„Secar 51“*, wie in **Abbildung A11** und **A12** zu sehen ist, zu einer Veränderung im aufgezeichneten Profil der Wärmefreisetzung. Dieses wird durch Zugabe von Alginat verbreitert sowie abgeflacht, sodass die Reaktionswärme über einen längeren Zeitraum freigesetzt wird (siehe **Abbildung A11** und **A12**). Dies impliziert eine verzögerte bzw. verlangsamte Sammelkristallisation der C-A-H-Phasen. In *„Secar 71“* und *„Ciment Fondu“* konnte dieses Phänomen nicht beobachtet werden.

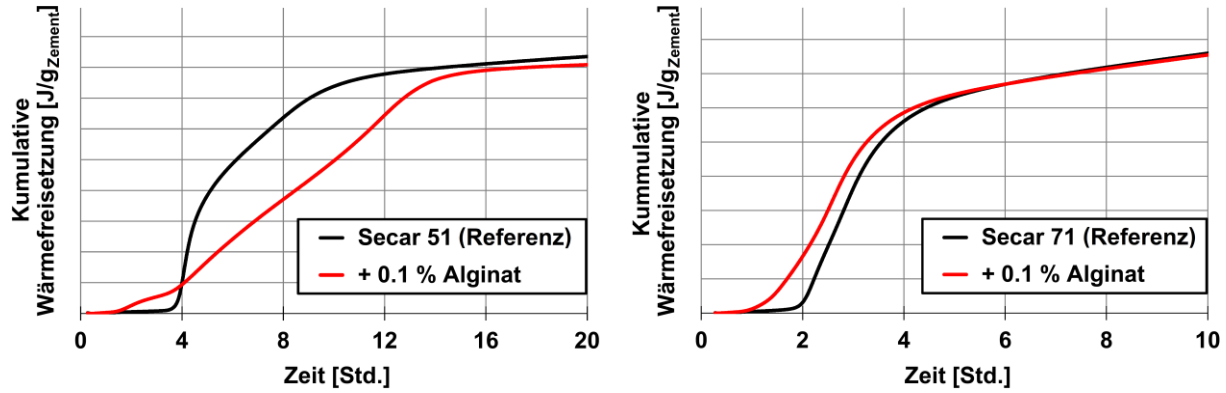

Abbildung A11: Kumulative Wärmefreisetzung zweier Aluminatzemente (*Secar 51* und *Secar 71*) in Anwesenheit (rot) und Abwesenheit (schwarz) von Alginat (*XEA 5036*) bei 40 °C im isothermen Wärmeflusskalorimeter.

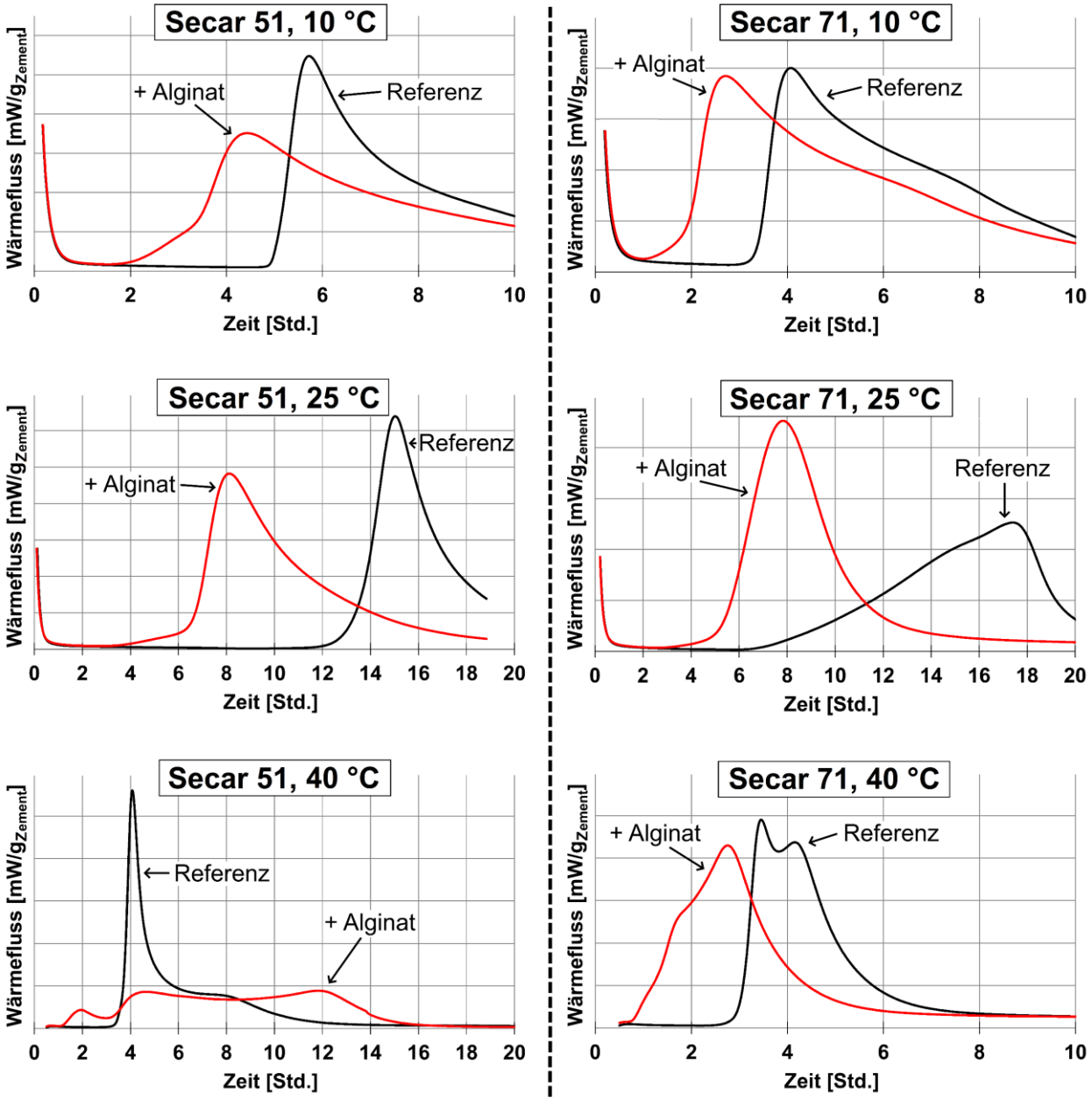

Abbildung A12: Abbindeprofile zweier Aluminatzemente (*Secar 51* und *Secar 71*) in Anwesenheit (rot) und Abwesenheit (schwarz) von Alginat (*XEA 5036*) bei verschiedenen Temperaturen (10, 25 und 40 °C) im isothermen Wärmeflusskalorimeter.

Die in Abhängigkeit von der Reaktionstemperatur gebildeten Hydratphasen wurden mittels XRD für den Aluminatzement *„Secar 71“* bestimmt (siehe **Abbildung A13**). Dieser zeigte bis 20 °C eine ausgeprägte CAH_{10}-Bildung, welche ab 20 °C durch die anfängliche Bildung von C_2AH_8 abgelöst wurde. C_2AH_8 ist neben C_3AH_6 bei 40 °C die dominante Phase, wobei bei höheren Reaktionstemperaturen (70 °C) erwartungsgemäß ausschließlich Katoit gebildet wird.

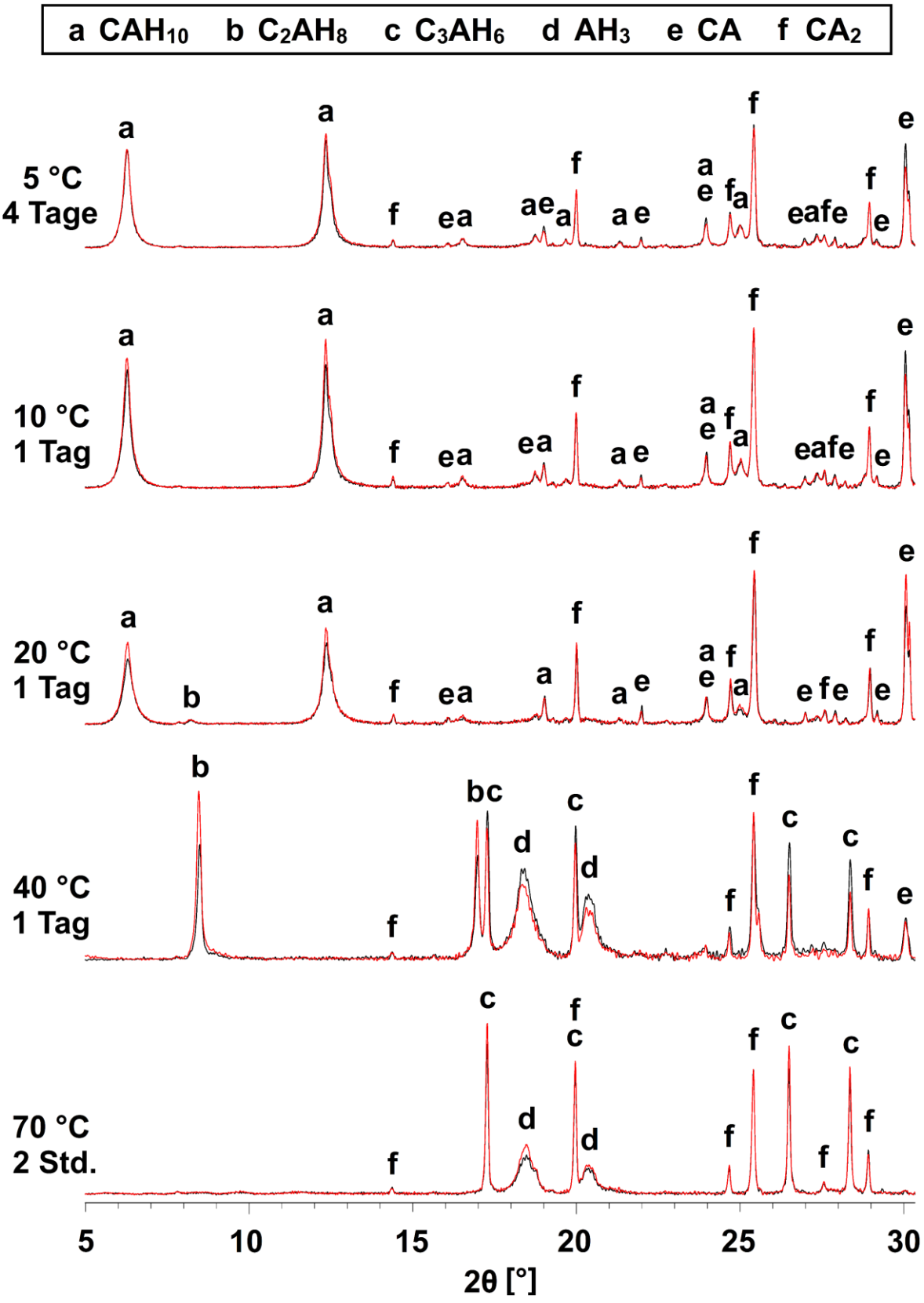

Abbildung A13: Röntgenpulverdiffraktogramme von „*Secar 71*“ ohne Zusatzmittel (schwarz) und mit Alginat „*XEA 5036*“ (rot) beschleunigt; hydratisiert bei unterschiedlichen Temperaturen.

7.4 XRD-Analyse der C-A-H-Alginat-Oberfläche

Die ursprünglich für die REM-Untersuchung entwickelte Probenpräparationsmethode wurde analog eingesetzt, um eine größere Materialprobe zu erhalten (siehe **Abbildung 24** in Kapitel 2.4.4) und diese mittels XRD charakterisiert. Hierbei zeigte die mittels Gefriertrocknung erhaltene Alginat-Probe nach Kontakt mit der Zementporenlösung in der Röntgenbeugung Reflexe (siehe **Abbildung A14**), die für ein getrocknetes Ca-Alginat-Hydrogel bzw. den Probenträger (Referenz) nicht zu beobachten waren. Diese können C-A-H-Phasen mit LDH-Struktur zugeordnet werden und kristallisieren, wie mittels REM gezeigt wurde, an der Polymeroberfläche. Die in diesem Diffraktogramm gefundenen Phasen C_2AH_5 und C_2AH_4, bei welchen es sich um dehydratisierte Formen des C_2AH_8/$C_2AH_{7,5}$ handelt [61,66], waren in einer erneuten Messung derselben Probe nach 4 Wochen Luftkontakt nicht mehr detektierbar.

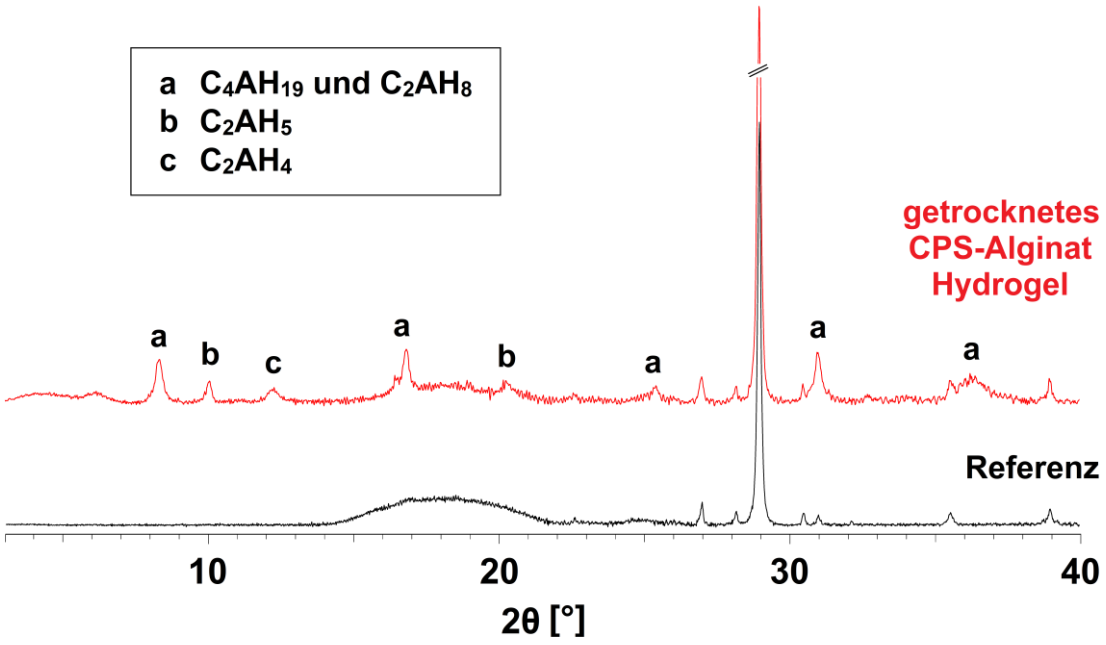

Abbildung A14: XRDs der Alginat-Oberfläche (*XEA 5036*) nach Kontakt mit Zementporenlösung und anschließender Gefriertrocknung.

7.5 Weitere REM-Aufnahmen zur C-A-H-Kristallisation

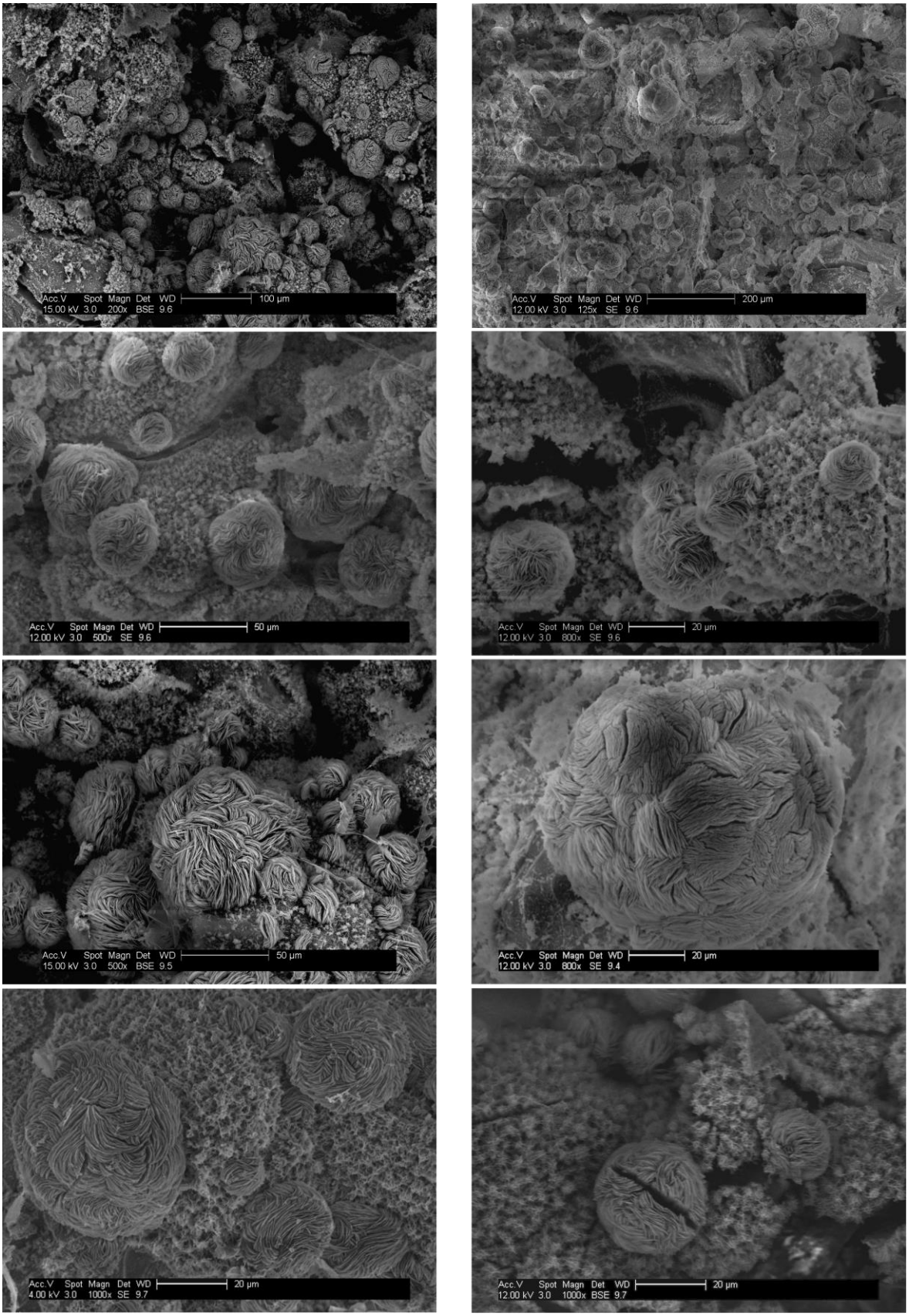

Abbildung A15: REM-Aufnahmen von Alginat, fixiert als Pulver auf dem Probenhalter nach 4-stündigem Kontakt mit Zementporenlösung.

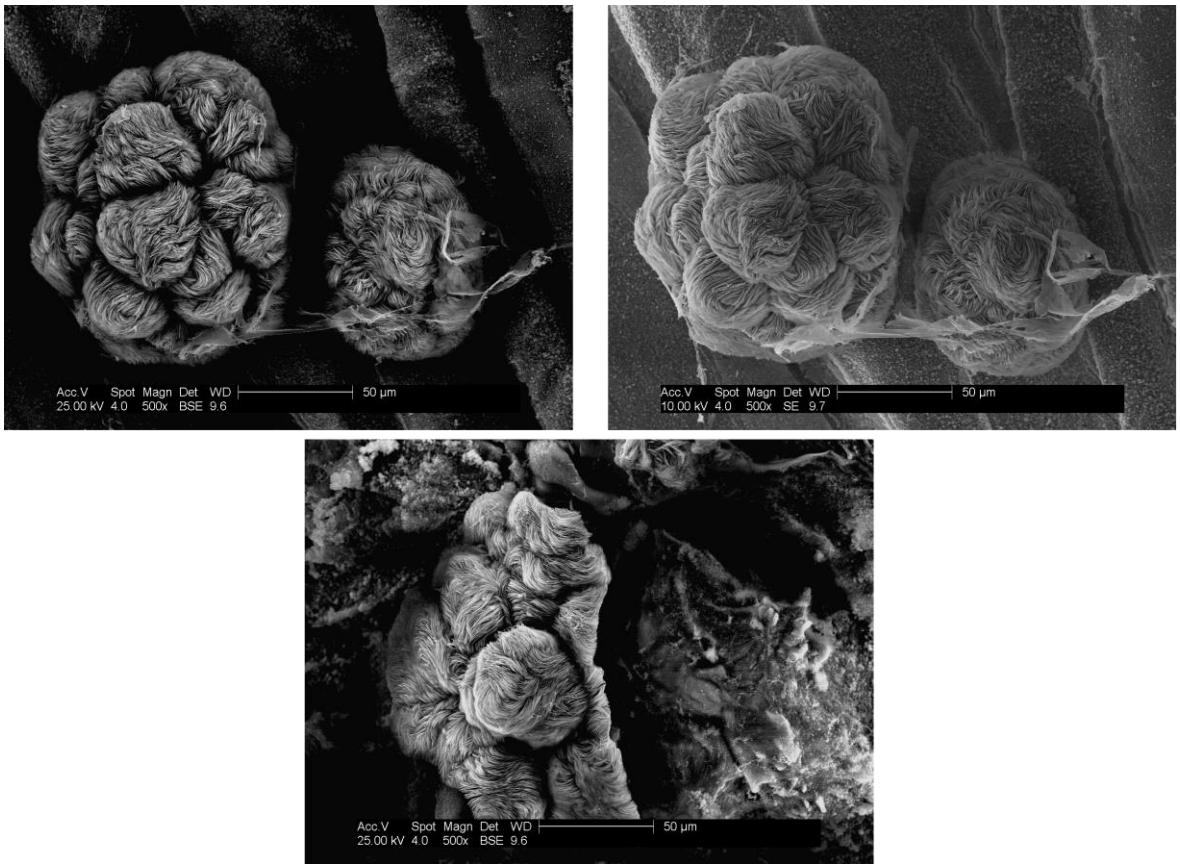

Abbildung A16: REM-Aufnahmen von Alginat, fixiert als Pulver auf dem Probenhalter nach 3-stündigem Kontakt mit Zementporenlösung.

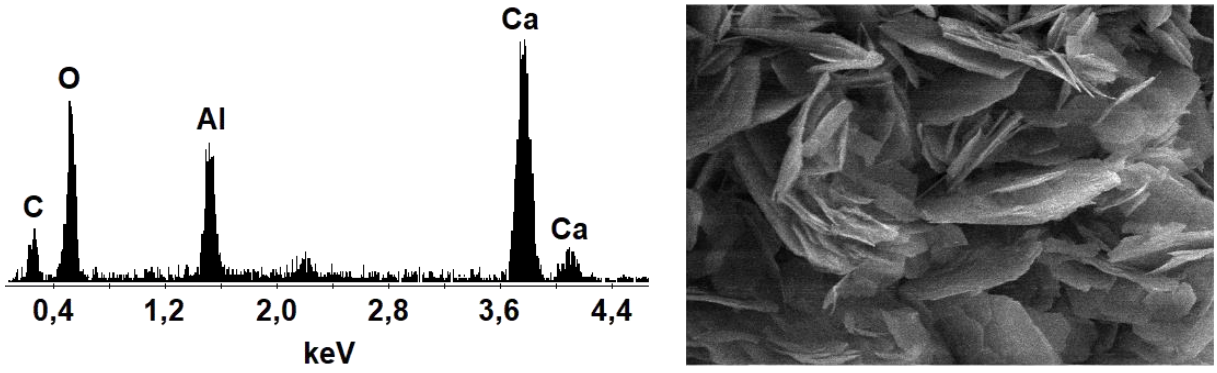

Abbildung A17: EDX-Untersuchung der Elementzusammensetzung (links) von gebildeten C-A-H-Phasen (rechts) auf der Oberfläche von Alginat, welches nach Mischen mit Zementporenlösung präzipitiert ist.

EDX-Untersuchungen (**Abbildung A17**) wurden an einer Probe von C-A-H-Phasen, welche durch den Kontakt einer Alginat-Lösung mit Zementporenlösung gebildet wurden und anschließend präzipitierten, durchgeführt und ergaben ein Ca/Al-Verhältnis von 1,25 ± 0,55. Hierbei ist anzumerken, dass verlässliche Ergebnisse nur schwer zu erhalten waren, da der Probenuntergrund störend wirkte. Der verwendete REM-Probenträger aus

Aluminium und das Ca-Alginat-Hydrogel unter den C-A-H-Phasen verfälschen hierbei das Messergebnis.

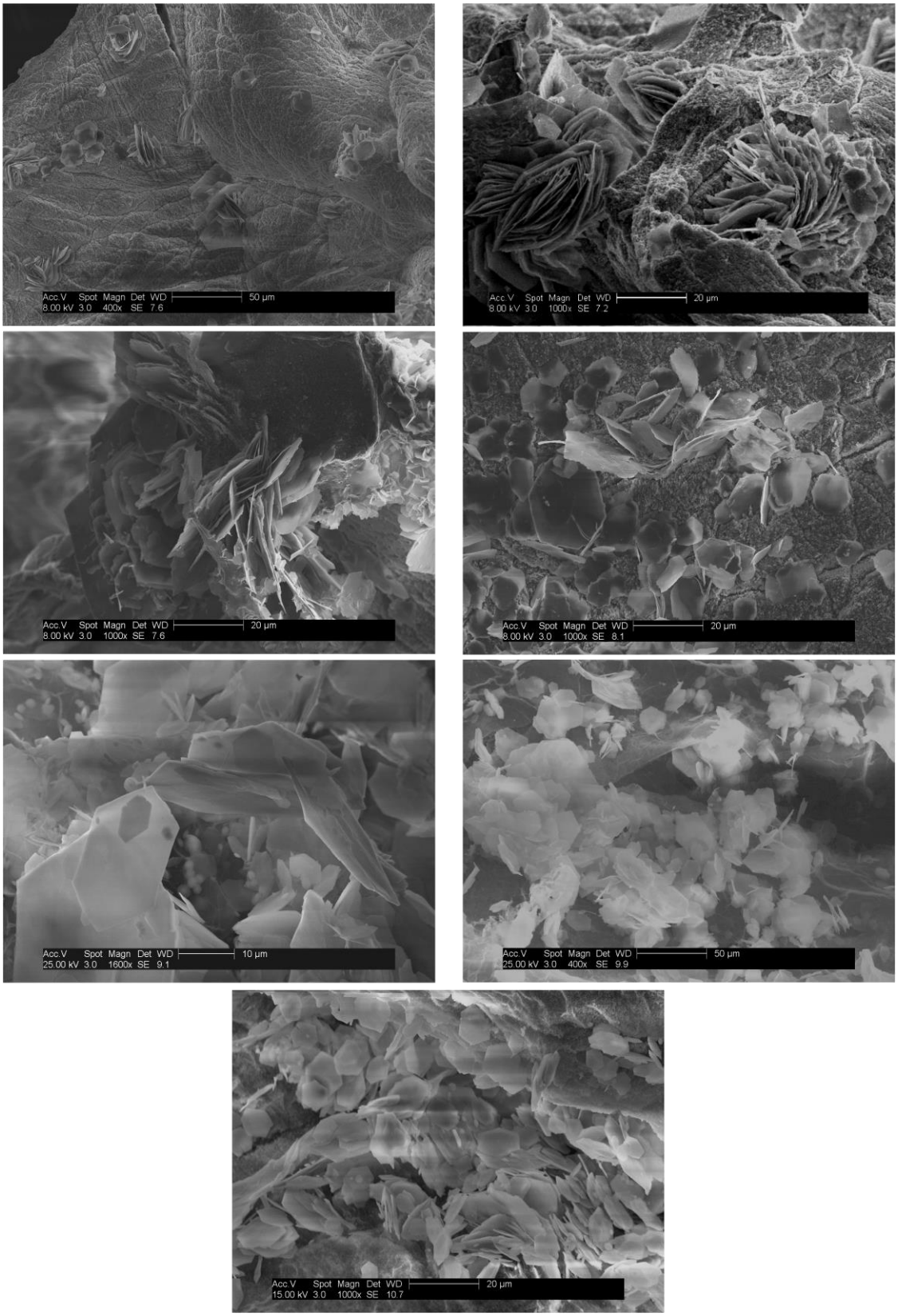

Abbildung A18: REM-Aufnahmen von der Oberfläche einer Alginat-Probe, welche nach Mischen (flüssig/flüssig) mit Zementporenlösung präzipitiert ist.

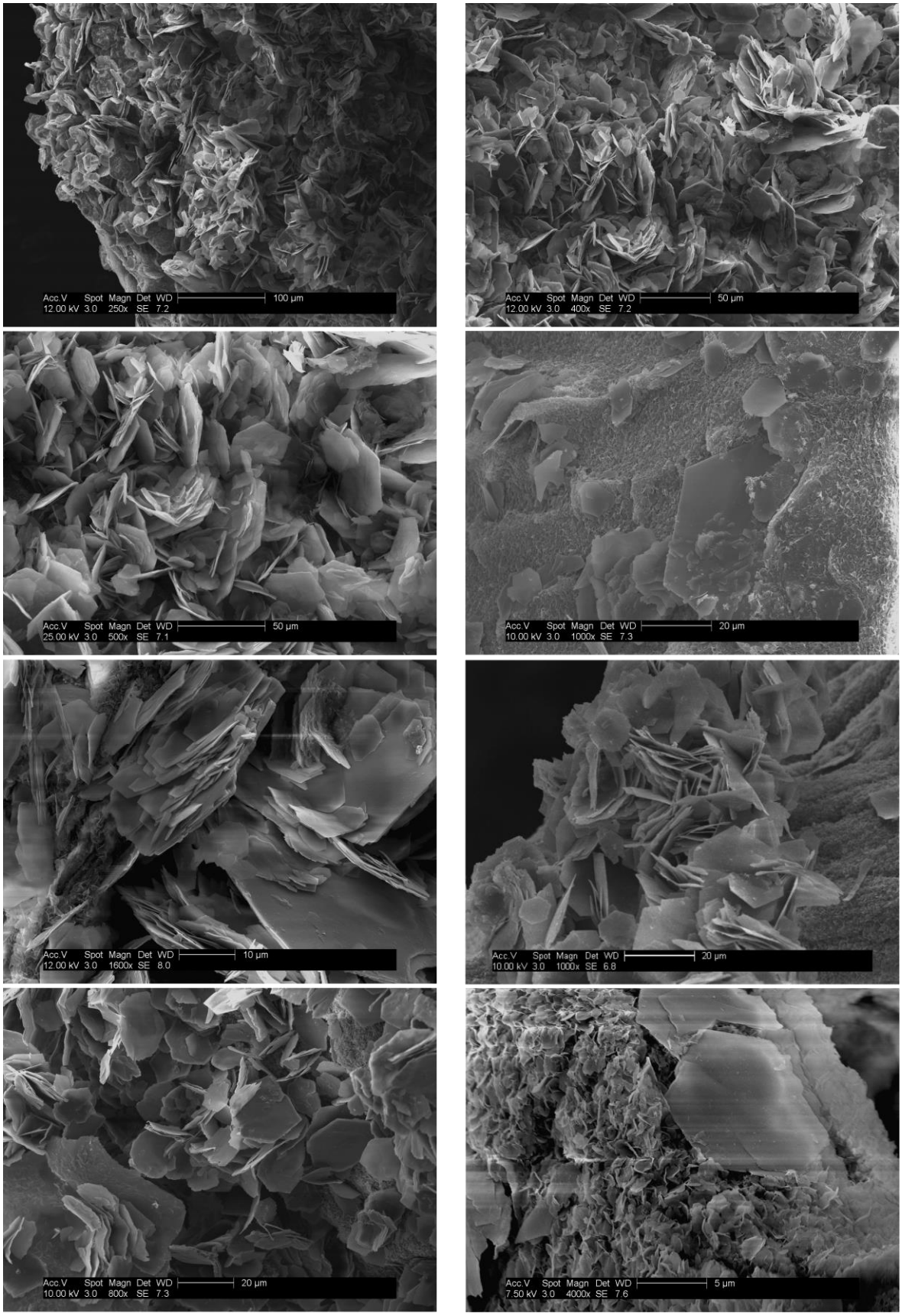

Abbildung A19: Weitere REM-Aufnahmen von der Oberfläche einer Alginat-Probe, welche nach Mischen (flüssig/flüssig) mit Zementporenlösung präzipitiert ist.

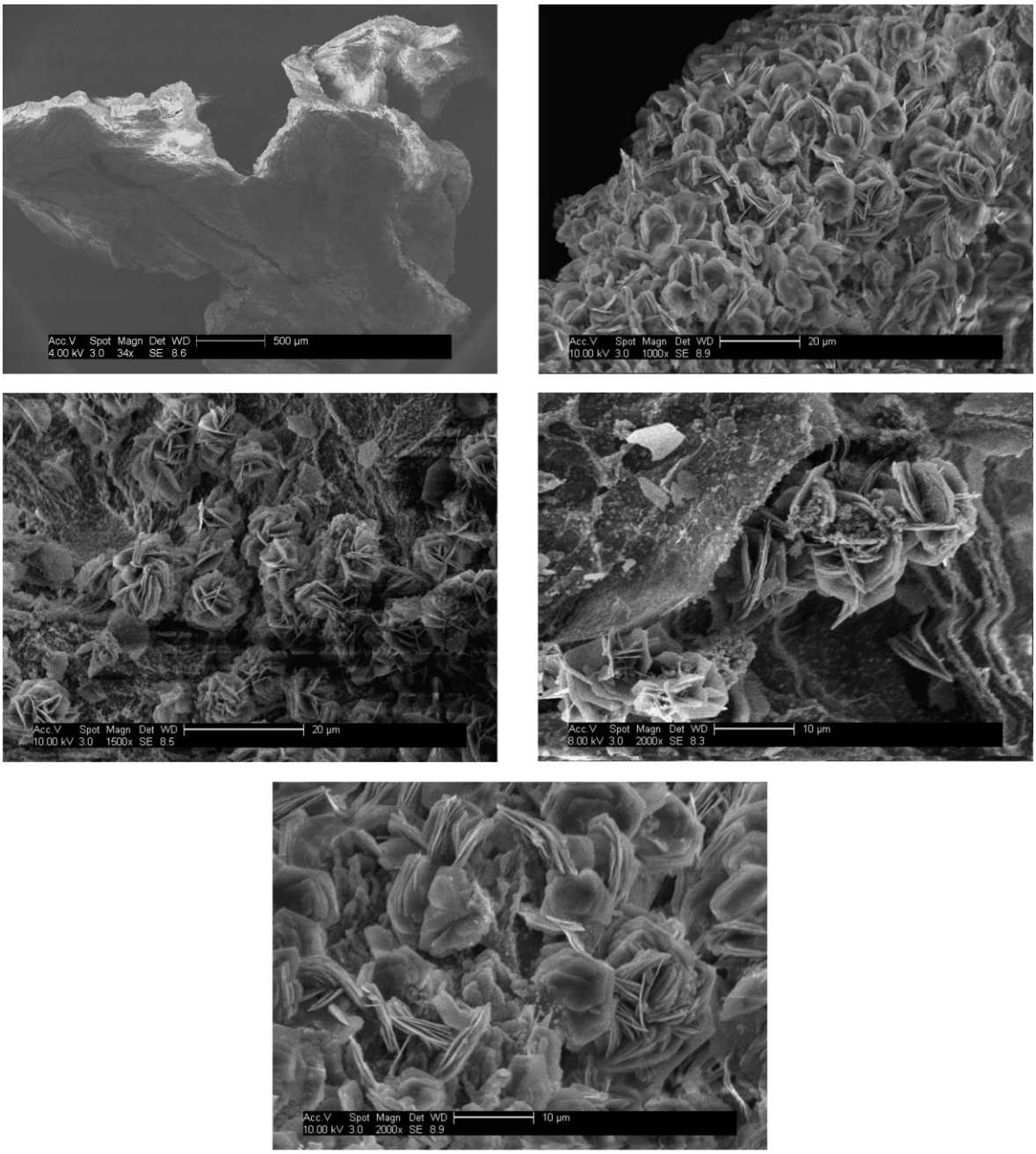

Abbildung A20: REM-Aufnahmen eines Ca-Alginat-Hydrogel-Fragments (wie es exemplarisch in **Abbildung 12** dargestellt ist), welches für 3 Stunden in Zementporenlösung gelagert wurde.

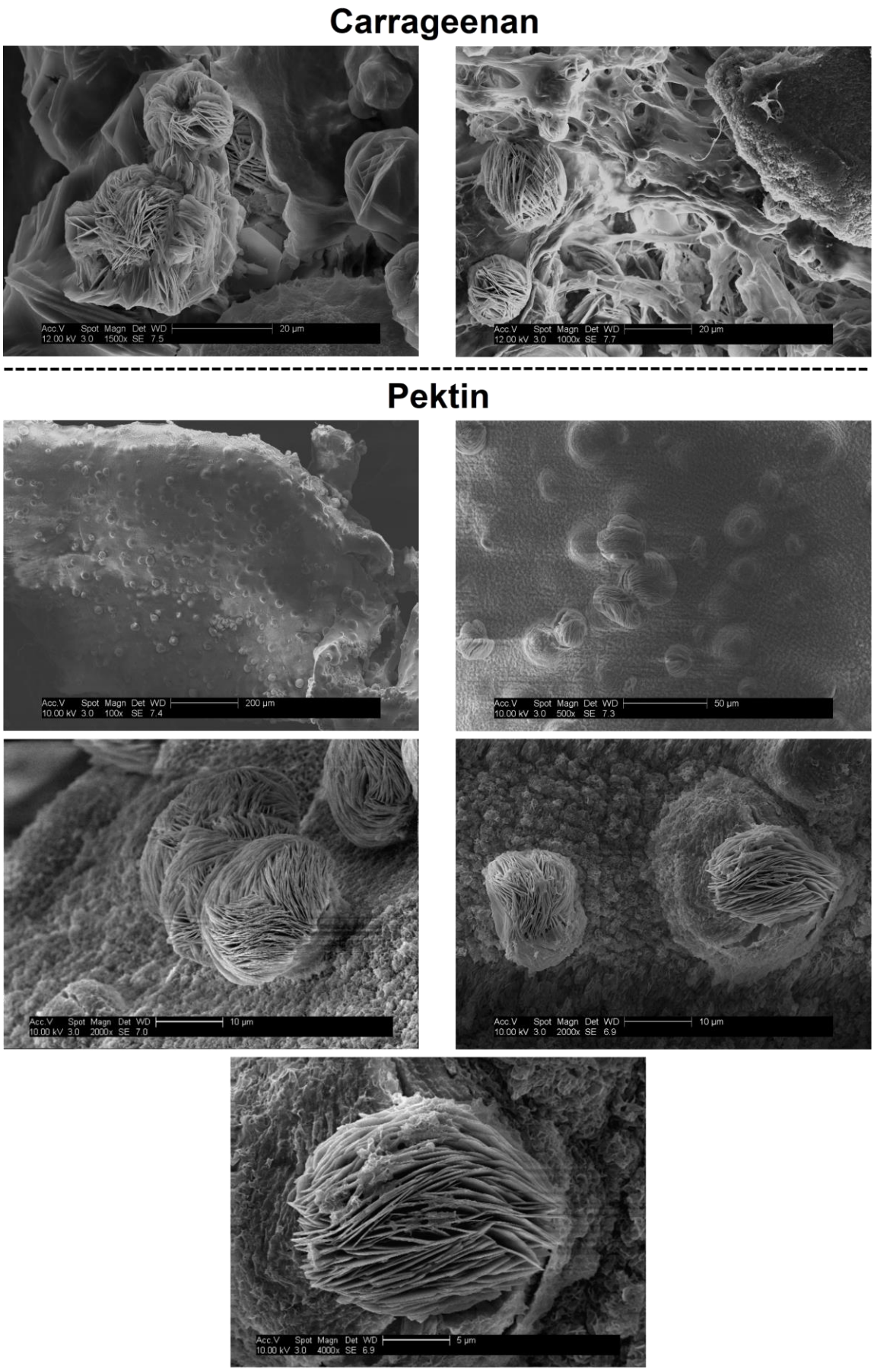

Abbildung A21: REM-Aufnahmen von Carrageen (oben) und Pektin (unten), welche nach Mischen (flüssig/flüssig) mit Zementporenlösung präzipitiert sind.

7.6 Konferenzbeiträge

Veröffentlichungen in Tagungsbänden
mit peer-review Verfahren

The unusual behaviour of specific biopolymers as accelerator in alumina cement

Alexander Engbert[a], Johann Plank[b]

Chemistry, Technische Universität München, Munich, Germany

[a]alexander.engbert@bauchemie.ch.tum.de
[b]sekretariat@bauchemie.ch.tum.de

ABSTRACT

Calorimetric studies on intercalation compounds made from different exo-polysaccharides with hydrocalumite (Ca2Al-OH-LDH) surprisingly resulted in alginate accelerating the hydration of calcium alumina cement (CAC). The following study of several commercial alginates and further polysaccharides came to the conclusion that most sodium alginates show a comparable accelerating effect. Recently this property could also be found for certain carrageenans. This accelerating action of polysaccharides is very unusual and is distinct in aluminous cements depending on their mineralogical phase composition.

In order to accelerate the setting of CAC salts of Lithium like Li2CO3 are used in ternary binders up-to-date. Lithium ions form on mixing with cement and water a layered double hydroxide compound ([Li2Al4(OH)12](OH)2·3H2O) which is isostructural to C2AH8 and accelerates its crystallization by forming a heterogeneous nucleation substrate. The use of Lithium in construction applications is endangered because of the increasingly problematic availability of supplies which are in demand by the continuous rising requisition for the production of lithium-ion-batteries for smartphones and electric cars.

The accelerating effect of alginates is limited to high-alumina cements and is not present in Portland cement or calcium sulfoaluminate cements.

Mechanistic studies revealed a high calcium binding capacity of the alginate in the cement paste. This finding is very astounding as a high calcium binding capacity is normally associated with a retarding effect and not an acceleration. A comparison of the chemical structure of alginate and carrageenan is without a striking joint feature or property on first glance which could help explaining this effect.

1. INTRODUCTION

Calcium aluminate cement (CAC) is used in many applications where ordinary portland cement shows insufficient performance. Especially the high acid and abrasion resistance as well as the quick heat evolution and hardening make CAC the cement of choice in challenging applications. Because of the different oxide composition of CAC (Al_2O_3 content of 35 % - 85 wt.%) and the thus increased sintering temperature (1450 – 1650 °C), its production is more cost intensive. The main hydraulic clinker phases of CAC are: CA, $C_{12}A_7$, CA_2, C_4AF, C_2S. By mass, monocalcium aluminate (CA) presents the most relevant phase in CAC. The hydration of CAC proceeds via dissolution and precipitation from solution. The crystallization of the hydrate phases is strongly dependent on the reaction temperature. In the end, C_3AH_6 (katoite) is formed after months or years from all metastable precursors and remains as the stable hydrate phase. At early ages, CAH_{10} and C_2AH_8 are first crystallized from the supersaturated solution and precipitated on and between the cement particles in the paste. Of them, C_2AH_8 is considered to be the trigger for the setting of CAC. Its formation proceeds either directly (equ. **I**) or through the formation of CAH_{10} (equ. **II**) and subsequent transformation (equ. **III**) to C_2AH_8 [1].

$$2\ CA + 11\ H \rightarrow C_2AH_8 + AH_3 \qquad \textbf{(equ. I)}$$

$$CA + 10\ H \rightarrow CAH_{10} \qquad \textbf{(equ. II)}$$

$$2\ CAH_{10} \rightarrow C_2AH_8 + AH_3 + 9\ H \qquad \textbf{(equ. III)}$$

1.1 Lithium salts as accelerator in CAC

Lithium salts are commonly used to accelerate the setting of CAC. Most frequently Li_2CO_3 (dosed between 0.005 and 0.1 wt.-% depending on application) is applied. It has been presented that lithium ions accelerate the hydration of alumina cement through six pathways: (1) improved dissolution of CA through an increased permeability of the aluminum hydroxo hydrate layer; (2) the thus increased Ca^{2+} / Al^{3+} ratio in solution promotes the formation of C_2AH_8 thermodynamically; (3) formation of $[Li_2Al_4(OH)_{12}](OH)_2 \cdot 3\ H_2O$ LDH as precursor acts as seeding material which decreases the activation energy necessary for the crystallization of C_2AH_8; (4) Li^+ is then continuously exchanged and replaced by Al^{3+} which then; (5) reduces the Al^{3+} concentration in solution and (6) further fosters the dissolution of CA by the lower Al^{3+} content in solution [2].

1.2 Biopolymers

Alginates and carrageenans are biopolymers of natural origin and can be extracted from brown (*Phaeophyceae)* and red algae (*Rhodophyceae)*. Because of different species, growth conditions and processing after harvest, their chemical composition and molecular weight is variable.

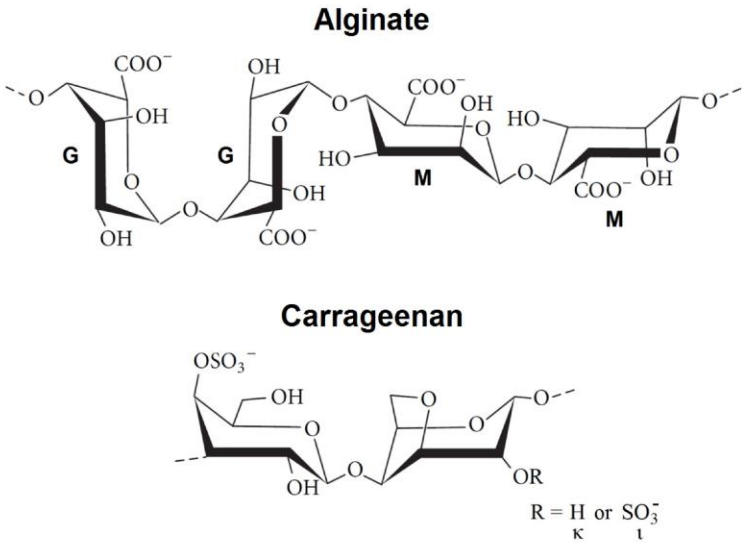

Figure 1. Chemical structures of alginate and carrageenan biopolymers.

15th International Congress on the Chemistry of Cement
Prague, Czech Republic, September 16-20, 2019

1.2.1 Alginates

Alginate is a copolymer of α-1→4 and β-1→4 glycosidically linked mannuronic (M) and guluronic (G) acid (**Figure 1**). Their average molecular weight lies between 10,000 and 600,000 Dalton. The monomer units (M and G) can be linked in different steric arrangements resulting from different tactical sequences. The ratio between M and G as well as the molecular weight (viscosity) determine the properties of alginates. Especially GG blocks exhibit a strong interaction with divalent cations like Ca^{2+} which is represented by the egg-box model and is responsible for the strong gelling properties of alginates (**Figure 2**) [3,4].

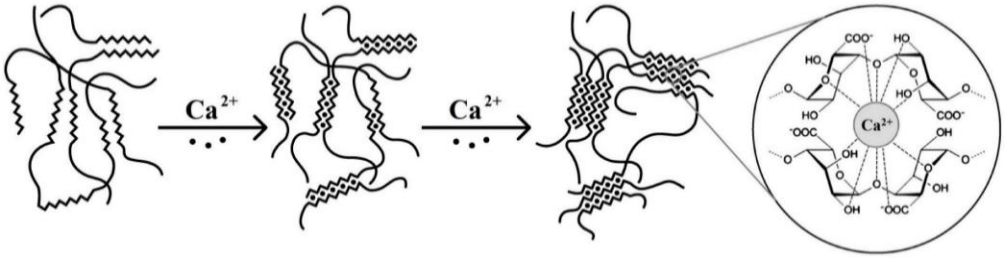

Figure 2. Calcium ion complexation by alginate according to the "egg-box" model (adapted from [5,6]).

1.2.2 Carrageenans

Carrageenans are a mostly alternating copolymers of α-1→4 and β-1→3 glycosidically linked galactose and 3,6-anhydro-galactose (**Figure 1**). Their average molecular weight lies between 200,000 and 800,000 Dalton. Kappa (κ) and iota (ι) carrageenan differ with respect to the degree of sulfatation while the lambda (λ) modification also is structurally different. Similar to alginates, κ- and ι-carrageenan form a gel in the presence of specific cations (e.g. Ca^{2+}) by bridging the sulfate groups (**Figure 3**). λ-carrageenan does not gelate and shows no accelerating effect on cement hydration [3,4].

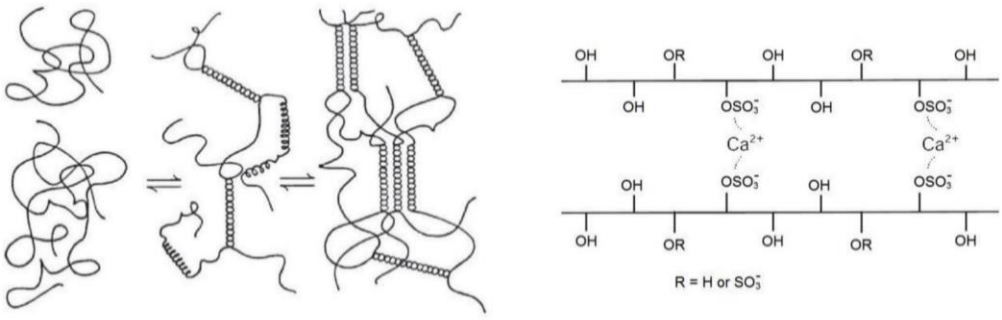

Figure 3. Complexation of calcium ions by κ - and ι – carrageenan (adapted from [4]).

1.3 Aim of this work

In this paper, the effect of different alginate and carrageenan biopolymer samples with respect to hydration acceleration of different alumina cements was investigated via heat flow calorimetry and determination of mortar strength. ICP-OES and in-situ XRD was applied to investigate this effect.

15th International Congress on the Chemistry of Cement
Prague, Czech Republic, September 16-20, 2019

2. EXPERIMENTAL

2.1 Cement Samples

A variety of differently composed calcium aluminate cements (*Ciment Fondu, Secar 41, Secar 51, Secar 71, Secar 712, Secar 80 as well as Ternal SE, Ternal LC and Ternal EP*) produced by *Kerneos* was studied. Their oxide contents were examined using XRF (*Axios*, PANalytical, Kassel, Germany) while their phase composition was investigated via XRD (*D8 advance*, Bruker AXS, Karlsruhe, Germany). The average particle size was determined by laser granulometry (*Cilas 1064*, Cilas Instruments, Orleans, France). Particle size was measured three times after complete dispersion in isopropanol using ultrasonic and the mean value was calculated. The specific surface area was determined according to *Blaine's* method.

Table 1. Oxide composition and properties of alumina cements studied.

Oxide / property	CAC sample (content in wt.%)			
	Ciment Fondu	Secar 51	Secar 71	Secar 712
Al_2O_3	38.2 %	51.5 %	68.9 %	68.3 %
CaO	38.1 %	37.8 %	29.3 %	28.7 %
Fe_2O_3	15.9 %	2.0 %	-	-
SiO_2	4.0 %	5.1 %	0.3 %	1,8 %
TiO_2	2.5 %	2.1 %	-	-
MgO	0.4 %	0.4 %	-	-
Blaine [g/cm³]	2,810	3,880	3,570	3,370
d_{50} [µm]	18.1 ± 0.3	10.1 ± 0.5	12.8 ± 0.2	13.4 ± 0.2

Oxide / property	Secar 41	Secar 80	Ternal SE	Ternal LC	Ternal EP
Al_2O_3	44.3 %	80.9 %	39.4 %	51.2 %	36.5 %
CaO	38.7 %	16.7 %	37.2 %	38.1 %	49.5 %
Fe_2O_3	7.2 %	-	15.9 %	1.8 %	7.1 %
SiO_2	5.2 %	-	4.1 %	5.0 %	4.3 %
TiO_2	2.3 %	-	1.8 %	2.4 %	1.7 %
MgO	0.3 %	-	0.4 %	0.3 %	0.3 %
Blaine [cm²/g]	3,580	10,600	3,650	3,330	3,140
d_{50} [µm]	15.6 ± 0.2	7.4 ± 0.5	11.2 ± 0.2	15.9 ± 0.3	17.1 ± 0.2

2.2 Chemicals

Deionized water obtained from a Barnstead Nanopore Diamond system (Werner Reinstwassersysteme, Leverkusen, Germany) was used as mixing water.
A polycarboxylate (PCE) superplasticizer based on ω-methoxy-poly(ethylene oxide)-methacrylate and methacrylic acid was utilized to reduce the viscosity of the CAC pastes. It was prepared via aqueous free radical copolymerization utilising sodium methallylsulfonate as chain transfer agent and sodium peroxodisulfate as initiator, as described in literature [7]. The molar ratio of the monomers was 6:1 (MAA : Ester), with the side chains made up of 114 ethylene oxide units. The product was analysed using aqueous GPC (Waters Alliance 2695; pre-column PL aquagel-OH; columns ultrahydrogel 120, 250 and 500; Wyatt Dawn EOS dynamic light scattering detector) with 0.1 M $NaNO_3$ (adjusted to pH = 12) as eluent. Molecular properties of the PCE sample are presented in Table 2.

Table 2. Molecular properties and GPC spectrum of the MPEG-PCE sample 114PC6

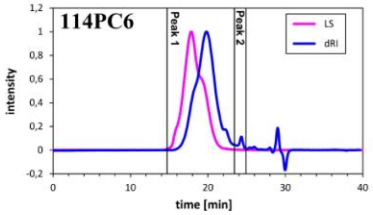

	Peak 1	Peak 2
time of eluation [min]	14.7 - 23.4	23.5 - 24.8
M_w [Da]	87,000 (0.6 %)	4,700 (19 %)
M_n [Da]	28,700 (2 %)	3,100 (22 %)
PDI	3.03 (2 %)	1.51 (29 %)
mass fraction	98 %	2 %

15th International Congress on the Chemistry of Cement
Prague, Czech Republic, September 16-20, 2019

2.3 Biopolymer samples

KIMICA, Eurogum, FMC (through IMCD), Roeper, Cargill, Danisco and Polygal generously supplied over thirty different samples of alginate and carrageenan biopolymers. Those differed by purity, particle size, chemical composition and viscosity grade. In the following work, alginate XEA5036 (alginate #1) and I-1 (alginate #2) as well as carrageenan GP379 (carrageenan #1) and XE4829 (carrageenan #2) were utilized.

2.4 Mortar preparation and testing

Mortar testing was conducted according to DIN EN 196-1 and the strength was determined at different times of hydration using a *ToniNORM* instrument setup (Toni Technik, Berlin, Germany). Measurements were performed on a *ToniNORM powerbox model 2010* equipped with two load frames *model 1543* and *model 1544*. The mortar was composed of 3 parts of norm sand and 1 part of cement which was blended with the biopolymer powder. Using a *ToniMIX* eccentric agitator (Toni Technik, Berlin, Germany), the mortar was automatically mixed with the water containing the superplasticizer as well as one drop of the defoamer *Dowfax DF 141*. The prisms (4 x 4 x 16 cm) were compacted using a *ToniVib* vibrating table (Toni Technik, Berlin, Germany) and stored at 20 °C / 90 % relative humidity until demoulding. Mortar density was calculated using the weight and size of the prisms. For measurement of the tensile strength, three specimens of each sample were used and the mean value calculated. Compressive strength was assessed using the broken specimens from the tensile strength tests. The mean value for the compressive strength was calculated from the results of the six pieces. The spread flow of the mortar was captured according to DIN EN 1015-3. First, the mortar was added in two steps into a Vicat cone and slightly compacted. Each layer was compacted 10 times with a tamping rod. Afterword's, the cone was lifted vertically and the flow table was lifted up 40 mm and then dropped 15 times, causing the mortar to spread out. The resulting spread was measured twice, the second measurement being at a 90° angle to the first and the mean value was reported.

2.5 Heat flow calorimetry

Four gram of cement were weighed into sealable 10 mL glass ampules and blended with biopolymer powder. The binder was mixed with deionised water and homogenised for two minutes with a vortex mixer *VWT 1419* (VWR, Ismaning, Germany). The ampoule was placed in an isothermal heat flow calorimeter *TAM air model 3116-2* (Thermometric, Järfälla, Sweden) to capture the heat flow. Measurements were conducted at 20 °C until heat evolution ceased.

2.6 In-situ X-ray diffraction

Cement paste was poured in the designated sample holder and covered with a *Kapton®* polyimide foil (VHG Labs, Manchester, UK). Measurements were performed every 30 minutes for 12 hours on a *D8 advance* (Bruker AXS, Karlsruhe, Germany) equipped with a *VÅNTEC-1* detector (5 – 50 ° 2θ, 40 kV, 30 mA, 0.034 ° step, t = 0.4 s, *Bragg-Brentano* geometry and Cu Kα source). Because of the heat generated by the x-ray tube, the temperature in the chamber of the XRD rose to about 27 °C during the in-situ measurement. Evaluation and processing of the diffraction patterns was performed using *Bruker's EVA2* software.

2.7 Inductively coupled plasma atomic emission spectroscopy

Concentrations of calcium and aluminum in the pore solution were measured on a *series 700* (Agilent Technologies, Santa Clara, CA, USA). The cement paste was prepared by admixing e.g. 10 g Ciment Fondu blended with 0.1 % bwob alginate in a centrifuge tube and homogenising with a vortex mixer (*VWT 1419* from VWR, Ismaning, Germany) for two minutes. The cement paste was centrifuged (8500 rpm, 15 min) and the pore solution collected using a 0.2 µm PES membrane filter. The resulting solution was diluted accordingly and measured five times. Calibration was performed at 1, 10 and 50 mg/L using an ICP multi-element standard (standard IV, *Merck*) and data collected at several wavelengths.

3. RESULTS AND DISCUSSION

3.1 Effect of biopolymers on CAC hydration

Normally, addition of polysaccharides to Portland or aluminate cements leads to a retardation of their hydration. However, screening of a broad variety of different biopolymers produced two major exceptions for CAC only. This accelerating effect is highly dependent on the structure of the biopolymer. Some exhibit minor acceleration only whereas alginate and carrageenan strongly promote CAC hydration. For example, addition of 0.1 % bwob of XEA 5036 (alginate #1) can reduce the time of maximum heat release by up to 50 % whereas XE4829 (carrageenan #2) reduces the time to maximum heat release only by 15 % (**Table 3, figure 4**).

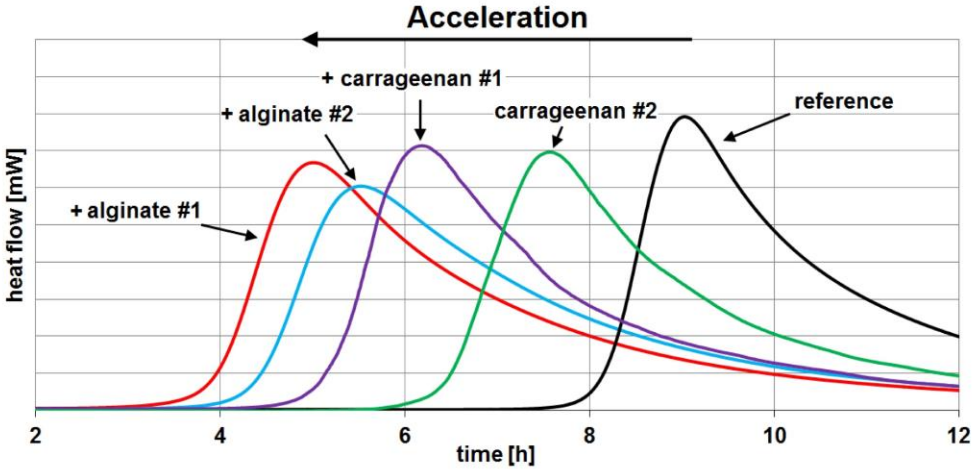

Figure 4. Accelerating effect of various alginate and carrageenan samples (dosage 0.1 % bwob) on CAC (Secar 51), determined via heat-flow calorimetry (w/c = 0.62).

From the samples tested it was observed that at comparable dosage alginates generally accelerate stronger than carrageenans. For example, at a dosage of 0.1 % bwoc alginate in Secar 51 the point of maximal heat release occurred 4 hours earlier then for the reference (**Figure 4**). This corresponds to an acceleration of 45 % (9 h for the reference vs. 5 h with alginate sample #1). The same trend was observed at different water-to-binder ratios, which were varied between 0.4 and 0.6.

Table 3. Accelerating effect of alginate #1 and carrageenan #1 on different CACs, determined via heat flow calorimetry (w/c = 0.62).

CAC sample	Earlier occurrence of heat release upon addition of		
	0.1 % alginate	0.2 % alginate	0.2 % ι-carrageenan
Fondu	≈ 30 %	≈ 25 %	≈ 20 %
Secar 41	≈ 30 %	≈ 20 %	≈ 20 %
Secar 51	≈ 45 %	≈ 50 %	≈ 45 %
Secar 71	≈ 45 %	≈ 50 %	≈ 30 %
Secar 712	≈ 50 %	≈ 55 %	≈ 35 %
Secar 80	≈ 5 %	≈ 15 %	≈ 15 %
Ternal SE	≈ 20 %	≈ 40 %	≈ 40 %
Ternal LC	≈ 50 %	≈ 60 %	≈ 55 %
Ternal EP	≈ 15 %	≈ 25 %	≈ 20 %

15th International Congress on the Chemistry of Cement
Prague, Czech Republic, September 16-20, 2019

Furthermore, alumina cements of different mineralogical compositions were differently effected by the biopolymers (**Table 3**). Some were accelerated very strongly (e.g. Secar 51 or Secar 712) whereas others were only slightly affected (e.g. Secar 80 or Ternal EP). This can be explained by their different clinker phase composition. Cements with an inherent high reactivity from a high content of $C_{12}A_7$ and C_4AF (e.g. Ciment Fondu) are less accelerated by the biopolymers. Whereas cements rich in CA_2 (e.g. Secar 71) which are characterized by a CaO/Al_2O_3 ratio less favourable for the crystallisation of CAC hydrate phases are strongly accelerated by the addition of these biopolymers. An exemption is Secar 80 which is accelerated only weekly. This might be owed to its high *Blaine* value in comparison to those of the other cements.

3.2 Early strength in mortar

To confirm the results from heat flow calorimetry, mortar testing was performed in different CACs using alginate #1 and carrageenan #1. In Ternal LC (≈ 52 % Al_2O_3), an increase in early strength after six hours of hydration of ≈ 75 % at 0.1 % dose of the alginate and of ≈ 150 % at 0.2 % bwob of the carrageenan sample was achieved (**Table 4**). Generally, alginates accelerate CAC hydration more strongly than carrageenan and both biopolymers reduce workability of the cement paste as will be discussed later. In CA_2 rich Secar 712 (≈ 69 % Al_2O_3), after 16 hours the compressive strength of the mortar was increased by 120 % from 15.8 N/mm² (reference) to 34.9 N/mm² for the carrageenan (dosage 0.2 % bwob) and by 110 % to 33.4 N/mm² for the alginate (dosage 0.1 % bwob) (**Table 5**). Moreover, after twelve hours of hydration, Secar 712 still had not developed any measureable strength while the mortar containing alginate or carrageen already exhibited 11.5 N/mm² or 18.7 N/mm² of compressive strength. Such a difference corresponds to an acceleration of about four hours.

Table 4. Mortar properties after 6 h of hydration in absence or presence of alginate sample #1 or carrageenan sample #1 in Ternal LC (w/c = 0.5).

	Ternal LC	+ alginate 0.10%	+ carrageenan 0.20%
compressive strength	9.7 N/mm²	17.2 N/mm² → **75 % increase**	25.0 N/mm² → **160 % increase**
tensile strength	1.4 N/mm²	2.5 N/mm² → **80 % increase**	3.6 N/mm² → **155 % increase**
mortar density	2,321 g/L	2,297 g/L	2,270 g/L
spread flow	24.1 cm	18.8 cm	17.9 cm

Addition of the biopolymers always strongly decreases workability of the pastes, as is indicated by lower spread flow values (**Table 4**). Due to the strong viscosifying effect of both biopolymers, their effective dosage range is limited and often necessitates the use of a (super)plasticizer to compensate their thickening effect.

Table 5. Mortar properties of Secar 712 (w/c = 0.5) after 16 h of hydration in absence or presence of alginate sample #1 and MPEG-PCE sample 114PC6.

	Secar 712	+ PCE 0.02%	+ PCE 0.02% + alginate 0.1%	+ alginate 0.1%
compressive strength	15.8 N/mm²	5.2 N/mm² → **70 % decrease**	36.9 N/mm² → **135 % increase**	33.4 N/mm² → **110 % increase**
tensile strength	2.1 N/mm²	0.8 N/mm² → **65 % decrease**	4.4 N/mm² → **110 % increase**	4.4 N/mm² → **110 % increase**
mortar density	**2,241 g/L**	**2,296 g/L**	**2,287 g/L**	**2,226 g/L**
spread flow	**19.7 cm**	**24.0 cm**	**21.3 cm**	**17.8 cm**

15th International Congress on the Chemistry of Cement
Prague, Czech Republic, September 16-20, 2019

To study potential options to improve the workability of CAC pastes accelerated with these biopolymers, combinations with polycarboxylate superplasticizers were studied. It was found that at only 0.02 % addition an MPEG-PCE (114PC6) can effectively fluidize the CAC paste and compensate the observed loss of workability due to viscosification and water binding by the biopolymer. However, PCE's significantly decrease the early strength after 16 hours of curing. In spite of this negative effect, the combination of alginate and PCE still produced significantly higher strength values, compared to the reference cement (36.9 N/mm² vs. 15.8 N/mm² which corresponds to an increase of 135 %) (**Table 5**).

3.3 Mechanism of acceleration

In the presence of calcium ions the anionic functional groups present in alginates and carrageenans form gels, which are responsible for their thickening effect in cement. Furthermore, this chelation of Ca^{2+} results in a reduction of the free calcium ion concentration by e.g. ≈ 25 % in Ciment Fondu at a dosage of 0.2 % bwob of alginate #1 (**Figure 5**). Complexation of aluminium or iron by the biopolymers is unlikely due to the formation of $[Al(OH)_4]^-$ and $[Fe(OH)_4]^-$ at the high pH in CAC. According to atomic emission spectroscopy, the aluminium concentration increased slightly in the presence of alginate. This can be attributed to an increased solubility of Al^{3+} resulting from the decreased calcium concentration.

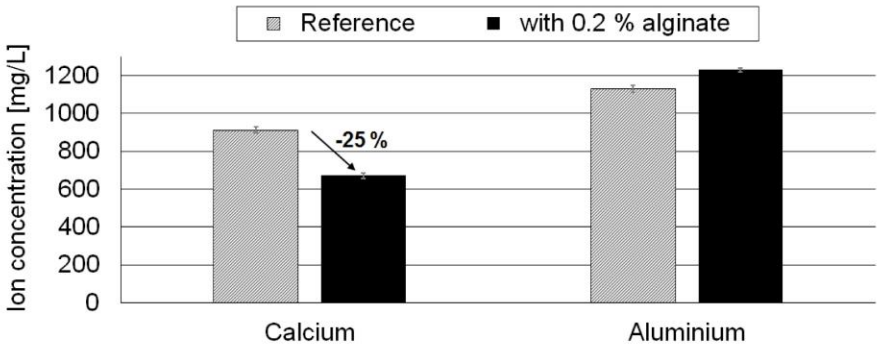

Figure 5. Ion concentrations of Ca^{2+} and Al^{3+} in the pore solution of freshly mixed Ciment Fondu in absence or presence of 0.2 % bwob alginate sample #1 (w/c = 0.5)

Mignon et al. have already reported that in a cement filtrate from OPC, ion exchange of sodium against calcium will occur in alginate. According to these authors, after 24 hours the resulting hydrogel consisted of 85 % calcium und 15 % sodium as counterions to the carboxylic functionalities in alginate [7]. Calcium becomes bound in the hydrogel while being removed from the cement pore solution, thus the decreased calcium concentration in the pore solution. To reduce the free Ca^{2+} ion concentration in pore solution is extremely surprising and uncommon for an accelerator, as such an effect is normally associated with retardation. To the contrary, common accelerators such as $CaCl_2$ increase the free Ca^{2+} concentration in the pore solution and do not decrease it.

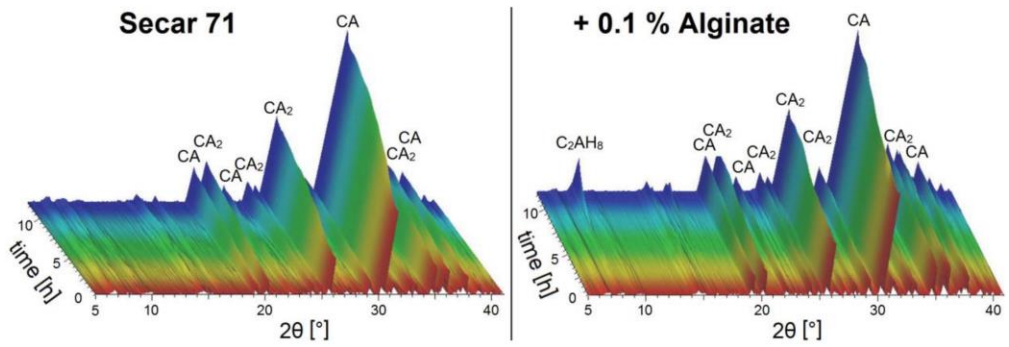

Figure 6. In-situ XRD measurement of the hydration of Secar 71 (w/c = 0.45) over 12 hours in absence or presence of 0.1 % bwob alginate.

15th International Congress on the Chemistry of Cement
Prague, Czech Republic, September 16-20, 2019

In-situ X-ray analysis of CAC hydration in the presence of an alginate progressed normally and no formation of unusual hydration products was observed. However, in the presence of alginate, crystallisation of C_2AH_8 occurs earlier. This effect was most noticed in slowly reacting high-alumina cements, such as Secar 71, where after 12 hours of hydration C_2AH_8 was observed only in the accelerated cement and not yet in the blank cement (**Figures 6**).

4. CONCLUSION

Biopolymers can significantly accelerate the hydration of aluminate cements, as is demonstrated by heat-flow calorimetry and strength tests in mortar. Addition of alginates or carrageenans shifts the beginning of the hydration reaction to earlier times. Because of this, noticeably higher early strength values, especially in the presence of PCE superplasticizers can be obtained. However, in comparison to lithium salts, these biopolymers require a significantly higher dosage and the addition of a superplasticizer to compensate their viscosifying effect. Still, to reduce the consumption of lithium in construction, a combined application of lithium salts and these biopolymers remains an interesting option.
Normally, biopolymers and especially polysaccharides retard cement hydration. As such, the accelerating properties of the studied biopolymers are most remarkable.
Regarding their chemical structures, alginates and carrageenans exhibit a common structural element, which allows efficient complexation of cations (**Figure 7**). Apparently, this ability to complex ions such as Ca^{2+} appears to be crucial for their accelerating effect, as was evidenced by a decrease in the free calcium ion concentration of the pore solution. On the other hand, the increased Al concentration as a consequence of the decreased Ca^{2+} content stimulates the earlier formation of CAH phases.

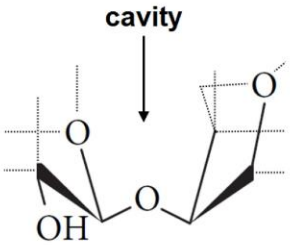

Figure 7: Joint structural element in alginate and carrageenan (common structural bonds marked by drawn lines, bonds specific for each biopolymer signified as dashed lines).

5. ACKNOWLEDGEMENTS

The authors are most grateful to Kerneos (now Imerys) for the generous supply of aluminate cement samples. Especially acknowledged is the support from Dipl.-Ing. Andreas Eisenreich and Dr. Rüdiger Kwasny-Echterhagen. Our thanks also go to KIMICA, Eurogum, FMC, Roeper, Cargill, Danisco and Polygal for providing different biopolymer samples for this study.

6. REFERENCES

[1] Barnes, P., Bensted, J. (2014). Structure and performance of cements. CRC Press.
[2] Götz-Neunhoeffer, F. (2005). *Kinetics of the hydration of calcium aluminate cement with additives*. ZKG international, 58(4), p. 65-72.
[3] Plank, J. (2005). *Applications of biopolymers in construction engineering*. Biopolymers Vol. 10. General Aspects and Special Applications. Wiley-VCH
[4] Imeson, A. (Ed.). (2011). *Food stabilisers, thickeners and gelling agents*. John Wiley & Sons.
[5] Stolarz, R. (2003). *Product brochure – alginates*. FMC Biopolymers.
[6] Pistone, S., Qoragllu, D., Smistad, G., Hiorth, M. (2015). *Formulation and preparation of stable cross-linked alginate–zinc nanoparticles in the presence of a monovalent salt*. Soft matter, *11*(28), p. 5765-5774.
[7] Plank, J., Pöllmann, K., Zouaoui, N., Andres, P. R., Schaefer, C. (2008). Synthesis and performance of methacrylic ester based polycarboxylate superplasticizers possessing hydroxy terminated poly (ethylene glycol) side chains. *Cement and Concrete Research*, *38*(10), 1210-1216.
[8] Mignon, A., et al. (2016). *Alginate biopolymers: Counteracting the impact of superabsorbent polymers on mortar strength*, Construction and Building Materials, 110, p. 169-174.

SPECIFIC BIOPOLYMERS AS ACCELERATOR FOR ALUMINA CEMENT

A. ENGBERT and J. PLANK*
Chair for Construction Chemistry, Technische Universität München
Lichtenbergstr. 4, 85747 Garching, Germany
sekretariat@bauchemie.ch.tum.de

SUMMARY: Investigations on intercalation compounds made from different exo-polysaccharides with hydrocalumite (Ca_2Al-OH-LDH) resulted in a surprising observation. Alginates (a biopolymer extracted from brown algae) accelerate the hydration of calcium alumina cement (CAC). This accelerating effect is limited to high-alumina cements and is not present in Portland cement or calcium sulfoaluminate cements. The following study of several commercial alginates came to the conclusion that most sodium alginates show a comparable acceleration. Recently this property could also be found in additional polymers. This accelerating effect of polysaccharides is very unusual and is distinct in aluminous cements depending on their mineralogical phase composition. Mechanistic studies on the accelerating effect of alginates revealed a high calcium binding capacity of the biopolymer in the cement paste. This finding is very astounding as a high calcium binding capacity is normally associated with a retarding effect and not an acceleration. But still an acceleration can be observed using heat-flow calorimetry and mortar testing. Accordingly the degree of hydration (investigated using ^{27}Al-MAS-NMR) started to increase earlier, thus indicating a shortening of the dormant period.
Keywords: accelerator, alginate, biopolymer, calcium aluminate cement, hydration.

INTRODUCTION

The most efficient way to accelerate the hydration of calcium alumina cements and ternary binder systems is the addition of a lithium salt. Most frequently used is Li_2CO_3 which is dosed between 0.005 and 0.1 wt.-%, depending on the specific application and the binder system. When lithium ions are present, the hydration of the aluminate phases is accelerated through six pathways. This leads to a potent effect in pure aluminate cement that is also strong in the presence of $C\bar{S}H$. Those six pathways are: (1) improved dissolution of CA through an increased permeability of the aluminum hydroxo hydrate layer; (2) the thus increased CaO/Al_2O_3 ratio in solution thermodynamically promotes the formation of C_2AH_8; (3) formation of $[Li_2Al_4(OH)_{12}](OH)_2 \cdot 3\ H_2O$ LDH as precursor decreases the activation energy necessary for the crystallization of C_2AH_8; (4) Li^+ is catalytically recycled by Al^{3+} fixation; (5) the LiAl-LDH reduces the Al^{3+} concentration in solution and (6) dissolution of CA is increased by a lower Al^{3+} content in solution [1].

Calcium Aluminates: Proceedings of International Conference, Cambridge, England. 1 –3 June 2020. Fentiman CH, Mangabhai RJ and Scrivener KL (Editors).

However, the availability of lithium salts in the construction industry is becoming increasingly problematic because of the high demand for lithium ion batteries. The growing market for mobile phones and electric cars will in the future negatively affect the price and the supply security for lithium to the construction industry.

While performing a study on the intercalation of exopolysaccharides into layered double hydroxide (LDH) compounds, an unusual behaviour was observed for alginates when tracking the hydration of alumina cement via heat flow calorimetry. An in-depth investigation concluded that alginates act as accelerator for CAC by prematurely triggering its hydration. This effect was very surprising, because so far polysaccharides were only known to retard cement hydration. Following this discovery, research on the interaction of the alginates with cement and their accelerating mechanism was intensified. When screening a broad variety of biopolymers, such an accelerating effect was also discovered for carrageenan and propylene glycol alginate.

Alginates are composed of mannuronic (M) and guluronic (G) acid that are linked α-1→4 and β-1→4 into a polymer with a molecular weight between 10.000 and 600.000 Dalton (Figure 1). The sugar monomers (M and G) can be linked in different sequences like MM, GM and GG which results in different steric arrangements. The ratio between those blocks is mostly responsible for the properties of the polymer. The GG blocks are important for the strong gelling properties of alginate in the presence of divalent cations like Ca^{2+}. Because of its characteristic appearance, this complexation mode with Ca^{2+} is named "egg-box" model (Figure 2) [2,3].

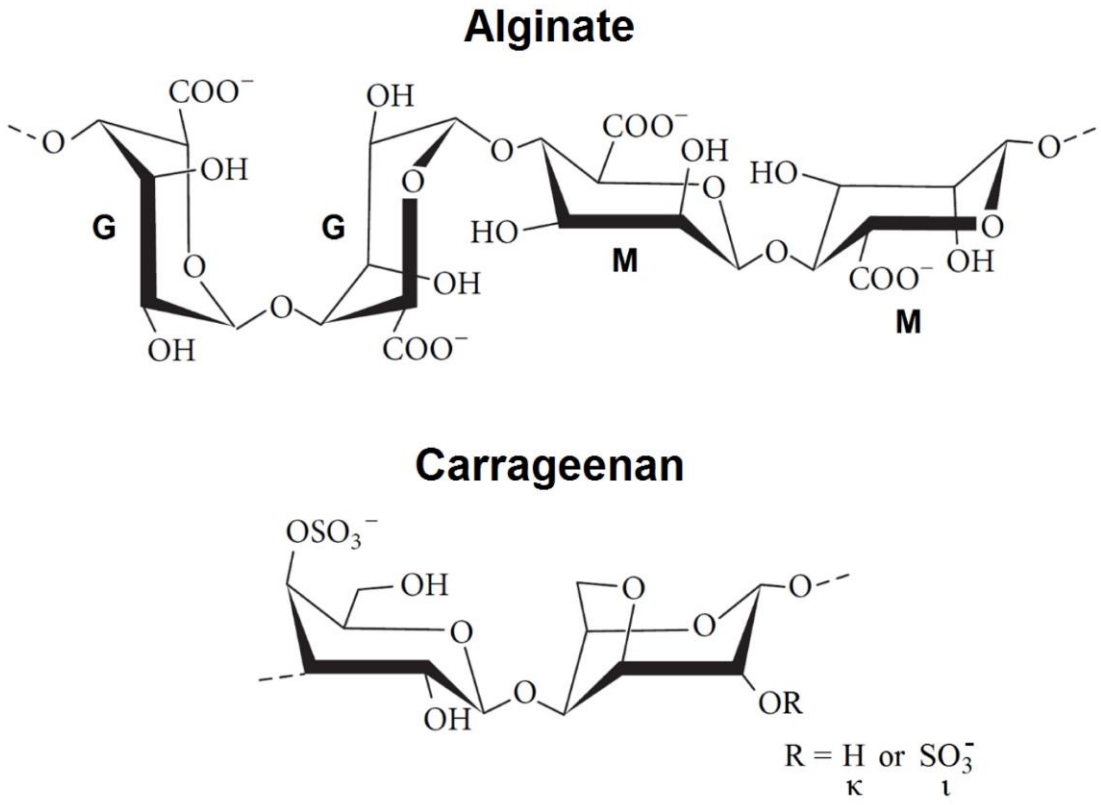

Figure 1: *Chemical structures of alginate and carrageenan.*

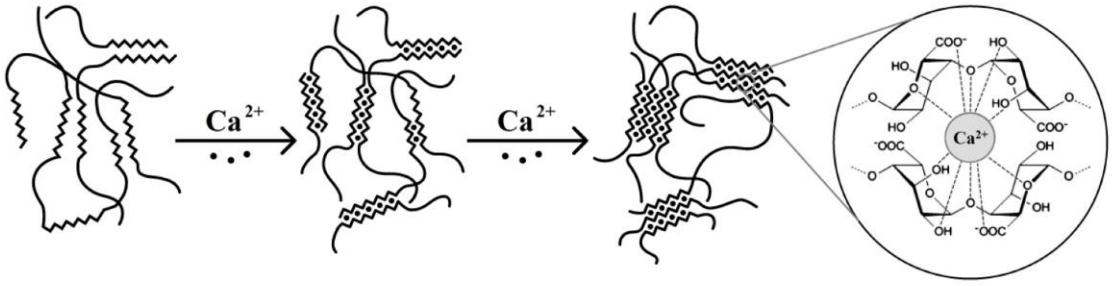

Figure 2: *Complexation of calcium ions by alginate according to the "egg-box" model resulting in gel formation* [4].

Carrageenans are generally composed of galactose and 3,6-anhydrogalactose which are linked α-1→4 and β-1→3 into a polymer with a molecular weight between 200.000 and 800.000 Dalton (Figure 1). Kappa (κ) and iota (ι) carrageenan differ by the degree of sulfatation while the lambda (λ) modification is structurally different and shows a different behavior in solution as well as relative to interaction with ions. Similar to alginates, κ- and ι-carrageenan form a gel in the presence of specific cations by bridging the sulfate groups (Figure 3) [2,3]. λ-carrageenan does not form such gels and shows no accelerating effect on cement hydration.

Alginates and carrageenans are biopolymers of natural origin and extracted from brown (alginate) or red (carrageenans) algae. Because of different algae species, growth conditions and processing after harvest, their chemical composition and molecular weight varies.

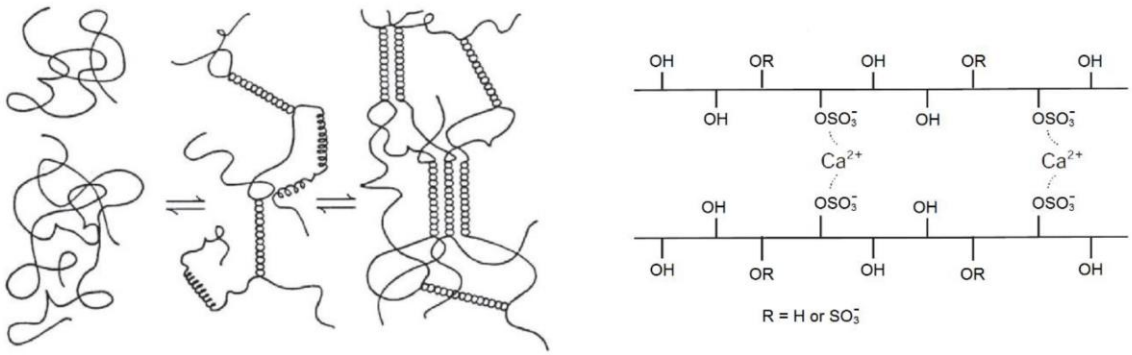

Figure 3: *Complexation of calcium ions by carrageenans leading to gel formation* [2].

The aim of this research was to characterise and understand this unusual property of both biopolymers. In order to probe the effect of diverse natural origin, different alginate as well as carrageenan products from different companies with variable properties were tested. Mechanistic investigations were conducted by studying the pore solution composition (ICP-OES) and the phase development (XRD and MAS-NMR).

EXPERIMENTAL

Polymers

KIMICA, Eurogum, FMC, Roeper, Cargill, Danisco and *Polygal* generously supplied over twenty different alginates. Ten different carrageenans were provided from *Eurogum, Roeper* and *FMC*.

The composition of the alginates (ratio between mannuronic and guluronic acid) was determined via IR spectroscopy. Using commercial samples of known composition, a

correlation between the M/G-ratio and the ratio of the IR absorption at about 1025 cm^{-1} and 1085 cm^{-1} was established [5].

In this study the alginate product *XEA 5036* from *Eurogum* is used exclusively for all investigations. It has a particle size below 80 µm and is of medium viscosity grade (300 – 600 mPa·s, 1 % solution at 20 °C). Its composition is slightly G-rich at a M/G-ratio of about 0.8.

Calcium aluminate cement

Imerys supplied alumina cements of various composition (*Ciment Fondu, Secar 51 and Ternal LC*). Their mineralogical composition was investigated using XRD (*D8 advance*, Bruker AXS, Karlsruhe, Germany).

Table 1. *Typical contents (wt.%) of hydraulic clinker phases in alumina cement samples used in the study, according to literature [6-10] and Rietveld analysis by TUM.*

Phase	CAC sample (wt.%)	
	Ciment Fondu Ternal SE	Secar 51 Ternal LC
CA	47 – 57 *[1,2]	64 - 74 *[1,2,3,4,5]
CA_2	*n.d.*	*n.d.*
C_2AS	1 - 10 *[1]	18 - 22 *[1,3,4,5]
C_4AF	10 - 20 *[1]	*n.d.*
C_2S	1 - 10 *[1]	1 - 5 *[1,3,4,5]
$C_{12}A_7$	1 - 5 *[1,2]	< 1 *[1,3,5]
other	C_3FT, $C_{20}A_{13}M_3S_3$ *[6]	CT, C_3FT *[3,4]

*[1] own analysis; *[2] data from [6]; *[3] data from [7]; *[4] data from [8]; *[5] data from [9]; *[6] data from [10]

Methods of investigation

Infrared spectra of the polymers were measured with an attenuated total reflectance Fourier transform spectrophotometer (ATR-FTIR) (*Vertex 70*, Bruker Optics, Karlsruhe, Germany). It was acquired in transmittance mode on a Diamond ATR crystal cell (*MPV-Pro*, Harrich Scientific Products, Pleasantville, USA) by accumulation of 20 scans with a resolution of 0.5 cm^{-1} and a spectral range of 2000–650 cm^{-1}.

The progress of cement hydration was tracked using isothermal heat flow calorimetry. Four grams of cement were added into sealable 10 mL glass ampules containing the previously placed biopolymer sample. The binder was mixed with deionised water and homogenised with a vortex mixer (*VWT 1419*, VWR, Ismaning, Germany) for two minutes. The ampoule was placed in an isothermal conduction calorimeter (*TAM air*, Thermometric, Järfälla, Sweden) for monitoring the heat flow.

Mortar testing was performed according to DIN EN 196-1 and the strength was determined at different times of hydration using a *ToniNORM* instrument (Toni Technik, Berlin, Germany). The mortar consists of 3 parts of norm sand and 1 part of cement which was blended with the solid biopolymers. Using a *ToniMIX* eccentric agitator (Toni Technik, Berlin, Germany), the mortar was automatically mixed with the water. The prisms (4 x 4 x 16 cm) were compacted using a *ToniVib* vibrating table (Toni Technik, Berlin, Germany) and stored at 20 °C / 90 % relative humidity until demoulding.

Inductively coupled plasma atomic emission spectroscopy was performed on a *series 700* instrument (Agilent Technologies, Santa Clara, CA, USA). The cement paste was prepared by mixing e.g. 10 g Ciment Fondu with water in a centrifuge tube and homogenising with a vortex

mixer *VWT 1419* for two minutes. The cement paste was then centrifuged (8500 rpm, 15 min) and the supernatant pore solution filtrated using a 0.2 µm PES membrane filter.

In-situ XRD was performed by placing the cement paste in the designated sample holder and covering the paste with a *Kapton®* polyimide foil (VHG Labs, Manchester, UK). Diffraction patterns were measured every 30 minutes for 12 hours with a *D8 advance* instrument (Bruker AXS, Karlsruhe, Germany) (5 – 40 ° 2θ, 40 kV, 30 mA, 0,025 ° step, t = 0,6 s). Temperature inside the measurement chamber was ≈ 27.5 °C. Powder diffraction patterns were also measured using the *D8 advance* instrument (5 – 70 ° 2θ, 30 kV, 30 mA, 0.0084 ° step, t = 0.5 s, *Bragg-Brentano* geometry and Cu Kα-source). Evaluation and processing of the diffraction patterns was performed using Bruker's *EVA2* software. Rietveld analysis of cement mineralogy was conducted using *TOPAS 4* software.

Solid-state NMR experiments were performed on an *Advance 300* (Bruker BioSpin, Karlsruhe, Germany) (Magnetic field strength of 7.0455 T, ^{27}Al resonance frequency 78.1 MHz). Samples were prepared ex-situ by admixing in a centrifuge tube or a sealable glass ampule and storage at 20 °C for different amounts of reaction time. Non-hardened samples were quenched with acetone and freeze-dried. Hardened samples were ground in a mortar and measured on time (acquisition time taken into account). Samples were investigated using a 4 mm zirconia rotor and rotated at 15 kHz. The chemical shifts were recorded relative to external standard $Al(NO)_3 \cdot 9\ H_2O$. Single-pulse technique was used with a pulse width of 3 milliseconds. Repetition time was 2 seconds and the number of scans was 1000. Deconvolution and integration of the signals was performed using *MestreNova 12* after phase and background correction.

RESULTS AND DISCUSSION

Effect of biopolymers on cement hydration

Addition of most polysaccharides normally results in retardation of cement hydration. Only few polymers seem to have no retarding effect or lead to a weak acceleration. Such a minor effect is attributed to the stabilizing properties of these water retaining polymers on the cement paste which improves water availability. In contrast to those polymers, alginates and carrageenans strongly accelerate alumina cement. They can reduce the time of maximum heat release by up to 50 % on addition of 0.1 wt.% (Figure 4).

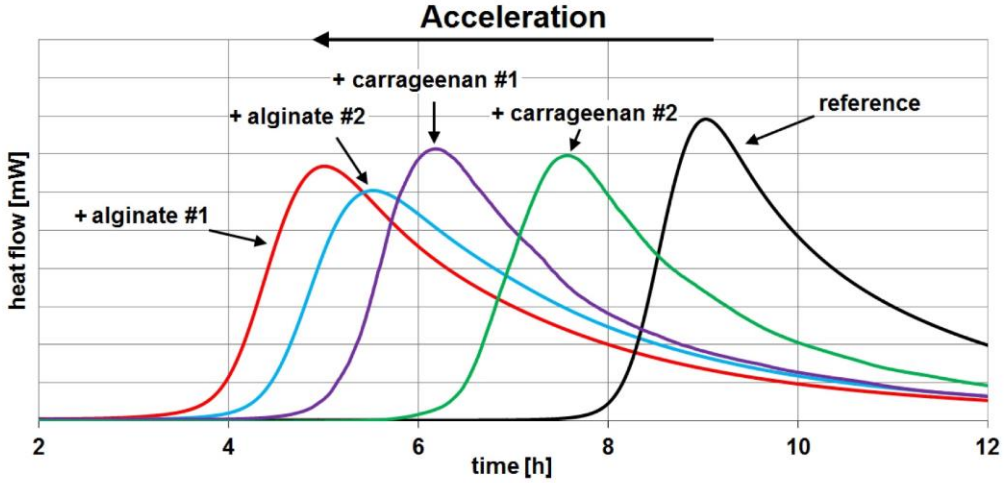

Figure 4: *Accelerating properties of various alginates and carrageenans at a dosage of 0.1 wt.% on CAC (Secar 51), determined by heat-flow calorimetry (w/c = 0.62).*

Generally, alginates were found to accelerate more than carrageenans at equal dosage. This effect of the biopolymers is independent of the w/c-ratio which were varied between 0.4 and 0.6 to exclude an impact of the water binding capacity of the biopolymers on the result.

Influence of molecular properties of the alginate on acceleration

Most sodium alginates showed a similar accelerating property. Different behaviours were observed for samples of insufficient purity, coarse particle size and ultra-low viscosity grade. Especially the viscosity grade of the alginate is most critical for its acceleration. At lower viscosities the acceleration becomes less and even changes to a retardation at ultra-low viscosity grades. Because in alginates viscosity correlates with the molecular weight it can be said that alginates with low M_w act like classical retarding polysaccharides. On the other hand, the ratio between mannuronic and guluronic acid in the alginate was found to be of no significant impact on the accelerating effect. Used products in our study had a M/G-ratio range between 0.4 and 1.6.

Strength development of mortar

In Ternal LC cement (≈ 52 % Al_2O_3) carrageenan achieves a much faster strength development than the alginate when applying an increased dosage (Table 2). Addition of the biopolymers

Table 2. *Mortar properties and strength values after 6h of hydration for Ternal LC (w/c = 0.5).*

Property	Reference	Alginate 0.10%	Carrageenan 0.20%
Compressive strength	9.7 N/mm²	17.2 N/mm² **→ 75 % increase**	25.0 N/mm² **→ 160 % increase**
Tensile strength	1.4 N/mm²	2.3 N/mm² 5 **→ 80 % increase**	3.6 N/mm² **→ 155 % increase**
Mortar density	2,320 g/L	2,300 g/L	2,270 g/L
Spread flow	24.1 cm	18.8 cm	17.9 cm

slightly reduces the fresh mortar density by retaining water and decreases the workability by reducing its flowability resulting from their viscosifying property. Because of the strong gelling properties of alginate the effective dosage range is limited, while carrageenan can be applied in higher dosage relative to alginates. In CA_2 rich Secar 712 (≈ 69 % Al_2O_3) both alginate and carrageenan result in an equally improved early strength. For example, after 16 hours the compressive strength of the mortar was increased by 120 % for carrageenan (dosage 0,2 % bwoc) and by 110 % for alginate (dosage 0.1 % bwoc) from 15.8 N/mm² to 34.9 N/mm² and 33.4 N/mm², respectively. Moreover, after twelve hours Secar 712 still was not hardened while the mortar containing carrageen or alginate already had developed 18.7 N/mm² or 11.5 N/mm² of compressive strength. This value is comparable to that of the neat cement after 16 h which represents an acceleration of four hours.

Interaction of accelerating biopolymers with other admixtures

The use of superplasticizers like PCEs results in a dose-dependent retardation of aluminate cements while flowability even at very low PCE dosages is much enhanced. The combination of PCE with alginate or carrageenan results in a slightly decreased workability, but still a distinct increase in early strength is observed, at improved workability from PCE, compared to the reference (Table 3).

Specific biopolymers as accelerator for alumina cement

Table 3. *Mortar properties and strength values after 16h of hydration for Secar 712 neat, with alginate, with superplasticizer and a combination of both (w/c = 0.5, MPEG-PCE 114PC6).*

Property	Reference	+ Alginate 0.1 %	+ PCE 0.02 % + Alginate 0.1 %	+ PCE 0.02 %
Compressive strength	15.8 N/mm²	33.4 N/mm² → **110 % increase**	36.9 N/mm² → **135 % increase**	5.2 N/mm² → **70 % decrease**
Tensile strength	2.1 N/mm²	4.4 N/mm² → **110 % increase**	4.4 N/mm² → **110 % increase**	0.8 N/mm² → **65 % decrease**
Mortar density	2,240 g/L	2,230 g/L	2,290 g/L	2,300 g/L
spread flow	19.7 cm	17.8 cm	21.3 cm	24.0 cm

If a stronger accelerating effect than from alginate is required, a combination of the lithium salt and the biopolymers was found to allow partial replacement of Li, resulting in reduced consumption of this rare element (Figure 5). However, alginate and lithium do not show a strong synergistic interaction. Up to a certain acceleration the biopolymers can completely replace lithium. However, beyond this point, the effect of lithium dominates the acceleration and the addition of a biopolymer only slightly further increases the acceleration.

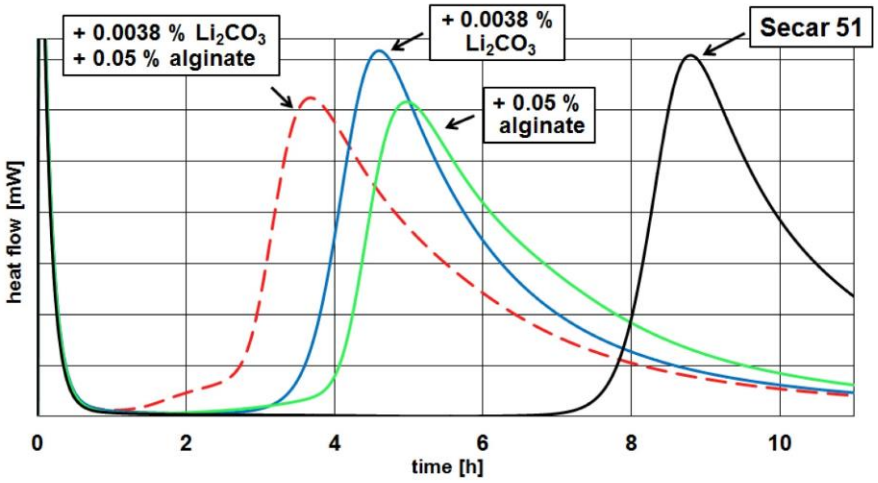

Figure 5. *Accelerating properties of alginate, lithium carbonate and a mixture of both on CAC (Secar 51), as determined by heat-flow calorimetry (w/c = 0.62).*

Interaction of accelerating biopolymers with ions in cement pore solution

As described in the introduction, alginates and carrageenans can interact with cations. Especially calcium ions are strongly complexed by the GG blocks of the alginate. This chemical binding reduces the concentration of Ca^{2+} in the cement pore solution of Ciment Fondu (w/c = 0.5) by 25 % after addition of 0.2 wt.% alginate (Figure 6). Over time a slight reduction in the calcium concentration is observed due to the crystallization of hydrate phases. When setting and hardening occurs resulting from bulk crystallization, then a stronger drop in the calcium concentration was monitored.

A comparison of the concentration evolution over time in cement paste with and without 0.2 % of alginate shows a difference in the slope of the Ca^{2+} concentration reduction. In the presence of alginate the amount of free calcium in solution decreases faster. This implies an earlier formation of CAH phases which is consistent with the earlier hydration and strength development of the CAC.

Theoretically, the complexation of Fe^{3+} or Al^{3+} is also possible, but because of the high pH in cement pore solution those ions will form either $[Al(OH)_4]^-$ or insoluble hydroxides (e.g. $Fe(OH)_3$). As such, an interaction with the negatively charged carboxylate groups is unlikely.

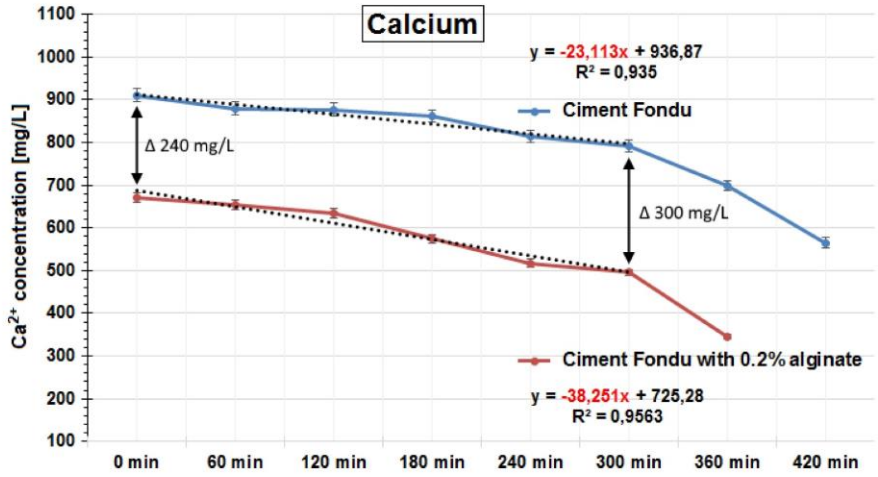

Figure 6. *Time dependent ion concentrations of Ca^{2+} in pore solutions extracted from Ciment Fondu with and without 0.2wt. % alginate at w/c = 0.5.*

Accordingly, the measurement of the aluminium concentration in solution showed a 10 % increased concentration in the presence of 0.2 % alginate (Figure 7). Such increased solubility of aluminate might be explained by the reduced amount of calcium in solution, which in turn increases the solubility of the clinker phases.

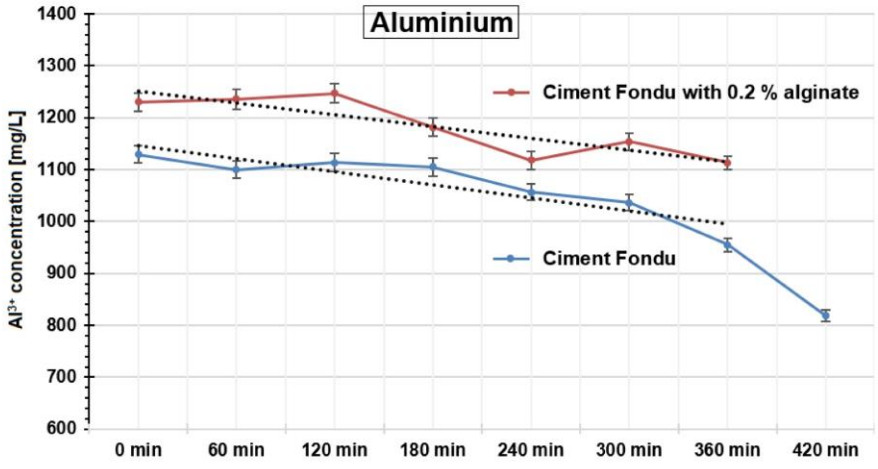

Figure 7. *Time dependent ion concentrations of Al^{3+} in pore solutions extracted from Ciment Fondu with and without 0.2 wt.% alginate at w/c = 0.5.*

The reduction in Ca^{2+} ion concentration is very surprising as this is normally associated with retarded cement hydration. Therefore, the question arose how alginate would behave in combination with known retarders. Here, it would be expected to find an increased retardation as the amount of free calcium would be reduced severely by the combined calcium complexing ability. To investigate, combinations of alginate with Na_3-citrate and KNa-tartrate were tested. When combined with them, alginate still accelerates and is able to not only compensate their retarding effect, but even produce a significant acceleration, inspite of the free calcium concentration in the pore solution being even substantially lower (≈ 40 % of the amount present

in the neat cement paste) than in the presence of the alginate only. Furthermore, the amount of aluminium ions in the pore solution was also reduced upon presence of the retarders in the CAC paste. Therefore should be expected that for the observed free ion concentrations of Ca^{2+} and Al^{3+}, the crystallisation of the CAH phases from the pore solution to be less favourable and result in a retardation. That such a retardation cannot be observed implies an influence of the alginate on the crystallisation of the hydrate phases.

Influence of accelerating biopolymers on phase development

When adding alginate to CAC, the hydration to CAH-phases proceeds as usual without the formation of other hydration products (Figures 8). However, the main hydrate phase C_2AH_8 forms earlier when alginate is present in the in-situ XRD. Because of elevated temperature (≈ 27.5°C) during the in-situ measurement, the hydration time and the hydration product differ compared to normal temperature of 20°C. But still the same accelerating effect on addition of the biopolymer could be observed.

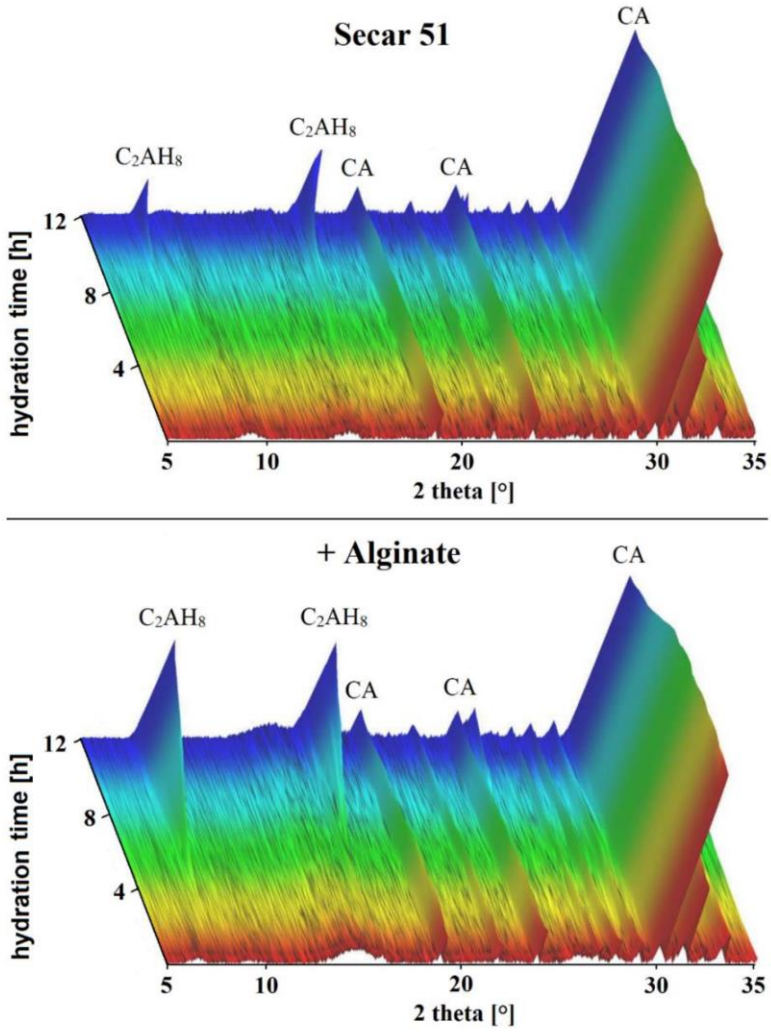

Figure 8: In-situ XRD of Secar 51 (w/c = 0.45) hydrated for 16h with and without alginate (≈ 27.5°C).

A quantitative study of the evolution of the degree of hydration (at 20°C) using solid state NMR spectroscopy accordingly came to the same conclusion. In the presence of alginate the consumption of clinker commenced earlier and subsequently resulted in a premature formation of hydrate phases compared to the reference (Figure 9). From the NMR investigation it can be

concluded that the dormant period of the hydration is shortened significantly upon addition of the biopolymer.

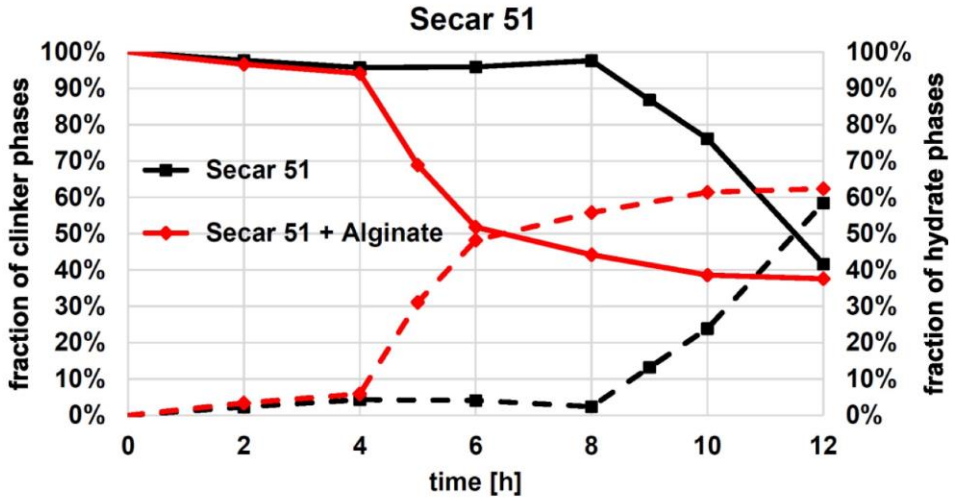

Figure 9. *Amount of clinker (Al-4) or hydrate (Al-6) phase after different reaction times (20 °C), determined using MAS-NMR.*

CONCLUSIONS

Alginate and carrageenan present suitable accelerators for aluminate cement, as proven by heat-flow calorimetry and strength tests of mortar samples. Addition of such biopolymers shifts the beginning of the hydration reaction to earlier times and results in higher early strength. Compared to lithium salts, these biopolymers require significantly higher dosages and addition of a superplasticizer to counteract their viscosifying effect. Combined application with lithium salts is an option to reduce the lithium consumption.

The ability to complex calcium ions seems to be critical for the accelerating effect and is very surprising. The reduction of the free calcium ion concentration in the pore solution is most remarkable, as it normally points to a substance being a retarder. Such retarding effect was only found for low-molecular weight alginates which in cement behave like other conventional polysaccharides. Investigation of the working mechanism of these biopolymers revealed a shortening of the dormant period as could be observed through earlier consumption of clinker as well as an earlier formation of hydrate phases, respectively. We contemplate that the alginate molecule interacts with the crystallization of these specific hydrate phases as no acceleration in different binder systems (CSH or ettringite) could be observed.

REFERENCES

[1] Götz-Neunhoeffer F. *Modelle zur Kinetik der Hydratation von Calciumaluminatzement mit Calciumsulfat aus kristallchemischer und mineralogischer Sicht*, Habilitation, Universitätsverbund Erlangen-Nürnberg, 2006.

[2] Imeson A P. *Food stabilisers, thickeners and gelling agents*, John Wiley & Sons, 2011.

[3] Plank J. *Applications of biopolymers in construction engineering*, in: Biopolymers, Vol. 10, General Aspects and Special Applications, Wiley-VCH, Weinheim, 2003, pp 29-95.

[4] Janetzky P. *Alginate in a glance*, Presentation DuPont / Danisco Deutschland GmbH, 2016.

[5] Sellimi S, Younes I, Ayed H B, Maalej H, Montero V, Rinaudo M, Dahia M, Mechichi

T, Hajji M and Nasri M. *Structural, physicochemical and antioxidant properties of sodium alginate isolated from a Tunisian brown seaweed*, International journal of biological macromolecules, *72*, 2015, pp 1358-1367.

[6] Parr C, Bin L, Alt C and Wohrmeyer C. *Interactions between Silica Fume and CAC and Methods to Optimise Castable Placing Properties*, Technical Paper 52, Kerneos

[7] Puerta-Falla G, Kumar A, Gomez-Zamorano L, Bauchy M, Neithalath N and Sant, G. *The influence of filler type and surface area on the hydration rates of calcium aluminate cement*, Construction and Building Materials, *96*, 2015, pp 657-665.

[8] Bizzozero J, Gosselin C and Scrivener K L. *Expansion mechanisms in calcium aluminate and sulfoaluminate systems with calcium sulfate*, Cement and Concrete Research, *56*, 2014, pp 190-202.

[9] Gosselin C and Scrivener K L. *Microstructure development of calcium aluminate cement accelerated with lithium sulphate*, Conference proceedings: Calcium Aluminate Cement, the Centenary Conference, 2008, pp 109-122.

[10] Touzo B, Gloter A and Scrivener K L. *Mineralogical composition of Fondu revisited*, Conference proceedings: Calcium Aluminate Cement, 2001, pp 129-138.

TOWARDS UNDERSTANDING THE AGEING BEHAVIOUR OF SLU FORMULATIONS: IMPACT OF PREHYDRATION ON INDIVIDUAL COMPONENTS AND THE ROLE OF ADMIXTURES

F. A. HARTMANN, A. ENGBERT and J. PLANK
Chair for Construction Chemistry, Technical University of Munich, Lichtenbergstrasse 4, 85748 Garching, Germany
florian.a.hartmann@tum.de
sekretariat@bauchemie.ch.tum.de

SUMMARY: Based on highly reactive multi-component binder systems, self-levelling underlayments (SLUs) are especially vulnerable to preliminary surface hydration when exposed to humidity and CO_2, in particular at elevated temperature. Such prehydrated SLUs exhibit reduced flowability and workability. Likewise, SLU performance can worsen when individual components suffer prehydration before the formulation is prepared.

The main constituents of a typical SLU ternary binder system are Portland cement (PC), calcium aluminate cement (CAC) and anhydrite. To gain a better understanding of the system's ageing behaviour, the constituents were prehydrated individually at 35 °C and 90 % relative humidity. Interestingly, CAC containing about 40 wt. % Al_2O_3 was found to age/prehydrate considerably less than Portland cement CEM I 52.5 N by measure of weight increase during storage. Anhydrite remained completely unaffected by these conditions.

In subsequent experiments, additives in powder form were mixed with the binders before ageing. The presence of lithium carbonate accelerator increased prehydration of CAC significantly. However, the common SLU retarders tartrate and citrate surprisingly accelerated CAC ageing as well.

To further investigate the impact of prehydration on flowability, a model SLU based on a PC/CAC/anhydrite ternary binder system was formulated with accelerator, retarder and PCE superplasticizer. The reduced flowability found for a prehydrated commercial SLU could be reproduced with this model system. To mitigate flowability reduction, addition of calcium hydroxide was investigated.

The results show that the individual components of a formulation exhibit different ageing behaviour, which is further changed by the presence of admixtures during ageing.

Keywords: Admixture, ageing, cement, clinker phase, prehydration, self-levelling underlayment (SLU), ternary binder system.

Calcium Aluminates: Proceedings of International Conference, Cambridge, England, 1 –3 June 2020. Fentiman CH, Mangabhai RJ and Scrivener KL (Editors).

INTRODUCTION

Self-levelling underlayments (SLUs) are used to obtain smooth surfaces on otherwise uneven foundations before floor coverings can be installed [1,2]. Conventionally, Portland cement (PC) is the basis for a SLU mortar. If rapid hardening is required in application, a ternary binder system of PC, calcium aluminate cement (CAC) and calcium sulphate is employed [3,4].

Upon contact with water, CAC-rich formulations quickly form large amounts of ettringite in the presence of sulphate. The needle-shaped crystal morphology of the ettringite along with its ability to incorporate high quantities of water cause rapid stiffening of the SLU slurry. Furthermore, this water uptake leads to volume expansion which counteracts shrinkage. However, to overcome the CAC's energy barrier for ettringite formation, accelerators are required, the most common of which is lithium carbonate Li_2CO_3. Lithium ions improve the dissolution of the main $CaAl_2O_4$ (CA) clinker phase and form lithium-aluminium layered double hydroxide (LDH) precursors, thereby decreasing the activation energy for aluminate hydrate formation [5].

Furthermore, overly quick stiffening can reduce the workability time of the slurry to such an extent that using a mechanical pump in application is no longer feasible. Therefore, hydration retarders are applied to maintain sufficient workability. Commonly used are α-hydroxycarboxylic acid salts such as tartrate and citrate. To achieve flowability and self-levelling capacity without greatly increasing the water to cement (w/c) ratio, superplasticizers are added. Thus, by design drymixed SLU formulations possess a high reaction potential towards water. While advantageous in application, it makes SLUs susceptible to premature hydration on particle surfaces upon exposure to atmospheric humidity. This "prehydration" occurs when the formulation is aged unintentionally due to insufficient protection against external environmental influences during storage. Moreover, individual components might undergo prehydration even before the SLU is formulated. An example is the milling of cement clinker after firing in the kiln. In this process water is injected into the mill for temperature regulation, resulting in a partially hydrated cement powder. Prehydration of cement can cause deficiencies in strength development as well as unpredictability in setting behaviour and interaction with additives [6, 7].

To get a better understanding of the prehydration mechanisms, we have investigated the water sorption capabilities of Portland cement constituents in earlier works [8,9]. It was discovered that individual clinker phases start to sorb water at different levels of relative humidity. The most hygroscopic clinker phase is orthorhombic (doped) C_3A which sorbs large amounts of water from 55 % RH upwards. It is followed by the silicate phases alite (C_3S) and belite (C_2S) showing a comparatively minor water uptake which starts around 65 % RH. Non-doped, cubic C_3A in turn sorbs a moderate amount of water, but only at a relative humidity of 80 % and higher.

For this reason, in follow-up studies on cements and binder systems humidity levels were increased to 90 % to guarantee that all clinker phases sorb water sufficiently. A SLU model formulation based on a ternary binder system of PC, CAC and fluoroanhydrite with the essential additives as described above was investigated [10,11]. Powder XRD made evident that the high atmospheric humidity was sufficient to trigger the characteristic strong ettringite formation of ternary binder systems within the first 24 hours of prehydration. This led to an increase in the water demand due to the ettringite overgrowth consuming water while also limiting access to the non-prehydrated inner part of the

particles. As a result, producing a free-flowing paste with the aged formulation required doubling the w/c ratio from 0.25 to 0.50.

Still, at w/c = 0.50 the SLU with tartrate showed a 40 % reduction in spread flow after one day of prehydration compared to the paste from the fresh formulation. After three days, this difference even increased to 70 %. Interestingly, prehydration inverted the performance of citrate. Using citrate instead of tartrate in a fresh SLU led to a higher initial spread flow but worse fluidity retention. However, after prehydrating the formulation for three days before adding citrate, initial flowability was nearly zero but increased constantly until reaching a maximum after two hours. Such unpredictable retarder behaviour after prehydration is not unique, we have also reported about varying performances of gluconate and pyrophosphate in PC and clinker phases [12].

Thus, our previous investigations revealed the profound impact of prehydration on binder systems and their constituents. In this work, we aimed to expand on the results obtained so far by taking a closer look at the ageing of the individual components of a ternary binder system, namely PC, CAC and anhydrite. Furthermore, to complement the research on Portland cement clinker, we investigated the ageing of the major aluminate cement clinker phases. Moreover, ageing of a model SLU formulation was investigated and the results were compared with those obtained from a commercial SLU. Finally, the differences between citrate and tartrate used in the formulation were studied.

EXPERIMENTAL PROCEDURES

SLU formulation

The composition of the model SLU formulation used in this study as displayed in Table 1 is based on previous works [10,11]. For the PC component of the ternary binder system a CEM I 52.5 N (Milke®, HeidelbergCement AG, Ennigerloh plant, Germany) which is regularly used in drymix applications was chosen. Ciment Fondu® (Kerneos S.A., Neuilly sur Seine, France) is a common CAC with an Al_2O_3 content of nearly 40 wt. %. Sulphate was provided in the form of fluoroanhydrite (Solvay Fluor, Bad Wimpfen, Germany), which contained a slight fluorite impurity and had a pH of 8.5 in H_2O.

Added to the ternary binder system were lithium carbonate (Chemetall, Frankfurt am Main, Germany), polycarboxylate ether (PCE) superplasticiser (Melflux® 2651 F, BASF, Ludwigshafen, Germany) and either sodium potassium tartrate (Jungbunzlauer, Basel, Switzerland) or sodium citrate (Merck, Darmstadt, Germany). The SLU formulation was prepared by drymixing binders and additives together for two hours using an overhead shaker Reax 20 (Heidolph, Schwabach, Germany).

Table 1. *Composition of simplified model SLU formulation used in this study.*

Constituent	Function	Share [wt. %]
PC (CEM I 52.5 N Milke®)	Binder	47.16
CAC (Ciment Fondu®, 40 % Al_2O_3)	Binder	32.70
$CaSO_4$ (Fluoroanhydrite)	Binder	19.04
Lithium carbonate	Accelerator	0.30
Sodium potassium tartrate tetrahydrate or sodium citrate dihydrate	Retarder	0.40
PCE (Melflux® 2651 F)	Superplasticiser	0.40
Total		100.00

Clinker phases

The aluminate clinker phases C_3A, $C_{12}A_7$, CA and CA_2 were synthesised according to [13] in a chamber furnace (Nabertherm, Lilienthal, Germany). After sintering, the calcium aluminates were ground and sieved to match the particle size of the Ciment Fondu® CAC used in this study (d_{50} = 18 µm). To enable ettringite formation, they were mixed on a 1 : 1 basis (by weight) with calcium sulphate dihydrate (gypsum).

Ageing of samples

The drymixed model SLU formulations, the commercial SLU and the individual components of the ternary binder system were spread out on 60 x 135 cm Plexiglas® plates in portions of 250 g each. The samples were then exposed to 35 ± 2 °C and 90 ± 5 % RH for varying periods in a custom-built climate controllable box (Figure 1). After ageing, the powders were scraped off the plates. Weight changes of the samples were then determined on a laboratory balance (Sartorius, Göttingen, Germany).

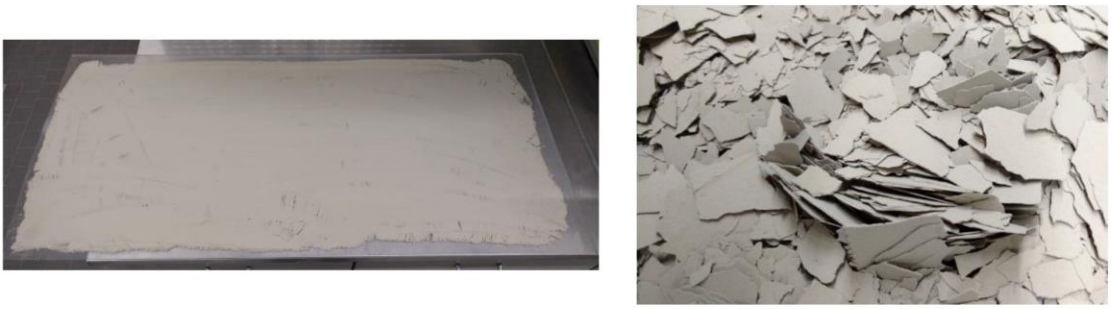

Fig. 1: *PC powder spread on a plate (left) prior to ageing at 35 °C / 90 %, and afterwards (right).*

Characterisation of ageing products

For monitoring the ageing progress with powder XRD, plastic sample carriers were prepared with samples of binders and clinker phases and continually aged in the climate box. XRD identification of the ageing products was carried out at a *D8 Advance* (Bruker AXS, Karlsruhe, Germany) instrument using a CuK_α source. As the peak intensities of the ageing products increased with ageing time, the peaks of the cement constituents simultaneously receded. Quantifying the conversion by means of XRD however proved not feasible. During prehydration water is not exclusively chemically sorbed, but also physically bond to the surface, thus lowering the XRD signal intensity of aged samples.

Paste flow

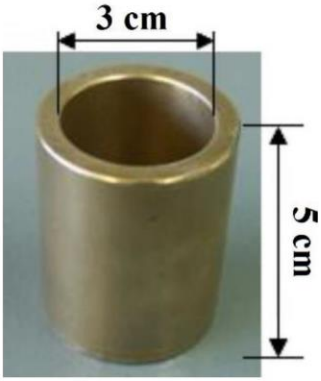

Fig. 2: *Slump cylinder used in flowability investigations.*

The flowability of both fresh and prehydrated formulations was tested by a "mini slump test" according to DIN EN 12706 [14] using a brass cylinder with an inner diameter of 30 mm and a height of 50 mm (Figure 2). First, the cylinder is positioned on a neat glass plate and completely filled with paste prepared from the formulation and DI water (w/f = 0.45). The cylinder is then lifted up and the paste allowed to flow out for ten seconds. After four minutes the paste spread on the glass plate is measured. The results for the model formulation were compared to those of a commercial SLU (*K15 DR*, Ardex, Witten, Germany).

RESULTS AND DISCUSSION

Ageing of ternary binder system components and clinker phases

Binders – PC, CAC and anhydrite

During ageing, cementitious materials increase in weight due to reaction with water and CO_2 from the atmosphere. Figure 3 shows the weight increase for the three components of a SLU ternary binder system after being individually exposed to 35 °C and 90 % relative humidity for 1, 3 and 7 days.

Of the three components, PC displayed the largest weight increase by far. A 7 days aged sample weighed ~ 12 % more than before prehydration. In the same timeframe, the weight of the CAC sample only increased by about 3.5 %, and anhydrite did not change in weight at all.

This was unexpected, since it was believed that the aluminate-rich CAC would quickly form large amounts of calcium aluminate hydrate (C-A-H) phases upon contact with moisture. Likewise, anhydrite was assumed to incorporate water resulting in hemihydrate (basanite) or dihydrate (gypsum). On the other hand, silicate rich PC was expected to age slower based on the aforementioned earlier investigations of alite and belite. Unlike CAC, PC contains sulphate and is therefore able to produce ettringite. However, considering that PC contains only ~ 4 % C_3A, this huge increase in weight after exposure to humidity is surprising.

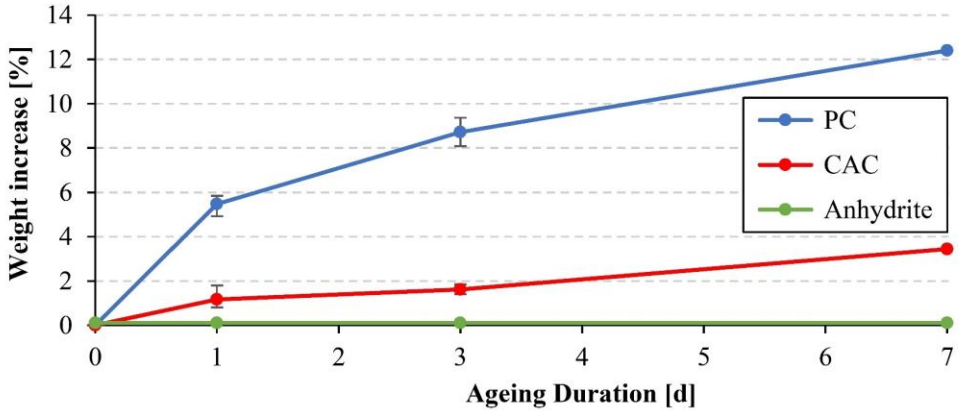

Fig. 3: *Weight increase of components of a ternary binder system during ageing at 35 °C and 90 % RH for up to seven days.*

To get a better understanding of the processes taking place during ageing, the surfaces of PC and CAC powders placed on plastic sample carriers were periodically examined by XRD, thus allowing for continuous monitoring of their surfaces. This makes the results for different ageing periods more comparable instead of samples which were prepared for every measurement individually and may show inconsistencies. Moreover, it avoids damaging the sensitive prehydrated particle surfaces which would occur during fixing aged samples onto the sample holders.

The XRD measurements of fresh and 14 days aged PC as well as CAC are displayed in Figure 4. The results match the earlier observations from determination of the weight increase, because the surface of the PC sample undergoes more significant changes than the CAC. Taking X-ray amorphous calcium silicate hydrates (C-S-H) out of the picture, PC predominantly formed calcium carbonate ($CaCO_3$) in the calcite modification. No portlandite was detected and ettringite only in a very small amount. This is a result of

carbonation. On contact with CO_2, portlandite and ettringite decompose to $CaCO_3$, aluminium hydroxide $Al(OH)_3$, calcium sulphate and water.

The CAC in comparison formed only minor quantities of a different $CaCO_3$ modification, aragonite. No C-A-H phases were detected, the only indicator of a reaction with H_2O consisted of a small amount of bayerite, an $Al(OH)_3$ polymorph. Pure anhydrite did not undergo any visible changes in the XRD during the first 14 days of ageing. Only after exposure for two months, a very low concentration of gypsum could be detected. In summary, the individual behaviours of the ternary binder system components displayed in weight increase and XRD are consistent.

Cement constituents	AH: Anhydrite	CA: $CaAl_2O_4$	C_3S: Ca_3SiO_5	C_3A: $Ca_3Al_2O_6$
Ageing products	A: Aragonite	B: Bayerite	C: Calcite	E: Ettringite

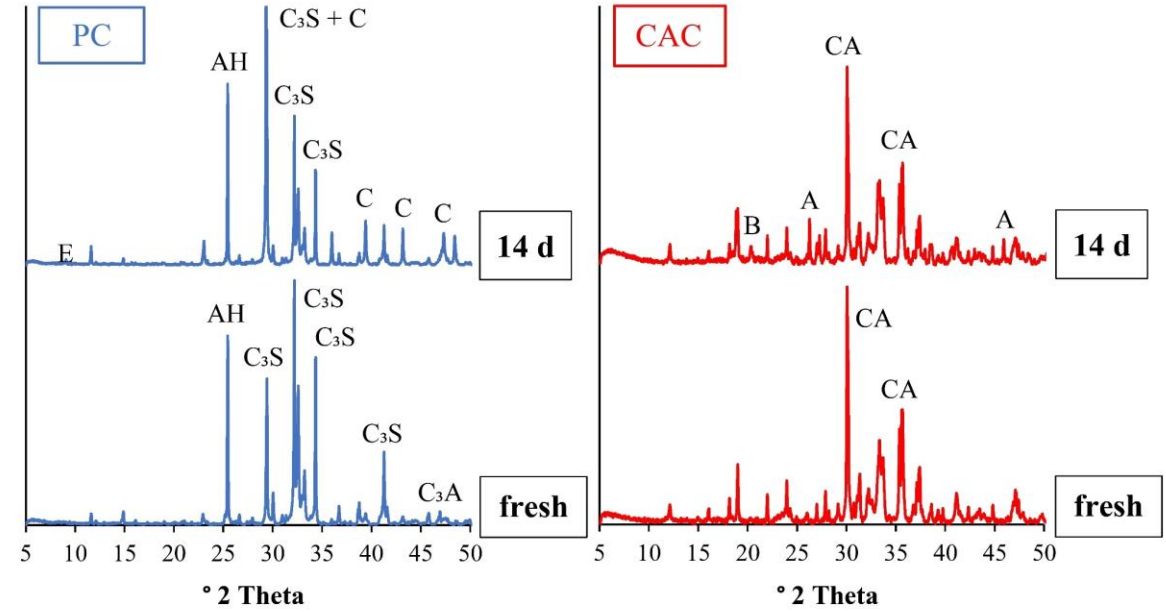

Fig. 4: *XRD patterns of fresh and 14 days aged PC (in blue, left) as well as CAC (in red, right), shown in the range of 5 – 50° 2θ with cement constituents and ageing products marked.*

Aluminate phases – C_3A, $C_{12}A_7$, CA, CA_2

In the previous part, the prehydration of CAC in the absence of sulphate was studied, hence ettringite formation was not possible. For this reason, the ageing of combinations of pure aluminate phases and sulphate was investigated next. The primary aluminate phase in PC used in this study is undoped, cubic C_3A. For Ciment Fondu® it is $CaAl_2O_4$ (CA). Other aluminate phases commonly encountered in aluminate cements are $C_{12}A_7$ and CA_2. All four phases were individually aged after drymixing with calcium sulphate dihydrate (gypsum) on a 1 : 1 basis (by weight) to enable ettringite formation. Gypsum was chosen over hemihydrate or anhydrite to eliminate sulphate hydration as a side reaction.

Figure 5 shows the XRD patterns of C_3A and CA combined with gypsum, both fresh and after 14 days of ageing. Aged C_3A exhibits strong ettringite formation while the CA does not react at all. $C_{12}A_7$ and CA_2 likewise remained unaffected after this ageing time. Only after 28 days at 35 °C and 90 % RH did the three aluminate phases show small concentrations of $Al(OH)_3$. In contrast, the ettringite formed by C_3A had decomposed at this point.

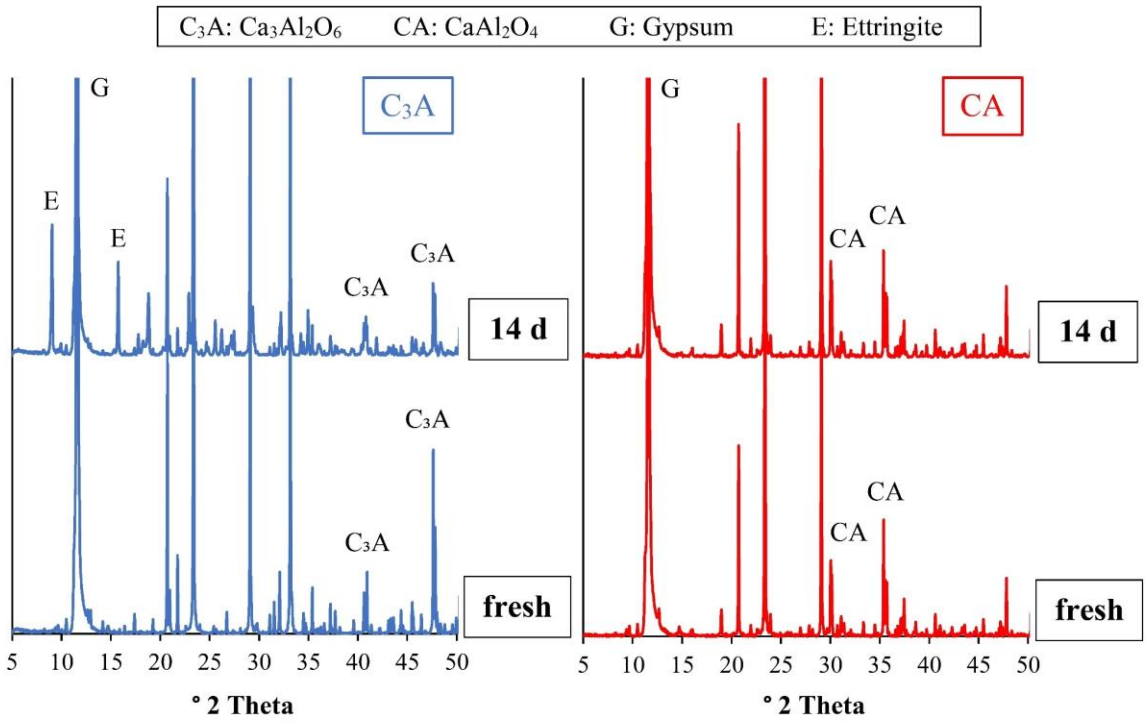

Fig. 5: *XRD patterns of fresh and 14 days aged aluminate clinker phases mixed with gypsum to enable ettringite formation. C_3A (blue, on the left) and CA (red, on the right) are shown in the range of 5 – 50° 2θ.*

Influence of additives on the ageing of PC and CAC

Lithium carbonate accelerator

The results presented so far indicate a low reactivity of the aluminate phases towards humidity, both their pure form and in the presence of sulphate. This underlines the need to use accelerators to activate the CAC, as is known from actual application. We subsequently mixed PC and CAC with lithium carbonate accelerator prior to ageing. The Li_2CO_3 dosage was chosen based on the relative portion of the two cements in the model SLU formulation (Table 1). PC comprises almost half of the formulation (47.16 wt.%), therefore it was mixed with 0.63 wt.% Li_2CO_3, which is slightly more than twice the 0.30 wt.% used in the SLU formulation. CAC makes up almost one third the formulation (32.70 wt.%), thus it was mixed with 0.91 wt.% Li_2CO_3.

A comparison of the weight increases with and without accelerator after 1 day of ageing at 35 °C and 90 % RH is shown in Figure 6. Lithium addition only slightly enhances weight increase of PC from 5.5 to 6.2 %. However, at 8.8 % the weight increase of CAC with accelerator is more than seven times higher than without (1.2 %). This difference was also visually observed, as the CAC sample aged with Li_2CO_3 formed large platelets like PC (Figure 1). In contrast, the pure CAC remained in a powdery form, more closely resembling the fresh cements.

XRD investigation of the CAC aged with lithium for 1 day revealed formation of $CaCO_3$ and $Al(OH)_3$ analogous to PC. In addition, the Li_2CO_3 had converted to the accelerating $[Li_2Al_4(OH)_{12}](OH)_2 \cdot 3\ H_2O$ layered double hydroxide (LDH). This shows that lithium acceleration does not require quantitative amounts of water and can already be activated during storage at elevated humidity.

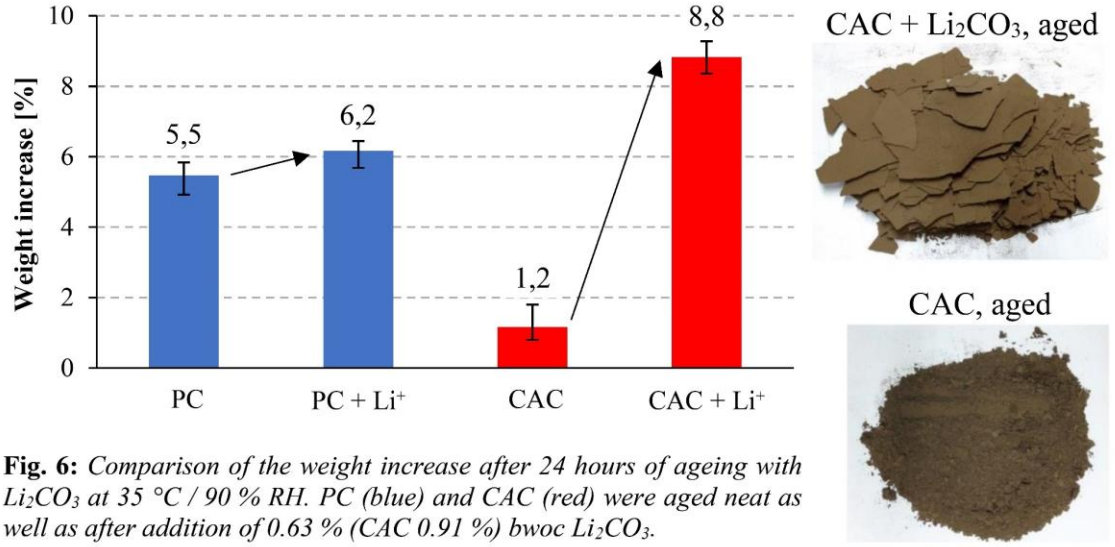

Fig. 6: *Comparison of the weight increase after 24 hours of ageing with Li_2CO_3 at 35 °C / 90 % RH. PC (blue) and CAC (red) were aged neat as well as after addition of 0.63 % (CAC 0.91 %) bwoc Li_2CO_3.*

Tartrate and citrate retarders

In a second series of experiments we added tartrate and citrate instead of lithium carbonate to the cements prior to ageing. Relative to the model SLU formulation, this amounted to dosages of 0.84 wt.% for PC and 1.21 wt.% for CAC respectively.

As is shown in Figure 7, both retarders surprisingly accelerated the weight increase over 24 hours, thus displaying a behaviour similar to Li_2CO_3. Tartrate had about the same effect on PC as lithium (6.4 % weight increase), whereas citrate addition led to a significantly higher weight increase of 10.0 %. Citrate had a stronger impact than tartrate in CAC as well. Unlike Li_2CO_3, the overall weight increase of CAC with retarders was lower than for PC. Furthermore, no compounds containing tartrate or citrate were detected by XRD, just $CaCO_3$ and $Al(OH)_3$. This makes a unique interaction between the retarders and the CAC such as the formation of LDH intercalation compounds unlikely.

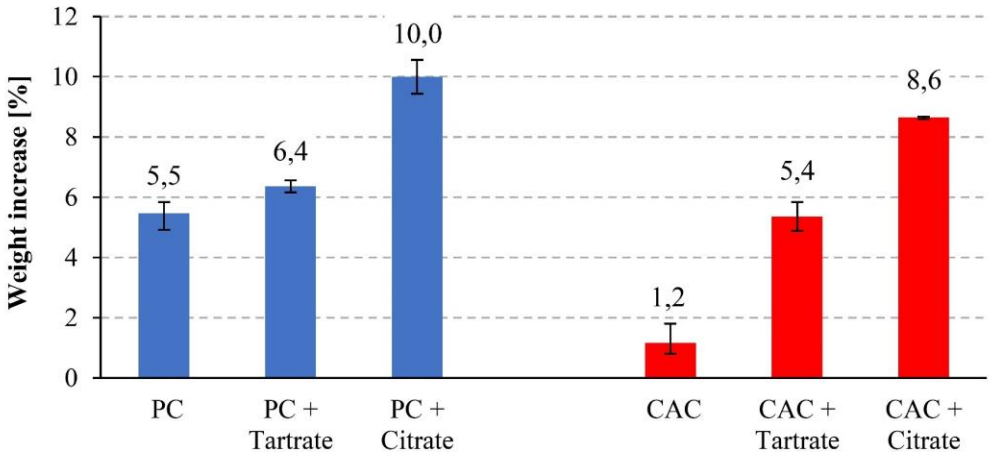

Fig. 7: *Comparison of the weight increase after 24 hours ageing with retarders at 35 °C / 90 % RH. PC (blue, on the left) and CAC (red, on the right) were aged neat as well as after addition of 0.84 % (CAC 1.21 %) bwoc of tartrate or citrate.*

Not only did retarder addition unexpectedly accelerate ageing, it also altered the outward appearance of the samples with spotty discolourations appearing on their surfaces during

ageing (Figure 8). In order to get more insight into the additives' reaction at elevated humidity and temperature, we exposed small quantities of pure Li_2CO_3 and retarders to 35 °C / 90 % RH as well.

Tartrate and citrate turned out to be hygroscopic, both increasing their weight by ~ 15 % over 7 days. The citrate even incorporated the sorbed moisture into its crystal structure, changing from a dihydrate to a pentahydrate. Li_2CO_3 on the other hand remained unaffected due to its low solubility in water compared to other lithium salts.

We assume that tartrate and citrate accelerate the weight increase of PC and CAC due to a combination of their hygroscopicity and particle size. After mixing, the coarse retarder crystals are distributed in the fine cement powder. The facilitated uptake of water via these isolated particles leads to areas of strong prehydration, visible as discolourations on the powder surfaces.

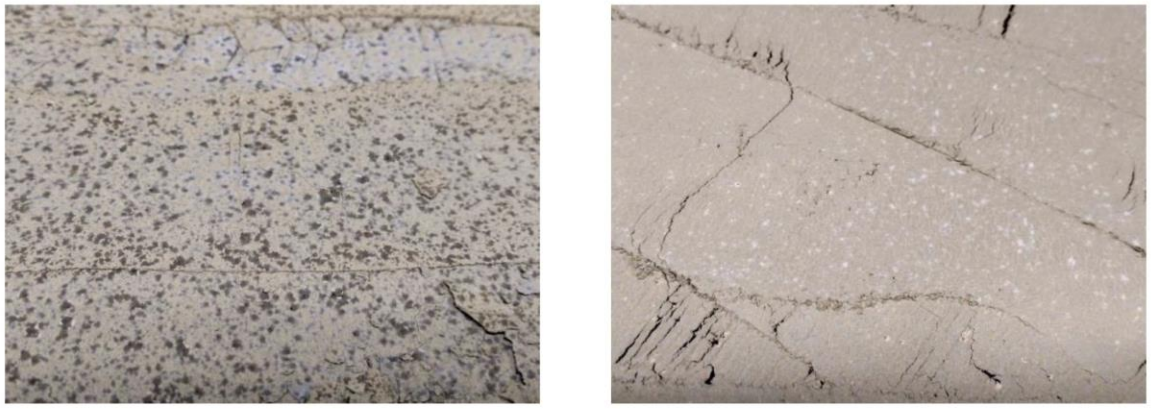

Fig. 8: *Surface discolourations of the model SLU formulation (left) and of pure PC (right), appearing when aged with citrate at 35 °C and 90 % RH.*

Impact of ageing on SLU flowability

Comparison between model SLU formulation and commercial SLU

The most important difference between the model SLU formulation and the commercial product is that the latter is "fully formulated", meaning it contains fillers like quartz sand and limestone as well as auxiliary additives such as redispersing polymers. The model formulation comprising the ternary binder system and its additives thus only represents the reactive key component (~ 35 wt.%) of a fully formulated SLU.

Figure 9 compares paste spread and mass increase of the model formulation (with tartrate as retarder) and the commercial SLU *K15 DR*. Before ageing, both reached a spread of 23 cm at a water-to-solid (w/s) ratio of 0.45. During ageing *K15 DR* lost flowability faster than the model formulation. It reached the minimum paste spread already after 24 hours of exposure to moisture. Increasing the ageing duration did not change the fluidity any further. This corresponds to the weight increase of the sample, which stopped after 1 day.

The model formulation on the other hand displayed a more gradual decline in flowability, the early stages of ageing still having the strongest impact. The corresponding weight increase mirrors the flowability development, similar to the commercial product.

The fillers in the *K15 DR* SLU are chemically inert towards water but can physically sorb moisture. This explains that the weight increase of the commercial product overall is lower but achieves its maximum after just 24 hours of exposure. The physical sorption of water further leads to agglomeration of filler particles which reduces initial flowability.

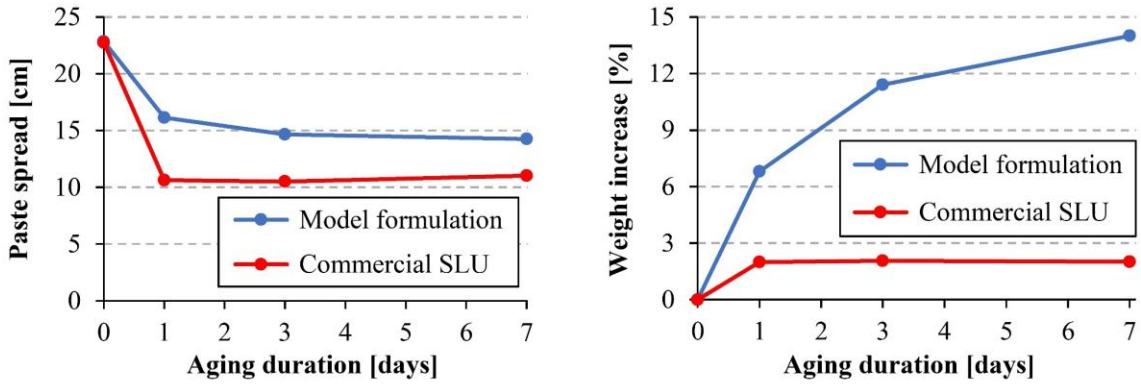

Fig. 9: *Comparison between model SLU formulation (with tartrate as retarder) and a commercial SLU (Ardex K15 DR). Shown are paste spread at a w/s ratio of 0.45 (left) and the weight increase (right) of samples aged at 35 °C / 90 % RH for up to seven days.*

Delayed plastification and measures to counteract ageing effects

In a previous study [11] we reported that ageing leads to delayed plastification, meaning that the flowability of a paste prepared from an aged sample of the model formulation increases over time. However there, the retarders had not been aged together with the other components of the model SLU and instead were added only during paste preparation. Now we conducted these experiments with the whole model formulation aged together. The results obtained were practically identical with those from the previous study and are shown in Figure 10 on the left for reference.

In order to find measures to mitigate the negative impact of ageing on paste flowability we investigated the impact of adding calcium hydroxide $Ca(OH)_2$ to the SLU formulation. $Ca(OH)_2$ addition has originally been suggested to prevent the formation of so-called hydrate spheres in ternary binder systems [15]. Hydrate spheres are inclusions inside the hardened matrix that develop due to inhomogeneous setting and are regularly encountered in tartrate-retarded ternary binder systems used in drymix applications [16].

In this study, we tested the addition of 1.0 and 2.5 wt.% $Ca(OH)_2$ to the model formulation containing tartrate prior to ageing for three days. As can be seen in Figure 10 on the right, $Ca(OH)_2$ generally increased fluidity which might be owed to its high hygroscopicity which prevents other phases from prehydration. The positive effect on flowability diminished over time due to the aforementioned delayed plastification.

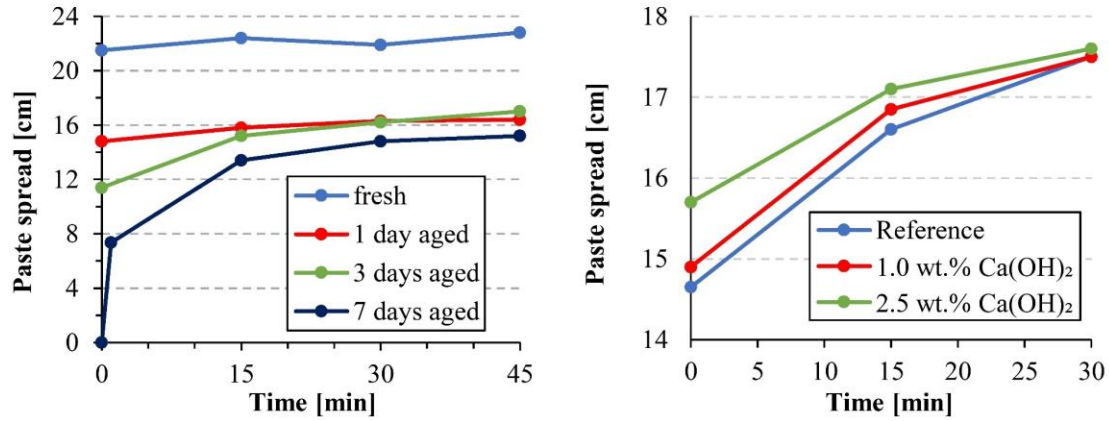

Fig. 10: *Paste spread of the model SLU formulation before and after ageing (w/s = 0.45). On the left, different ageing periods are compared. The results shown on the right were obtained with addition of $Ca(OH)_2$ prior to ageing for 3 days.*

CONCLUSION

The aim of this study was to further our understanding of the ageing behaviour of SLU formulations. First, we investigated the impact of prehydration on individual constituents of the ternary binder system which presents the basis of a SLU. Samples were exposed to 35 °C and 90 % RH over varying periods of time in a climate box.

Unexpectedly, PC displayed a higher weight increase during ageing than CAC, while anhydrite did not change in weight at all. This was confirmed by XRD analysis with PC samples undergoing significant changes on their surface. PC predominantly formed $CaCO_3$ (calcite modification) with atmospheric CO_2 and minor quantities of ettringite. CAC on the other hand produced only small amounts of $CaCO_3$ and $Al(OH)_3$, with no C-A-H being formed under the ageing conditions applied.

We investigated potential ettringite formation during ageing by mixing pure aluminate clinker phases with gypsum prior to prehydration. As was observed for neat PC, C_3A also produced quantitative amounts of ettringite during ageing while CA, $C_{12}A_7$ and CA_2 remained unaffected by moisture.

These results confirmed the need to use accelerators to activate the CAC contained in the ternary binder system. While the weight increase of PC aged with Li_2CO_3 was only slightly accelerated, the weight of CAC increased sevenfold. XRD analysis confirmed the formation of a $[Li_2Al_4(OH)_{12}](OH)_2 \cdot 3\ H_2O$ LDH in CAC during ageing.

Ageing of PC and CAC with tartrate or citrate retarder instead of Li_2CO_3 surprisingly accelerated the weight increase as well. In their pure form the retarders turned out to be hygroscopic at 90 % RH. In combination with the relatively large particle size of the retarders, this led to isolated spots of strong prehydration on the cement surface.

We compared the paste spread of a model SLU formulation with that of a commercial SLU (*K15 DR*). Before ageing, both reached a similar spread, whereas after 24 hours in the climate box the commercial product showed a stronger reduction in flowability than the model formulation. *K15 DR* contains fillers like quartz sand and limestone besides the ternary binder system. These non-hydrating fillers can physically sorb moisture, thus possibly causing particle agglomeration which results in additional flowability loss. To counteract the ageing effect on SLUs, we tested the addition of $Ca(OH)_2$ to the model formulation which had a positive impact on early flowability.

The experiments conducted in this study show that the combination of numerous components contained in a SLU increases its susceptibility to ageing. Apart from the binder system, additives and even aggregates play a role in determining ageing behaviour.

ACKNOWLEDGEMENTS

The authors are most grateful to the Deutsche Forschungsgemeinschaft (DFG, German Research Foundation) for funding this project under the grant PL-472/9-2. Thanks go also to HeidelbergCement and Kerneos S.A. for providing the cements used in this study.

REFERENCES

[1] Plank J. *Technology Trends in the European Dry Mix Mortar Industry.* Proceedings of 1st Conference on Research and Application of Commercial Mortar, Shanghai/China, 2005. pp 26-40.

[2] Winter C and Plank J. *The European Dry-Mix Mortar Industry (Part 1).* Zement-Kalk-Gips International, 2007, 60(6), pp 62-69.

[3] Harbron R. *A general description of flow-applied floor screeds - an important application for complex formulations based on CAC.* Calcium Aluminate Cements: Proceedings of the International Conference 2001, Edinburgh. Mangabhai R J and Glasser F P. (Eds). London: IOM Communications, 2001, pp 597-604.

[4] Amathieu L, Bier T A and Scrivener K L. *Mechanisms of set acceleration of Portland cement through CAC addition*. Calcium Aluminate Cements: Proceedings of the International Conference 2001, Edinburgh. Mangabhai R J and Glasser F P. (Eds). London: IOM Communications, 2001, pp 303-317.

[5] Götz-Neunhoeffer F. *Modelle zur Kinetik der Hydratation von Calciumaluminatzement mit Calciumsulfat aus kristallchemischer und mineralogischer Sicht*, Universitätsverbund Erlangen-Nürnberg, 2006.

[6] Al-Mutawa F, Whittaker M, Arkless L, Dubina E, Plank J and Black L. *The Effects of Prehydration at Moderate Humidities on the Engineering Properties of Portland Cement.* Proceedings of Cement and Concrete Science, Birmingham, 2010.

[7] Winnefeld F. *Influence of cement ageing and addition time on the performance of superplasticisers.* Zement-Kalk-Gips International, 2008, 61(11), pp 68-77.

[8] Dubina E, Black L, Sieber R and Plank J. *Interaction of water vapour with anhydrous cement minerals.* Advances in Applied Ceramics 109(5), 2010, 260-268.

[9] Dubina E, Wadsö L and Plank J. *A sorption balance study of water vapour sorption on anhydrous cement minerals and cement constituents.* Cement and Concrete Research, 2011, 41, pp 1196-1204.

[10] Dubina E and Plank J. *Investigation of the long-term stability during storage of drymix mortars, Part 2. Influence of Moisture Exposure on the Performance of Self-levelling mortars (SLUs).* ALITinform, 2012, 26(4-5), pp 86-99.

[11] Plank J, Dubina E and Meier M R. *Ageing Behavior of SLU Mortar Formulations Based on a Ternary Binder System Comprising PC/CAC/Anhydrite Exposed to Environmental Moisture and CO_2*. Calcium Aluminate Cements: Proceedings of the International Conference 2014, Avignon. Fentiman C H, Mangabhai R J and Scrivener K L. (Eds). London: IOM Communications, 2014, pp 407-421.

[12] Hartmann F A, Meier M R and Plank J. *The impact of cement and clinker prehydration on retarder performance.* Proceedings of 15th International Congress on the Chemistry of Cement, Prague, 2019.

[13] Wesselsky A and Jensen O M. *Synthesis of pure Portland cement phases*. Cement and Concrete Research, 2009, 39, pp 973-980.

[14] DIN EN 12706. *Adhesives-test methods for hydraulic setting floor smoothing and/or levelling compounds - determination of flow characteristics.* 1999.

[15] Zurbriggen R. *High Performing Self-Levelling Underlayments - Learnings from Material Science Studies*, Proceedings of 5th American Drymix Mortar Conference, Philadelphia, 2016

[16] Götz-Neunhoeffer F and Zurbriggen R. *Formation of hydrate spheres in ternary binder systems*. Zement-Kalk-Gips International, 2008, 61(12), pp 68-76.

Veröffentlichungen in Tagungsbänden ohne peer-review Verfahren

Alginate als neue Beschleuniger für Aluminatzemente

A. Engbert, M. Dinkel, J. Plank
Technische Universität München, Lehrstuhl für Bauchemie
Lichtenbergstr. 4, 85747 Garching, Deutschland

Einleitung

Für die Beschleunigung von Aluminatzementen werden Lithiumsalze wie z.B. Li_2CO_3 eingesetzt. Dieses bildet beim Anmischen eine LDH-Verbindung ($[Li_2Al_4(OH)_{12}](OH)_2 \cdot 3H_2O$), welche isostrukturell zu C_2AH_8 ist, und als heterogenes Nukleationssubstrat für die Kristallisation dient /1/. Der Einsatz von Lithium in der Bauindustrie wird jedoch durch die zunehmend problematischere Versorgungssituation, bedingt durch den stetig steigenden Bedarf an Lithiumbatterien für Smartphones und Elektromobilität, gefährdet.

Alginate sind Polysaccharide, welche aus $1 \rightarrow 4$ glycosidisch verknüpften Mannuron- und Guluronsäuren aufgebaut sind. Durch unterschiedliche Verknüpfungssequenzen (siehe **Abbildung 1**) der

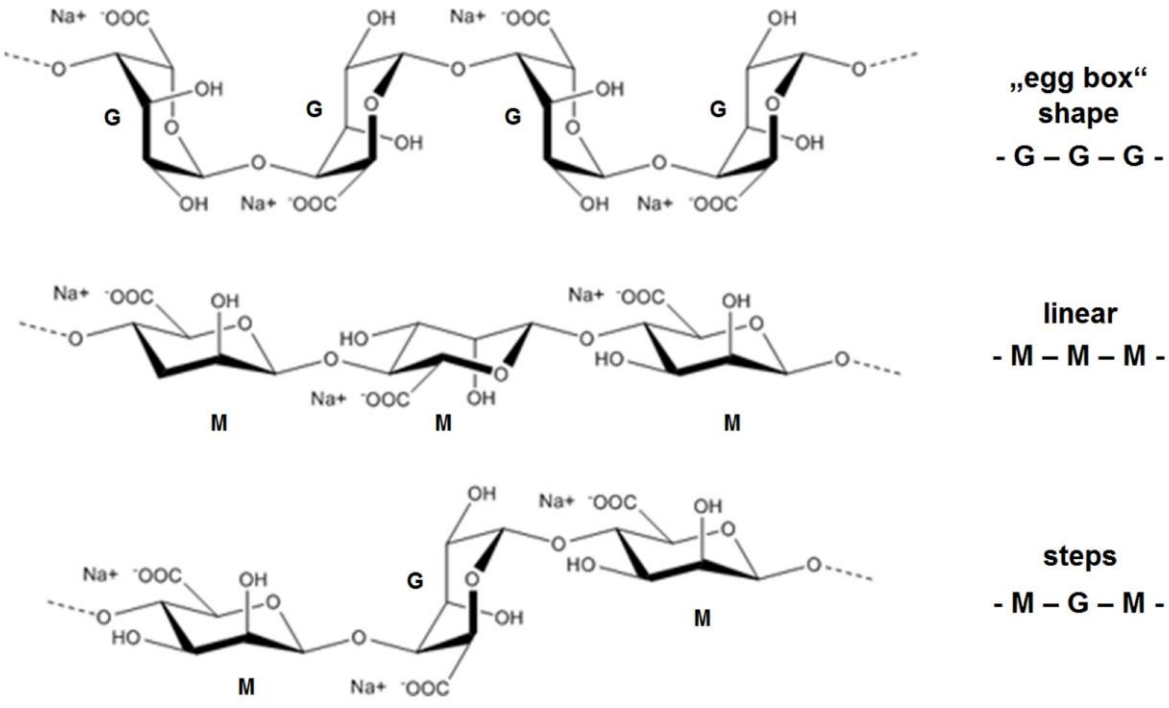

Abb. 1: Chemischer Aufbau sowie unterschiedliche Verknüpfungsmöglichkeiten von Mannuronsäure (M) und Guluronsäure (G) in Alginaten.

Zucker werden die Sekundärstruktur und damit die Eigenschaften des Alginats stark beeinflusst. Die Carboxylat-Gruppen ermöglichen eine Bindung von Ca^{2+}, welches in den G-Blöcken („egg box“) konformationsbedingt besonders günstig komplexiert werden kann (siehe **Abb. 2**) /2/. Aufgrund dieser Fähigkeit, die mit bestimmten Kationen wie z.B. Ca^{2+} zu einer starken Gelbildung führt, findet das Hydrokolloid Alginat z.B. in Lebensmittelzubereitungen Anwendung.

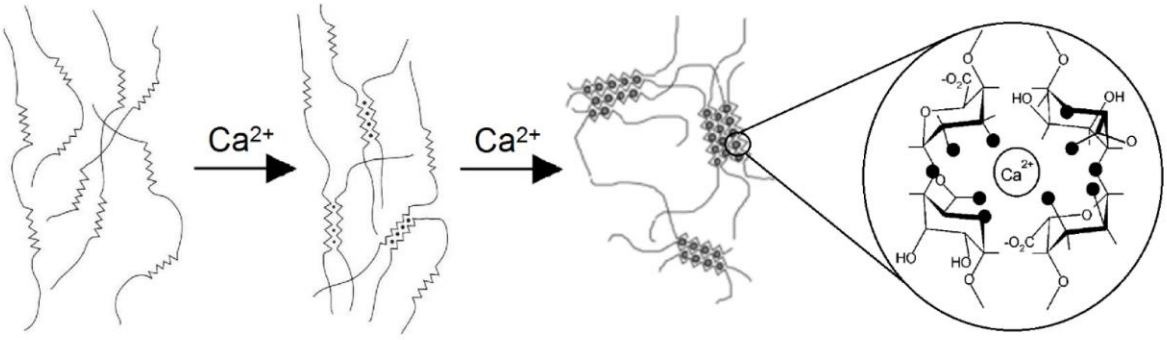

Abb. 2: Schematische Darstellung der intermolekularen Wechselwirkung zwischen Metallkationen (hier: Ca^{2+}) und einem Alginat nach dem egg-box-Modell /2/.

Überraschenderweise wurde gefunden, dass das Biomolekül Alginat bezüglich der Beschleunigung von CAC eine Alternative zu Lithiumsalzen darstellt. In früheren Untersuchungen zur Interkalation von Exo-Polysacchariden in LDH-Strukturen hatte sich gezeigt, dass Alginate Calciumaluminatzemente, nicht jedoch Portlandzement beschleunigen /3, 4/.

Ziel der vorliegenden Studie war es, diesen beschleunigenden Effekt auf die Hydratation von CAC, welcher für Polysaccharide untypisch ist (alle bisher getesteten Polyssaccharide verzögern), zu quantifizieren und Einblicke in den Wirkmechanismus zu erhalten.

Da es sich bei Alginaten um Naturprodukte handelt, welche aus verschiedenen Braunalgen-Spezies (*phaeophyceae*) extrahiert werden, kann ihre chemische Zusammensetzung je nach Gattung und Art der Alge sowie der Erntezeit stark variieren. Aus diesem Grund wurde eine sehr breite Auswahl an Alginaten untersucht.

Material und Methoden

Insgesamt 26 verschiedene Alginat-Muster wurden von den Firmen KIMICA, FMC, Eurogum, Cargill, Danisco, Roeper und Polygal

bezogen. Polyguluronsäure und Polymannuronsäure (Mw >5000 Da) wurden von Carbosynth erhalten. Die Aluminatzemente Secar 41, 51, 71, 712, 80 sowie Ciment Fondu, Ternal LC und Ternal SE stellte die Firma Kerneos zur Verfügung.

Der Hydratationsverlauf wurde an CAC-Pasten durch Anmischen von 4 g Zement, welchem die Alginate trocken zugegeben waren, bei einem Wasser/Zement-Wert von 0,62 untersucht. Hierfür wurde die Probe zwei Minuten mittels eines Vibrations-Mischers homogenisiert und anschließend die Ampulle in ein TAM AIR Wärmeflusskalorimeter eingeführt. Alle Proben wurden mindestens zweimal vermessen, das Ergebnis gemittelt und daraus die Genauigkeit bestimmt.

Die Bestimmung der Ionenkonzentration in Porenlösung erfolgte mittels ICP-OES. Hierfür wurde der Zement bei w/z = 0,45 ohne bzw. mit 0,1 % (bezogen auf Zement, bwoc) an Alginat für zwei Minuten am Vibrations-Mischer homogenisiert und für 15 Minuten abzentrifugiert /3/.

Ergebnisse und Diskussion

Wirkung in Calciumaluminatzement

Ein Screening von 26 kommerziellen Alginaten der oben genannten Firmen zeigte, dass alle Natriumalginate eine recht ähnliche beschleunigende Wirkung aufweisen (Beispiele siehe in **Abb. 3**). Die Unterschiede sind u.a. auf die Viskosität, welche mit dem Molekulargewicht korreliert, und die Partikelgröße des Alginatpulvers zurückzuführen.

Mit Propylenglycol veresterte Alginate, welche einen Veresterungsgrad von >70 % und somit im Wesentlichen Carboxylatgruppen aufweisen, welche für die Wechselwirkung mit Kationen blockiert sind, zeigen ebenfalls einen beschleunigenden Effekt (siehe **Abb. 3**). Somit ist die Carboxylatgruppe für die Beschleunigung nicht maßgeblich.

Weitere Hydrokolloide (λ-Carrageen, Pektin und verschiedene Gums) ergaben die für Polysaccharide übliche verzögernde Wirkung. Die Homopolymere Polymannuron- und Polyguluronsäure zeigten im Gegensatz zum Alginat keine Beschleunigung, sondern eine verzögernde Wirkung.

Die beschleunigende Wirkung eines Alginats auf CAC ist je nach verwendetem Aluminatzemente sehr unterschiedlich. **Tabelle 1** zeigt beispielhaft die Ergebnisse des Na-Alginats XEA5036 der Fa. Eurogum. Es zeigte sich, dass eine Dosierung von 0,1 % bwoc des Alginats eine

Verkürzung des Maximums der Hydratationswärme um 15 - 45 % abhängig vom Aluminatzement ergibt. Eine Ausnahme stellt Secar 80 dar, bei welchem nur eine vernachlässigbare Beschleunigung zu beobachten war, welche evtl. auf die wesentlich höhere Feinheit dieses Zements im Vergleich zu den Anderen zurückzuführen ist.

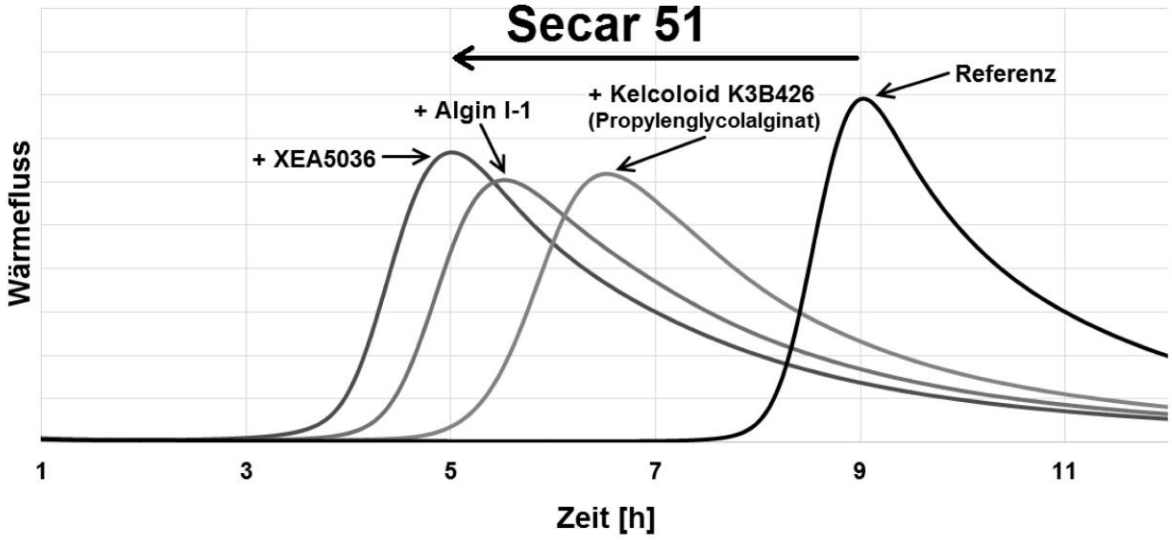

Abb. 3: Wärmeflusskalorimetrie von CAC (Secar 51) ohne und mit verschiedenen Alginaten (Dosierung jeweils 0,1 % bwoc ; w/z=0,62).

Tab. 1: Vergleich der beschleunigenden Wirkung des Alginates XEA5036 bei 0,1 % sowie 0,2 % Dosierung in verschiedenen Aluminatzementen.

CAC	Dosierung des Alginats	
	0,1 %	0,2 %
Ciment Fondu	~ 30 %	~ 25 %
Secar 41	~ 30 %	~ 20 %
Secar 51	~ 45 %	~ 50 %
Secar 71	~ 30 %	~ 40 %
Secar 712	~ 30 %	~ 40 %
Secar 80	~ 5 %	~ 15 %
Ternal SE	~ 20 %	~ 40 %
Ternal LC	~ 50 %	~ 60 %

Es wird vermutet, dass die unterschiedliche Beschleunigung auf die verschiedene mineralogische Zusammensetzung der Zemente zurückzuführen ist.

Höhere Alginat-Dosierungen (0,2 % bwoc) führten in der Regel zu keiner wesentlichen Verbesserung der Beschleunigung (siehe **Tab. 1**). Eine Ausnahme stellen die Zemente der Ternal-Serie dar, welche in ihrer Partikelgröße gröber sind als die homologen Zemente der Secar-Serie. Sie werden bei einer Dosierung von 0,2 % Alginat um bis zu 60 % beschleunigt.

Wirkung in anderen Zementen

In einem Calciumsulfoaluminatzement (≥ 58 % Ye'elimite, i.tech ALI PRE der Firma ItalCementi) zeigte das Alginat keine nenneswerte Beschleunigung (5 % bei 0,2 % Dosierung). Auch OPC-reiche ternäre Bindemittelsysteme, welche ihre Frühfestigkeit aus der Ettringitbildung beziehen, ergaben ebenfalls keine signifikante Beschleunigung (siehe **Abb. 4**).

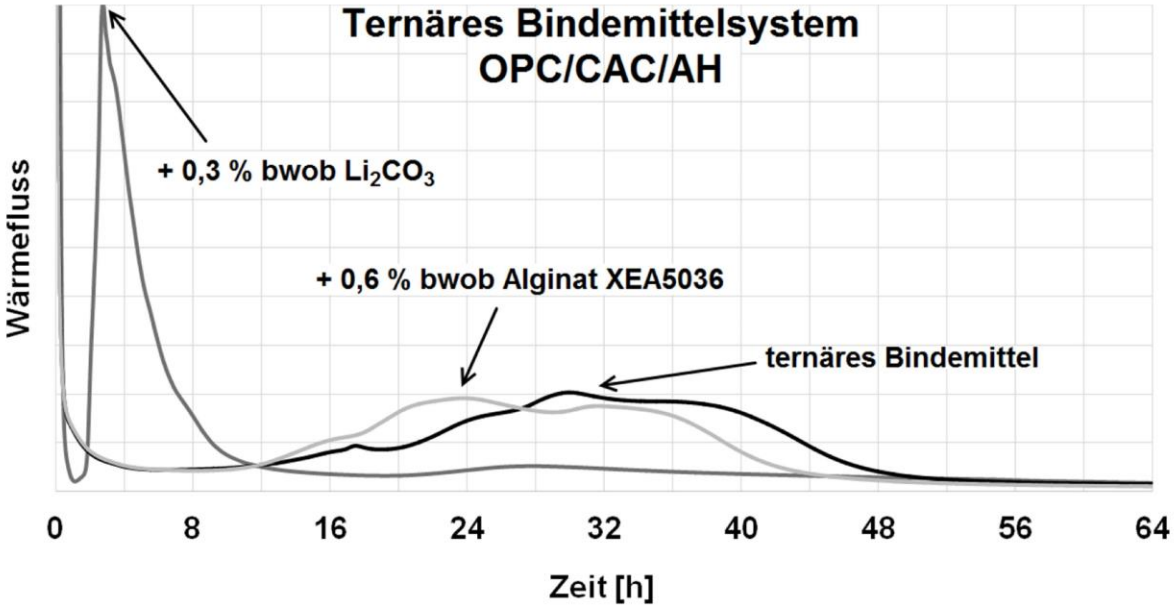

Abb. 4: Wärmefluss eines ternären Bindemittelsystems ohne und mit Alginat im Vergleich zu Lithiumcarbonat (w/z=0,5, bestehend aus CEM I 52.5N/ Ciment Fondu/Anhydrit und Seignettesalz sowie einem PCE-Fließmittel).

Eine Untersuchung der Ionengehalte in der Zementporenlösung von Ciment Fondu zeigte für 0,1 % Alginat eine Reduktion der Ca^{2+}-Konzentration um 16 % /3/. Dies spricht für eine deutliche Ionenbindefähigkeit des Alginats, welche für einen Beschleuniger untypisch ist, denn Ca^{2+}-Komplexierung führt in der Regel zu einer Verzögerung der Hydratation, da die Calciumionen dann zur Bildung der Hydratphasen

nicht zur Verfügung stehen. Es ist deshalb erstaunlich, dass Alginate trotz dieses Effektes als Beschleuniger wirken.

Zusammenfassung

Alginate eignen sich als Beschleuniger für Aluminatzemente, wie mittels kalorimetrischer Untersuchungen gezeigt wurde. Die Alginate beschleunigen - bei gleicher Dosierung - jedoch wesentlich geringer als Li_2CO_3. Sie stellen deshalb nur dann einen Ersatz für Lithium-Salze dar, wenn eine Beschleunigung von 30 % bis 45 % gewünscht ist. Ist eine stärkere Beschleunigung erforderlich, kann Lithiumcarbonat mit Alginat kombiniert werden, sodass sich immerhin ein geringerer Verbrauch an Lithiumsalz ergibt. Zu beachten ist beim Einsatz von Alginaten ihre verdickende Wirkung im Zement, die vorteilhaft oder nachteilig sein kann, je nach Anwendung.

Mechanistische Untersuchungen zeigten, dass Alginat die Ca^{2+}-Konzentration in der Porenlösung von Aluminatzementen reduziert, was für einen Beschleuniger untypisch ist. Das für die beschleunigende Wirkung des Alginats verantwortliche Strukturelement konnte bisher nicht ermittelt werden. Es ist denkbar, dass dieses Strukturelement eine noch wesentlich stärkere Beschleunigung hervorruft, welche allerdings durch die nachgewiesene Calcium-Komplexierung zum Teil wieder neutralisiert wird.

Die aktuellen Untersuchungen konzentrieren sich auf die Wirkung der Alginate auf reine CAC-Klinkerphasen. Des Weiteren werden derzeit Alginate von Braunalgen anderer Arten besorgt (vor allem aus Asien, die bisher nicht untersucht wurden), um deren Einfluss auf das Abbinden von CAC zu ermitteln. Schließlich dienen weitere Untersuchungen dazu, die für die Beschleunigung verantwortliche Struktureinheit im Alginat bzw. den Wirkmechanismus aufzuklären.

Referenzen

/1/ F. Götz-Neunhoeffer: „Modelle zur Kinetik der Hydratation von Calciumaluminatzement mit Calciumsulfat aus kristallchemischer und mineralogischer Sicht“
Habilitationsschrift, Universitätsverbund Erlangen-Nürnberg (2006)

/2/ Janetzky: „*Alginate in a* glance“, Präsentation DuPont/Danisco Deutschland GmbH (2016)

/3/ M. Dinkel: „Wirkung von Alginaten und Hectorit als Hydratationsbeschleuniger von Calciumaluminatzementen“
Masterarbeit, Technische Universität München (2016)

/4/ J. de Reese: „Wechselwirkung von Bionanokompositen und Fließmitteln mit zementären Systemen“
Dissertation, Technische Universität München (2016)

Engbert, A., Dinkel, M., Plank, J.

Biopolymers As Novel Accelerators For Alumina Cement

1. Introduction

The most efficient way to accelerate the hydration of calcium alumina cements and ternary binder systems is the addition of a lithium salt. Most frequently used is Li_2CO_3 which is dosed between 0.005 and 0.1 wt.-%, depending on the specific application and the binder system. When lithium ions are present, the hydration of the aluminate phases is accelerated through six pathways. This leads to a potent effect in pure aluminate cement that is also strong in the presence of $C\bar{S}H$. Those six pathways are: (1) improved dissolution of CA through an increased permeability of the aluminum hydroxo hydrate layer; (2) the thus increased CaO/Al_2O_3 ratio in solution thermodynamically promotes the formation of C_2AH_8; (3) formation of $[Li_2Al_4(OH)_{12}](OH)_2 \cdot 3H_2O$ LDH as precursor decreases the activation energy necessary for the crystallization of C_2AH_8; (4) Li^+ is catalytically recycled by Al^{3+} fixation; (5) the LiAl-LDH reduces the Al^{3+} concentration in solution and (6) dissolution of CA is increased by a lower Al^{3+} content in solution [1].

However, the availability of lithium salts in the construction industry is becoming increasingly problematic because of the high demand for lithium ion batteries. The growing market for mobile phones and electric cars will in the future negatively affect the price and the supply security for lithium to the construction industry.

While performing a study on the intercalation of exopolysaccharides into layered double hydroxide (LDH) compounds, an unusual behavior was observed for alginates when tracking the hydration of alumina cement via heat flow calorimetry. An in-depth investigation concluded that alginates act as accelerator for CAC by prematurely triggering its hydration. This effect was very surprising, because so far polysaccharides were only known to retard cement hydration. Following this discovery, research on the interaction of the alginates with cement and their accelerating mechanism was intensified. When screening a broad variety of biopolymers, such an accelerating effect was also discovered for carrageenan and propylene glycol alginate.

Alginates are composed of mannuronic (M) and guluronic (G) acid that are linked α-1→4 and β-1→4 into a polymer with a molecular weight between 10.000 and 600.000 Dalton (**Figure 1**). The sugar monomers (M and G) can be linked in different sequences like MM, GM and GG which results in different steric arrangements. The ratio between those blocks is mostly responsible for the properties of the polymer. The GG blocks are important for the strong gelling properties of alginate in the presence of divalent cations like Ca^{2+}. Because of its characteristic appearance, this complexation mode with Ca^{2+} is named “egg-box” model (**Figure 2**) [2,3].

Carrageenans are generally composed of galactose and 3,6-anhydrogalactose which are linked α-1→4 and β-1→3 into a polymer with a molecular weight between 200.000 and 800.000 Dalton (**Figure 1**). Kappa (κ) and iota (ι) carrageenan differ by the degree of sulfatation while the lambda (λ) modification is structurally different and shows a different behavior in solution as well as relative to interaction with ions. Similar to alginates, κ- and ι-carrageenan form a gel in the presence of specific cations by bridging the sulfate groups (**Figure 3**) [2,3]. λ-carrageenan does not form such gels and shows no accelerating effect on cement hydration.

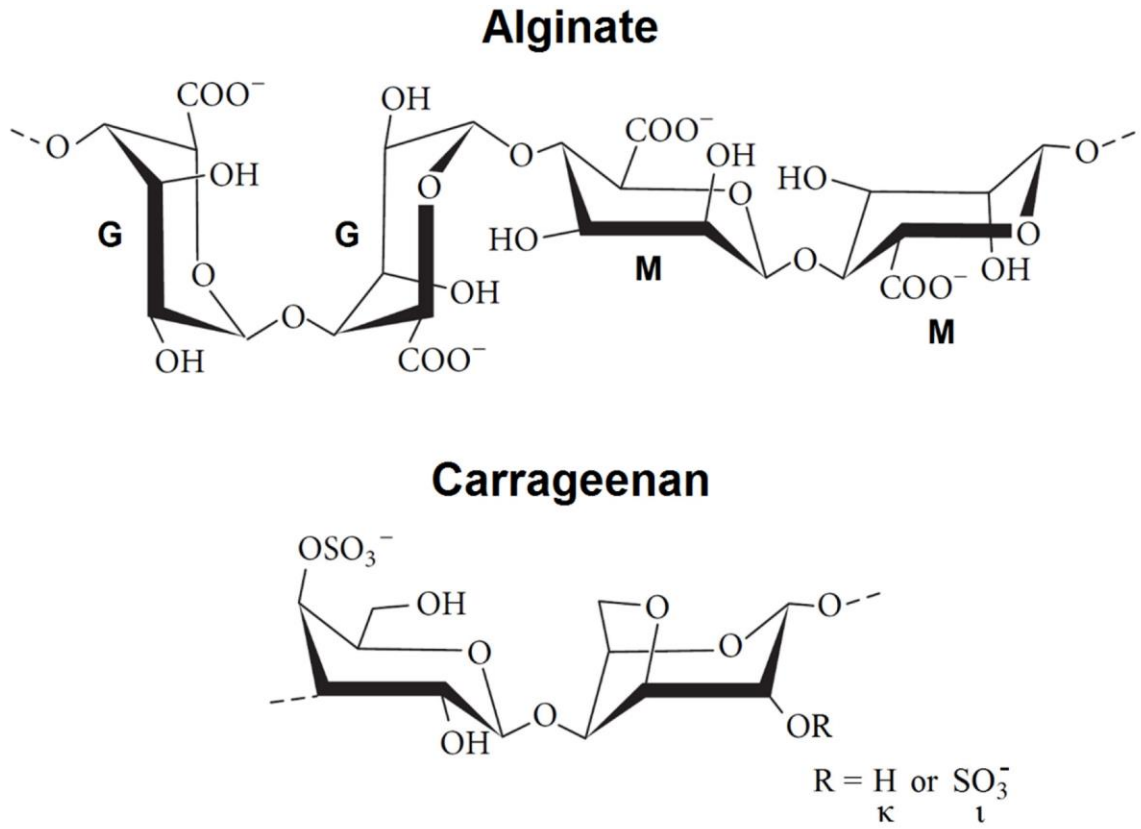

Figure 1: Chemical structures of alginate and carrageenan.

Alginates and carrageenans are biopolymers of natural origin and extracted from brown (alginate) or red (carrageenans) algae. Because of different algae species, growth conditions and processing after harvest, their chemical composition and molecular weight varies.

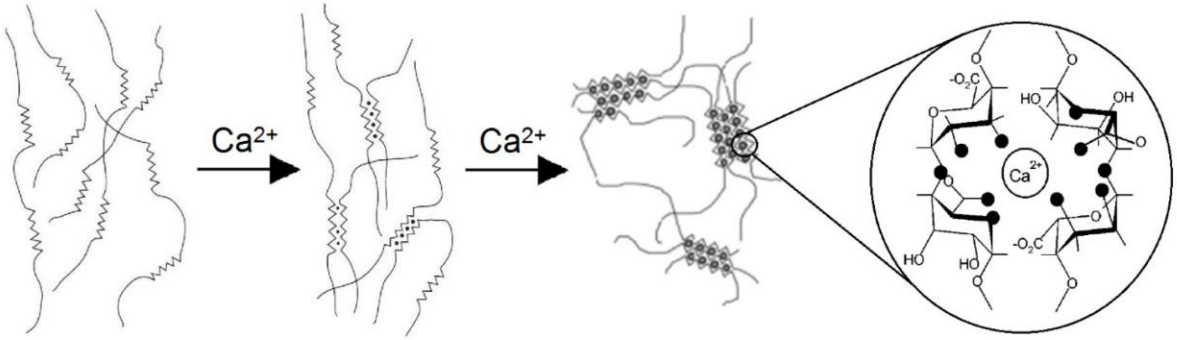

Figure 2: Complexation of calcium ions by alginate according to the “egg-box” model resulting in gel formation [4].

The aim of this research was to characterise and understand this unusual property of both biopolymers. In order to investigate the effect of diverse natural origin, different alginate as well as carrageenan products from different companies with variable properties were tested. Additionally, their accelerating effect on different alumina cements was investigated. This is necessary because of the different mineralogical compositions resulting mainly from the ratio of $CaO / Al_2O_3 / Fe_2O_3$ present in the clinker production.

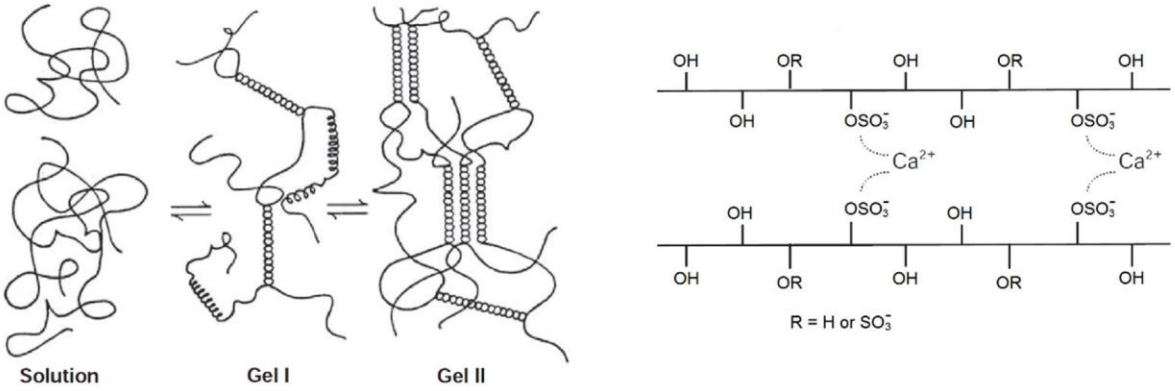

Figure 3: Complexation of calcium ions by carrageenans leading to gel formation [2].

2. Experimental program

2.1. Raw materials

KIMICA, Eurogum, FMC, Roeper, Cargill, Danisco and Polygal generously supplied over twenty different alginates. Ten different carrageenans were provided from Eurogum, Roeper and FMC. Kerneos supplied various alumina cements.

2.2. Experimental procedures

The progress of cement hydration was tracked using isothermal heat flow calorimetry. Four grams of cement were added into sealable 10 mL glass ampules containing the previously placed biopolymer sample. The binder was mixed with deionised water and homogenised with a vortex mixer (*VWT 1419*, VWR, Ismaning, Germany) for two minutes. The ampoule was placed in an isothermal conduction calorimeter (*TAM air*, Thermometric, Järfälla, Sweden) for monitoring the heat flow.

Mortar testing was performed according to DIN EN 196-1 and the strength was determined at different times of hydration using a *ToniNORM* instrument (Toni Technik, Berlin, Germany). The mortar consists of 3 parts of norm sand and 1 part of cement which was blended with the solid biopolymers. Using a *ToniMIX* eccentric agitator (Toni Technik, Berlin, Germany), the mortar was automatically mixed with the water. The prisms (4 x 4 x 16 cm) were compacted using a *ToniVib* vibrating table (Toni Technik, Berlin, Germany) and stored at 20°C / 90 % relative humidity until demoulding.

Ion concentrations in cement pore solution were determined using an ICP-OES spectrometer. The pore solution was extracted by mixing water and cement holding the biopolymer in a centrifuge tube for two minutes using a vortex mixer and afterwards separating the solution by centrifuging for 15 minutes at 8500 rpm.

In-situ XRD was performed by placing the cement paste in the designated sample holder and covering the paste with a *Kapton*® polyimide foil (VHG Labs, Manchester, UK). Diffraction patterns were measured every 30 minutes for 12 hours with a *D8 advance* instrument (Bruker AXS, Karlsruhe, Germany) (5 – 50 ° 2θ, 40 kV, 30 mA, 0,034 ° step, t = 0,4 s). Temperature inside the measurement chamber was ~ 26 °C.

Anionic charge amounts of the biopolymers were captured by charge titration using the cationic counter-polymer PolyDADMAC. 0.1 g/L alginate were titrated in water, 0.1 M NaOH and CPS using a *PCD 03 pH* instrument (BTG Mütek, Herrsching, Deutschland) until charge neutralisation was achieved. The CPS was extracted by mixing CAC (Secar 51) at w/c = 0.6 and vacuum filtration of the cement paste.

3. Results and discussion

3.1 Effect of biopolymers on cement hydration

Addition of most polysaccharides normally results in retardation of cement hydration. Only few polymers seem to have no retarding effect or lead to a weak acceleration. Such a minor effect was observed for Karaya Gum and Gellan Gum under certain conditions. It diminishes at increased dosages and is attributed to the stabilizing properties of these water retaining polymers on the cement paste which improves water availability. In contrast to those polymers, alginates and carrageenans strongly accelerate alumina cement. They can reduce the time of maximum heat release by up to 50 % (**Figure 4**).

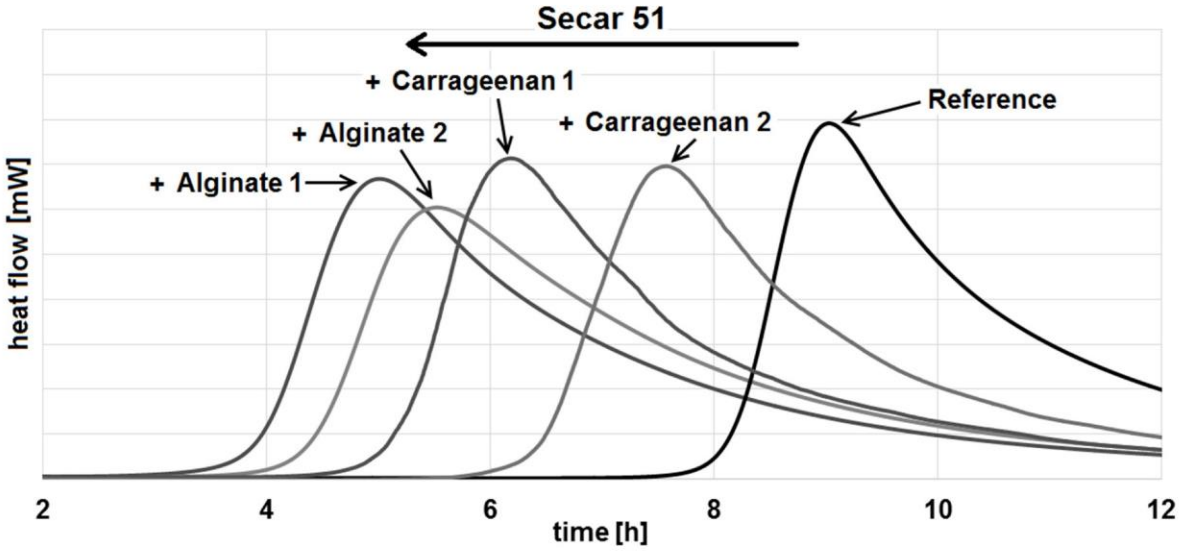

Figure 4: Accelerating properties of alginates and carrageenans at a dosage of 0.1 % bwob on CAC (Secar 51), determined by heat-flow calorimetry (w/c = 0.62).

Generally, alginates were found to accelerate more than carrageenans at equal dosage. This effect of the biopolymers is independent of the w/c-ratio which were varied between 0.4 and 0.6 to exclude an impact of the water binding capacity of the biopolymers on the result.

3.2. Strength development of mortar

In addition to heat-flow calorimetry, mortar testing was conducted using an alginate and a ι carrageenan sample in three different CACs. In fast-setting Ciment Fondu (≈ 38 % Al_2O_3), addition of the alginate accelerates strength development by ~ 1 hour (**Figure 5**). In less reactive Ternal LC cement (≈ 52 % Al_2O_3) carrageenan achieves a much faster strength development than the alginate when applying an increased dosage (**Table 1**). Addition of the biopolymers slightly reduces the fresh mortar density by retaining water and decreases the workability by reducing its flowability resulting from their viscosifying property. Because of the strong gelling properties of alginate the effective dosage range is limited, while carrageenan can be applied in higher dosage relative to alginates. In CA_2 rich Secar 712 (≈ 69 % Al_2O_3) both alginate and carrageenan result in an equally improved early strength. For example, after 16 hours the compressive strength of the mortar was increased by 120 % for carrageenan (dosage 0,2 % bwoc) and by 110 % for alginate (dosage 0,1 % bwoc) from 15.8 N/mm^2 to 34.9 N/mm^2 and 33.4 N/mm^2,

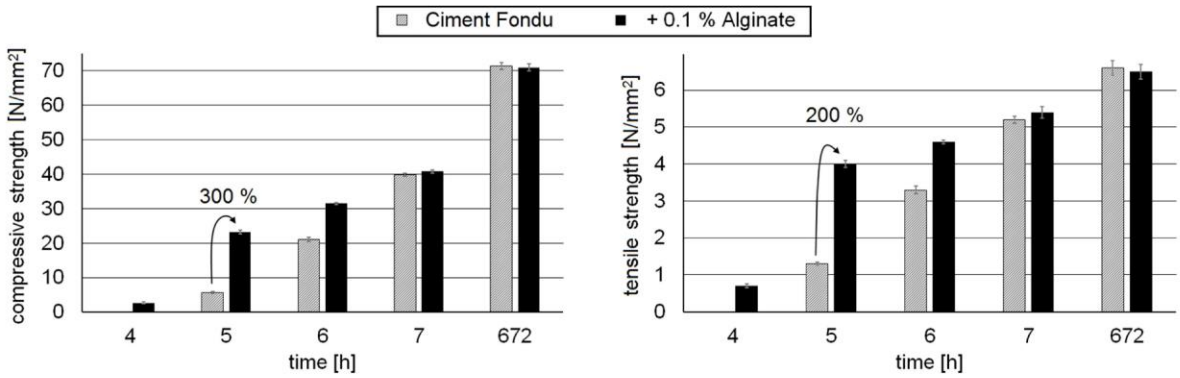

Figure 5: Compressive and tensile strengths at different curing periods for Ciment Fondu with and without alginate (0.1 % bwob Alginate, w/c = 0.5, 0.04 % bwob MPEG-PCE 45PC6)

respectively. Moreover, after twelve hours Secar 712 still was not hardened while the mortar containing carrageen or alginate already had developed 18.7 N/mm^2 or 11.5 N/mm^2 of compressive strength. This value is comparable to that of the neat cement after 16 h which represents an acceleration of four hours.

Table 1: Mortar properties and strength values after 6h of hydration for Ternal LC (w/c = 0.5).

6h	Reference	Alginate 0.10%	Carrageenan 0.20%
compressive strength	9.71 N/mm^2 ± 0.98 N/mm^2	17.15 N/mm^2 ± 0.83 N/mm^2 **→ 75 % increase**	25.03 N/mm^2 ± 1.05 N/mm^2 **→ 160 % increase**
tensile strength	1.39 N/mm^2 ± 0.07 N/mm^2	2.53 N/mm^2 ± 0.16 N/mm^2 **→ 80 % increase**	3.57 N/mm^2 ± 0.11 N/mm^2 **→ 155 % increase**
mortar density	2321 g/L ± 2 g/L	2297 g/L ± 5 g/L	2270 g/L ± 7 g/L
spread flow	24.1 cm	18.8 cm	17.9 cm

3.3. Interaction of accelerating biopolymers with other admixtures

The use of superplasticizers like PCEs results in a dose-dependent retardation of aluminate cements while flowability even at very low PCE dosages is much enhanced. The combination of PCE with alginate or carrageenan results in a slightly decreased workability, but still the increase in early strength is recorded, at improved workability compared to the reference. Combination of a lithium salt and the biopolymers allows partial replacement of Li resulting in a reduced consumption of this rare metal.

3.4. Interaction of accelerating biopolymers with ions in cement pore solution

As described in the introduction, alginates and carrageenans can interact with cations. Especially calcium ions are strongly complexed by the GG blocks of the alginate. This

chemical binding reduces the concentration of Ca^{2+} in the cement pore solution of Ciment Fondu (w/c = 0.45) by 15 % after addition of 0.1 % bwob alginate (**Figure 6**). Theoretically, the complexation of Fe^{2+}, Fe^{3+} or Al^{3+} is also possible, but because of the high pH in cement pore solution those ions will form $[M(OH)_4]^-$. This is mirrored by the slightly increased concentration of Al^{3+} in the pore solution. This increased solubility of Al^{3+} can be explained by the decreased Ca^{2+} concentration. When sodium alginate dissolves in the cement paste, then about 85 % of the sodium will be exchanged against calcium, forming a viscous gel [5].

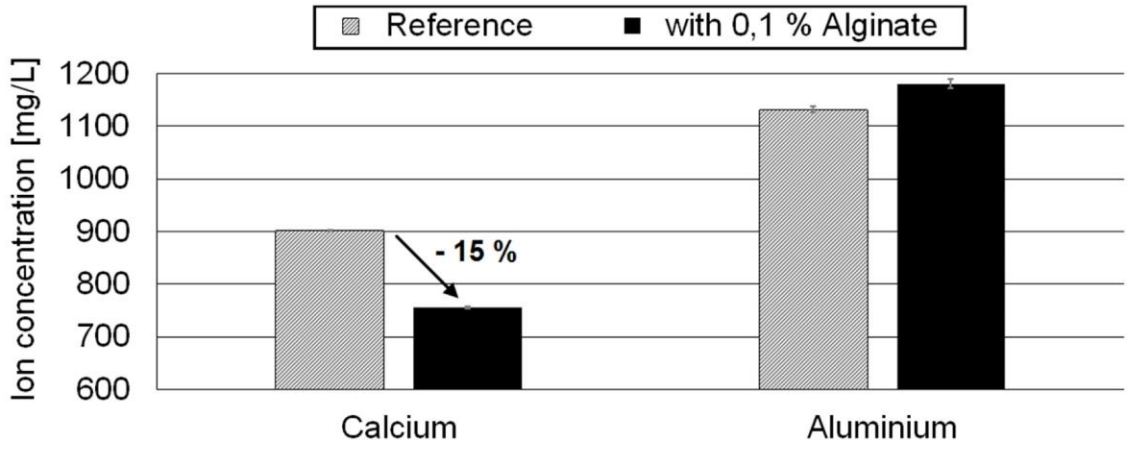

Figure 6: Ion concentrations of Ca^{2+} and Al^{3+} in extracted pore solution of Ciment Fondu with and without 0.1 % bwob alginate at w/c = 0.45.

The reduction in Ca^{2+} ion concentration is very surprising as this is normally associated with a retarded cement hydration. Combination of alginate or carrageen with retarders (citrate or tartrate) does not increase retardation as a consequence of even stronger reduction of the Ca^{2+} concentration, as would be expected. Experiments with sodium alginate in a calcium salt solutions concluded that calcium is not irreversibly bound in the calcium alginate gel, but can be exchanged when calcium is incorporated into an energetically more favourable complex.

A comparison of the charge density of alginate, propylene glycol alginate (PGA) and carrageenan in water, alkaline solution and cement pore solution helps to better understand the behaviour of the biopolymers in cement (**Figure 7**).

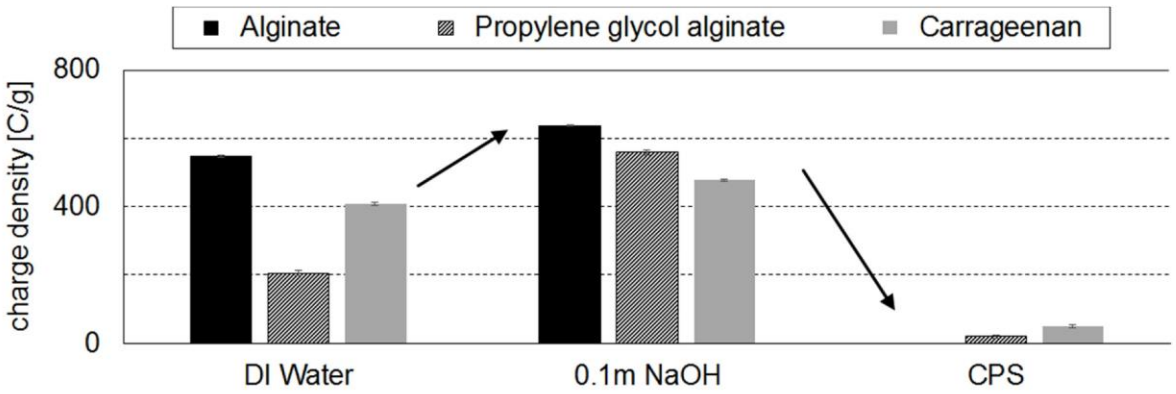

Figure 7: Anionic charge amounts of alginate, PGA and carrageenan in different solutions.

In alkaline environment, the functional groups are fully deprotonated and develop a strong interaction with ions in the cement pore solution. This was expected for alginates as they are known to form gels in the presence of divalent cations which makes charge density measurements for them in CPS not possible. For PGA (70 - 80 % degree of substitution of carboxylate groups) the results suggest a strong interaction with the hydroxyl groups of the alginate.

3.5. Molecular properties of the biopolymers studied

Most sodium alginates showed a similar accelerating property. Different behaviors were observed for samples of insufficient purity, coarse particle size and ultra-low viscosity grade. Especially the viscosity grade of the alginate is most critical for its acceleration. At lower viscosities the acceleration becomes less and even changes to a retardation. Because in alginates viscosity correlates with the molecular weight it can be said that alginates with low M_w act like classical retarding polysaccharides while the ratio between M/G in the alginate was found to be of no significant impact on acceleration.

3.6. Influence of accelerating biopolymers on phase development

When adding alginate to CAC, the hydration to CAH-phases proceeds as usual without the formation of other hydration products (**Figures 8 and 9**). However, the main hydrate phase C_2AH_8 forms earlier when alginate is present. This effect was particularly strong

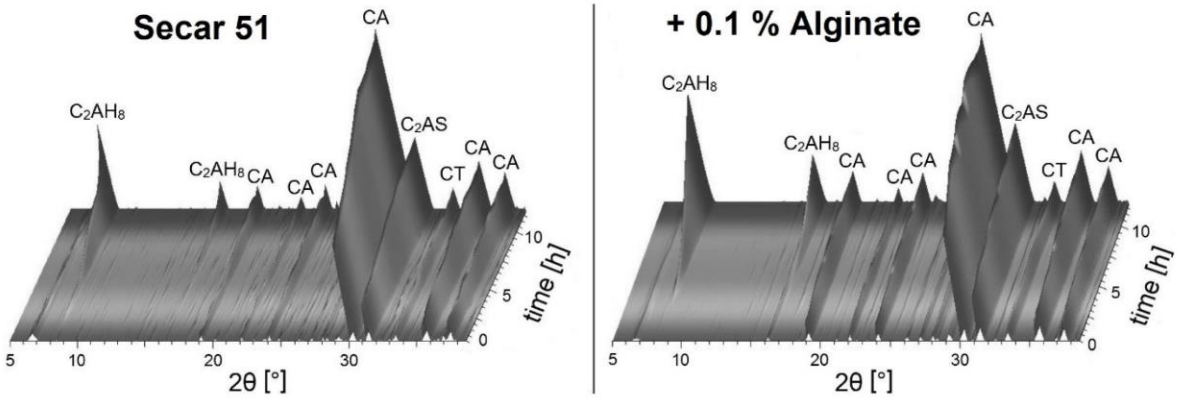

Figure 8: In-situ XRD measurement of Secar 51 (w/c = 0.45) for 12h with and without alginate.

in the slowly reacting high-alumina cement, where after 12 hours of hydration C_2AH_8 was only found in the accelerated cement and not in the reference **(Figure 9)**.

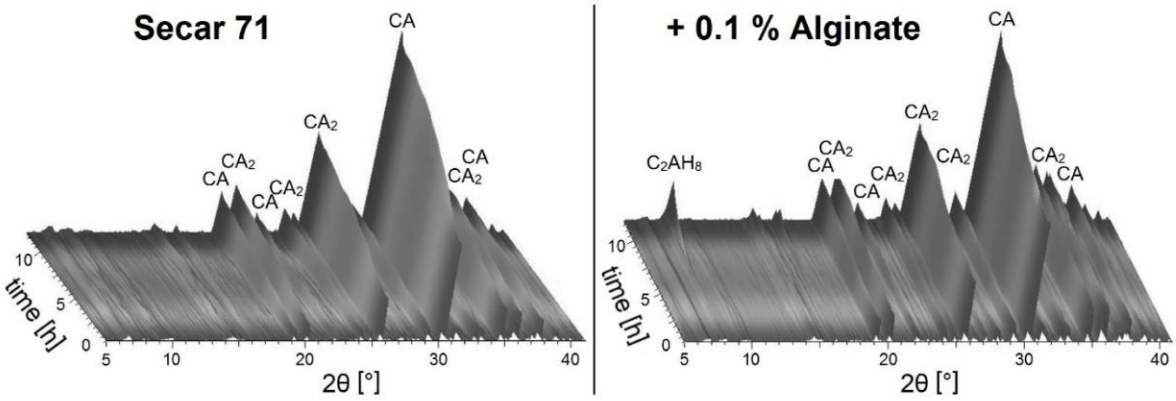

Figure 9: In-situ XRD measurement of Secar 71 (w/c = 0.45) for 12h with and without alginate.

4. Conclusions

Alginate and carrageenan present suitable accelerators for aluminate cement, as was proven by heat-flow calorimetry and strength tests of mortar samples. Addition of such biopolymers shifts the beginning of the hydration reaction to earlier times and results in higher early strength. Compared to lithium salts, these biopolymers require significantly higher dosages and addition of a superplasticizer to counteract their viscosifying effect. Combined application with lithium salts is an option to reduce the lithium consumption.

When comparing the chemical structures of the two biopolymers, a common structural element which allows the efficient complexation of ions sticks out (**Figure 10**).

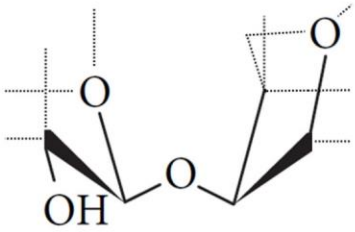

Figure 10: Common structural element present in alginate and carrageenan (common structural bonds shown in drawn lines, bonds specific to each biopolymer shown as dashed lines).

Apparently, both biopolymers share the ability to complex ions which seems to be critical for the accelerating effect. Especially the reduction of the calcium ion concentration in the pore solution is most remarkable, as it normally points to a substance being a retarder. Such retarding effect was only found for low-molecular weight alginates which in cement behave like other conventional polysaccharides.

References

[1] Götz-Neunhoeffer, F., *Modelle zur Kinetik der Hydratation von Calciumaluminatzement mit Calciumsulfat aus kristallchemischer und mineralogischer Sicht*, Habilitation, Universitäts-verbund Erlangen-Nürnberg, **2006**.

[2] Imeson, A. P., *Food stabilisers, thickeners and gelling agents*, John Wiley & Sons, **2011**.

[3] Plank, J., *Applications of biopolymers in construction engineering*, in: Biopolymers, Vol. 10, General Aspects and Special Applications, Wiley-VCH, Weinheim, **2003**, p. 29-95.

[4] Janetzky, P.: „*Alginate in a glance*“, Präsentation DuPont / Danisco Deutschland GmbH, **2016**.

[5] Mignon, A., et al., *Alginate biopolymers: Counteracting the impact of superabsorbent polymers on mortar strength*, Construction and Building Materials, 110, **2016**.

Authors:

M. Sc. Alexander Engbert alexander.engbert@bauchemie.ch.tum.de

Prof. Dr. Johann Plank sekretariat@bauchemie.ch.tum.de

Technische Universität München, Lehrstuhl für Bauchemie

Lichtenbergstraße 4

85747 Garching bei München